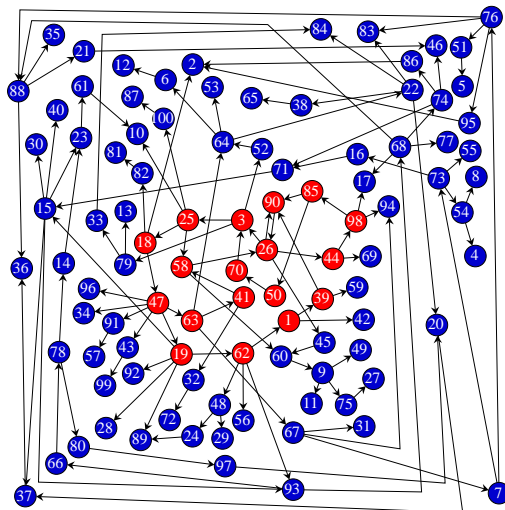


Formation and Destruction of Autocatalytic Sets in an Evolving Network Model



A thesis submitted for the degree of
Doctor of Philosophy in the Faculty of Science

Sandeep Krishna



Centre for Theoretical Studies
Indian Institute of Science
Bangalore - 560012, India

August 2003

Declaration

This thesis describes work done by me during my tenure as a PhD student at the Centre for Theoretical Studies, Indian Institute of Science, Bangalore. This thesis has not formed the basis for the award of any degree, diploma, membership, associateship or similar title of any university or institution.

Sandeep Krishna

August 2003

Centre for Theoretical Studies

Indian Institute of Science

Bangalore - 560012

India

Contents

1	Introduction	9
1.1	Networks in chemical, biological and social systems	9
1.2	Graph representation of a network	17
1.3	Difficulties of creating a graph representation	17
1.4	Structure of networks	18
1.5	Dynamical systems on networks	21
1.6	Evolution of networks	23
1.7	Framework of a model in which the network co-evolves with other variables	26
1.8	Extensions of the framework	28
1.9	The origin of life: evolution of a chemical network	28
1.10	Catastrophes and recoveries in evolving networks	30
1.10.1	Innovations	30
1.11	A map of subsequent chapters	31
2	Definitions and Terminology	33
2.1	Directed graphs and adjacency matrices	33
2.2	Degrees and dependency	35
2.2.1	Degree of a node and degree distribution of a graph	35
2.2.2	Dependency and interdependency	35
2.3	Walks, paths and cycles	36
2.4	Connected components of a graph	37
2.5	Partitioning a graph into its strong components	38
2.6	Condensation of a graph	38
2.7	Irreducible graphs and matrices	39
2.8	Perron-Frobenius eigenvectors (PFEs)	39
2.8.1	The Perron-Frobenius theorem	40
2.8.2	Basic subgraphs	41
2.9	Random graphs	42

3	Autocatalytic Sets	43
3.1	Autocatalytic sets (ACSs)	43
3.2	Relationship between Perron-Frobenius eigenvectors and autocatalytic sets	44
3.3	Eigenvector profile theorem	45
3.4	Core and periphery of a simple PFE	46
3.5	Core and periphery of a non-simple PFE	47
3.6	The profile of PFEs when there is no ACS	49
3.7	The profile of PFEs when there is an ACS but only one basic subgraph	49
3.8	The profile of PFEs when there is an ACS and many basic subgraphs	49
4	Population Dynamics	51
4.1	The population dynamics equation	51
4.2	Attractors of the population dynamics equation	52
4.3	Attractor profile theorem	54
4.4	The attractor for a graph with no ACS	54
4.5	The dominant ACS of a graph	54
4.6	Examples of the attractor for specific graphs	55
4.7	Timescale for reaching the attractor	60
4.8	Core and periphery of a graph	60
4.9	Keystone nodes	61
5	Graph Dynamics	63
5.1	Graph dynamics rules	63
5.2	Features of the graph dynamics	65
5.2.1	Evolution in a prebiotic pool	65
5.2.2	Coupling of population and graph dynamics: two timescales	65
5.2.3	Absence of self-replicators	65
5.2.4	Selection and novelty	66
5.3	Implementation	67
5.4	Results of graph evolution	67
6	Formation and Growth of Autocatalytic Sets	77
6.1	The random phase	77
6.2	The growth phase	80
6.2.1	Timescale for growth of the dominant ACS	81
6.3	Fully autocatalytic graphs	82
6.3.1	Probability of a random graph being fully autocatalytic	84
6.3.2	Clustering coefficient	85
6.3.3	Degree and dependency distributions	85

7	Destruction of Autocatalytic Sets	89
7.1	Catastrophes and recoveries in the organized and growth phases	89
7.2	Crashes and core-shifts	92
7.3	Addition and deletion of nodes from a graph	93
7.3.1	Deletion of a node: keystone nodes	93
7.3.2	Addition of a node: innovations	95
7.4	Classification of core-shifts	97
7.4.1	Complete crashes	98
7.4.2	Takeovers by core transforming innovations	98
7.4.3	Takeovers by dormant innovations	100
7.5	Timescale of crashes	100
7.6	Recoveries	103
7.7	Structure of the graph just before a crash	103
8	Robustness of the ACS Growth Mechanism	105
8.1	Variants of the model	105
8.2	Variable link strengths	106
8.3	Negative links: emergence of cooperation	108
8.4	Self-replicators	113
8.5	Non-extremal selection	114
8.6	Variable number of nodes	118
8.7	Different population dynamics	120
9	Concluding Remarks	123
9.1	Interesting features of the model	123
9.2	Implications for the origin of life	128
9.3	Limitations of the model as a description of a chemical network	129
9.4	Possible extensions of the model	130
9.5	Modeling other systems within the same framework	131
A	Proofs of Propositions	133
B	Programs to simulate the model	149
B.1	Variables and data types	149
B.2	Creating the initial random graph	149
B.3	The graph update	150

B.4	Program that uses the attractor profile theorem	150
B.4.1	Determining which node to remove	150
B.4.2	Output files	151
B.5	Program that finds the attractor numerically	152
B.5.1	Numerical method for determining the attractor	152
B.5.2	Output files	153
C	Contents of the attached CD	155
	Bibliography	157
	Acknowledgements	168

Chapter 1

Introduction

In this thesis I will analyze a model of an evolving set of catalytically interacting molecules. The dynamical rules of the model attempt to capture key features of the evolution of chemical organizations on the prebiotic Earth. Such a set of molecules is an ideal example of a ‘network’ – a system of several interconnected components. The concept of a network is often used as a metaphor in describing a variety of chemical, biological and social systems, as overviewed in section 1.1. Graphs provide a natural way of representing networks in a mathematical model. I describe how a graph can be used to represent a network and the difficulties involved in creating such a representation in sections 1.2 and 1.3. Sections 1.4, 1.5 and 1.6 discuss several studies of network systems, broadly classified according to whether they focus on the structure, function or evolution of networks. This classification is not meant to be precise – several studies could be placed in more than one category. In analyzing the model I will be mainly interested in the evolution of the graph representing the chemical network. Some issues of interest are discussed in section 1.6, including the spontaneous growth of non-random graph structures, the effect of different graph structures on the selective pressures that drive the evolution and sudden mass extinctions of species. Sections 1.7 and 1.8 describe a framework for modeling an evolving network, within which some of these issues can be addressed. The specific model I will analyze will be an instance of this framework. Sections 1.9 and 1.10 mention some of the interesting phenomena observed in the model and discuss its possible use in addressing puzzles connected with the evolution of chemical networks on the prebiotic Earth. Finally, I provide a ‘map’ of subsequent chapters in section 1.11.

1.1 Networks in chemical, biological and social systems

The term ‘network’ is often used to describe a variety of chemical, biological and social systems: The metabolism of a cell is a network of substrates and enzymes interacting via chemical reactions, ecosystems are networks of biological organisms with predator-prey, competitive or symbiotic interactions, the brain is a network of interconnected neurons, and the Internet is a network of interconnected computers.

Reviews of recent work on 'networks' (Watts, 1999; Strogatz, 2001; Bose, 2002; Albert and Barabási, 2002; Dorogovtsev and Mendes, 2002, 2003a; Bornholdt and Schuster, 2003) testify to the diversity of systems for which the term is used:

- **Ecological networks:** Williams and Martinez (2000), Montoya and Solé (2002) and Camacho et al. (2002) have studied a number of food webs found in freshwater, marine-freshwater interface and terrestrial environments. They have constructed graph representations of these food webs. A graph consists of a set of 'nodes', pairs of which may be connected by 'links'. It is usually drawn as a set of circles (the nodes) with arrows (the links) connecting pairs of nodes. In the graph representations created by Montoya and Solé, the nodes represent species, genera and sometimes higher taxa, and links represent predator-prey interactions. Figure 1.1 shows a graph for the Ythan estuary food web. It has 135 nodes and 601 links; each link points from a species to one of its predators.
- **Transcription regulatory networks** (Milo et al., 2002; Sengupta et al., 2002; Shen-Orr et al., 2002; Farkas et al., 2003; Maslov et al., 2003): Transcription of a gene is the process of constructing an mRNA from the DNA sequence of the gene. This process is regulated by proteins, called transcription factors, that enhance or inhibit transcription by binding to sites on the DNA, usually upstream of the gene, which in turn helps or prevents RNA polymerase and the rest of the basal transcription machinery from binding and initiating transcription. The protein product of one gene may act as a transcription factor for another gene – this network of interacting genes is called a transcription regulatory network.
- **Biochemical signaling networks:** A number of biochemical signaling pathways exist in cells which receive and transmit information, and perform computational functions that are necessary for regulating various cellular activities. These pathways are highly interconnected, with different pathways sharing several common components, and thus forming a signaling network. One example is the mitogen-activated protein kinase network, which is involved in regulating the cell cycle (Bhalla et al., 2002).
- **Neural networks:** The complete neural network of the nematode *Caenorhabditis elegans* has been mapped and can be represented as a graph with 302 nodes, each corresponding to one neuron, and more than 5000 links corresponding to synaptic or gap junction connections between neurons (White et al., 1986; Watts and Strogatz, 1998; Koch and Laurent, 1999).
- **Polymer chain networks:** The conformation space of a lattice polymer chain can be represented as a graph, with the nodes representing possible conformations of the polymer chain and the links representing the possibility of transforming one conformation to the other through local movements of the chain (Scala et al., 2001). Sen and Chakrabarti (2001) consider a different type of network – they represent a linear polymer as a regular one-dimensional graph with nearest neighbour links and some long range links.

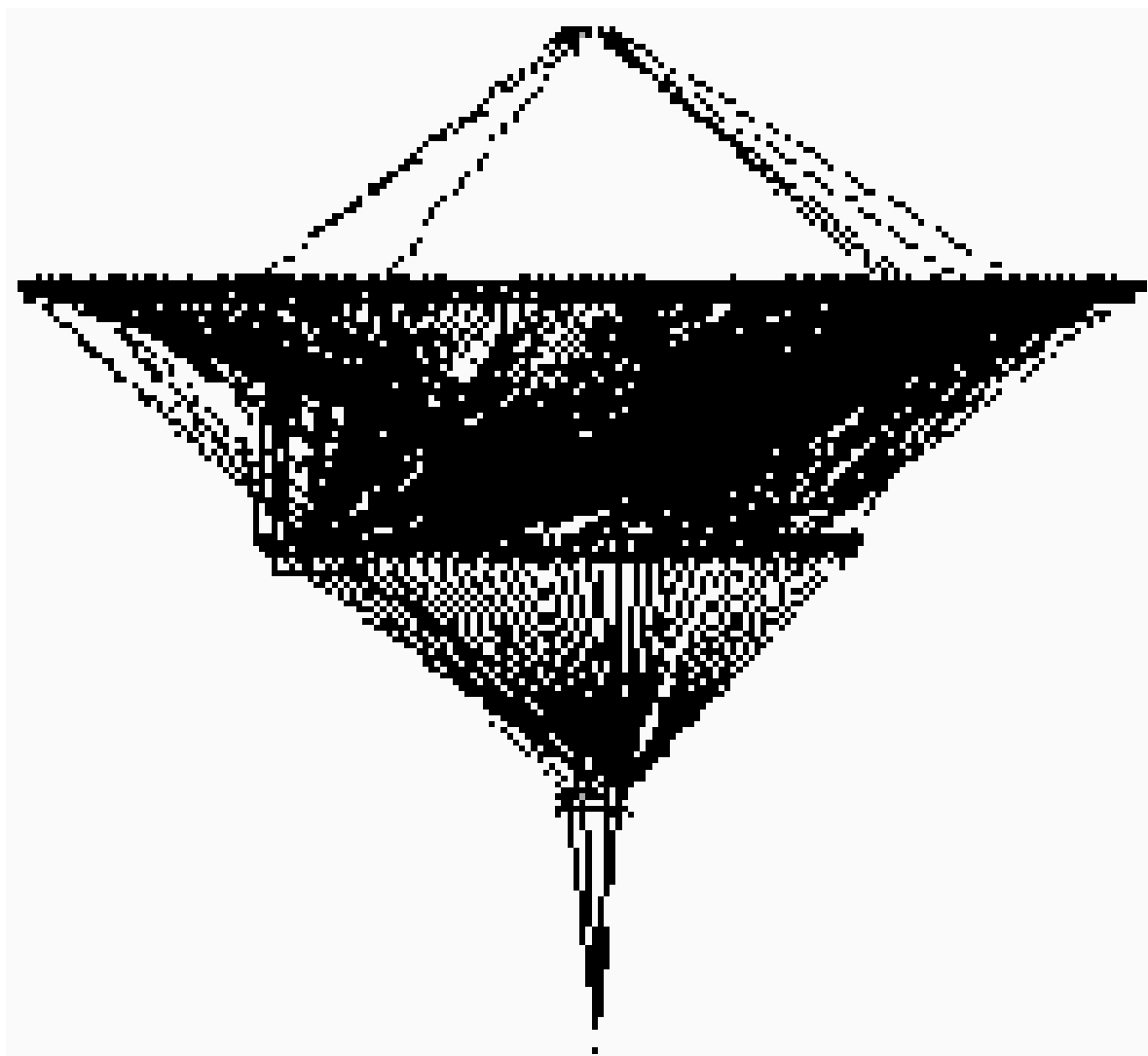


Figure 1.1: Ythan estuary food web. Each of the 135 nodes (circles) represents a species and there are 601 directed links (arrows, pointing from prey to predator). This data is freely available from the website of the COSIN project (<http://www.cosin.org>). The graph has been drawn using LEDA, the Library of Efficient Data types and Algorithms, which is now a proprietary software distributed by Algorithmic Solutions Software GmbH (<http://www.algorithmic-solutions.com/en/leda.htm>). The vertical positioning of each node is decided by the length of the shortest path leading to it from the basal species (the bottom node).

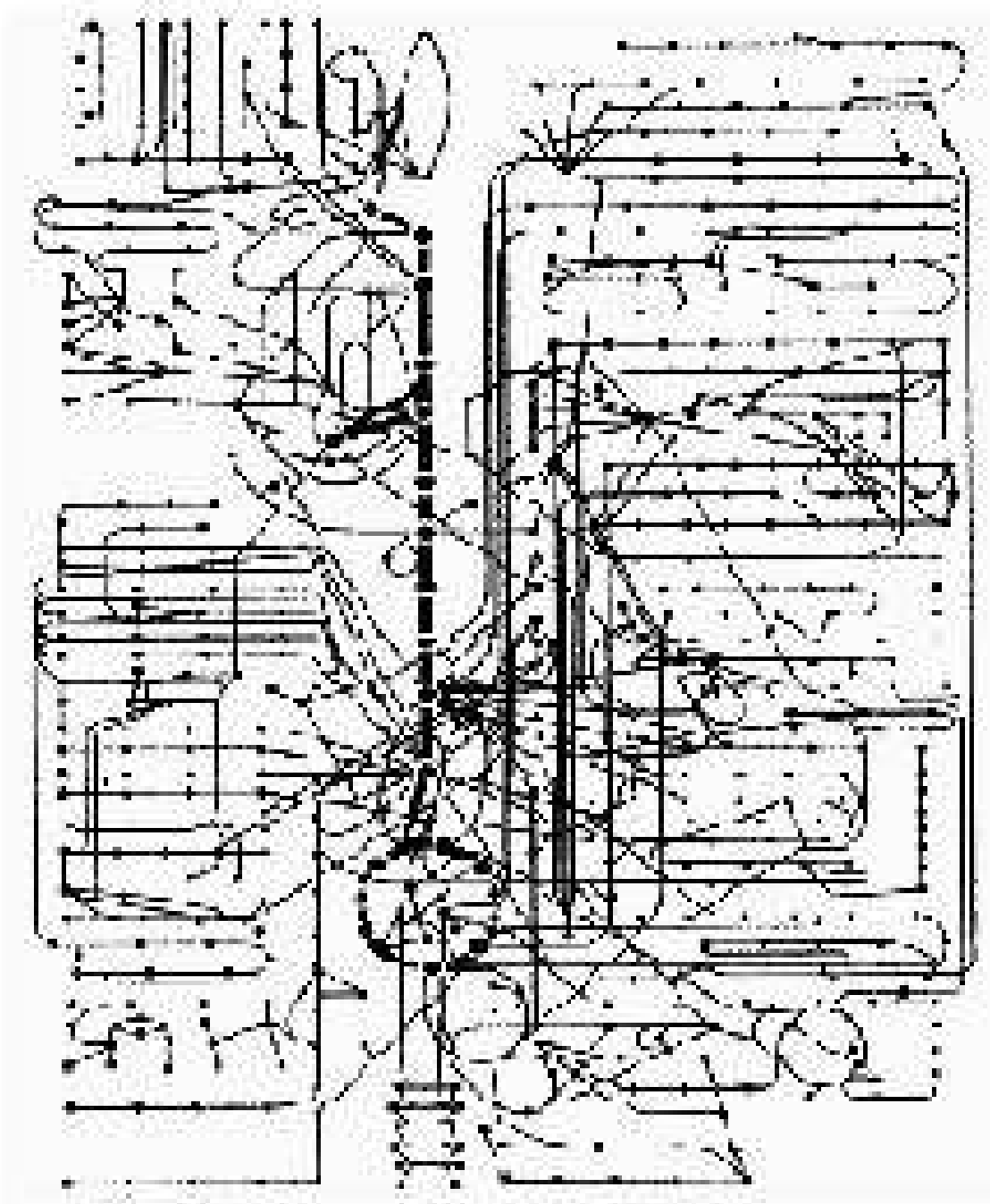


Figure 1.2: A graph of around 500 chemical reactions that take place in cells; image by Dennis Bray, Cambridge Univ. Each node represents a chemical species. Two species are linked if there is a reaction in which one species is a reactant and the other a product.

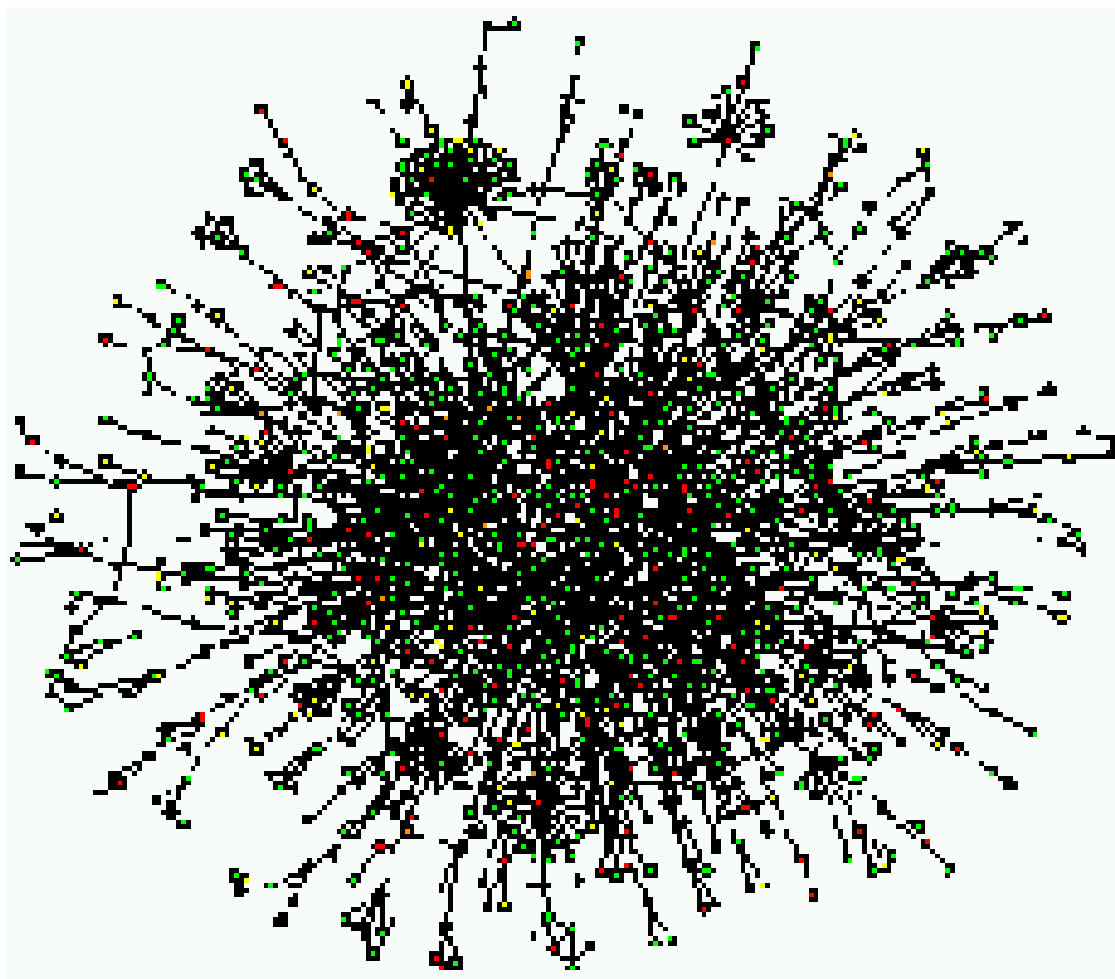


Figure 1.3: The protein interaction network for the yeast *Saccharomyces cerevisiae*. The nodes represent proteins. Pairs of proteins that are known to interact are linked. There are 1870 nodes and 2240 links. A node is coloured red if removing the corresponding protein is lethal for the cell, green if non-lethal, orange if removing the protein results in slower growth, and yellow if the effect of removing the protein is not known. Image available at <http://www.nd.edu/~networks/gallery.htm>, courtesy Hawoong Jeong, Korea Advanced Institute of Science and Technology.

- **Metabolic networks** (Fell and Wagner, 2000; Jeong et al., 2000): The metabolism of an organism, such as the bacterium *Escherichia coli*, is typically specified by a set of chemical reactions involving different substrates that are catalyzed by various enzymes. Figure 1.2 shows a graph of around 500 metabolic reactions. Each node represents one chemical species; a link connects two species if there is a reaction in which one species is a reactant and the other a product. This graph, unlike that in Figure 1.1, is an undirected one – the links have no associated direction and are therefore drawn as lines, not arrows.
- **Protein interaction networks**: The protein-protein interactions in the yeast *Saccharomyces cerevisiae* have been modeled as graphs by Jeong et al. (2001), Wagner (2001), Maslov and Sneppen (2002), Solé et al. (2002) and Vázquez et al. (2003) using data from two-hybrid assays and other experiments (Uetz et al., 2000; Ito et al., 2001). Figure 1.3 shows the protein interaction map for *S. cerevisiae*. In the graph each node represents a protein and an undirected link connects two proteins if they are known to interact. There are 1870 nodes and 2240 links.
- **Internet**: The Internet is a network of interconnected computers. Typically a few computers at one physical location (say a university or a company) are connected by a ‘local area network’. These LANs interact with each other via ‘routers’ or ‘gateways’. The topology of the Internet can be studied at various levels of detail. For example, Faloutsos et al. (1999) have studied a graph of the Internet at both the router level, where each node corresponds to a router, and at a more coarse-grained level, where each node corresponds to a group of routers. Another study of the Internet at the router level was done by Govindan and Tangmunarunkit (2000). Figure 1.4 shows a graph of the Internet at the router level. Another representation of the Internet is in terms of ‘autonomous systems’; each autonomous system “approximately maps to an internet service provider (ISP) and its links are inter-ISP connections” (Pastor-Satorras et al., 2001).
- **World-Wide Web**: The WWW is a network of interconnected hypertext documents. The connections are in the form of ‘hyperlinks’ that can be followed to other documents on the WWW. The structure of the WWW has been studied at this level of resolution (Albert et al., 1999; Broder et al., 2000; Kumar et al., 2000) as well as at the level of ‘sites’, collections of all the documents stored on the same web server (Huberman and Adamic, 1999).
- **Peer to peer networks**: The Gnutella network is one example. It consists of a set of computers connected to each other for the purpose of sharing files, with no central coordinating computer (Adamic et al., 2003).
- **Power grid networks**: Watts and Strogatz (1998) have studied a graph of the electricity transmission grid of western USA. The nodes of the graph represent generators, transformers and substations, and links represent transmission lines.

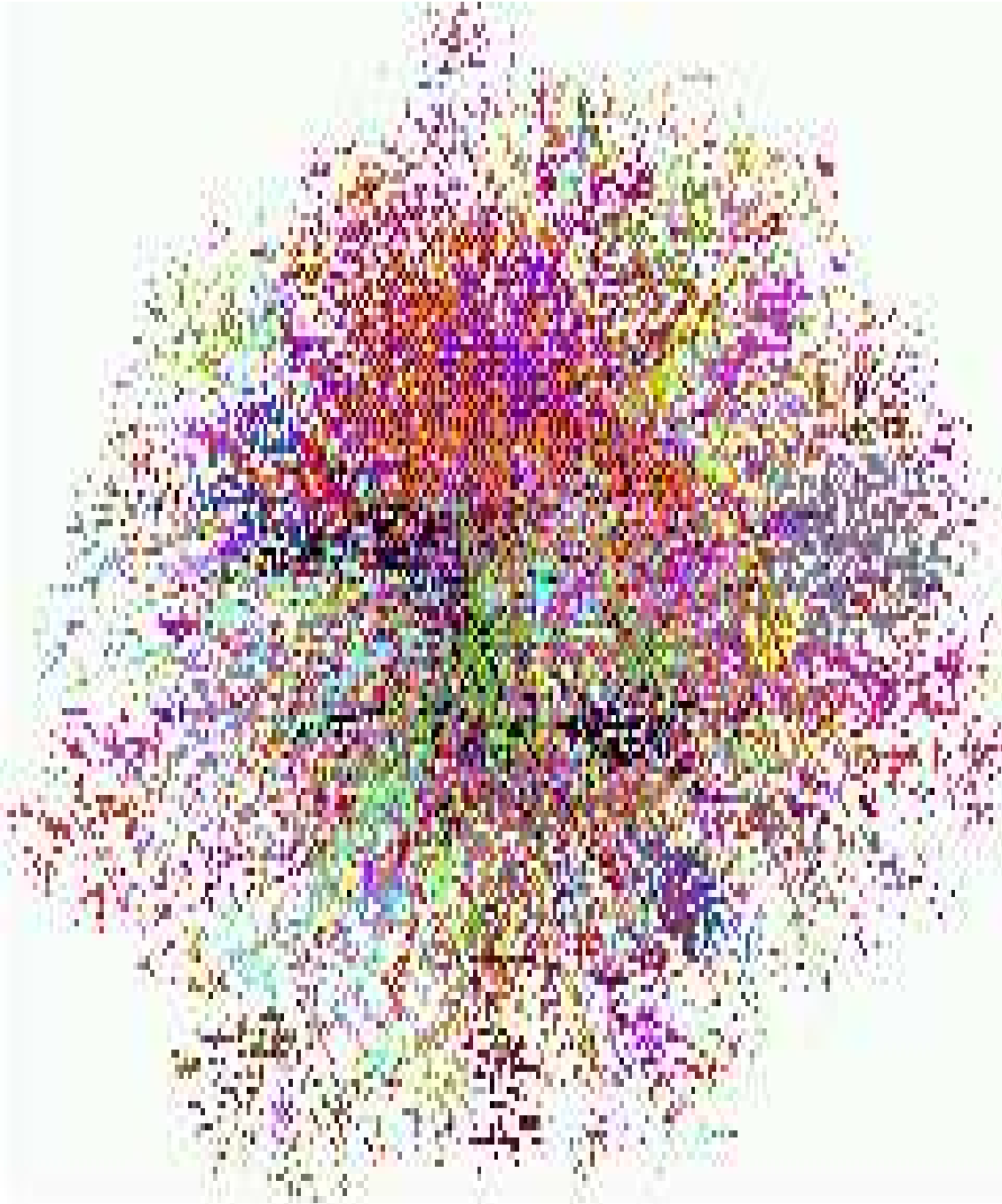


Figure 1.4: A graph of the Internet at the router level, as of September 1998. Image by Hal Burt and Bill Cheswick, courtesy Lumeta Corporation.

- **Transportation networks:** The Indian railway system, consisting of a network of stations connected by train services, has been studied by Sen et al. (2003). A similar network of the world's airports has been reconstructed from data on number of passengers arriving and leaving each airport (Amaral et al., 2000).
- **Economic networks** (Kirman, 2003): An economic system can be thought of as a network of interacting 'agents' (individuals, companies or even nations). Several different types of interactions can be visualized. For instance, one company may use the product of another as a raw material. In a market, individuals may interact by barter or monetary transactions. Stock market traders interact by buying and selling stocks and shares.
- **Word co-occurrence network:** i Cancho and Solé (2001) and Dorogovtsev and Mendes (2001) have studied a graph representing the English language. The nodes represent the different words of the English language and links signify that two words occur adjacent to each other in at least one sentence in the database of texts studied. The resulting graph has approximately 470 thousand nodes and 17 million links.
- **Friendship networks:** Amaral et al. (2000) have studied the properties of a graph representing the friendship network of a group of 417 high school students in USA.
- **Sexual contact network:** A graph with each node representing an individual and links representing sexual contacts was constructed and studied by Liljeros et al. (2001), based on a Swedish survey of 2810 people in the age range 18-74 years.
- **Film actor/actress collaboration network:** A graph can be constructed where nodes represent actors and actresses and a link is put between two if they have acted together in any film. Watts and Strogatz (1998) have studied such a graph of collaborations for all actors listed in the Internet Movie Database (<http://us.imdb.com>).
- **Scientific collaboration networks:** A similar graph can be constructed for scientific collaborations, where nodes represent researchers and a link represents co-authorship of one or more papers. Newman (2000a,b) has studied such a graph of collaborations constructed from databases of papers in physics, biomedical research and computer science.
- **Citation networks** (Seglen, 1992; Redner, 1998): It is common for research papers to cite several other papers. Thus a network of mutual citations interconnects research papers.

1.2 Graph representation of a network

As is evident from the list above, the starting point of many studies is to model networks using graphs. A graph representation is useful for formulating questions about the structure and functioning of a network more precisely. Graph theory suggests several quantities that can characterize the structure of a graph. These can be computed for a real network and used for comparison with, for instance, random and regular graphs.

The correlation of these graph theoretic quantities with the functioning of the network can also be studied, thus exposing, in a more precise way, the connection between a network's structure and its functioning. Another possibility a graph representation allows is of a cross comparison of very different systems – for instance, the metabolic network of a cell can be compared with the Internet.

In many natural systems, the network of interactions is itself a dynamical variable: The transcription regulatory network of an organism changes as genes evolve, the World Wide Web changes as web pages get added and deleted, and ecosystems change as species become extinct and new species arise. With a graph representation of the network, one can model processes that alter the graph with time, either in discrete steps or continuously.

1.3 Difficulties of creating a graph representation

Representing a network as a graph is not as straightforward as it may seem at first glance. Firstly, it is likely that several different graphs can be drawn for a given system, each of which focus on different aspects of the network. Consider, for example, the metabolism of the bacterium *Escherichia coli*, which is specified by a set of chemical reactions involving different substrates that are catalyzed by various enzymes. Fell and Wagner (2000) construct two different graphs from this information. The 'reaction graph' has a node for each chemical reaction with a directed link from one reaction to another if a product of the first reaction is used as a reactant for the second. The 'substrate graph' has one node for each substrate with a directed link from one substrate to another if there is a reaction in which the first substrate is a reactant and the second a product. Jeong et al. (2000) represent the metabolic network of each of 43 organisms as a graph consisting of two types of nodes, one type for each substrate and one type for each reaction. The graph is bipartite with links from substrate nodes to reaction nodes and reaction nodes to substrate nodes but no links connecting two substrate or two reaction nodes. This graph has more information than the previous two but also leaves out some information, for example, the stoichiometry of the reactions. Thus, each of these three types of graphs encodes different information about the metabolic network, and each of them excludes certain information.

Another problem is the incompleteness and uncertainty of data (Kohn, 1999). When the system consists of a complex network of interactions, even a single missed interaction or an erroneously added interaction, can drastically affect the dynamics. Food webs tend to suffer from a bias

against including parasites (Williams and Martinez, 2000). Incompleteness of data is suggested by Williams and Martinez (2000) and Camacho et al. (2002) as one of the possible reasons why the Ythan estuary food web appears to differ, in several properties, from the other food webs they have studied. Protein interaction networks are another example. The two hybrid experiments that have been used to build these networks are susceptible to both false positives as well as false negatives, i.e., some protein interactions may be erroneously missed and some non-existent protein interactions may be included (Uetz et al., 2000; Ito et al., 2001).

1.4 Structure of networks

How can one characterize the structure of the Internet, the neural network of *Caenorhabditis elegans*, or the Indian railway system? Representing a network as a graph makes it possible to use various graph theoretic measures to characterize its structure. For instance, one can compute the length of the shortest path between two nodes averaged over all pairs of nodes in the graph. This quantity can be compared with that expected for a ‘random graph’. Random graphs – graphs where each pair of nodes has a probability, p , to be connected by a link (see section 2.9 for a more precise definition) – were introduced by Erdős and Rényi (1959), and have several known structural characteristics. In the limit where the number of nodes of the graph, N , tends toward infinity, then if $p < 1/N$ (equivalently, if the number of links $l < N/2$) the graph consists of several connected clusters of nodes, each of which has only a finite number of nodes, and if $p \geq 1/N$ (or $l \geq N/2$) a ‘giant’ connected cluster exists which has an infinite number of nodes (Bollobás, 2001). The average shortest path length for an undirected random graph of N nodes, with enough links to contain a giant cluster, grows as $\ln N$ (Bollobás, 2001). At the other extreme are regular graphs, such as a one-dimensional chain of N nodes whose average shortest path length scales in proportion to N (for a d -dimensional hyper-cubic lattice it would scale as $N^{1/d}$).

Graphs of the Indian railway network (Sen et al., 2003), the western USA power grid network, the movie actor network, the neural network of *C. elegans* (Watts and Strogatz, 1998), the world airport network and polymer chain networks (Amaral et al., 2000), and ecological networks (Montoya and Solé, 2002) are known to have low average path lengths similar to random graphs with the same number of nodes and links.

However they differ from random graphs in other characteristics, like ‘clustering’. A set of nodes is ‘clustered’ if in some sense the nodes are more ‘strongly connected’ to each other than to other nodes of the graph outside the set. One measure of the amount of clustering in a graph is the ‘clustering coefficient’, which is the probability that two neighbours of any node are also neighbours of each other. Regular graphs have a relatively large clustering coefficient, while random graphs have a relatively low coefficient.

The networks mentioned above, which have a low average path length, have much higher clustering coefficients than random graphs with the same number of nodes and links. Graphs of

this type which have a comparable average path length but a much higher clustering coefficient than a similar random graph have been dubbed ‘small-world’ graphs (Watts and Strogatz, 1998; Watts, 1999).

Another measure is the degree distribution of a graph. The degree of a node (the total number of outgoing and incoming links to a node, see section 2.2) takes a range of values over all the nodes of any graph. The distribution of these values can be analytically calculated for the random graph described above, and is a binomial distribution. Given a graph of a real network, say the Internet, one can compute its degree distribution and compare with the binomial distribution expected for a random graph with the same number of nodes and links. In contrast, a regular graph, such as the lattice of a crystal solid, has nodes whose degrees take at most a few different values. For example, in a body-centred cubic lattice (such as that formed by iron or CsCl) each node (atom) has a degree eight. Many networks, such as the metabolic network of *E. coli* (Jeong et al., 2000), the Internet (Faloutsos et al., 1999) and citation networks (Seglen, 1992; Redner, 1998) have neither the binomial degree distribution of a random graph nor the discrete distribution of a regular graph. Instead their degree distribution has a power law tail. Such networks have been termed ‘scale-free’ (Barabási and Albert, 1999). Montoya and Solé (2002) claim that ecological networks also have a scale-free degree distribution, a conclusion that is disputed by Camacho et al. (2002). Several properties of scale-free graphs have been elucidated (Newman et al., 2001; Bollobás and Riordan, 2003). For instance, scale-free graphs are small-world, having a small average shortest path length (Barabási and Albert, 1999) and a high clustering coefficient (Watts, 1999). However, the converse is not true: Amaral et al. (2000) show that not all small-world networks are scale-free – among several different networks that are small-world, the degree distribution of some have an exponential tail like random graphs, some are scale-free, while others have a power-law distribution which is truncated by an exponential or a gaussian tail.

Yet another measure used to characterize a graph is its eigenvalue spectrum. Any graph with N nodes can be specified by an $N \times N$ ‘adjacency’ matrix. The collection of eigenvalues of this matrix is the eigenvalue spectrum of the graph. Some structural characteristics of a graph are reflected in the eigenvalue spectrum. For instance, in a directed graph, the largest eigenvalue is directly related to the presence or absence of cycles in the graph (see section 2.8). Though only some aspects of the connection between the spectrum and the structure of the graph have been worked out, it nevertheless serves to classify graphs into different groups. Once again, some properties of the spectrum of a random graph are known. For an undirected random graph, with enough links to contain a giant cluster, the value of the largest eigenvalue scales as pN , when $N \rightarrow \infty$, while the distribution of the rest of the eigenvalues converges to a semi-circle whose width is proportional to \sqrt{N} (Farkas et al., 2001). Therefore, the amount by which the eigenvalue spectrum of a real network deviates from this ‘semi-circle law’ is a measure of the non-randomness of the graph. Farkas et al. (2001) and Goh et al. (2001) have shown that the eigenvalue distributions of sparse random graphs and scale-free graphs are very different from the semi-circle distribution.

The clustering and degree of a node are ‘local’ quantities, in the sense that they depend only on the immediate links of the node or at most the links of its neighbours. In contrast, shortest path lengths, eigenvalues and eigenvectors are ‘non-local’ quantities, in the sense that the shortest path between two nodes, or the component of an eigenvector corresponding to a node, depends on the entire graph and not just on the immediate links of the nodes in question. It is therefore not surprising that the possibility of missing or extra links is a more serious problem for the non-local quantities than for the local quantities. The addition or removal of a small number of links will not significantly affect the degree distribution or the clustering coefficient. In contrast, adding a small number of random links to a regular graph reduces the average path length drastically (Watts and Strogatz, 1998). Similarly, the addition of a single link can create a cycle, where there was none before, thereby changing the largest eigenvalue.

Another non-local graph-theoretic measure is the dependency of a node, which, for a directed graph, is defined to be the number of links that lie on paths leading to the node in question (Jain and Krishna, 1999). The average dependency of nodes of a graph is termed the ‘interdependency’ of the graph because it is a measure of how interdependent are the nodes of the graph. Section 2.2 will discuss more about these measures.

A structural characteristic that is of interest, especially for chemical networks, is the property of autocatalysis. The concept of an autocatalytic set of chemical species was introduced by Eigen (1971), Kauffman (1971) and Rossler (1971), and is defined in that context to be a set of molecular species that contains, within itself, a catalyst for each of its member species. This notion is closely related to that of positive feedback loops and can be generalized to different systems which have other kinds of ‘beneficial’ interactions – for instance, symbiosis in ecological networks. Hong et al. (1992) and Lee et al. (1997) have each constructed a pair of different molecules that catalyze one another’s (as well as their own) production and hence form an autocatalytic set of this kind. Wächterhäuser (1990) and Morowitz et al. (2000) use a slightly different, but related, definition of autocatalysis to argue that the reductive citric acid cycle is autocatalytic. A graph-theoretic definition of autocatalytic sets (Jain and Krishna, 1998) is discussed in section 3.1. Autocatalytic sets will play a major role in the dynamics of the model studied in this thesis.

Several other structural characteristics of graphs that have this non-local character have been studied: Dhar et al. (1987) have analyzed the structure of the shortest path spanning all nodes in a variety of graphs derived from regular lattices; Janaki and Gupte (2003) define the “weight-bearing capacity” of a branching hierarchical network and analyze which network structures enhance this capacity; Hartwell et al. (1999) and Lauffenburger (2000) argue that cellular networks are ‘modular’, i.e., consisting of distinguishable clusters of nodes that play some functional role; Ravasz et al. (2002) suggest that the metabolic network of *E. coli* may have a hierarchical structure; Milo et al. (2002), Shen-Orr et al. (2002) and Maslov et al. (2003) describe a way of decomposing the transcription regulatory network of *E. coli* into commonly occurring ‘motifs’, which are specific patterns of connections between a small set of nodes.

1.5 Dynamical systems on networks

A different set of questions about such networks concerns the dynamics of variables ‘living’ on the graph – for example, the concentrations of different chemical substrates in a cell, or the populations of species in an ecosystem, or the number of times a document on the WWW is accessed. The network topology affects the dynamics of these variables. The food-web structure of an ecosystem affects the dynamics of its constituent species’ populations; the network of human contacts influences the spread of a contagious disease.

Such dynamical systems on networks are often modeled as a set of coupled differential equations in which the couplings are specified by the network of interactions. An example is a network of coupled (possibly nonlinear) oscillators where one common question asked is whether groups of oscillators eventually synchronize despite different natural frequencies and initial phases. The synchronization properties of coupled dynamical systems have been studied for network structures ranging from a fully connected graph (Strogatz, 2000) to regular lattices (Kaneko, 1989; Pérez et al., 1996), to trees (Gade et al., 1995), and a variety of sparse network structures (Jalan and Amritkar, 2003; Sinha, 2002). Ramaswamy (1997) has described the synchronization of coupled strange non-chaotic attractors. The stability of the synchronization to perturbations of the coupling strengths has been studied by Chen et al. (2003) for a large class of coupled maps and differential equations.

In ecosystem models, the Lotka-Volterra equation, replicator equation and other more complicated differential equations have been used to represent the dynamics of the populations of species (Drossel and McKane, 2003). The replicator equation, for example, displays a range of different behaviour depending on the network structure – fixed point, limit cycle, heteroclinic cycle and chaotic attractors have been observed (Hofbauer and Sigmund, 1988). Biochemical signaling networks too exhibit a variety of dynamics (Bhalla and Iyengar, 1999; Bhalla, 2002).

The dynamics of neural networks has been extensively studied. One example is a model of a neural network that exhibits a periodic cycling between different meta-stable states (“memories”) as well as intermittent transitions to a high activity state resembling epileptic seizures (Biswal and Dasgupta, 2002a,b). Sinha and Chakrabarti (1999) review what is known about synchronization in neural network models. For a comprehensive review of neural network models see (Arbib, 1995).

Some dynamical systems on networks have the property of displaying a variety of different dynamics even for the same network topology. Suguna et al. (1999) describe a simple model of a biochemical pathway that can show fixed point, periodic, birhythmic and chaotic dynamics as the rates of the reactions comprising the pathway are changed, while keeping the topology of the pathway fixed. Bhalla et al. (2002) analyze a biochemical signaling pathway whose dynamics is either monostable or bistable depending on the parameter values.

In some systems it is more appropriate to represent the dynamics by difference equations, rather than differential equations, or by cellular automata. This is especially true for systems where the variables of interest take discrete values and assuming them to be continuous variables is a bad

approximation. For instance, models of traffic on transportation networks in which particles (vehicles) are individually represented often show a different behaviour (e.g., different phase transitions from a free flowing state to a traffic jam state) from models in which a continuous traffic flow rate is the dynamical variable. Nagel (2003) reviews different traffic models on various types of networks. Several studies of neural networks model the neurons as cellular automata (Arbib, 1995). Two studies where the dynamics occurs in discrete time steps are described by Pandit and Amritkar (2001), who have studied the dynamics of random walkers on a class of small-world networks, and Dube et al. (2002), who have studied the effect of different pricing schemes on the dynamics of queues of people accessing an Internet web server.

When the dynamics can be assumed to be reaching some steady state or fixed point, there may be short cuts to finding the steady state without actually having to solve the equations of motion. For instance, Edwards et al. (2001) describe a procedure for determining the rates of the chemical reactions comprising the intermediary metabolism of *E. coli*, assuming a steady state. Instead of finding the rates as the attractor of some difference or differential equations, the procedure is based on linear optimization of a specifically chosen function under the constraints imposed by the stoichiometry of the reactions. The structure of the steady state reaction fluxes can be studied as a function of different network topologies.

Local search strategies are another example of dynamical systems on a network (Adamic et al., 2003). The Gnutella file sharing system consists of a network of computers; there is no central coordinating computer that has information about the entire network, in particular, which files are available at which nodes. Therefore, each user must use a local search strategy, an algorithm that uses only local information, such as the identities and connections of a particular node's neighbours, its neighbour's neighbours, etc., to find where a particular file is located on the network. Again, the network topology is crucial because, for example, the most efficient search algorithms for regular graphs are quite different from those for random or scale-free graphs (Adamic et al., 2003).

Another set of studies involving dynamics on networks is in the field of epidemiology. In the models studied by Watts and Strogatz (1998) and Pastor-Satorras and Vespignani (2003) diseases spread faster in small-world or scale-free graphs than in regular and random graphs. Similar models are used to study the spread of computer viruses through the Internet. These models can suggest efficient immunization techniques by identifying which links or nodes of the graphs are contributing most to the spread of the virus (Pandit and Amritkar, 1999; Pastor-Satorras and Vespignani, 2003).

Closely related to this are studies of 'attacks' on a network by the removal of nodes of the network. Albert et al. (2000), Callaway et al. (2000) and Cohen, R., et al. (2000, 2001) show that scale-free networks are more robust to random attacks than random graphs but are susceptible to directed attacks at the nodes with the highest degree. These studies contain networks that are changing with time, though the dynamics simply involves nodes getting removed in a specified order. The next section deals with studies of evolving networks with more complicated dynamics.

1.6 Evolution of networks

So far I have focused mainly on the structure of, and the behaviour of dynamical systems on, fixed networks. However, real networks are rarely static. An obvious question, therefore, is how (and why) did a particular network evolve into the specific structure we see? For instance, has the structure of a network evolved to optimize certain functionality? Further, one can ask what are the mechanisms that cause the network to change? Is the evolution driven by Darwinian natural selection, or Lamarckian selection, or by other self-organizing processes?

Some of the structural and dynamical studies in the previous two sections can be used to make some guesses about the evolution of the network. For instance, Fell and Wagner (2000) suggest that the small-world structure of metabolic networks may have evolved to enable a cell to react rapidly to perturbations. Watts and Strogatz (1998) suggest that the visual cortex may have evolved into a small-world architecture because that would aid the synchronization of neuron firing patterns. The robustness of scale-free networks to random removal of nodes has been suggested as an evolutionary reason for the prevalence of scale-free networks (Albert et al., 2000).

While studies of static networks do provide some insight into network evolution, it is natural to address such evolution-related questions in models where the network is also a dynamical variable. One possibility is to analyze a variety of simple models of changing networks, with different rules governing the dynamics of the network, and see which rules produce structures like small-world or scale-free graphs that are commonly observed in real networks: Watts and Strogatz (1998) describe a model that produces a small-world graph by randomly rewiring or adding links to a regular graph. A similar model (where the number of nodes is fixed but links are repeatedly added) that produces scale-free networks, is described by Mukherjee and Manna (2003). Several other 'growing network' models start from an empty network and add nodes and links at discrete time steps. The 'preferential attachment' rule – new nodes are preferentially assigned links to nodes with a high degree – produces scale-free graphs (Barabási and Albert, 1999). Albert and Barabási (2002) and Dorogovtsev and Mendes (2002) review several different models of this type, using both deterministic and stochastic rules, that give rise to scale-free graphs. The growing network model described by Manna (2003) adds another level of complexity by making the addition of new links to the network dependent on the dynamics of several random walkers on a regular lattice. Variants of these models exist where the preferential attachment to nodes of high degree competes with the preferential attachment to nodes of a lesser age, i.e., nodes that have been added to the network more recently. Amaral et al. (2000) have shown that such aging effects can result in a graph whose power-law degree distribution is truncated by an exponential tail. Dorogovtsev and Mendes (2003b) discuss models of accelerated growth of networks, where the rate of addition of new nodes increases with time. Williams and Martinez (2000) describe a simple set of rules to grow a network, that produces graphs remarkably similar in structure to many ecological food webs (Camacho et al., 2002).

One aspect missing from these growing network models is that the dynamics of the network is not intertwined with the dynamics of other variables. The models that include aging are implicitly using a dynamical variable, the age of a node, but the dynamics of that variable is not coupled to the structure of the graph. In many natural systems the dynamics of the network is tightly coupled to the dynamics of the variables living on it, and vice versa. For example, a food-web influences the dynamics of the species' populations, and if a species becomes extinct, the food-web changes. The firing pattern of neurons depends on the structure of the neural network and the strengths of synaptic connections are in turn modified by the repeated firing or non-firing of neurons (Arbib, 1995). There exist a number of models that incorporate this feature too. Models of learning and memory in neural networks typically have neuron firing patterns co-evolving with the network connection strengths (Arbib, 1995). A number of such evolving ecosystem models have been studied (Lindgren and Nordahl, 1994; Solé and Manrubia, 1996; Chowdhury et al., 2003) (see Drossel and McKane, 2003, for a review). Evolving replicator networks have been described by Happel and Stadler (1998) and Tokita and Yasutomi (2003).

In addition to creating evolving network models that produce graphs having a similar structure to existing networks, one can also use evolving network models to address a number of other evolution-related questions. For instance, how does the existing structure of a network influence its subsequent evolution? This question is best addressed in a model where the evolution of the network is coupled to the dynamics of other variables, which, in turn, are affected by the network structure. Because of this coupling, the different (sub)structures in the network affect its evolution. For instance, autocatalytic sets in prebiotic chemical networks might have been more stable to perturbations because of their ability to self-replicate. If so, an interesting question is: Can such stable structures grow, or spread through a network and, if they can, over what timescales? Further, one can ask how the existing structures determine the short and long term effects of a perturbation on the evolution of the network; in an ecosystem, whether an invading species will be able to survive, and for how long, will depend on the competition and resources provided by the existing species.

A related set of (meta)questions can be asked about the 'evolvability' of networks. Kirschner and Gerhart (1998) have defined the evolvability of a biological organism as the capacity to generate heritable, selectable phenotypic variation. This definition can be extended to other types of networks. Then one can ask: How evolvable is a network? Is this evolvability also subject to selection and has it, therefore, itself evolved over time?

One of the inspirations for the model I will discuss in this thesis are the models of Kauffman, Farmer, Fontana and others who have explored questions about self-organization, the origin of life and some of the above evolvability issues in work on artificial chemistries. An artificial chemistry is a system whose components 'react' with each other in a way analogous to molecules participating in chemical reactions. Thus, Kauffman (1983) and Bagley et al. (1991) consider systems composed of strings of arbitrary length made from a binary alphabet. Strings can participate in 'cleavage'

and 'ligation reactions' which involve the splitting or concatenation of strings to form new ones. Just as with a real chemistry, not all reactions will be allowed and there are different ways of specifying which strings participate in which reactions. The simplest way is to randomly decide which reactions are allowed, resulting in a 'random chemistry' of the type studied by Kauffman. He found that there is a critical number of links, such that if a random chemistry has more than that number of links, it is almost certain to contain an autocatalytic set (Kauffman, 1993).

Bagley et al. (1991) have explored an artificial chemistry consisting of catalyzed ligation and cleavage reactions. Their network evolves with time as new molecules can be created by the ligation of existing ones. They address the puzzle of how large molecules with highly specialized functionality, like enzymes and DNA, could have evolved from an initial condition that contained only small molecules which interacted weakly and non-specifically. Again, autocatalytic sets play an important role in the overall dynamics and are suggested as one of the possible means by which a complex chemical organization, a 'metabolism', could have evolved on the prebiotic Earth. Fontana (1991) and Fontana and Buss (1994) study more abstract artificial chemistries consisting of functions expressed in the lambda-calculus. Each function can 'react' with other functions, producing a new function by the composition of the 'reactant' functions. They find that in such a chemistry there is a spontaneous emergence of groups of cooperative reactions such as self-replicators, self-replicating sets, autocatalytic cycles, symbiotic and parasitic functions.

If Darwinian natural selection is driving the evolution of the network one can ask, what were the selective pressures acting on the network at different times? How do the selective pressures change with the structure of the network? Whenever the dynamics of the network has a stochastic component the detailed structure of the network is typically a result of many chance events. Nevertheless, some patterns may still be predictable. Thus, it is of interest to ask which patterns are predictable and which are a result of historical accidents.

Another aspect of the dynamics of evolutionary systems is the destruction of structures. In evolving systems, non-random structures not only emerge but also get destroyed in some circumstances. A number of mass extinctions are documented in the fossil record (Newman and Palmer, 1999). Financial markets suffer sudden large crashes (Bouchaud, 2001; Johansen and Sornette, 2001). Discovering markers that can be used to predict an imminent crash would obviously be very useful in the context of financial markets. It is of interest to try to identify the possibly multiple causes of such crashes. Many mechanisms have been suggested to explain mass extinctions in the fossil record (Maynard-Smith, 1989; Glen, 1994). The model of Bak and Sneppen (1993) is one example of attempts to explain the distribution of extinction sizes. Tokita and Yasutomi (1999) have studied various statistical properties of the extinction events in their model of an ecosystem. In ecosystems there can exist 'keystone' species whose extinctions are likely to trigger a cascade of further extinctions (Paine, 1969; Jordán et al., 1999; Solé and Montoya, 2001). This raises several interesting questions: Knowing the structure of an ecological network can one predict which species are keystone? Are there any mechanisms that exist to 'protect' such important species?

In this thesis I will try to address some of these issues within the context of a specific mathematical model of an evolving network. Many of the phenomena exhibited by the model are reminiscent of the phenomena seen in a variety of evolving networks – the growth of non-random structure (in the form of autocatalytic sets), the growth of interdependence and cooperation between nodes of the network, sudden mass extinctions due to the extinction of keystone species or the creation of certain new structures in the network (termed ‘innovations’). The model provides a simple mathematical framework within which to analyze the mechanisms that produce such phenomena. The basic model, and its variants, will be specific instances of a broad framework for modeling evolving networks that I present in the following section.

1.7 Framework of a model in which the network co-evolves with other variables

Consider a process that alters a network, represented by a graph, in discrete steps. The series of graphs produced can be denoted $C_n, n = 1, 2, \dots$. Each step of the process, taking a graph from C_{n-1} to C_n , will be called a ‘graph update event’. The following framework defines a class of evolving network models that consist of a graph evolving, by a series of graph update events, along with other system variables:

Variables: The dynamical variables are a directed graph C and a variable x_i associated with each node i of the graph. For example, x_i could represent:

- the concentrations of substrates and enzymes in a metabolic network,
- the expression level of genes in a genetic regulatory network,
- the populations of species in an ecosystem,
- the state (firing or not firing) of neurons in the brain,
- the number of times each web page on the world wide web has been accessed,
- the number of films each actor/actress has worked in,
- the profits of each of a set of interacting companies.

Initialization: To start with, the graph C and the variables x_i are given some initial values. The particular choice of values will depend on the system being modeled.

Dynamics:

Step 1: First, keeping the graph (C_{n-1} at step $n - 1$) fixed, the x_i are evolved for a specified time T according to a set of differential equations that can be schematically written in

the form: $\dot{x}_i = f_i(C_{n-1}, x_1, x_2, \dots)$, where f_i are certain functions that depend upon the graph C_{n-1} and on all the x_i variables.

- Step 2: After this, some nodes may be removed from the graph, along with their links. Some links may also be removed from the graph. Which nodes and links are removed will, in general, depend on the x_i values of the nodes and the graph C_{n-1} .
- Step 3: Similarly, some nodes may be added to the graph. These new nodes will be assigned links with existing nodes. The rules for specifying which links will be assigned may depend on the x_i values of the other nodes and C_{n-1} . The new node will be given its own x_i variable, which will be assigned some initial value. Some new links may be added between existing nodes, which again may depend on the x_i values of the nodes and C_{n-1} .

Steps 2 and 3 produce a new graph which will be the graph at time step n , C_n . This process, from step 1 onward, is iterated.

The above provides a nonequilibrium statistical mechanics framework for a model of an evolving network. The graph is generically in a nonequilibrium state because of the constant flux of nodes and links into and out of the graph. The x_i variables may also be in a nonequilibrium state depending on the form of f_i . The graph dynamics in this framework is a specific case of a Markov process on the space of graphs. For a general Markov process, at time $n - 1$, the graph C_{n-1} determines the transition probability to all other graphs. The stochastic process picks the new graph for time n , C_n , using this probability distribution. In the example here, the transition probability is not specified explicitly. It arises implicitly as a consequence of the dynamics of the x_i variables (step 1) and the way the specified rules for steps 2 and 3 use the x_i values to determine which nodes and links will be removed or added.

There are two timescales built into this framework. On a timescale much shorter than T , the x_i variables can evolve while the graph remains fixed. On a longer timescale, the graph changes in discrete steps that involve the possible removal and addition of nodes and links. The operation of the x_i dynamics and the graph dynamics on different timescales is common to many systems. In the brain, over short times neurons fire or not depending on their fixed synaptic connections and the firing of other neurons, while over a long timescale the firing pattern can cause the synaptic connections to strengthen or weaken. In an ecosystem, over short timescales the species composition is fixed while the populations change, and over long times the network changes because of the extinction and mutation of existing species and the invasion of the system by new species. In a genetic regulatory network, over short times the genes and regulatory interactions are fixed and it is the expression level of genes that changes with time, and on a longer timescale the genes themselves evolve. These examples also reiterate what was mentioned before – the x_i dynamics and the graph dynamics are interdependent. This feature is also built into the above framework: The dependence of the x_i dynamics on the graph lies in the dependence of the functions f_i on C .

The dependence of the graph dynamics on x_i lies in steps 2 and 3. The particular choices of f_i as well as the rules determining which, if any, nodes and links will be removed or added will depend on the particular system that is being modeled.

1.8 Extensions of the framework

This framework can be extended to include a larger class of evolving network models. Firstly, as mentioned in section 1.5, it may be preferable to model some systems using difference equations or cellular automata. For instance, if the populations of all species in an ecosystem can be assumed to be large then treating them as continuous variables and representing their dynamics by differential equations may be reasonable. But if the populations are close to zero this could be a bad approximation. It is easy to alter step 1 to take into account these possibilities. Secondly, it may be more appropriate to model some systems using two or more graphs, or by some generalization of a graph like a hypergraph. For example, in a cell, the metabolic network is linked to the genetic regulatory network and the dynamics on one network can affect the dynamics on the other. A number of neural network models of learning consist of two interacting networks, the 'teacher' and the 'student'; Kinzel (2003) has reviewed several models that consist of more than one neural network interacting with one another. The framework described above can be generalized to deal with such systems: Kohn (1999) has described a generalized form of a graph that he uses to represent all the different types of interactions in the mammalian cell cycle control and DNA repair systems. Thirdly, as is the case in some neural network models (Arbib, 1995), it may be worthwhile to consider dynamical rules where the network changes continuously with time, rather than in discrete steps as in the above framework.

1.9 The origin of life: evolution of a chemical network

In this thesis I will describe a model – a particular instance of the above framework – whose rules attempt to describe some aspects of the dynamics of a chemical network in a pool on the prebiotic Earth (Jain and Krishna, 1998). Assume that the pool contains many amino acid monomers or nucleotide bases, as well as some small polypeptide chains or short RNA molecules which may have a weak catalytic activity (Joyce, 1989). For instance, some of these polypeptides or catalytic RNA might catalyze the production of other polypeptides or RNA from the monomers present in the pool. Such a chemical network can be represented as a graph in which the nodes are the polypeptides/RNA and the links represent their catalytic interactions. This would be the graph C in the model. The x_i could represent the concentrations or relative populations of each type, or species, of polypeptide or RNA. x_i would change with time as the possible chemical reactions proceed to produce or deplete the different molecular species. Focusing only on the catalyzed reactions which produce different molecular species from the monomers, one can imagine that for

a short timescale, over which the pool remains undisturbed, the chemical network (i.e., C) will be fixed with no molecular species entering or exiting the pool. Thus, the x_i will evolve according to the chemical rate equations, with C fixed. In section 4.1, I derive the form of f_i for such chemical rate equations under the following assumptions:

- only reactions involving the catalyzed production of each molecular species are modeled,
- the catalyzed reactions are described by the Michaelis-Menten theory of enzyme catalysis,
- the Michaelis constants for each reaction are very large compared to the populations,
- the concentrations of all the required reactants are non-zero and fixed,
- all catalysts have the same strength,
- the pool is well-stirred, i.e., there are no spatial degrees of freedom.

Over long timescales imagine that the pool is subject to perturbations in the form of floods, tides or storms which may flush out part of the pool and possibly introduce new molecules into the pool. Removing a node from the graph would correspond to removing all the molecules of a particular type from the pool. When a perturbation removes a random lot of molecules, the molecular species with smaller x_i are more likely to be completely wiped out from the pool. For step 2, I will choose a rule that implements an extreme version of such selection: the node with the least x_i will be removed along with all its links. A perturbation can add a new node to the graph, with a small x_i value. An added node corresponds to a new type of molecule being brought into the pool by the perturbation. As there is no reason to assume such a node would have any particular relationship with existing nodes it is reasonable to assign the links of the new node randomly. Therefore, for step 3, I choose the rule: add one new node, whose links with existing nodes are assigned randomly. In this scenario one can assume that the perturbation would not remove existing links without removing a node, or create a new link between existing nodes. Therefore, these possibilities can be excluded from the model. A detailed description of the model rules is given in chapter 5.

Such a model could address some questions concerning the origin of life on Earth (Jain and Krishna, 2001). The chemical network of a bacterial cell of today consists of several thousand types of molecules involved in thousands of different chemical reactions. Each type of molecule plays a definite functional role and the entire chemical network is organized to enable the cell to perform the various functions it needs to survive and reproduce in often extreme conditions. This chemical organization is highly non-random – the molecules found in cells are a small subset in a very large space of possible molecules and the graph that describes their interactions is a special kind of graph in the very large space of graphs. The probability of such a structured chemical organization arising by pure chance is extremely small. After the oceans condensed about 4 billion years back on the prebiotic Earth there was no such chemical network of interactions existing anywhere. However, if we assume that life originated on Earth about 3.5 to 3.8 billion years ago as suggested by the

microfossil evidence (Schopf, 1993), then that leaves a few hundred million years for the first living cells to form. A puzzle of the origin of life on Earth is: how did such a structured, non-random chemical organization form in such a short time? This question can be addressed in the above model. One can start with a random graph, representing the situation just after the oceans would have condensed on Earth, where the pool would be likely to contain a random set of molecules with no particular non-random chemical organization. As I will show, starting from this initial state, the chemical network in the model described above evolves inevitably into a highly non-random, autocatalytic network (Jain and Krishna, 1998, 1999). The mechanisms that cause this growth might throw light on the above puzzle.

1.10 Catastrophes and recoveries in evolving networks

The model I will analyze also exhibits sudden catastrophes – mass extinctions where the relative populations of many species fall to zero in a short time – which are followed by slow recoveries. The asymmetry between catastrophe and recovery times, and fat tails in the size distribution of catastrophes in the model (Jain and Krishna, 2002a) are also observed in catastrophes and recoveries seen in the fossil record (Newman and Palmer, 1999) and in financial markets (Bouchaud, 2001; Johansen and Sornette, 2001). The mechanisms that cause such mass extinctions are a matter of much debate (Maynard-Smith, 1989; Glen, 1994). The model of Bak and Sneppen (1993) is an attempt to explain the frequency distribution of extinction events of different sizes using the mechanism of self-organized criticality. The model I will study is similar in some ways to the Bak-Sneppen model, with the addition of another dynamical variable – the network structure of the system. The advantage of explicitly modeling the network structure is that the mechanisms causing the catastrophes and their dependence on the network structure can be analyzed in detail.

I will show that, in the model, the largest extinctions are caused mainly by three mechanisms (Jain and Krishna, 2002b). One of the mechanisms involves the removal of specific species. This is reminiscent of the notion of ‘keystone species’ that was discussed in section 1.6. Thus, in this model, one can give a graph-theoretic definition of keystone species and explain why their removal causes mass extinctions (Jain and Krishna, 2002b).

1.10.1 Innovations

Apart from the removal of species, it is interesting that ‘innovations’ – the creation of new structures in the network – can also cause catastrophes. In the context of the model it is possible to create a graph-theoretic definition for the term ‘innovation’ (Jain and Krishna, 2002b, 2003b). This definition allows me to construct a hierarchy of innovations and correlate the graph-theoretic structure of an innovation to its short and long term effects on the evolution of the network (Jain and Krishna, 2003a,b).

1.11 A map of subsequent chapters

Chapters 2–4 describe different segments of the basic model, that are put together in chapter 5, and introduce various results from graph theory that will be useful for analyzing the model. The later chapters analyze the diverse phenomena observed in the model using the results from the previous chapters. In more detail:

Chapter 2 introduces certain elements of graph theory. I set out the notation that will be used and give definitions of directed graphs, degree of a node, paths, cycles and connected components of a graph. I introduce the notions of ‘dependency’ of a node, and ‘interdependency’ of a graph. I define the Perron-Frobenius eigenvalue and eigenvectors of a graph and describe some of their properties. Random graphs are briefly discussed at the end of the chapter.

Chapter 3 introduces the concept of an ‘autocatalytic set’. I describe the relation between algebraic properties of a graph, such as the Perron-Frobenius eigenvalue and eigenvectors, and topological properties, such as the presence or absence of autocatalytic sets in a graph. I then present the eigenvector profile theorem which, for any graph, specifies the ‘profile’ (which components are zero and which non-zero) of all possible Perron-Frobenius eigenvectors of the graph. The notion of a core and periphery of a Perron-Frobenius eigenvector is introduced.

Chapter 4 presents a dynamical system whose variables ‘live’ on the nodes of the graph. Their dynamics is described by a set of coupled differential equations, where the couplings are specified by the graph. The equations are derived from an idealized version of the chemical rate equations that would describe the dynamics of catalytic molecules in a well-stirred chemical reactor. I show that the attractors are fixed points and for generic initial conditions are Perron-Frobenius eigenvectors of the graph. I present the attractor profile theorem which identifies the subset of Perron-Frobenius eigenvectors that are attractors of the system for a given graph. The ‘core’ and ‘periphery’ of a graph are defined and the notion of a ‘keystone node’ is introduced.

Chapter 5 introduces a model of an evolving graph along the lines of section 1.7. The model uses the dynamical system discussed in chapter 4 for step 1 of the dynamics. Some specific rules are chosen for steps 2 and 3 that aim to capture the way storms, floods or tides would remove molecular species from, and add new molecular species to, a pool on the prebiotic Earth. I display the evolution of various quantities – the total number of links in the graph, the number of nodes with non-zero relative population in the attractor, the Perron-Frobenius eigenvalue, and the interdependency of the graph – as a function of time for some example runs of the model. I also exhibit snapshots of the graph at various times for one run. Three ‘phases’ of behaviour are observed in these runs which are dubbed the ‘random’, ‘growth’ and ‘organized’ phases.

Chapter 6 discusses the random and growth phases. Autocatalytic sets are shown to play an important role. I argue that no graph structure is stable for very long during the random phase, and that this is because there is no ACS in the graph. I show that the chance formation of an ACS triggers the growth phase, in which the number of links of the graph grow exponentially as the ACS expands by accreting more and more nodes to itself. This continues until the entire graph is an ACS at which point the organized phase starts. The timescales of appearance and growth of the ACS are analytically estimated. I show that the final fully autocatalytic graph is a highly non-random graph. The degree and dependency distributions for the fully autocatalytic graphs produced in the runs are discussed.

Chapter 7 discusses the sudden extinctions of large numbers of molecular species observed occasionally in the organized phase. I show that the largest extinction events are 'core-shifts', a complete change of the core of the graph. The notion of an 'innovation' is introduced. I show that core-shifts can occur due to the removal of a keystone species from the graph, or due to a particular type of innovation (the addition of a species which creates a new 'self-sustaining' structure in the graph), or a specific combination of both. The timescales of these large extinction events, as well as the recovery of the system afterward, are discussed. The structure of the graphs just before each large extinction, in particular their degree and dependency distributions, are analyzed.

Chapter 8 discusses the robustness of the formation and growth of autocatalytic sets to changes in the model rules. I list various simplifications in the model rules that depart from realism but make the system analytically tractable. Variants of the model that relax these simplifications are presented and are shown to exhibit the formation and growth of autocatalytic sets.

Chapter 9 summarizes the interesting features of the model and its variants, and discusses the limitations and possible extensions of the model.

Appendix A contains detailed proofs of all propositions made in the thesis, including the eigenvector, and attractor, profile theorems.

Appendix B describes two computer programs that use different methods to simulate the model and its variants. The source code of the programs are provided in the attached CD.

Appendix C describes the contents of the attached CD.

Chapter 2

Definitions and Terminology

2.1 Directed graphs and adjacency matrices

Definition 2.1: Directed graph.

A *directed graph* $G = G(S, L)$ is defined by a set S of 'nodes' and a set L of 'links', where each link is an ordered pair of nodes (Harary, 1969; Robinson and Foulds, 1980).

The set of nodes can be conveniently labeled by integers, $S = \{1, 2, \dots, s\}$ for a directed graph of s nodes. Henceforth I will use the term 'graph' to refer to a labeled, directed graph.

An example of a graph is given in Figure 2.1a where each node is represented by a small labeled circle, and a link (j, i) is represented by an arrow pointing from node j to node i . A graph with s nodes is completely specified by an $s \times s$ matrix, $C = (c_{ij})$, called the 'adjacency matrix' of the graph, and vice versa.

Definition 2.2: Adjacency matrix.

The *adjacency matrix* of a graph $G = G(S, L)$ with s nodes is an $s \times s$ matrix, denoted $C = (c_{ij})$, where $c_{ij} = 1$ if L contains a directed link (j, i) (arrow pointing from node j to node i), and $c_{ij} = 0$ otherwise.

This convention differs from the usual one (Harary, 1969; Robinson and Foulds, 1980; Bollobás, 1998) where $c_{ij} = 1$ if and only if there is a link from node i to node j ; the transpose of the adjacency matrix defined above. This convention has been chosen because it is more convenient in the context of the dynamical system to be discussed in chapter 4. Figure 2.1b shows the adjacency matrix corresponding to the graph in Figure 2.1a. I will use the terms 'graph' and 'adjacency matrix' interchangeably: the phrase 'a graph with adjacency matrix C ' will often be abbreviated to 'a graph C '.

Undirected graphs are special cases of directed graphs whose adjacency matrices are symmetric (Harary, 1969; Robinson and Foulds, 1980). A single (undirected) link of an undirected graph between, say, nodes j and i , can be viewed as two directed links of a directed graph, one from j to i and the other from i to j . See Bollobás (1998) for many results concerning undirected graphs.

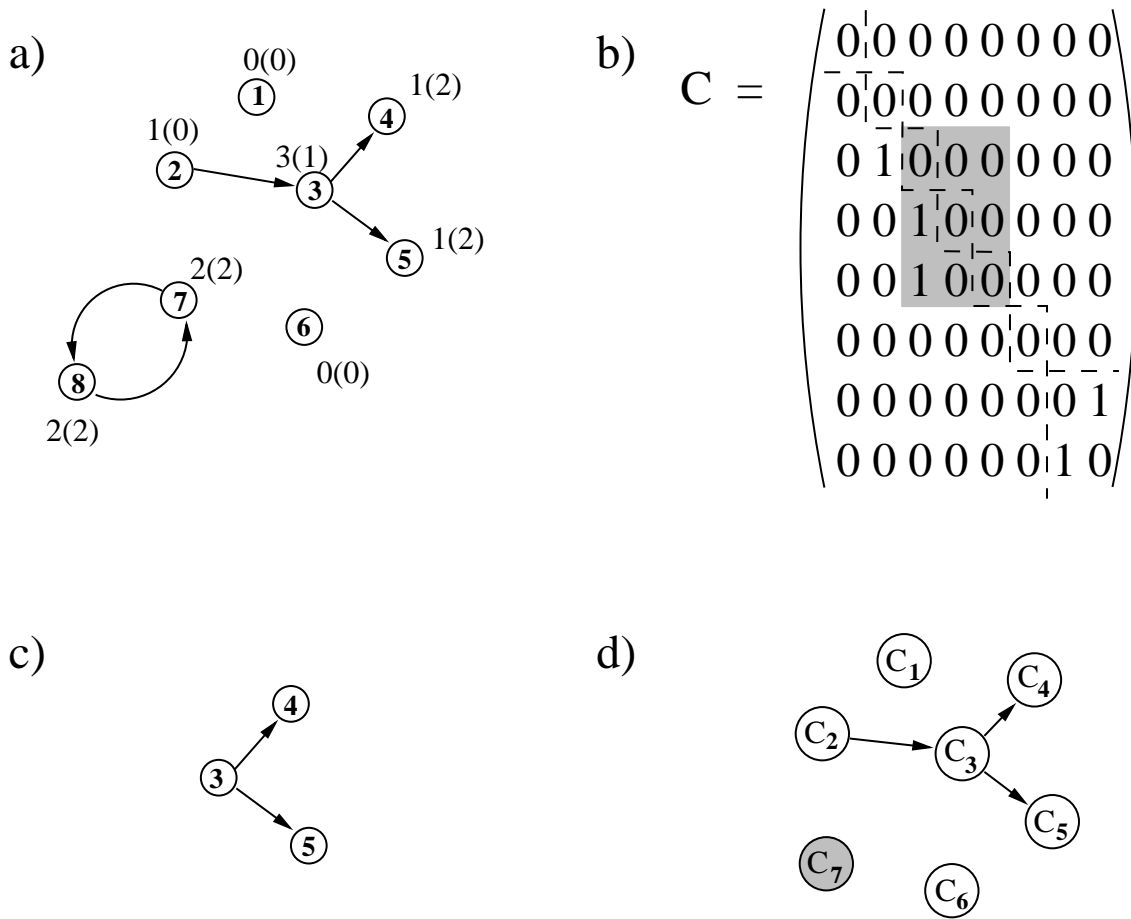


Figure 2.1: **a.** A directed graph with 8 nodes. The unbracketed number adjacent to each node is the degree of that node, and the bracketed number is the dependency. **b.** The adjacency matrix of the graph in (a). **c.** A subgraph of the graph in (a) induced by $S' = \{3, 4, 5\}$. The adjacency matrix of the subgraph is the shaded portion of the matrix in (b). **d.** The condensation of the graph in (a). The dashed lines in (b) demarcate the portions that correspond to the strong components C_α . The only basic subgraph, C_7 , is shaded.

Definition 2.3: Subgraph.

A graph $G' = G'(S', L')$ is called a *subgraph* of $G(S, L)$ if $S' \subset S$ and $L' \subset L$ (Harary, 1969; Bollobás, 1998).

Definition 2.4: Induced subgraph.

A graph $G' = G'(S', L')$ is called an *induced subgraph* of $G(S, L)$, or the *subgraph of $G(S, L)$ induced by S'* , if $S' \subset S$ and L' contains all (and only) those links in L with both endpoints in S' (Harary, 1969; Bollobás, 1998).

The graph in Figure 2.1c is thus an induced subgraph of the graph in Figure 2.1a (induced by $S' = \{3, 4, 5\}$). For a subgraph it is often more convenient to label the nodes not by integers starting from 1, but by the same labels the corresponding nodes had in the parent graph. The adjacency matrix of an induced subgraph can be obtained by deleting all the rows and columns from the full adjacency matrix that correspond to the nodes outside the subgraph. The highlighted portion of the matrix in Figure 2.1b is the adjacency matrix of the induced subgraph in Figure 2.1c.

2.2 Degrees and dependency

2.2.1 Degree of a node and degree distribution of a graph

Definition 2.5: Degree, in-degree and out-degree.

The *degree*, or *total degree*, of a node is the total number of incoming plus outgoing links from that node, i.e., the degree of node i is $\sum_{j=1}^s (c_{ji} + c_{ji})$.

The *in-degree* of a node is the total number of incoming links to that node, i.e., the in-degree of node i is $\sum_{j=1}^s c_{ji}$.

The *out-degree* of a node is the total number of outgoing links from that node, i.e., the out-degree of node i is $\sum_{j=1}^s c_{ji}$ (Harary, 1969; Bollobás, 1998).

The unbracketed numbers adjacent to each node in Figure 2.1a show the degree of that node.

Definition 2.6: Degree distribution.

The *degree distribution* of a graph, denoted $P(k)$, is the fraction of nodes with degree k .

The *out-degree distribution*, $P_{out}(k)$, and the *in-degree distribution*, $P_{in}(k)$, are similarly defined (Harary, 1969; Bollobás, 1998).

2.2.2 Dependency and interdependency

Definition 2.7: Dependency.

The *dependency*, denoted d_i , of a node i is the total number of links in all paths that terminate at that node, each link counted only once (Jain and Krishna, 1999).

Definition 2.8: Dependency distribution.

The *dependency distribution* of a graph, denoted $D(d)$, is the fraction of nodes with dependency d .

Definition 2.9: Interdependency.

The *interdependency* of a graph is defined to be the average dependency:

$$\bar{d} \equiv (1/s) \sum_{i=1}^s d_i = \sum_{d=0}^{\infty} d \times D(d)$$

(Jain and Krishna, 1999).

The bracketed numbers adjacent to each node in Figure 2.1a show the dependency of that node. The interdependency of the graph in Figure 2.1a is 9/8.

Because d_i counts how many links ultimately 'feed into' the node i , it is a measure of how 'dependent' node i is on other nodes. Thus \bar{d} is a measure of how interdependent are the nodes in the graph. While the degree of a node is a 'local' measure as it depends only on the immediate connections of a node, the dependency is more 'non-local' in character because links far away from the node contribute to it.

2.3 Walks, paths and cycles

Definition 2.10: Walk, closed walk.

A *walk* of length n (from node i_1 to node i_{n+1}) is an alternating sequence of nodes and links $i_1 l_1 i_2 l_2 \dots i_n l_n i_{n+1}$ such that link l_1 points from node i_1 to node i_2 (i.e. $l_1 = (i_1, i_2)$), l_2 points from i_2 to i_3 and so on. If the first and last nodes i_1 and i_{n+1} of a walk are the same, it will be referred to as a *closed walk*

(Harary, 1969; Robinson and Foulds, 1980; Bollobás, 1998).

The existence of even one closed walk in the graph implies the existence of an infinite number of distinct walks in the graph. In the graph of Figure 2.1a, there are an infinite number of walks from node 7 to node 8 (e.g., $7 \rightarrow 8$, $7 \rightarrow 8 \rightarrow 7 \rightarrow 8$, ...) but no walk from node 7 to node 2. An undirected graph trivially has closed walks if it has any undirected links at all.

If C is the adjacency matrix of a graph then it is easy to see that $(C^n)_{ij}$ equals the number of distinct walks of length n from node j to node i . E.g., $(C^2)_{ij} = \sum_{k=1}^s c_{ik} c_{kj}$; each term in the sum is unity if and only if there exists a link from j to k and from k to i , hence the sum counts the number of walks from j to i of length 2.

Definition 2.11: Path.

A walk with all nodes distinct is a *path*

(Harary, 1969; Robinson and Foulds, 1980; Bollobás, 1998).

In a directed graph C , I will say node j 'has access to' node i , or node i 'has access from' node j , if there is a path from node j to node i , i.e., for some $n \geq 0$ $(C^n)_{ij} > 0$ (Rothblum, 1975). I refer

to a node i as being 'downstream' from a node j if j has access to i , but i does not have access to j . Similarly i is 'upstream' from j if i has access to j , but j does not have access to i . Thus in Figure 2.1a, node 5 is downstream from node 2, or equivalently node 2 is upstream from node 5 because node 2 has access to 5 but not vice versa. Node 2 is neither upstream nor downstream from node 7 as neither have access to the other. Node 8 is also neither upstream nor downstream from 7 because each has access to the other along some directed path.

Definition 2.12: Cycle, n -cycle.

An n -cycle is a closed walk with n links, and all intermediate nodes distinct (Harary, 1969; Robinson and Foulds, 1980; Bollobás, 1998).

I will also use the term 'cycle' to refer to the subgraph consisting of the nodes and links that form the cycle. Thus any subgraph with $n \geq 1$ nodes that contains exactly n links and also contains a closed walk that covers all n nodes is an n -cycle. E.g., the subgraph induced by nodes 7 and 8 in Figure 2.1a is a 2-cycle. Clearly any graph that has a closed walk contains a cycle.

2.4 Connected components of a graph

Given a directed graph C , its 'associated undirected graph' (or 'symmetrized version') $C^{(s)}$ can be obtained by adding additional links as follows: for every link (j, i) in L , add another link (i, j) if the latter is not already in L .

Definition 2.13: Strongly, weakly and unilaterally connected nodes.

Two nodes i and j of a directed graph C will be said to be

- (i) *strongly connected* if i has access to j and j also has access to i ,
- (ii) *unilaterally connected* if either i has access to j , or j has access to i ,
- (iii) *weakly connected* if there exists a path between them in the associated undirected graph $C^{(s)}$,
- (iv) *disconnected* if none of the above is true (Harary, 1969; Robinson and Foulds, 1980).

It is evident that any strongly connected nodes are also unilaterally connected, and any unilaterally connected nodes are weakly connected, but the converse need not be true. A graph will be termed strongly, unilaterally, or weakly connected if *all* pairs of its nodes are, respectively, strongly, unilaterally or weakly connected. Any directed graph can be decomposed into strongly-, unilaterally- and weakly-connected components which are subgraphs induced by maximal sets of strongly, unilaterally and weakly connected nodes (Harary, 1969; Robinson and Foulds, 1980) (e.g., the graph of Figure 2.1a has five weakly connected components induced, respectively, by the nodes $\{1\}$, $\{2, 3, 4, 5\}$, $\{6\}$ and $\{7, 8\}$). By convention a single node is considered strongly-connected to itself even if there is no self-link (Harary, 1969; Robinson and Foulds, 1980). Therefore, if a graph contains a single node with no links the single node is also considered a (trivial) strong component of the graph.

2.5 Partitioning a graph into its strong components

The nodes of any graph can be grouped into a unique set of strong components as follows:

1. Pick any node, say i . Find all the nodes having access from i . Denote this set by S_1 ; it may include i itself. Similarly find all the nodes having access to i . Denote this set by S_2 . Denote the subgraph induced by the set of nodes $\{i\} \cup (S_1 \cap S_2)$ as C_1 . C_1 is one strongly connected component of the graph.
2. Pick another node that is not in C_1 and repeat the procedure with that node to get another subgraph, C_2 . The sets of nodes comprising the two subgraphs will be disjoint.
3. Repeat this process until all nodes have been placed in some C_α , $\alpha = 1, 2, \dots, M$. Each C_α is a strong component of the graph.

Irrespective of which nodes are picked and in which order, this procedure will produce for any graph a unique (upto labeling of the C_α) set of disjoint subgraphs, each of which is strongly connected, encompassing all the nodes of the graph (Harary, 1969; Robinson and Foulds, 1980). The graph in Figure 2.1a will decompose into 7 such subgraphs (comprising nodes $\{1\}$, $\{2\}$, $\{3\}$, $\{4\}$, $\{5\}$, $\{6\}$ and $\{7, 8\}$).

One says there is a path from a strong component C_1 to another strong component C_2 if there is a path in C from any node of C_1 to any node of C_2 . The terms 'access', 'downstream' and 'upstream' can thus be used unambiguously for the C_α .

2.6 Condensation of a graph

Definition 2.14: Condensation of a graph.

Determine all the strong components C_1, C_2, \dots, C_M of the graph as described above. Construct a new graph of M nodes, one node for each C_α , $\alpha = 1, \dots, M$. The new graph has a directed link from C_β to C_α if, in the original graph, any node of C_β has a link to any node of C_α . This new graph is called the *condensation of the graph C* (Harary, 1969; Robinson and Foulds, 1980).

Figure 2.1d illustrates the condensation of Figure 2.1a. Clearly the condensed graph cannot have any closed walks. For if it were to have a closed walk then the C_α subgraphs comprising the closed walk would together have formed a larger strong component in the first place. Therefore one can renumber the C_α such that if $\alpha > \beta$, C_β is never downstream from C_α . Now one can renumber the nodes of the original graph such that nodes belonging to a given C_α are labeled by contiguous node numbers, and whenever a pair of nodes i and j belong to different subgraphs C_α and C_β respectively, then $\alpha > \beta$ implies $i > j$. Such a renumbering is in general not unique, but with any such renumbering the adjacency matrix takes the following canonical form:

$$C = \begin{pmatrix} C_1 & & & 0 \\ & C_2 & & \\ & & \ddots & \\ & & & C_M \\ R & & & \end{pmatrix},$$

where 0 indicates that the upper block triangular part of the matrix contains only zeroes while the lower block triangular part, R , is not equal to zero in general. The matrix in Figure 2.1b is already in this canonical form; the dashed lines demarcate the portions that correspond to the C_α .

2.7 Irreducible graphs and matrices

Definition 2.15: Irreducible graph.

A graph is termed *irreducible* if each node in the graph has access to every other node (Harary, 1969; Seneta, 1973).

The simplest irreducible subgraph is a 1-cycle. In Figure 2.1a the subgraph induced by nodes 7 and 8 is irreducible, but the subgraph induced by nodes 2, 3, 4, and 5 is not irreducible as there is, for example, no path from node 5 to node 2.

Definition 2.16: Irreducible matrix.

A matrix C is *irreducible* if for every ordered pair of nodes i and j there exists a positive integer k such that $(C^k)_{ij} > 0$ (Seneta, 1973).

Thus, if a graph is irreducible then its adjacency matrix is also irreducible, and vice versa. Irreducible graphs are, by definition, strongly connected graphs. In fact all strongly connected graphs are irreducible, except the graph consisting of a single node with no self-link which is strongly connected (by definition) but not irreducible.

2.8 Perron-Frobenius eigenvectors (PFEs)

Definition 2.17: Eigenvector, eigenvalue.

A column vector $\mathbf{x} = (x_1, x_2, \dots, x_s)^T$ is said to be a *right eigenvector* of an $s \times s$ matrix C with an eigenvalue λ if for each i , $\sum_{j=1}^s c_{ij}x_j = \lambda x_i$. The *eigenvalues* of a matrix C are roots of the characteristic equation of the matrix: $|C - \lambda I| = 0$, where I is the identity matrix of the same dimensionality as C and $|A|$ denotes the determinant of the matrix A (Seneta, 1973).

A 'left eigenvector' is similarly defined to be a row vector $\mathbf{x} = (x_1, x_2, \dots, x_s)$ such that for each i , $\sum_{j=1}^s c_{ji}x_j = \lambda x_i$; the left eigenvectors of C are simply the transpose of the right eigenvectors of C^T , the transpose of C . In this thesis I will only use right eigenvectors and will therefore refer to them simply as eigenvectors. Note that the set of eigenvalues corresponding to all right eigenvectors is identical to the set of eigenvalues corresponding to the left eigenvectors. In general a matrix will have complex eigenvalues and eigenvectors, but an adjacency matrix of a graph has special properties, because it is a 'non-negative' matrix, i.e., it has no negative entries.

2.8.1 The Perron-Frobenius theorem

The Perron-Frobenius theorem for irreducible non-negative matrices states (Seneta, 1973):

Suppose T is an $s \times s$ non-negative irreducible matrix. Then there exists an eigenvalue r such that:

- a) r is real, > 0 ;
- b) with r can be associated strictly positive left and right eigenvectors;
- c) $r \geq |\lambda|$ for any eigenvalue $\lambda \neq r$;
- d) the eigenvectors associated with r are unique to constant multiples;
- e) Let B be any $s \times s$ non-negative matrix. If $0 \leq B \leq T$ and β is an eigenvalue of B , then $|\beta| \leq r$. Moreover, $|\beta| = r$ implies $B = T$;
- f) r is a simple root of the characteristic equation of T .

If the matrix is not irreducible a weaker form of the above theorem holds. The Perron-Frobenius theorem for a general non-negative matrix states (Seneta, 1973):

Suppose T is an $s \times s$ non-negative matrix. Then there exists an eigenvalue r such that:

- a') r is real, ≥ 0 ;
- b') with r can be associated non-negative left and right eigenvectors;
- c') $r \geq |\lambda|$ for any eigenvalue $\lambda \neq r$;
- e') Let B be any $s \times s$ non-negative matrix. If $0 \leq B \leq T$ and β is an eigenvalue of B , then $|\beta| \leq r$.

Definition 2.18: Perron-Frobenius eigenvalue.

For any graph C , the eigenvalue of C that is real and larger than or equal to all other eigenvalues in magnitude will be called the *Perron-Frobenius eigenvalue* of the graph and denoted by $\lambda_1(C)$. The Perron-Frobenius theorem guarantees the existence of such an eigenvalue.

Definition 2.19: Perron-Frobenius eigenvector (PFE).

For any graph C , each eigenvector corresponding to $\lambda_1(C)$ consisting only of real and non-negative components will be referred to as *Perron-Frobenius eigenvector (PFE)*. The Perron-Frobenius theorem guarantees the existence of at least one such eigenvector.

The Perron-Frobenius eigenvalue of the graph in Figure 2.1a is 1 and $\mathbf{x} = (0, 0, 0, 0, 0, 0, 1, 1)^T$ is a Perron-Frobenius eigenvector.

The presence or absence of closed walks in a graph can be determined from the Perron-Frobenius eigenvalue of its adjacency matrix:

Proposition 2.1: If a graph, C ,

- (i) has no closed walk then $\lambda_1(C) = 0$,
- (ii) has a closed walk then $\lambda_1(C) \geq 1$.

The proof of this and all subsequent propositions can be found in appendix A.

Note that λ_1 cannot take values between zero and one because of the discreteness of the entries of C , which are either zero or unity.

2.8.2 Basic subgraphs

In section 2.6 it was shown that the adjacency matrix of any graph can always be written in the following canonical form by an appropriate renumbering of the nodes:

$$C = \begin{pmatrix} C_1 & & & & 0 \\ & C_2 & & & \\ & & \ddots & & \\ & & & \ddots & \\ R & & & & C_M \end{pmatrix}.$$

From the above form of C it follows that

$$|C - \lambda I| = |C_1 - \lambda I| \times |C_2 - \lambda I| \times \dots \times |C_M - \lambda I|.$$

Therefore the set of eigenvalues of C is the union of the sets of eigenvalues of C_1, \dots, C_M , which implies that $\lambda_1(C) = \max_{\alpha} \{\lambda_1(C_{\alpha})\}$. Thus, if a given graph C has a Perron-Frobenius eigenvalue λ_1 then it contains at least one strong component with Perron-Frobenius eigenvalue λ_1 .

Definition 2.20: Basic subgraph.

Each strong components of C with Perron-Frobenius eigenvalue equal to $\lambda_1(C)$ is referred to as a *basic subgraph* (Rothblum, 1975).

The shaded node in Figure 2.1d corresponds to the only basic subgraph of Figure 2.1a.

Proposition 2.2: If all the basic subgraphs of a graph C are cycles then $\lambda_1(C) = 1$, and vice versa.

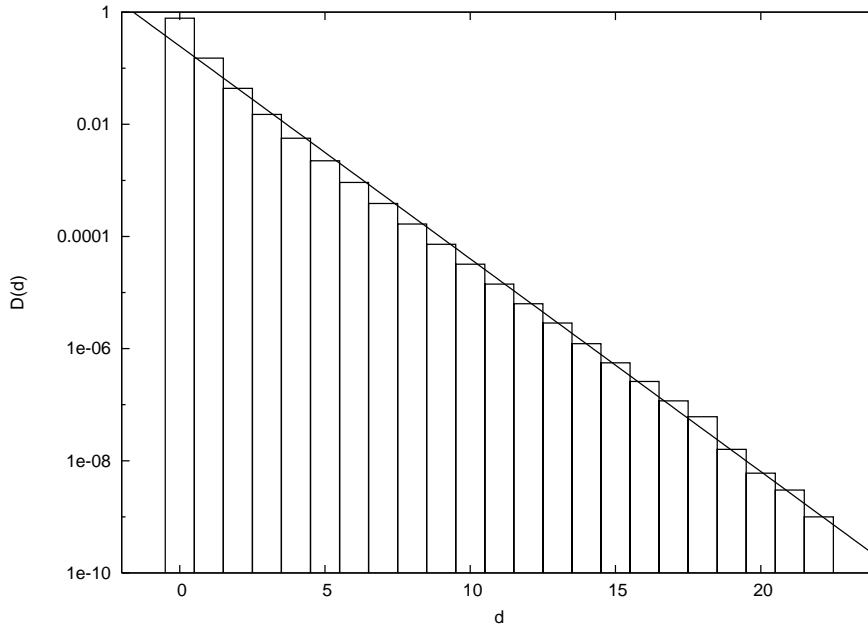


Figure 2.2: Dependency distribution of nodes of 10^7 random graphs from the ensemble G_s^p with $s = 100, p = 0.0025$. The average dependency is 0.33 and the standard deviation of dependency values is 0.76. The straight line plots the function $A \exp(-\alpha d)$ with $A = 0.25, \alpha = -0.87$. This is the best straight line fit to the dependency distribution on a semi-log plot.

2.9 Random graphs

A random graph is an ensemble of graphs with each member of the ensemble having an associated probability (introduced by Erdős and Rényi, 1959). Two ensembles have been extensively studied. One, denoted G_s^l , is the ensemble of graphs with s vertices and l links (and no self-links) with a uniform associated probability. The second is the ensemble of graphs, denoted G_s^p , having s vertices, with each possible link (except self-links) present with probability p ; in other words the ensemble of all graphs with the probability associated with a graph being $p^l(1-p)^{s(s-1)-l}$ if it has l links. These two ensembles have the same properties in the $s \rightarrow \infty$ limit if $l = ps(s-1)$ (Bollobás, 1998, 2001). For the random graph G_s^p the average number of links is $ps(s-1)$, while the (total) degree distribution is binomial: $P(k) = \binom{2s-2}{k} p^k (1-p)^{2s-2-k}$ (Bollobás, 1998, 2001). Figure 2.2 shows the dependency distribution of nodes of 10^7 graphs picked from the ensemble G_s^p with $s = 100, p = 0.0025$ (the program `rndgraph.cpp` that is included in the attached CD, see appendix C, was used to generate the random graphs). The dependency averaged over all nodes was 0.33, and the standard deviation of dependency values was 0.76. The distribution appears to decline exponentially as a function of dependency value, but much slower than would be expected for a Poisson distribution with the same mean. See (Bollobás, 1998, 2001) for further results concerning random graphs.

Chapter 3

Autocatalytic Sets

This chapter discusses the notion of an ‘autocatalytic set’, which will play an important role in the dynamics of the model studied in this thesis. After first providing a graph-theoretic definition of an autocatalytic set, I discuss its relationship with the Perron-Frobenius eigenvectors of a graph. The rest of the chapter analyzes the structure of PFEs of different graphs, both ones which contains autocatalytic sets and ones which do not. The results derived here will prove useful in the analysis of the dynamical system discussed in chapter 4.

3.1 Autocatalytic sets (ACSs)

Definition 3.1: Autocatalytic set (ACS).

An *autocatalytic set* is a graph, each of whose nodes has at least one incoming link from a node belonging to the same graph (Jain and Krishna, 1998).

The concept of an ACS was introduced in the context of a set of catalytically interacting molecules where it was defined to be a set of molecular species that contains, within itself, a catalyst for each of its member species (Eigen, 1971; Kauffman, 1971; Rössler, 1971). Such a set of molecular species can collectively self-replicate under certain circumstances even if none of its component molecular species can individually self-replicate. This definition matches the one above if you imagine a node in a directed graph to represent a molecular species and a link from j to i to signify that j is a catalyst for i .

Figure 3.1 shows various ACSs. The simplest is a 1-cycle; Figure 3.1a. Figures 3.1a and 3.1b are graphs that are irreducible as well as cycles, 3.1c is an ACS that is not an irreducible graph and hence not a cycle, while 3.1d and 3.1e are irreducible graphs that are not cycles.

Proposition 3.1: (i) All cycles are irreducible graphs and all irreducible graphs are ACSs.

(ii) Not all ACSs are irreducible graphs and not all irreducible graphs are cycles.

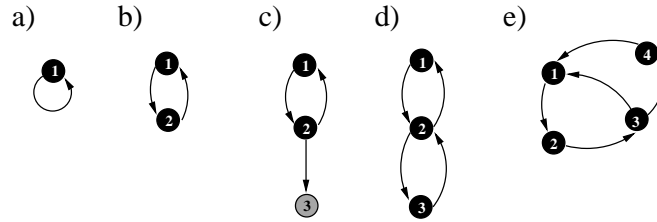


Figure 3.1: Examples of autocatalytic sets (ACSs). **a.** A 1-cycle, the simplest ACS. **b.** A 2-cycle. **c.** An ACS that is not an irreducible graph. **d,e** Examples of ACSs that are irreducible graphs but not cycles.

3.2 Relationship between Perron-Frobenius eigenvectors and autocatalytic sets

The ACS is a useful graph-theoretic construct in part because of its connection with the PFE. Firstly, the Perron-Frobenius eigenvalue of a graph is an indicator of the existence of an ACS in the graph (Jain and Krishna, 1998, 1999):

- Proposition 3.2:** (i) An ACS must contain a closed walk. Consequently,
- (ii) If a graph C has no ACS then $\lambda_1(C) = 0$.
 - (iii) If a graph C has an ACS then $\lambda_1(C) \geq 1$.

Let \mathbf{x} be a PFE of a graph. Consider the set of all nodes i for which x_i is non-zero. I will call the subgraph induced by these nodes the ‘subgraph of the PFE \mathbf{x} ’. For example consider the graph in Figure 3.2a. For this graph $\lambda_1 = 1$. Figure 3.2b shows a PFE of the graph and how it satisfies the eigenvalue equation. For this PFE, nodes 1, 5 and 6 have $x_i = 0$. Removing these nodes produces the PFE subgraph shown in Figure 3.2c. If all the components of the PFE are non-zero then the subgraph of the PFE is the entire graph. One can show that (Jain and Krishna, 1998, 1999):

Proposition 3.3: If $\lambda_1(C) \geq 1$, then the subgraph of any PFE of C is an ACS.

For the PFE of Figure 3.2b this is immediately verified by inspection. Note that this result relates an algebraic property of a graph, its PFE, to a topological structure, an ACS. Further, this result is not true if we considered irreducible graphs instead of ACSs.

Proposition 3.4: Let \mathbf{x} be a PFE of a graph C , and let C' denote the adjacency matrix of the subgraph of \mathbf{x} . Let $\lambda_1(C')$ denote the Perron-Frobenius eigenvalue of C' . Then $\lambda_1(C') = \lambda_1(C)$ and C' must contain at least one of the basic subgraphs of C .

Figure 3.2 illustrates this point. The adjacency matrix of the PFE subgraph, C' , is obtained by removing rows 1, 5, 6 and columns 1, 5, 6 from the original matrix. Figure 3.2d illustrates that

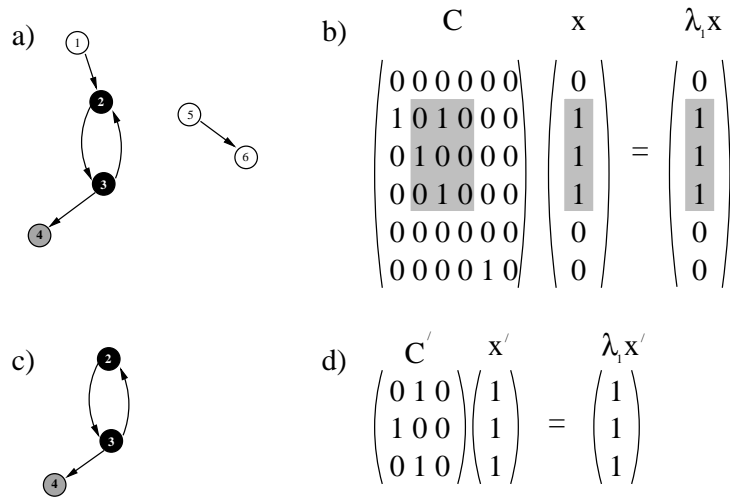


Figure 3.2: **a.** A graph with 6 nodes. **b.** \mathbf{x} is an eigenvector of its adjacency matrix C with eigenvalue $\lambda_1 = 1$, which is the Perron-Frobenius eigenvalue of the graph. The non-zero components of \mathbf{x} and the corresponding rows and columns of C are shaded. **c.** The subgraph of the PFE \mathbf{x} . The subgraph is an ACS and contains one of the basic subgraphs of the graph in (a). **d.** The vector \mathbf{x}' constructed by removing the zero components of \mathbf{x} is an eigenvector of the adjacency matrix, C' , of the PFE subgraph. Its corresponding eigenvalue is unity, which is also the Perron-Frobenius eigenvalue of the PFE subgraph.

the vector constructed by removing the zero components of the PFE is an eigenvector of C' with eigenvalue 1. C' contains one basic subgraph of C – the one induced by the nodes 2 and 3.

Definition 3.2: Simple PFE.

If the subgraph of a PFE contains only one basic subgraph then the PFE is termed a *simple PFE* (Jain and Krishna, 2003a).

The PFE in Figure 3.2 is simple.

3.3 Eigenvector profile theorem

I now present a series of propositions that describe some aspects of the ‘profile’ of possible PFEs of a graph, i.e., which components of the PFE are zero and which are non-zero. These propositions lead toward the eigenvector profile theorem which provides an algorithm for finding the profile of all the simple PFEs of a graph, and consequently the profile of the possible non-simple PFEs also. This theorem is completely general, applying to any given graph. After I had generated the proofs for the theorem and the propositions it depends upon, I found that these results had already been derived by Rothblum (1975) as part of a more general theorem concerning the profile of generalized eigenvectors of a non-negative matrix. The proofs provided in appendix A (Krishna

and Jain, forthcoming) are, however, different from his; they make no use of the principle of mathematical induction, which Rothblum uses extensively.

For convenience I will often abbreviate statements like ‘there exists a PFE in which the components corresponding to the nodes in subgraph C_1 are non-zero/zero’ to ‘there exists a PFE in which the nodes in subgraph C_1 are non-zero/zero’.

Proposition 3.5: If a node is non-zero in a PFE then all nodes it has access to are non-zero in that PFE.

It follows that if any node of an irreducible subgraph is non-zero in a PFE then all the other nodes in that subgraph must be non-zero in that PFE. A situation where some nodes of an irreducible subgraph are non-zero and some are zero in the same PFE cannot happen.

Proposition 3.6: If a node is upstream from a basic subgraph then that node is zero in any PFE.

Proposition 3.7: If a node does not have access from a basic subgraph then it is zero in any PFE.

Propositions 3.6 and 3.7 describe which nodes will be zero in the PFEs, while proposition 3.4 and 3.5 describe which nodes will be non-zero – at least one of the basic subgraphs will be non-zero in every PFE along with all nodes it has access to. In other words the subgraph of any PFE consists of one or more of the basic subgraphs and those nodes that they have access to, i.e., the subgraph of any PFE is necessarily an ACS (recall proposition 3.3, this is an alternate proof of that proposition).

Propositions 3.4–3.7 can be used to prove the following theorem about the profile of PFEs of any graph:

Theorem 3.1: Eigenvector profile theorem

For any graph C , determine all the basic subgraphs of C . Denote them by D_1, \dots, D_K . Determine which of these does not have any other D_i downstream from it. Denote these by E_1, \dots, E_N . Then:

- (i) For each $i = 1, \dots, N$ there exists a unique (upto constant multiples) PFE in which the nodes of E_i and all nodes having access from them are non-zero and all other nodes are zero. It is evident that these PFEs are simple. Moreover these are the only simple PFEs of the graph C .
- (ii) Any PFE is a linear combination of these N simple PFEs.

3.4 Core and periphery of a simple PFE

Definition 3.3: Core and periphery of a simple PFE.

If C is the subgraph of a simple PFE, the basic subgraph contained in C will be called the *core* of the simple PFE (or equivalently, the ‘core of C ’), and denoted Q . The set of the remaining nodes and links of C that are not in its core will together be said to constitute the *periphery* of the simple PFE (Jain and Krishna, 2003a).

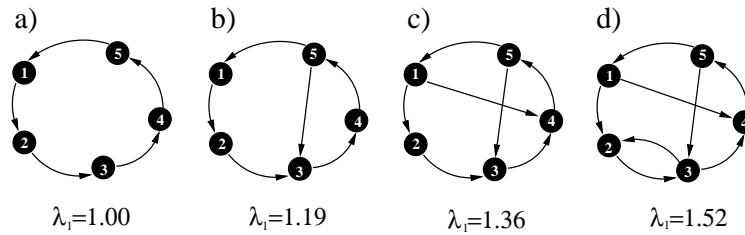


Figure 3.3: λ_1 is a measure of the multiplicity of internal pathways in the core of a simple PFE. Four irreducible graphs are shown. An irreducible graph always has a unique PFE that is simple and whose core is the entire graph. The Perron-Frobenius theorem ensures that adding a link to the core of a simple PFE necessarily increases its Perron-Frobenius eigenvalue λ_1 .

For example, for the PFE in Figure 3.2b the core is the 2-cycle comprising nodes 2 and 3. In Figure 3.2 the core nodes are black and the periphery nodes grey. Note that the periphery is not a subgraph because it contains links not just between periphery nodes but also from nodes outside the periphery (like the link from node 3 to 4 in Figure 3.2c).

It follows from the Perron-Frobenius theorem for irreducible graphs that $\lambda_1(Q)$ will necessarily increase if any link is added to the core. Similarly removing any link will decrease $\lambda_1(Q)$. Thus λ_1 measures the multiplicity of internal pathways in the core. Figure 3.3 illustrates this point.

The core and periphery can be shown to have the following topological property (Jain and Krishna, 2003a):

Proposition 3.8: Every node in the core of a simple PFE has access to every other node of the PFE subgraph. No periphery node has access to any core node.

Thus starting from the core one can reach the periphery but not vice versa.

3.5 Core and periphery of a non-simple PFE

Because any PFE of a graph can be written as a linear combination of the simple PFEs (which, upto constant multiples, are unique for any graph), the definitions of core and periphery can be readily extended to any PFE as follows:

Definition 3.4: Core and periphery of a (non-simple) PFE.

The *core* of a PFE, denoted Q , is the union of the cores of those simple PFEs whose linear combination forms the given PFE. The rest of the nodes and links of the PFE subgraph constitute its *periphery* (Jain and Krishna, 2003a).

It follows from the above discussion that $\lambda_1(Q) = \lambda_1(C)$. When the core is a union of disjoint cycles then $\lambda_1(Q) = 1$, and vice versa (recall proposition 2.2).

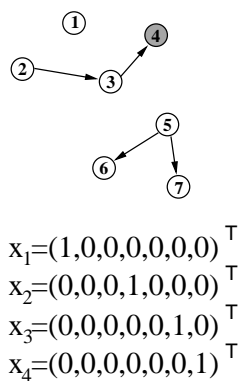


Figure 3.4: A graph that has no ACS. The graph has four simple PFEs (upto constant multiples).

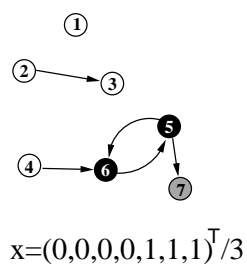


Figure 3.5: A graph that has an ACS, but only one basic subgraph, along with various non-ACS structures. The only simple PFE of the graph is also displayed.

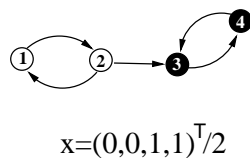


Figure 3.6: One 2-cycle downstream from another. Both 2-cycles are basic subgraphs. The graph has one simple PFE in which only the downstream cycle is non-zero.

3.6 The profile of PFEs when there is no ACS

If $\lambda_1(C) = 0$, the graph has no ACS, then the profile of PFEs is as follows: for every node that has no outgoing links, there is a PFE with that node non-zero and all other nodes zero. For example the graph in Figure 3.4 has four (upto constant multiples) simple PFEs that are displayed in the same figure. This follows from theorem 3.1 because for a graph with $\lambda_1 = 0$ each node is a basic subgraph. A general PFE is a linear combination of all such simple PFEs. Because there is no closed walk there is no core (or periphery) for any PFE of the graph. The core of all PFEs of such a graph may be defined to be the null set, $Q = \Phi$.

3.7 The profile of PFEs when there is an ACS but only one basic subgraph

Now consider a graph that has $\lambda_1 \geq 1$, i.e., it contains an ACS, but has only one basic subgraph. In addition to the ACS it could possibly have various non-ACS structures such as chains, trees and isolated nodes. An example is the graph in Figure 3.5. For such a graph theorem 3.1 says that there is only one simple PFE in which the nodes in the basic subgraph and all nodes having access from it are non-zero, while the other nodes are zero (displayed in Figure 3.5). In particular the nodes in all non-ACS structures are zero in the (unique) PFE of the graph because they are don't have access from the basic subgraph. The core nodes (nodes of the single basic subgraph) are black and the periphery nodes are grey in Figure 3.5. The white nodes are the nodes that are zero in the PFE of the graph.

3.8 The profile of PFEs when there is an ACS and many basic subgraphs

For any graph containing an ACS, i.e., one that has $\lambda_1 \geq 1$, there are possibly several simple PFEs as specified by theorem 3.1. However it follows from the theorem that in all the simple PFEs the nodes of non-ACS structures will be zero because they are not downstream from any basic subgraph.

While the nodes of non-ACS structures are guaranteed to be zero, it can also happen that the nodes of some basic subgraphs are zero in every PFE. Figure 3.6 illustrates such a case where the graph consists of one 2-cycle downstream from another. The Perron-Frobenius eigenvalue of this graph is $\lambda_1 = 1$, and each 2-cycle is a basic subgraph. From theorem 3.1 it follows that this graph has only one (simple) PFE (displayed in Figure 3.6) in which the upstream 2-cycle is zero.

Chapter 4

Population Dynamics

4.1 The population dynamics equation

In this chapter, I will analyze the attractors of the dynamical system described by the equation:

$$\dot{x}_i = \sum_{j=1}^s c_{ij}x_j - x_i \sum_{k,j=1}^s c_{kj}x_j, \quad (4.1)$$

where \mathbf{x} lies on the simplex $J = \{\mathbf{x} \equiv (x_1, x_2, \dots, x_s)^T \in \mathbf{R}^s | 0 \leq x_i \leq 1, \sum_{i=1}^s x_i = 1\}$ of normalized non-negative vectors in s dimensions.

As discussed in section 1.7, the set of variables x_i can be thought of as 'living' on the nodes of a graph whose adjacency matrix is $C = (c_{ij})$. The links of the graph represent the interactions between the variables x_i . It is useful to see how equation (4.1) arises in a chemical context.

Let $i \in \{1, \dots, s\}$ denote a chemical (or molecular) species in a well-stirred chemical reactor. Molecules can react with one another in various ways; I focus on only one aspect of their interactions: catalysis. The catalytic interactions can be described by a directed graph with s nodes. The nodes represent the s species and the existence of a link from node j to node i means that species j is a catalyst for the production of species i . In terms of the adjacency matrix, $C = (c_{ij})$ of this graph, c_{ij} is set to unity if j is a catalyst of i and is set to zero otherwise. The operational meaning of catalysis is as follows:

Each species i will have an associated non-negative population y_i in the reactor that changes with time. Let species j catalyze the ligation of reactants A and B to form the species i , $A+B \xrightarrow{j} i$. Assuming that the rate of this catalyzed reaction is given by the Michaelis-Menten theory of enzyme catalysis, $\dot{y}_i = V_{max}ab \frac{y_j}{K_M + y_j}$ (Gutfreund, 1995), where a, b are the reactant concentrations, and V_{max} and K_M are constants that characterize the reaction. If the Michaelis constant K_M is very large this can be approximated as $\dot{y}_i \propto y_j ab$. Combining the rates of the spontaneous and catalyzed reactions and also putting in a dilution flux ϕ , the rate of growth of species i is given by $\dot{y}_i = k(1 + \nu y_j)ab - \phi y_i$, where k is the rate constant for the spontaneous reaction, and ν is the

catalytic efficiency. Assuming the catalyzed reaction is much faster than the spontaneous reaction, and that the concentrations of the reactants are non-zero and fixed, the rate equation becomes $\dot{y}_i = Ky_j - \phi y_i$, where K is a constant. In general because species i can have multiple catalysts, $\dot{y}_i = \sum_{j=1}^s K_{ij}y_j - \phi y_i$, with $K_{ij} \sim c_{ij}$. I make the further idealization $K_{ij} = c_{ij}$ giving:

$$\dot{y}_i = \sum_{j=1}^s c_{ij}y_j - \phi y_i. \quad (4.2)$$

The relative population of species i is by definition $x_i \equiv y_i / \sum_{j=1}^s y_j$. As $0 \leq x_i \leq 1$, $\sum_{i=1}^s x_i = 1$, $\mathbf{x} \equiv (x_1, \dots, x_s)^T \in J$. Taking the time derivative of x_i and using (4.2) it is easy to see that \dot{x}_i is given by (4.1). Note that the ϕ term, present in (4.2), cancels out and is absent in (4.1).

Because we ultimately ignore the concentrations of the reactants we would get the same rate equations even if the reaction scheme were different, e.g., if only one reactant was required as in the reaction $A \xrightarrow{j} i$. Such dynamics might also be relevant in an economic context where the presence of one commodity increases the rate of production of another commodity.

Equation (4.1) has been used by Eigen et al. (1989) to describe the dynamics of the relative populations of self-replicating strings. Each node of C represents one string. Two strings are connected by an undirected link if mutations of one string can produce the other; the strength of the link being a decreasing function of the number of mutations required. Eigen et al. have determined the attractor of equation (4.1) for the specific form this interpretation imposes on C . Below, I analyze the attractors of equation (4.1) for an arbitrary graph C , with no restrictions placed on its structure.

4.2 Attractors of the population dynamics equation

An important motivation for the choice of the population dynamics (4.1) is its analytical tractability. The following properties of the attractor can be derived (Jain and Krishna, 2003a; Krishna and Jain, forthcoming):

Proposition 4.1: For any graph C ,

- (i) Every eigenvector of C that belongs to the simplex J is a fixed point of equation (4.1), and vice versa.
- (ii) Starting from any initial condition in the simplex J , the trajectory converges to some fixed point (generically denoted \mathbf{X}) in J .
- (iii) For generic initial conditions in J , \mathbf{X} is a Perron-Frobenius eigenvector (PFE) of C .
- (iv) If C has a unique (upto constant multiples) PFE, it is the unique stable attractor of equation (4.1).

(v) If C has more than one linearly independent PFE, then \mathbf{X} can depend upon the initial conditions. The set of allowed \mathbf{X} is a linear combination of a subset of the PFEs. The interior of this set in J may then be said to be the 'attractor' of (4.1), in the sense that for generic initial conditions all trajectories converge to a point in this set.

Statement (i) is easy to see: let $\mathbf{x}^\lambda \in J$ be an eigenvector of C , $\sum_j c_{ij}x_j^\lambda = \lambda x_i^\lambda$. Substituting this on the r.h.s. of (4.1), one gets zero. Conversely, if the r.h.s. of (4.1) is zero, $\mathbf{x} = \mathbf{x}^\lambda$, with $\lambda = \sum_{k,j} c_{kj}x_j$.

Appendix A provides proof of the above propositions but they can be motivated by considering the underlying dynamics (4.2) from which (4.1) is derived. Because (4.1) is independent of ϕ , we can set $\phi = 0$ in (4.2) without any loss of generality. With $\phi = 0$ the general solution of (4.2), which is a linear system, can be schematically written as:

$$\mathbf{y}(t) = e^{Ct}\mathbf{y}(0),$$

where $\mathbf{y}(0)$ and $\mathbf{y}(t)$ are viewed as column vectors. Suppose $\mathbf{y}(0)$ is a right eigenvector of C with eigenvalue λ , denoted \mathbf{y}^λ . Then

$$\mathbf{y}(t) = e^{\lambda t}\mathbf{y}^\lambda.$$

As this time dependence is merely a rescaling of the eigenvector, this is an alternative way of showing that $\mathbf{x}^\lambda = \mathbf{y}^\lambda / \sum_{j=1}^s y_j^\lambda$ is a fixed point of (4.1). If the eigenvectors of C form a basis in R^s , $\mathbf{y}(0)$ is a linear combination: $\mathbf{y}(0) = \sum_\lambda a_\lambda \mathbf{y}^\lambda$. In that case, for large t it is clear that the term with the largest value of $\text{Re}(\lambda)$ will grow fastest, hence,

$$\mathbf{y}(t) \stackrel{t \rightarrow \infty}{\sim} e^{\lambda_1 t} \mathbf{y}^{\lambda_1},$$

where λ_1 is the eigenvalue of C with the largest real part (which is the same as its Perron-Frobenius eigenvalue) and \mathbf{y}^{λ_1} an associated eigenvector. Therefore, for generic initial conditions the trajectory of (4.1) will converge to $\mathbf{X} = \mathbf{x}^{\lambda_1}$, a PFE of C . If the eigenvectors of C do not form a basis in R^s , the above result is still true (see appendix A).

Note that λ_1 can be interpreted as the 'population growth rate' at large t , because $\dot{\mathbf{y}}(t) \stackrel{t \rightarrow \infty}{\sim} \lambda_1 \mathbf{y}$. In section 3.4, I had mentioned that λ_1 measures a topological property of the graph, the multiplicity of internal pathways in the core of the graph. Thus, in the present model, λ_1 has both a topological and dynamical significance, which relates two distinct properties of the system, one structural (multiplicity of pathways in the core of the graph), and the other dynamical (population growth rate). The higher the multiplicity of pathways in the core, the greater is the population growth rate of the dominant ACS.

4.3 Attractor profile theorem

While any eigenvector of C is a fixed point it need not be stable. In other words, only for special initial conditions, forming a space of measure zero in J , can \mathbf{X} be some other eigenvector of C , not a PFE. Henceforth, I ignore such special initial conditions. However, not all PFEs are attractors either. The following theorem indicates which subset of PFEs form the attractor set (Krishna and Jain, forthcoming):

Theorem 4.1: Attractor profile theorem

- 1) Determine all the strong components of the given graph C . Denote these by C_1, \dots, C_M .
- 2) Determine which of these are basic subgraphs. Denote them by D_1, \dots, D_K .
- 3) Construct a graph, denoted D^* , with K nodes, representing the D_i , and a link from node j to node i if there is a path from any node of D_j to any node of D_i that does not contain a node of any other basic subgraph.
- 4) Determine which of the D_i are at the ends of the longest paths in the above graph D^* . Denote these by $F_i, i = 1, \dots, N$.

For each $i = 1, \dots, N$ there exists a unique (upto constant multiples) PFE that has only nodes of F_i and all nodes having access from them non-zero, and all other nodes zero. The attractor set consists of all linear combinations of these PFEs that lie on the simplex J .

4.4 The attractor for a graph with no ACS

For any graph that consists of only chains, trees and isolated nodes, i.e. any graph with $\lambda_1 = 0$, the theorem reduces to the following (Jain and Krishna, 1998, 1999):

Proposition 4.2: For any graph with $\lambda_1(C) = 0$, in the attractor only the nodes at the ends of the longest paths are non-zero. All other nodes are zero.

This follows from theorem 4.1 because for a graph with $\lambda_1 = 0$ each node is a basic subgraph. Appendix A has an alternate proof based directly on the underlying y_i dynamics. Figure 4.1 shows a graph that has $\lambda_1 = 0$. The white nodes are those that are zero in the attractor and the grey node is the only non-zero node in the attractor. This graph is the same as the one in Figure 3.4. Notice that of the four PFEs of the graph only one, $(0, 0, 0, 1, 0, 0, 0)^T$, is the attractor.

4.5 The dominant ACS of a graph

For graphs with an ACS, i.e., with $\lambda_1 \geq 1$, recall that proposition 3.3 showed a close relationship between the PFEs of the graph and ACSs. A similar result holds for the attractor (Jain and Krishna, 1998, 1999):

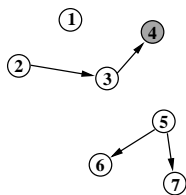


Figure 4.1: A graph that has no ACS. Only node 4, coloured grey, is non-zero in the attractor.

Proposition 4.3: For any graph C ,

- (i) For every \mathbf{X} belonging to the attractor set, the set of nodes i for which $X_i > 0$ is the same and is uniquely determined by C . The subgraph formed by this set of nodes will be called the 'subgraph of the attractor' of (4.1) for the graph C .
- (ii) If $\lambda_1(C) \geq 1$, the subgraph of the attractor is an ACS.

Definition 4.1: Dominant ACS.

For any graph with $\lambda_1 \geq 1$ the subgraph of the attractor, which is an ACS, will be called the *dominant ACS* of the graph (Jain and Krishna, 1998, 1999).

The dominant ACS is independent of (generic) initial conditions and is the subgraph induced by the set of nodes belonging to all the F_i and all nodes having access from them in C . The following sections use theorem 4.1 to determine the structure of the dominant ACS of several different types of graphs.

4.6 Examples of the attractor for specific graphs

It is instructive to consider examples of graphs and see how the trajectory converges to a PFE, and what the dominant ACS looks like in each case.

Example 1. A simple chain, Figure 4.2a:

The adjacency matrix of this graph has all eigenvalues zero; $\lambda_1 = 0$. The unique PFE (upto constant multiples) of this graph is $\mathbf{e} = (0, 0, 1)^T$. Because node 1 has no catalyst, its rate equation is (henceforth taking $\phi = 0$) $\dot{y}_1 = 0$. Therefore $y_1(t) = y_1(0)$, which is a constant independent of t . The rate equation for node 2 is $\dot{y}_2 = y_1 = y_1(0)$. Thus $y_2(t) = y_2(0) + y_1(0)t$. Similarly $\dot{y}_3 = y_2$ implies that $y_3(t) = (1/2)y_1(0)t^2 + y_2(0)t + y_3(0)$. At large t , $y_1 = \text{constant}$, $y_2 \sim t$, $y_3 \sim t^2$; hence y_3 dominates. Therefore, $X_i = \lim_{t \rightarrow \infty} x_i(t)$ is given by $X_1 = 0, X_2 = 0, X_3 = 1$. Thus \mathbf{X} equals the unique PFE \mathbf{e} , independent of initial conditions.

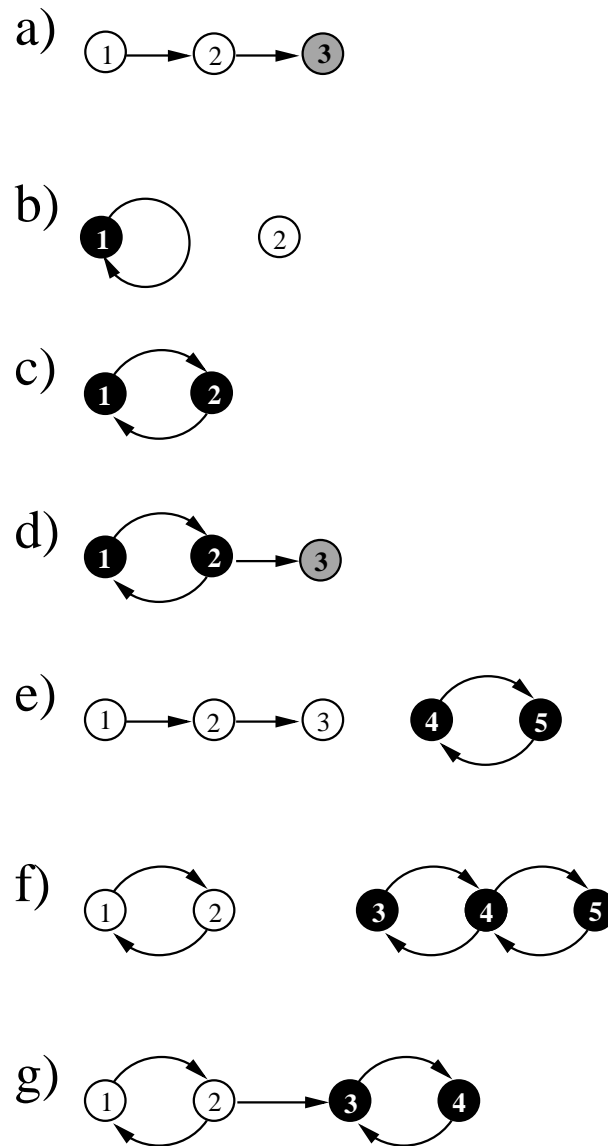


Figure 4.2: Examples of graphs with a unique PFE (upto constant multiples), which is, therefore, the unique stable attractor. The coloured nodes show the subgraph of the PFE, i.e., the nodes that are non-zero in the attractor. The black nodes are core nodes, the grey nodes are periphery nodes and the white nodes are the nodes that are zero in the attractor.

Example 2. A 1-cycle, Figure 4.2b:

This graph has two eigenvalues, $\lambda_1 = 1$, $\lambda_2 = 0$. The unique PFE is $\mathbf{e} = (1, 0)^T$. The rate equations are $\dot{y}_1 = y_1, \dot{y}_2 = 0$, with the solutions $y_1(t) = y_1(0)e^t, y_2(t) = y_2(0)$. At large t node 1 dominates, hence $\mathbf{X} = (1, 0)^T = \mathbf{e}$. The exponentially growing population of 1 is a consequence of the fact that 1 is a self-replicator, as embodied in the equation $\dot{y}_1 = y_1$.

Example 3. A 2-cycle, Figure 4.2c:

The corresponding adjacency matrix has eigenvalues $\lambda_1 = 1, \lambda_2 = -1$. The unique normalized PFE is $\mathbf{e} = (1, 1)^T/2$. The population dynamics equations are $\dot{y}_1 = y_2, \dot{y}_2 = y_1$.

The general solution to these is (note $\ddot{y}_1 = y_1$)

$$y_1(t) = Ae^t + Be^{-t}, \quad y_2(t) = Ae^t - Be^{-t}.$$

Therefore at large t , $y_1 \rightarrow Ae^t, y_2 \rightarrow Ae^t$, hence $\mathbf{X} = (1, 1)^T/2 = \mathbf{e}$. Neither 1 nor 2 is individually a self-replicating node, but collectively they function as a self-replicating entity.

Example 4. A 2-cycle with a periphery, Figure 4.2d:

This graph has $\lambda_1 = 1$ and a unique normalized PFE $\mathbf{e} = (1, 1, 1)^T/3$. The population equations for y_1 and y_2 and consequently their general solutions are the same as Example 3, but now in addition $\dot{y}_3 = y_2$, yielding $y_3(t) = Ae^t + Be^{-t} + \text{constant}$. Again for large t , y_1, y_2, y_3 grow as $\sim Ae^t$, hence $\mathbf{X} = (1, 1, 1)^T/3 = \mathbf{e}$. The dominant ACS includes all the three nodes.

This example shows how a parasitic periphery (which does not feed back into the core) is supported by an autocatalytic core. This is also an example of the following general result: when a subgraph C' , with largest eigenvalue λ'_1 , is downstream from another subgraph C'' with largest eigenvalue $\lambda''_1 > \lambda'_1$, then the populations of the former also grow at the rate at which the populations of C'' are growing. Therefore if C'' is non-zero in the attractor, so is C' . In this example C' is the single node 3 with $\lambda'_1 = 0$ and C'' is the 2-cycle of nodes 1 and 2 with $\lambda''_1 = 1$.

Example 5. A 2-cycle and a chain, Figure 4.2e:

The graph in Figure 4.2e combines the graphs of Figures 4.2a and c. Following the analysis of those two examples it is evident that for large t , $y_1 \sim t^0, y_2 \sim t^1, y_3 \sim t^2, y_4 \sim e^t, y_5 \sim e^t$. Because the populations of the 2-cycle are growing exponentially they will eventually completely overshadow the populations of the chain which are growing only as powers of t . Therefore the attractor will be $\mathbf{X} = (0, 0, 0, 1, 1)^T/2$ which, it can be verified, is a PFE of the graph (it is an eigenvector with eigenvalue 1). In general when a graph consists of one or more ACSs and other nodes that are not part of any ACS, the populations of the ACS nodes grow exponentially while the populations of the latter nodes grow at best as powers of t . Hence ACSs always outperform non-ACS structures in the population dynamics (see also Example 2).

Example 6. A 2-cycle and another irreducible graph disconnected from it, Figure 4.2f:

One can ask, when there is more than one ACS in the graph which is the dominant ACS? Figure 4.2f shows a graph containing two strong components. The 2-cycle subgraph has a Perron-Frobenius eigenvalue 1, while the other strong component has a Perron-Frobenius eigenvalue $\sqrt{2}$. The unique PFE of the entire graph is $\mathbf{e} = (0, 0, 1, \sqrt{2}, 1)^T / (2 + \sqrt{2})$ with eigenvalue $\sqrt{2}$. The population dynamics equations are $\dot{y}_1 = y_2, \dot{y}_2 = y_1, \dot{y}_3 = y_4, \dot{y}_4 = y_3 + y_5, \dot{y}_5 = y_4$. The first two equations are completely decoupled from the last three and the solutions for y_1 and y_2 are the same as for Example 3. For the other irreducible graph the solution is (because $\ddot{y}_4 = \dot{y}_3 + \dot{y}_5 = 2y_4$)

$$y_4(t) = Ae^{\sqrt{2}t} + Be^{-\sqrt{2}t}, \quad y_3(t) = \frac{1}{\sqrt{2}}(Ae^{\sqrt{2}t} + Be^{-\sqrt{2}t}) + C,$$

$$y_5(t) = \frac{1}{\sqrt{2}}(Ae^{\sqrt{2}t} + Be^{-\sqrt{2}t}) - C.$$

Thus, the populations of nodes 3, 4 and 5 also grow exponentially but at a faster rate, reflecting the higher Perron-Frobenius eigenvalue of the subgraph comprising those nodes. Therefore, this structure eventually overshadows the 2-cycle, and the attractor is $\mathbf{X} = \mathbf{e}$. The dominant ACS in this case is the irreducible subgraph formed by nodes 3, 4 and 5. More generally, when a graph consists of several disconnected ACSs with different individual λ_1 , only the ACSs whose λ_1 are the largest (and equal to $\lambda_1(C)$) end up with non-zero relative populations in the attractor.

Example 7. A 2-cycle downstream from another 2-cycle, Figure 4.2g:

What happens when the graph contains two ACSs whose individual λ_1 equals $\lambda_1(C)$, and one of those ACSs is downstream of another? In Figure 4.2g nodes 3 and 4 form a 2-cycle that is downstream from another 2-cycle comprising nodes 1 and 2. The unique PFE of this graph, with $\lambda_1 = 1$, is $\mathbf{e} = (0, 0, 1, 1)^T / 2$. The population dynamics equations are $\dot{y}_1 = y_2, \dot{y}_2 = y_1, \dot{y}_3 = y_4 + y_2, \dot{y}_4 = y_3$. Their general solution is:

$$y_1(t) = Ae^t + Be^{-t}, \quad y_2(t) = Ae^t - Be^{-t},$$

$$y_3(t) = \frac{t}{2}(Ae^t - Be^{-t}) + Ce^t + De^{-t},$$

$$y_4(t) = \frac{t}{2}(Ae^t + Be^{-t}) + (C - \frac{A}{2})e^t + (\frac{B}{2} - D)e^{-t}.$$

It is clear that for large t , $y_1 \sim e^t, y_2 \sim e^t, y_3 \sim te^t, y_4 \sim te^t$. While all four grow exponentially with the same rate λ_1 , as $t \rightarrow \infty$ y_3 and y_4 will overshadow y_1 and y_2 . The attractor will be therefore be $\mathbf{X} = (0, 0, 1, 1)^T / 2 = \mathbf{e}$. Here the dominant ACS is the 2-cycle of nodes 3 and 4. This result generalizes to other kinds of ACSs: if one strong component is downstream of another with the same Perron-Frobenius eigenvalue, the latter will have zero relative population in the attractor.

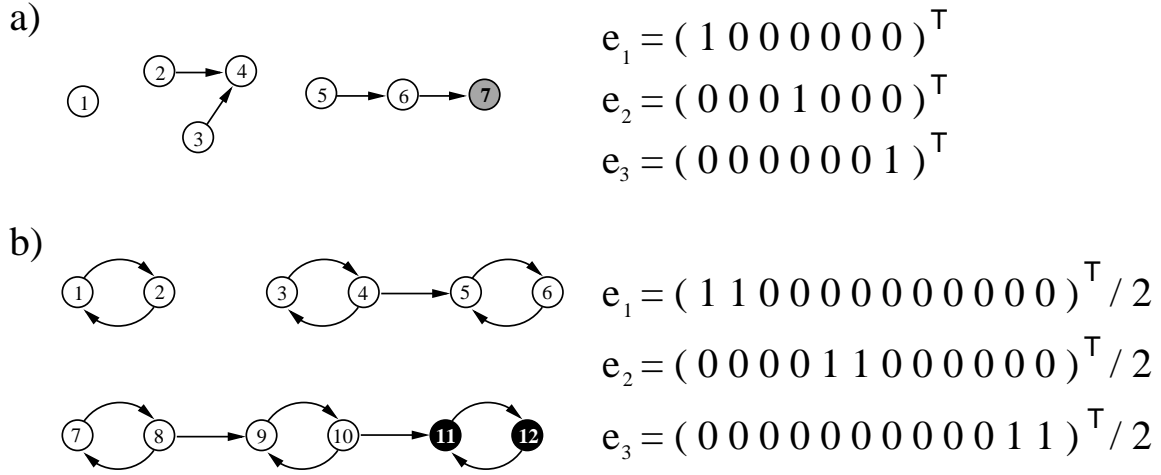


Figure 4.3: Examples of graphs with multiple PFEs. **a.** $\mathbf{e}_1, \mathbf{e}_2, \mathbf{e}_3$ are all eigenvectors with eigenvalue $\lambda_1 = 0$. Only \mathbf{e}_3 is the attractor. Thus for generic initial conditions, only node 7, which sits at the end point of the longest chain of nodes is non-zero in the attractor. **b.** $\mathbf{e}_1, \mathbf{e}_2, \mathbf{e}_3$ are all eigenvectors with eigenvalue $\lambda_1 = 1$, but only \mathbf{e}_3 is the attractor. Only the 2-cycle, of nodes 11 and 12, which sits at the end of the longest chain of cycles, is non-zero in the attractor.

The above examples displayed graphs with a unique PFE, and illustrated proposition 4.1(iv). The stability of the attractor follows from the fact that the constants A, B, C, D , etc., in the above examples, that can be traded for the initial conditions of the populations, do not appear anywhere in the attractor \mathbf{X} . Now I consider examples where the PFE is not unique.

Example 8. Graph with $\lambda_1 = 0$ and three weakly connected components, Figure 4.3a:

This graph has three independent PFEs, displayed in Figure 4.3a. The attractor is $\mathbf{X} = \mathbf{e}_3$. This is an immediate generalization of Example 1 above. Using the same argument as for Example 1, we can see that $y_i \sim t^k$ if the longest path ending at node i is of length k . Thus, the populations of nodes 1, 2, 3 and 5 are constant, those of 4 and 6 increase $\sim t$ for large t , and of 7 as $\sim t^2$. Therefore, only nodes at the ends of the longest paths will be non-zero in the attractor.

Example 9. Several weakly connected components containing 2-cycles, Figure 4.3b:

Here again there are three PFEs, one for each weakly connected component. The population of nodes in 2-cycles that are not downstream of other 2-cycles (nodes 1,2,3,4,7 and 8) will grow as e^t . As in Example 7, Figure 4.2g, the nodes of 2-cycles that are downstream of one 2-cycle (nodes 5, 6, 9 and 10) will grow as te^t . It can be verified that the populations of nodes in 2-cycles downstream from two other 2-cycles (nodes 11 and 12) will grow as t^2e^t . The pattern is clear: in the attractor only the 2-cycles at the ends of the longest chains of 2-cycles will have non-zero relative populations. Therefore, the attractor is $\mathbf{X} = \mathbf{e}_3$.

4.7 Timescale for reaching the attractor

How long does it take the system to reach the attractor? This depends on the structure of the graph C . For instance in Example 2, the attractor is approached as the population of node 1, y_1 , overwhelms the population y_2 . Because y_1 grows exponentially as e^t , the attractor is reached on a timescale $\lambda_1^{-1} = 1$. (In general, when I say that ‘the timescale for the system to reach the attractor is τ ’, I mean that for $t \gg \tau$, $\mathbf{x}(t)$ is ‘exponentially close’ to its final destination $\mathbf{X} \equiv \lim_{t \rightarrow \infty} \mathbf{x}(t)$, i.e. for all i , $|x_i(t) - X_i| \sim e^{-t/\tau} t^\alpha$, with some finite α .) In contrast, in Example 1, the attractor is approached as y_3 overwhelms y_1 and y_2 . Because in this case all the populations are growing as powers of t , the timescale for reaching the attractor is infinite. When the populations of different nodes are growing at different rates, this timescale depends on the difference in growth rate between the fastest growing population and the next fastest growing population.

For graphs with $\lambda_1 = 0$ like those in Example 1 and 8, all populations grow as powers of t , hence the timescale for reaching the attractor is infinite.

For graphs that have $\lambda_1 \geq 1$ but all the basic subgraphs are in different weakly connected components, such as Examples 2-6, the timescale for reaching the attractor is given by $(\lambda_1 - \text{Re}\lambda_2)^{-1}$, where λ_2 is the eigenvalue of C with the next largest real part, compared to λ_1 .

For graphs having $\lambda_1 \geq 1$ with at least one basic subgraph downstream from another basic subgraph, the ratio of the fastest growing population to the next fastest growing one will always be a power of t (as in Examples 7 and 9), therefore, the timescale for reaching the attractor is again infinite.

4.8 Core and periphery of a graph

As the dominant ACS is specified by a particular PFE, I will define the core of the dominant ACS to be the core of the corresponding PFE. If the PFE is simple, the core of the dominant ACS consists of just one basic subgraph. If the PFE is non-simple the core of the dominant ACS will be a union of more than one basic subgraph. The dominant ACS is uniquely determined by the graph. This motivates the definition of the core and periphery of a graph:

Definition 4.2: Core and periphery of a graph.

The *core* of a graph C , denoted $Q(C)$, is the core of the dominant ACS of C , if an ACS exists in the graph. The *periphery* of C is the periphery of the dominant ACS of C . If no ACS exists in the graph, i.e., $\lambda_1(C) = 0$ then $Q(C) = \Phi$ (Jain and Krishna, 2003a).

In all cases $\lambda_1(Q(C)) = \lambda_1(C)$. Henceforth all graphs will be depicted with the following colour scheme: black for core nodes, grey for periphery nodes (and for nodes with non-zero X_i when there is no ACS), and white for nodes that are not in any of the PFE subgraphs.

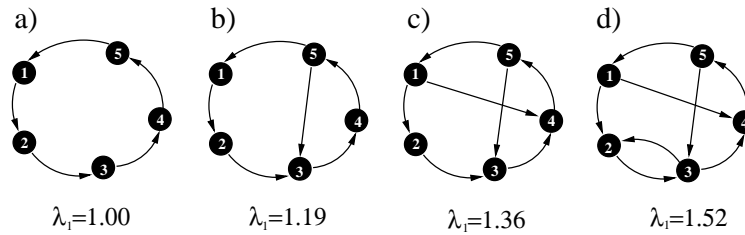


Figure 4.4: Keystone nodes. **a.** All nodes of the graph are keystone. **b.** Nodes 3, 4 and 5 are keystone. **c.** Nodes 4 and 5 are keystone. **d.** None of the nodes are keystone.

4.9 Keystone nodes

In ecology certain species are referred to as keystone species – those whose extinction or removal would seriously disturb the ecosystem (Paine, 1969; Jordán et al., 1999; Solé and Montoya, 2001). One might similarly look for the notion of a keystone node in a directed graph that captures some important organizational role played by a node. Consider the impact of the hypothetical removal of any node i from a graph C . One can, for example, study the structure of the core of the graph $C - i$ that would result if node i (along with all its links) were removed from C .

Definition 4.3: Core overlap.

Given any two graphs C and C' whose nodes are labeled, the *core overlap* between them, denoted $Ov(C, C')$, is the number of common links in the cores of C and C' , i.e., the number of ordered pairs (j, i) for which Q_{ij} and Q'_{ij} are both non-zero. If either C or C' does not have a core, $Ov(C, C')$ is defined to be zero (Jain and Krishna, 2002a).

Definition 4.4: Keystone node.

I will refer to a node i of a graph C as a *keystone node* if C has a non-vanishing core and $Ov(C, C - i) = 0$ (Jain and Krishna, 2002b, 2003a).

Thus a keystone node is one whose removal modifies the organizational structure of the graph (as represented by its core) drastically. In each of Figures 4.4a-d, for example, the core is the entire graph. In Figure 4.4a, all the nodes are keystone, because the removal of any one of them would leave the graph without an ACS (and hence without a core). In general when the core of a graph is a single n -cycle, for any n , all the core nodes are keystone. In Figure 4.4b, nodes 3, 4 and 5 are keystone but the other nodes are not, and in Figure 4.4c only nodes 4 and 5 are keystone. In Figure 4.4d, there are no keystone nodes. These examples show that the more internal pathways a core has (generally, this implies a higher value of λ_1), the less likely it is to have keystone nodes, and hence the more robust its structure is to removal of nodes.

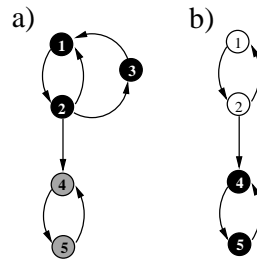


Figure 4.5: Another example of a keystone node. Node 3 is a keystone node of the graph (a) because its removal produces the graph (b) which has a zero core overlap with the graph (a). The core nodes of both graphs are coloured black.

Figure 4.5 illustrates another type of graph structure that has a keystone node. The graph in Figure 4.5a consists of two strong components – a 2-cycle (nodes 4 and 5) downstream from an irreducible subgraph consisting of nodes 1, 2 and 3. The core of this graph is the latter irreducible subgraph. Figure 4.5b shows the graph that results if node 3 is removed with all its links. This consists of one 2-cycle downstream from another. Though both 2-cycles are basic subgraphs of the graph, as discussed in Example 7, Figure 4.2g, this graph has a unique (upto constant multiples) PFE, whose subgraph consists of the downstream cycle (nodes 4 and 5) only. Thus the 2-cycle 4-5 is the core of the graph in Figure 4.5b. Clearly $Ov(C, C - 3) = 0$. Therefore, node 3 in Figure 4.5a is a keystone node.

The above purely graph theoretic definition of a keystone node turns out to be useful in the dynamical system discussed in this and the following chapters. For other dynamical systems, alternate definitions of keystone might be more useful.

Chapter 5

Graph Dynamics

In this chapter, I present a model of an evolving network that is a specific instance of the framework described in section 1.7. The dynamical system described in the previous chapter is used for step 1 of the dynamics, and certain rules are chosen for steps 2 and 3 that aim to capture some features of the evolution of chemical networks on the prebiotic Earth.

5.1 Graph dynamics rules

The initial graph is constructed as follows: For every ordered pair (i, j) with $i \neq j$ (where $i, j \in S = \{1, 2, \dots, s\}$), c_{ij} is independently chosen to be unity with a probability p and zero with a probability $1 - p$. c_{ii} is set to zero for all $i \in S$. Thus the initial graph is a random graph, a member of the ensemble G_s^p described in section 2.9. Each x_i is chosen randomly, with uniform probability, in $[0, 1]$ and all x_i are rescaled so that $\sum_{i=1}^s x_i = 1$.

- Step 1. With C fixed, \mathbf{x} is evolved according to (4.1) until it converges to a fixed point, denoted \mathbf{X} .
- Step 2. The set \mathcal{L} of nodes with the least X_i is determined, i.e, $\mathcal{L} = \{i \in S | X_i = \min_{j \in S} X_j\}$. A node, say node k , is picked randomly from \mathcal{L} and is removed from the graph along with all its links.
- Step 3. A new node (also denoted k) is added to the graph. Links to and from k to other nodes are assigned randomly according to the same rule, i.e, for every $i \neq k$ c_{ik} and c_{ki} are independently reassigned to unity with probability p and zero with probability $1 - p$, irrespective of their earlier values, and c_{kk} is set to zero. All other matrix elements of C remain unchanged. x_k is set to a small constant x_0 , all other x_i are perturbed by a small amount from their existing value X_i , and all x_i are rescaled so that $\sum_{i=1}^s x_i = 1$.

This process, from step 1 onward, is iterated many times. Figure 5.1 depicts the graph dynamics schematically.

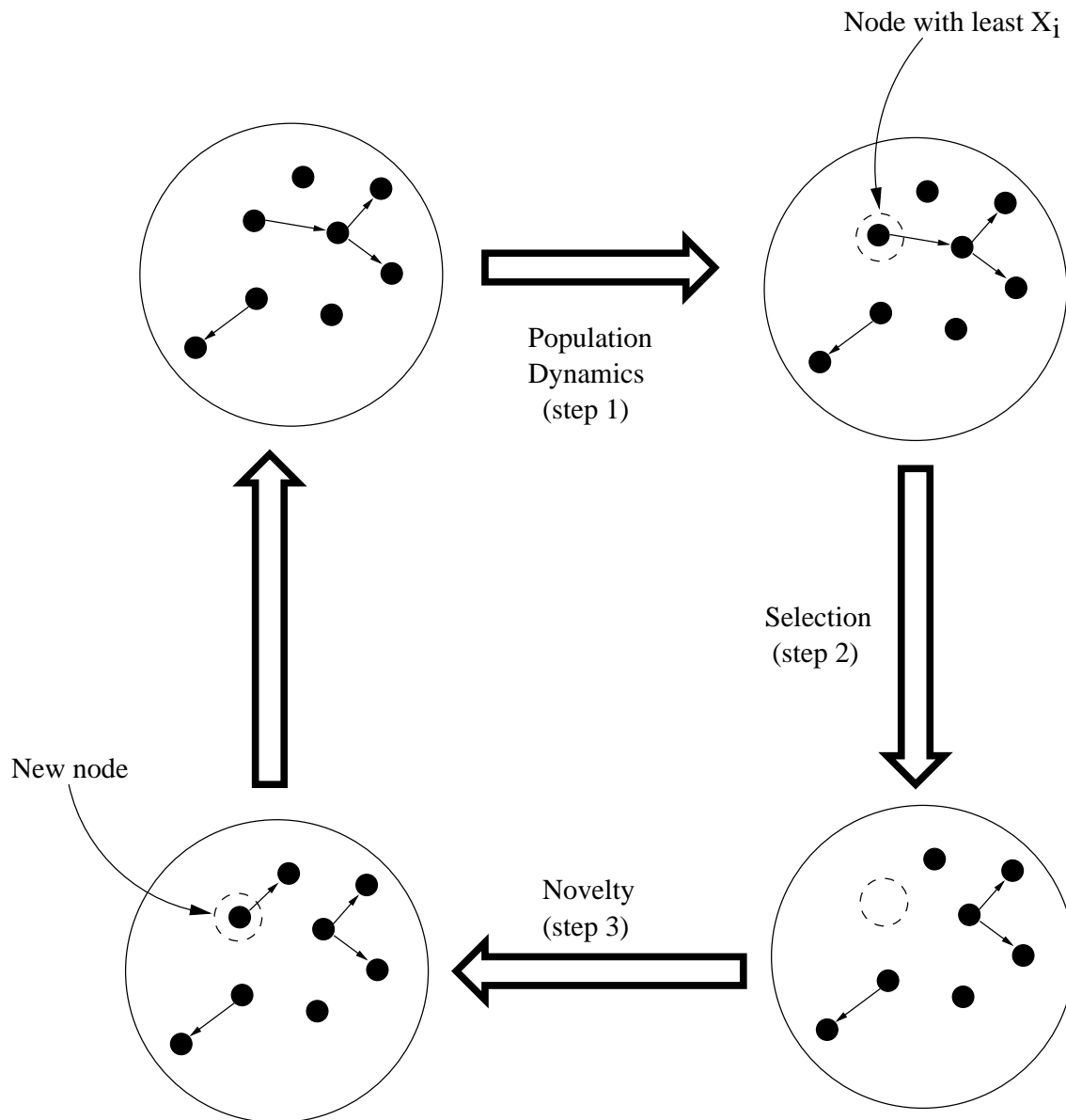


Figure 5.1: Schematic depiction of the graph dynamics. Starting with a random graph, first the population dynamics is allowed to run until the relative populations reach their attractor (step 1). Then one of the nodes with the least relative population is removed from the graph (selection, step 2). It is replaced by a new node which is assigned random links to existing nodes (novelty, step 3). This process is then iterated.

5.2 Features of the graph dynamics

5.2.1 Evolution in a prebiotic pool

These graph dynamics rules are motivated by the puzzle of how a complex chemical organization might have emerged from an initial ‘random soup’ of chemicals. As discussed in section 1.9, the rules model the imagined dynamics of an evolving chemical network such as might have existed in a pool on the prebiotic Earth. Several assumptions and idealizations underlie such a chemical interpretation of the model rules. Some of these have been mentioned in sections 1.9 and 4.1, however I will defer a more detailed discussion to section 9.3.

The model has two main sources of inspiration. One is the set of models studied by Farmer, Kauffman, Packard and others (Kauffman, 1983, 1993; Farmer et al., 1986; Bagley and Farmer, 1991; Bagley et al., 1991), and by Fontana (1991), and Fontana and Buss (1994) (see also Stadler et al., 1993; Dyson, 1985). Like these models, the present one employs an artificial chemistry of catalyzed reactions, albeit a much simpler one, in which populations of species evolve over time. To this I add the feature, inspired by the model of Bak and Sneppen (1993), that the ‘least fit species mutates’ with ‘fitness’ here being equated to the relative population. Unlike the Bak-Sneppen model, however, the ‘mutation’ of a species also changes its links to other species.

5.2.2 Coupling of population and graph dynamics: two timescales

As discussed in section 1.7, the coupling of the population dynamics and the graph dynamics is built into the framework of the model: the evolution of the x_i depends on the graph C in step 1, and the evolution of C in turn depends on the x_i through the choice of which node to remove in step 2. There are two timescales in the dynamics, a short timescale over which the graph is fixed while the x_i evolve, and a longer timescale over which the graph is changed.

5.2.3 Absence of self-replicators

While in previous sections I have considered graphs with 1-cycles, the requirement $c_{ii} = 0$ in the present section forbids 1-cycles in the graph. The motivation is the following: 1-cycles represent self-replicating species (see previous section, Example 2). Such species, e.g., RNA molecules, are difficult to produce and maintain in a prebiotic scenario and it is possible that it requires a self-supporting molecular organization to be in place *before* an RNA world, for example, can take off (Joyce et al., 1987; Joyce, 1989). Thus, I wish to address the question: can one get molecular organizations that can collectively self-replicate without introducing self-replicating species ‘by hand’ into the system?

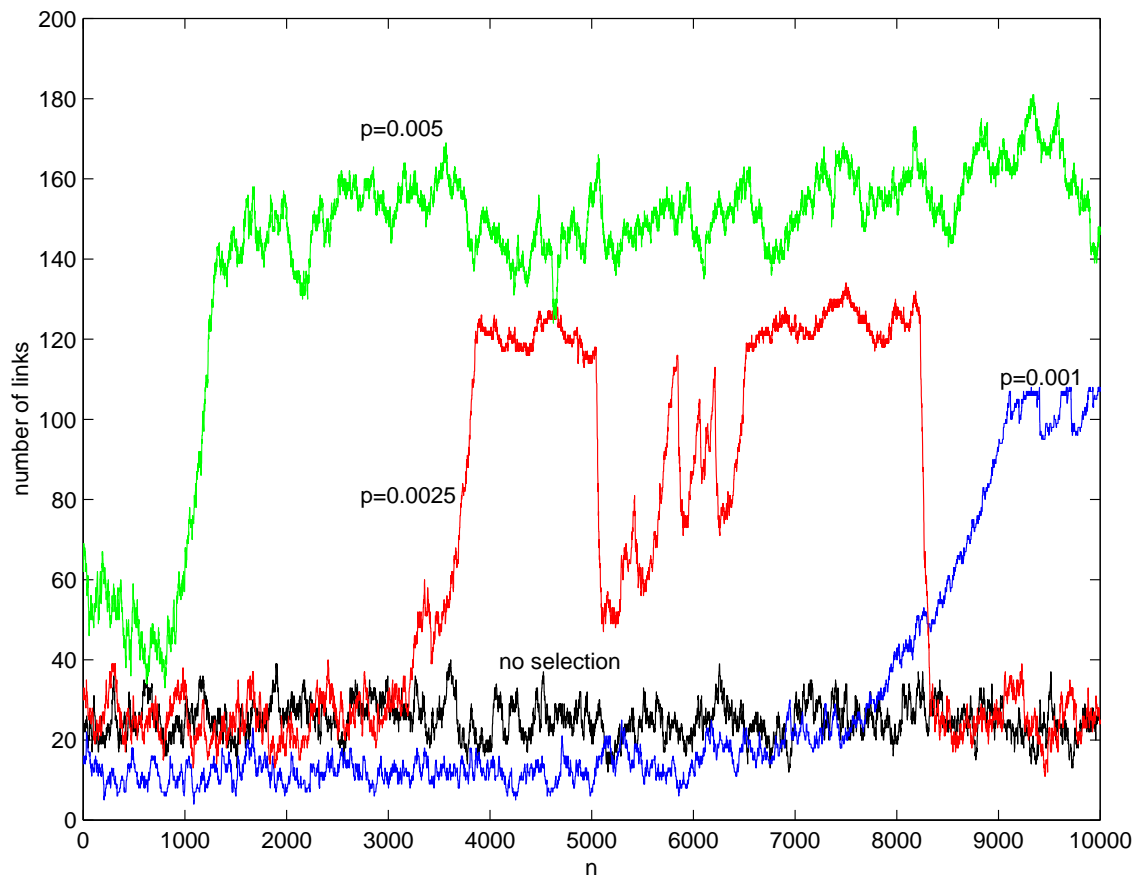


Figure 5.2: The number of links versus time, n , for various runs. Each run had $s = 100$. The black curve is a run with no selection: a random node is picked for removal at each graph update. The other curves show runs with selection and with different p values: blue, $p = 0.001$; red, $p = 0.0025$; green, $p = 0.005$.

5.2.4 Selection and novelty

The rules for changing the graph implement *selection* and *novelty*, two important features of natural evolution. Selection is implemented by removing the node that is 'performing the worst', with 'performance' in this case being equated to a node's relative population (step 2). Adding a new node introduces novelty into the system (step 3). Note that although the actual connections of a new node with other nodes are created randomly, the new node has the same average connectivity as the initial set of nodes. Thus, the new node is not biased in any way toward increasing the complexity of the chemical organization. Steps 2 and 3 implement the interaction of the system with the external environment. The phenomena to be described in the following sections are all consequences of the interplay between selection, novelty and the population dynamics.

5.3 Implementation

Two programs are described in appendix B, and are included in the attached CD, that use different methods to implement the graph dynamics. The programs differ in the way the attractor is determined at each time step. The first program uses theorem 4.1. The second numerically integrates equation (4.1) to find its attractor. The programs are written in C++, with Matlab 5.2 being used to determine eigenvalues and eigenvectors where required.

5.4 Results of graph evolution

Figure 5.2 shows the total number of links in the graph versus time (n , the number of graph updates). Three runs of the model described in the previous section, each with $s = 100$ and different values of p are exhibited. Also exhibited is a run where there was *no selection* (in which step 2 is modified: instead of picking one of the nodes of \mathcal{L} , any one of the s nodes is picked randomly and removed from the graph along with all its links. The rest of the procedure remains the same). Figure 5.3 shows the time evolution of two more quantities for the same three runs with selection displayed in Figure 5.2. The quantities plotted are s_1 , the number of nodes with $X_i > 0$, and λ_1 , the Perron-Frobenius eigenvalue of the graph. Figure 5.4 shows the evolution of another graph theoretic measure, the interdependency of the graph, \bar{d} , for the run of Figure 5.3b (the data files for these runs are included in the attached CD, see appendix C).

For all the displayed runs the size of the network has been taken to be $s = 100$. Computational constraints have prevented a detailed exploration of larger values of s , though the few runs I have studied with values of s upto 250 and $ps < 1$ have shown a similar behaviour. The values of the parameters p and s for the displayed runs were chosen to lie in the regime $ps < 1$, and much of the analytical work described in later chapters, such as estimation of various timescales, assumes that $ps \ll 1$. This range is the one of interest from the point of view of the origin of life problem because it is likely that the catalytic networks existing in prebiotic pools would have been quite sparse. However, it is worthwhile to extend the analysis and simulations to other parameter ranges, such as large s or large p values, and compare with the $ps < 1$ behaviour.

Coming back to the runs displayed in Figure 5.2, it is clear why the number of links fluctuates about its random graph value $\approx ps^2$ in the run without selection. This is because each graph update replaces a randomly chosen node with another that has on average the same connectivity and, therefore, the graph remains random like the starting graph. As soon as selection is added the behaviour becomes more interesting. Three regimes can be observed. First, the 'random phase' where the number of links fluctuates around ps^2 , while s_1 and \bar{d} are small. Second, the 'growth phase' where l , s_1 and \bar{d} show a clear rising tendency. Finally, the 'organized phase' where l and \bar{d} hover (with large fluctuations) about a value much higher than the initial random graph value, and s_1 remains close to its maximum value s (with some fluctuations). The time spent in each phase depends on p and s . I analyze the structure of the graph in the three phases in chapter 6.

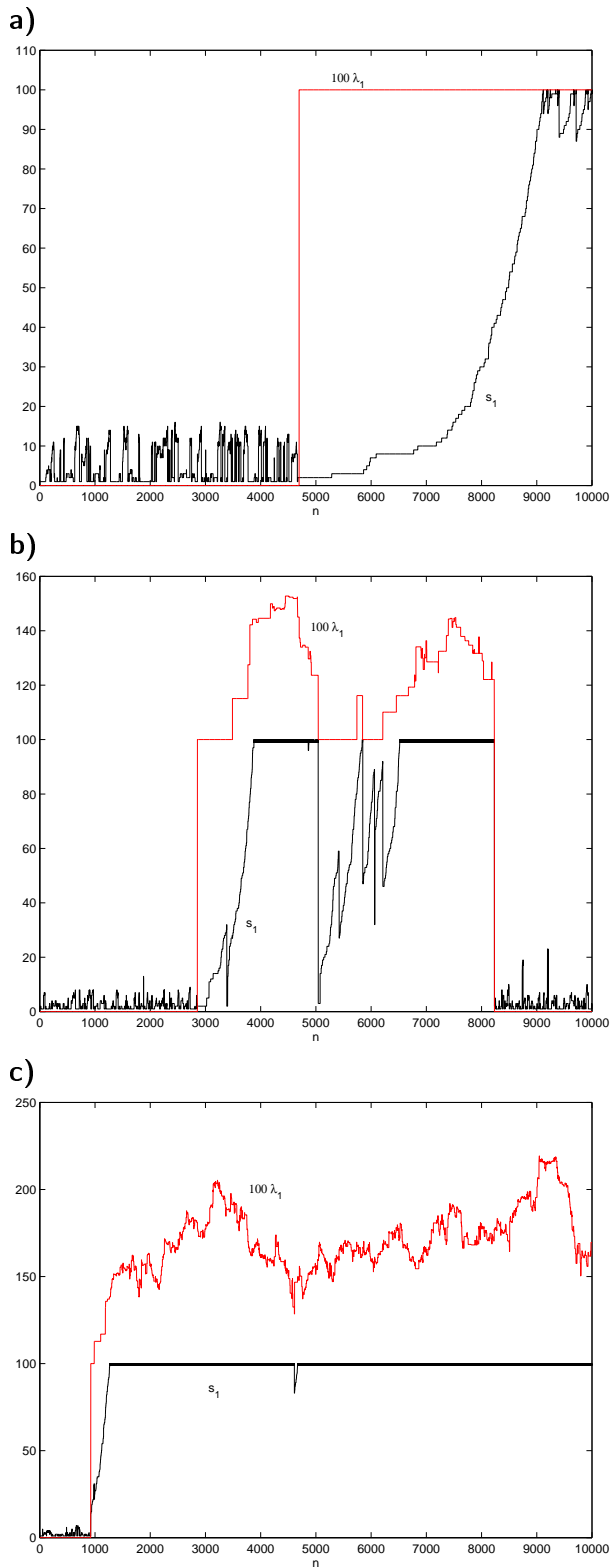


Figure 5.3: Number of nodes with $X_i > 0$, s_1 , (black curve) and the Perron-Frobenius eigenvalue of the graph, λ_1 , (red curve) versus time, n , for the same three runs shown in Figure 5.2. Each run has $s = 100$ and, **a.** $p = 0.001$, **b.** $p = 0.0025$ and **c.** $p = 0.005$, respectively. The λ_1 values shown have been multiplied by 100 to ease comparison with the s_1 curves.

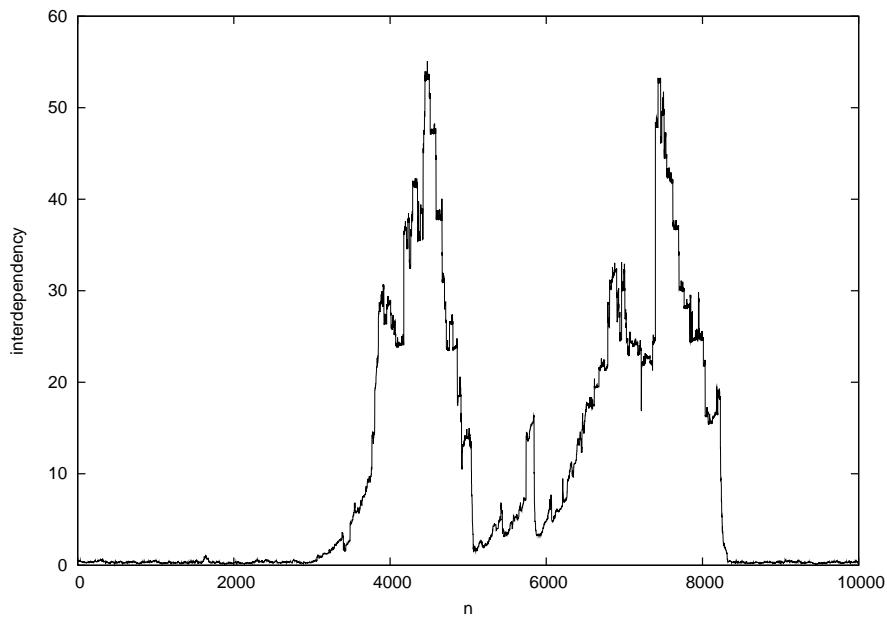


Figure 5.4: Interdependency vs. n for the run with $s = 100$ and $p = 0.0025$ that is displayed in Figure 5.3b.

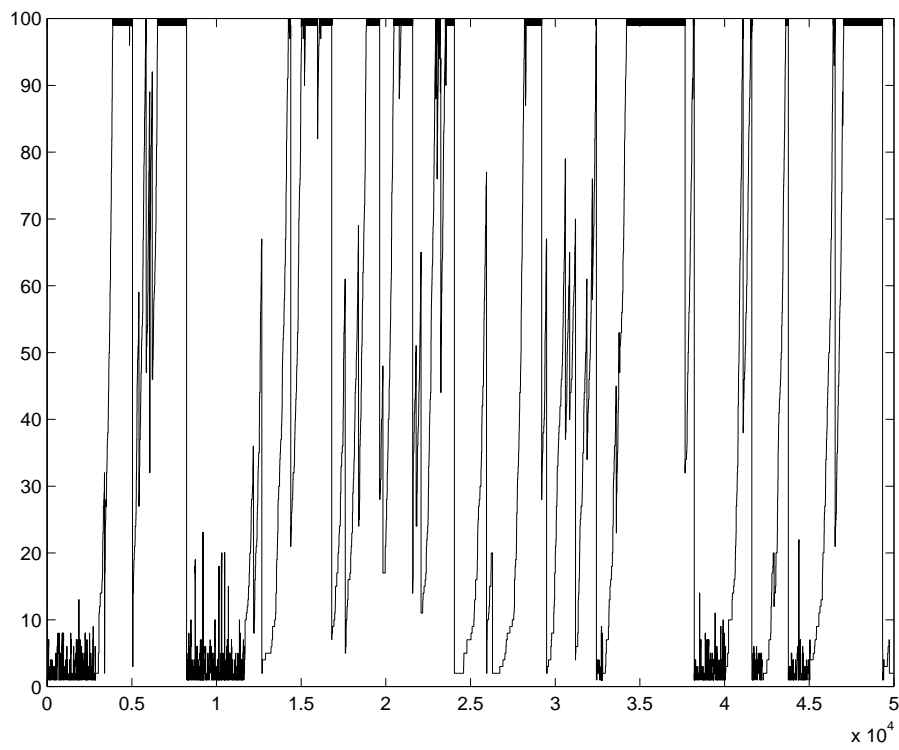


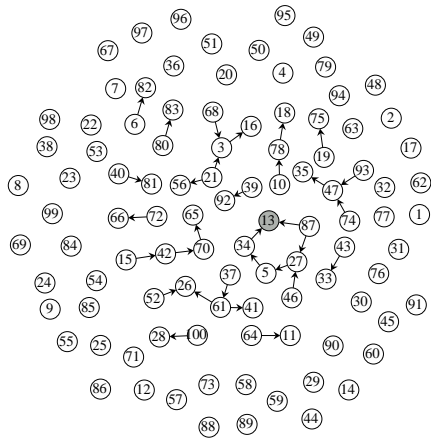
Figure 5.5: s_1 vs. n for the same run displayed in Figure 5.3b ($s = 100$, $p = 0.0025$) for a longer time, till $n = 50000$. Repeated rounds of catastrophes and recoveries are seen.

Figure 5.5 shows s_1 for the same run as that of Figure 5.3b for a longer time, from $n = 1$ to $n = 50,000$. In this long run one can see several sudden, large drops in s_1 : ‘catastrophes’ in which a large fraction of the s nodes become extinct, i.e., the X_i values of the nodes fell to zero. Some of the drops seem to take the system back into the random phase, others are followed by ‘recoveries’ in which s_1 rises back towards its maximum value s . The recoveries are comparatively slower than the catastrophes, which in fact occur in a single time step. An analysis of crashes and recoveries is the subject of chapter 7.

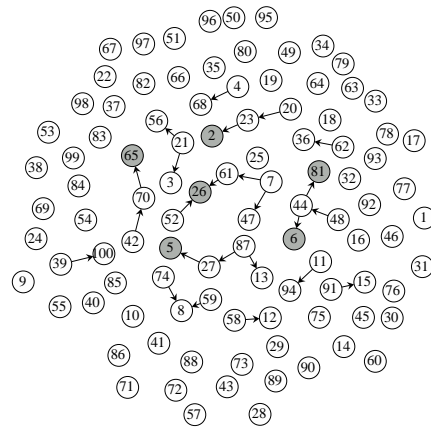
It may be useful for the reader to trace the steps through one example run. Figure 5.6 shows snapshots of the graph at various times for the run shown in Figure 5.3b, which has $p = 0.0025$. The initial random graph ($n = 1$, Figure 5.6a) has 31 links. 55 nodes are isolated with no incoming or outgoing links, and there are no cycles. In the attractor only node 13 is non-zero, all others are zero. Figures 5.6b-d show further snapshots of the graph in the random phase.

The first cycle comprising nodes 26 and 90 forms at $n = 2854$ (Figure 5.6e), and these nodes are the only non-zero ones in the attractor. This marks the beginning of the growth phase. At $n = 3022$ (Figure 5.6f) more nodes get attached to the cycle and their relative populations also become non-zero. By $n = 3386$ (Figure 5.6g) 28 nodes have added onto the 2-cycle. All these 30 nodes are non-zero in the attractor, while the other nodes are zero. At $n = 3387$ (Figure 5.6h) there is a sudden drop in s_1 as a new 2-cycle comprising nodes 41 and 98 is formed. This 2-cycle is downstream from the earlier 2-cycle, and for such a graph, as explained in section 4.6 (Example 7), only the downstream cycle will be non-zero. By $n = 3402$ (Figure 5.6i) the situation has not altered much, the old 2-cycle still survives by chance. But then node 38 gets removed, which breaks the path connecting the cycles. So at $n = 3403$ (Figure 5.6j) the graph consists of two disconnected 2-cycles. Both these cycles and all nodes having access from them are non-zero in the attractor. By $n = 3488$ (Figure 5.6k) several nodes have joined the 26-90 cycle. By chance none have joined the 41-98 cycle. At $n = 3489$ (Figure 5.6l) the 26-90 cycle gets strengthened by a second cycle. This subgraph now has a larger Perron-Frobenius eigenvalue and so the other cycle is zero in the attractor. After this the dominant ACS keeps accreting nodes until it spans the entire graph for the first time at $n = 3880$ (Figure 5.6m) signaling the start of the organized phase. At $n = 4448$ (Figure 5.6n) the core is at its largest. Most subsequent graph updates involve the removal of a node with no more drastic effect on the dominant ACS. This removed node will keep getting repeatedly replaced until it rejoins the dominant ACS. At $n = 4695$ (Figure 5.6o) the node 36 which is outside the ACS and therefore zero in the attractor, gets replaced and the new node rejoins the ACS resulting in the graph at $n = 4696$ (Figure 5.6p). Notice that node 36 forms a 2-cycle with node 74. Thus, this graph update has created a new irreducible subgraph in the periphery. At the moment this structure does not affect the dominant ACS because the core has a larger λ_1 . However, a few hundred time steps later this 2-cycle plays a significant role.

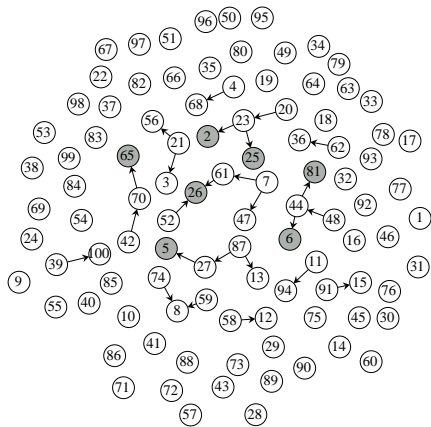
a) $n=1$



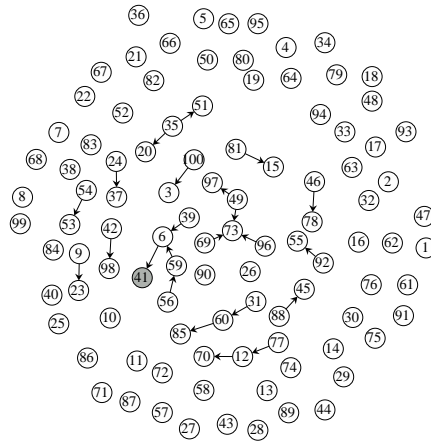
b) $n=78$



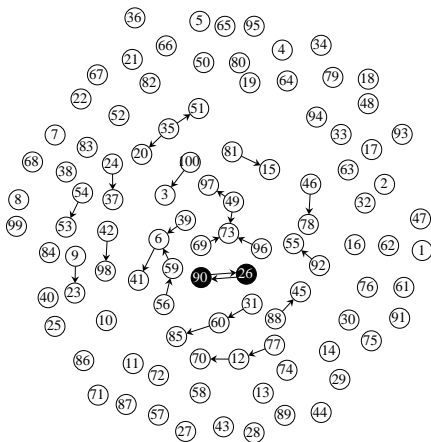
c) $n=79$



d) $n=2853$



e) $n=2854$



f) $n=3022$

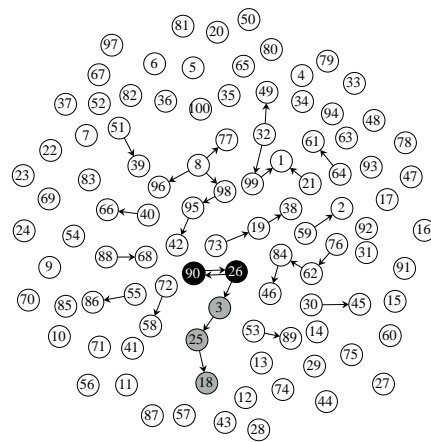
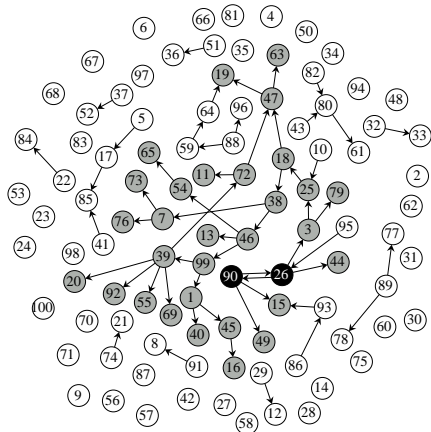
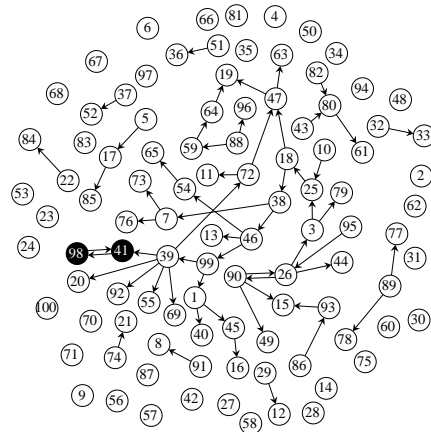


Figure 5.6a–f, continued on next page.

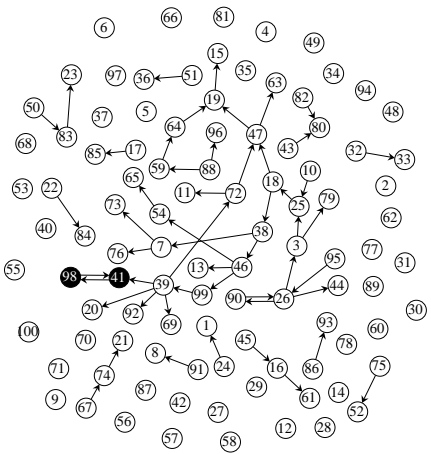
g) n=3386



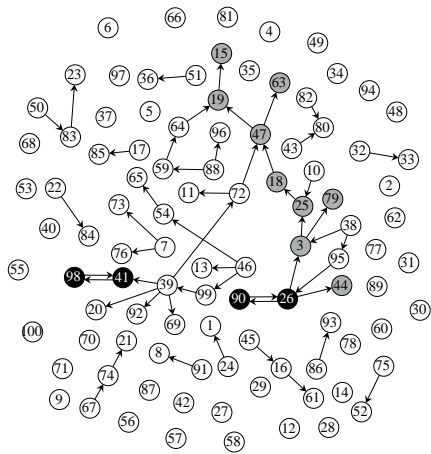
h) n=3387



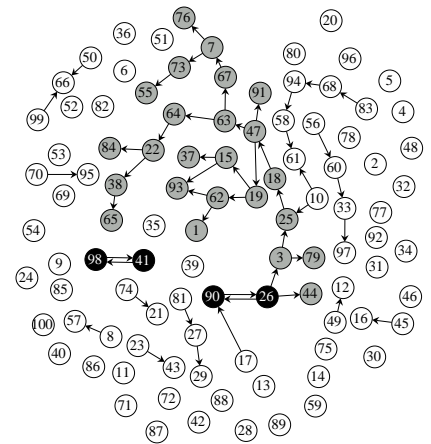
i) n=3402



j) n=3403



k) n=3488



l) n=3489

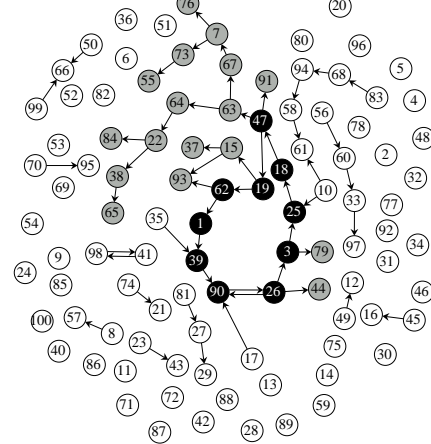
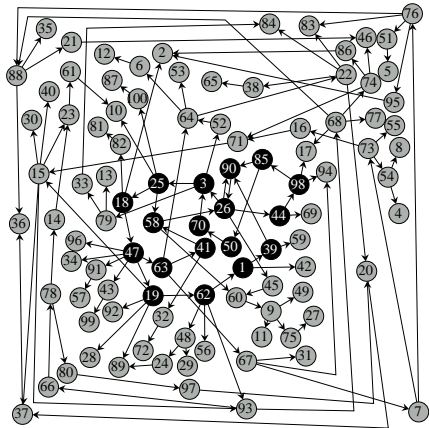
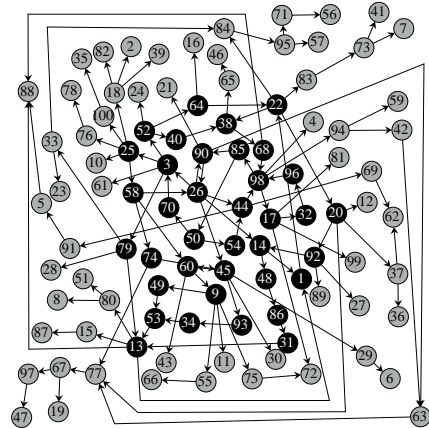


Figure 5.6g-l, continued on next page.

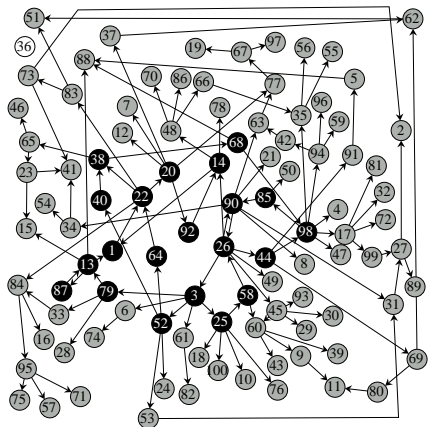
m) n=3880



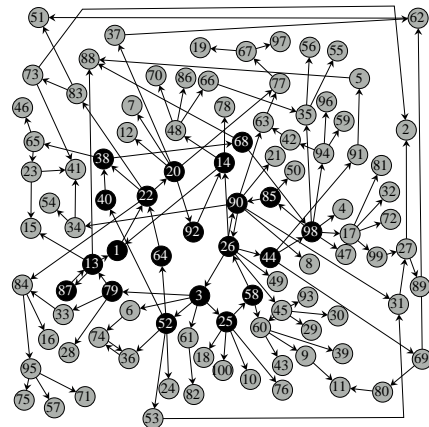
n) n=4448



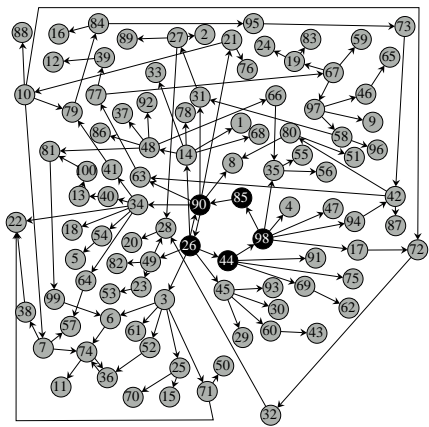
o) n=4695



p) n=4696



q) n=5041



r) n=5042

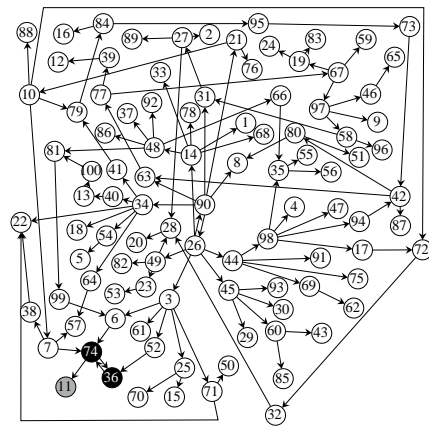
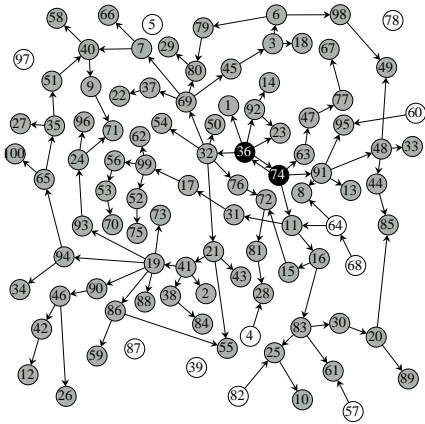
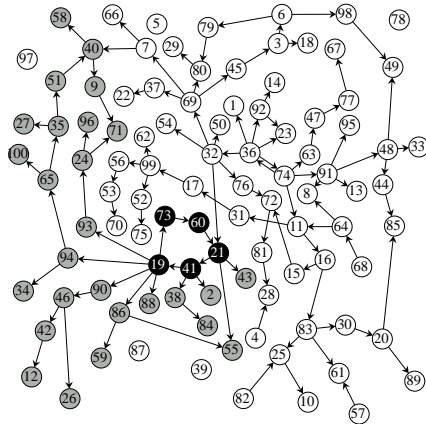


Figure 5.6m-r, continued on next page.

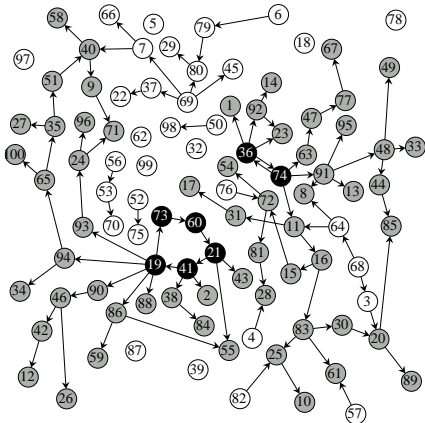
s) n=6061



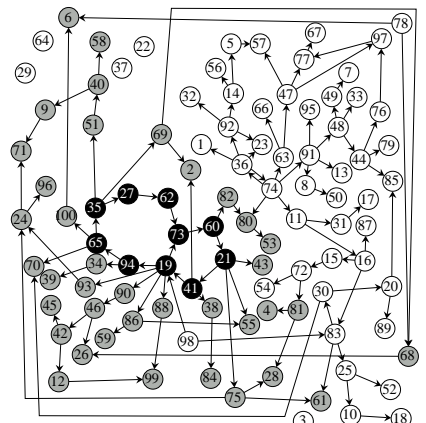
t) n=6062



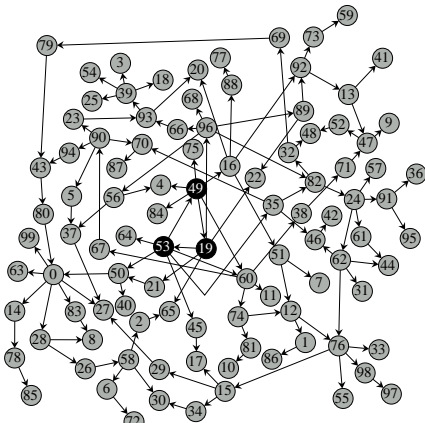
u) n=6070



v) n=6212



w) n=8232



x) n=8233

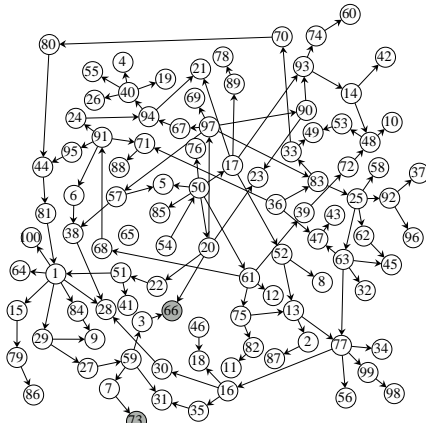


Figure 5.6s-x, continued on next page.

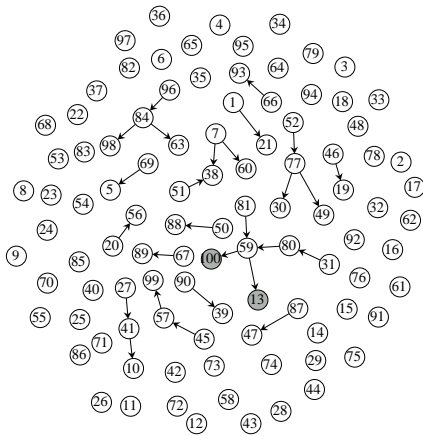
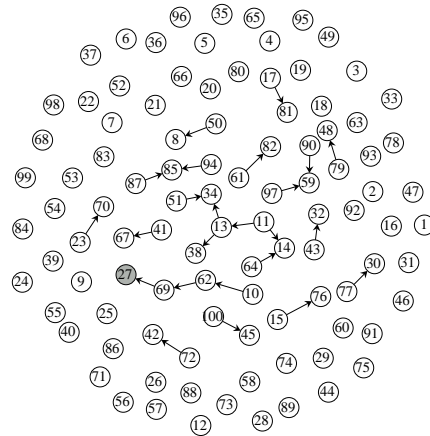
y) $n=8500$ z) $n=10000$ 

Figure 5.6: (see previous pages also) Snapshots of the graph at various times for the run shown in Figure 5.3b with $s = 100$ and $p = 0.0025$. See the text for a description of the major events. In all graphs, white nodes are those with $X_i = 0$. All shaded nodes have $X_i > 0$. If there is an ACS in the graph, the core nodes are coloured black and the periphery nodes grey. The graphs have been drawn using LEDA. Data files for these graphs, in LEDA format, and files containing their adjacency matrices can be found in the attached CD (see appendix C).

By $n = 5041$ (Figure 5.6q) the core has shrunk to 5 nodes. Node 85 gets removed which leaves the graph at $n = 5042$ (Figure 5.6r) with one 2-cycle (nodes 36 and 74) downstream from another (26 and 90). Only nodes 36, 74 and node 11 (downstream from 74) are non-zero in the new attractor. All other nodes have become extinct, triggering a drop in s_1 from 100 to 3. Over the next thousand time steps the dominant ACS rebuilds itself around the new core comprising nodes 36 and 74 ($n = 6061$, Figure 5.6s). Then node 60 comes in, completing a cycle of 5 nodes that is downstream from the 36-74 cycle ($n = 6062$, Figure 5.6t) and again there is a large drop in s_1 as 36, 74 and many nodes having access from them become extinct. At $n = 6070$ (Figure 5.6u), however, the 36-74 cycle is resurrected as the path connecting it to the 5-cycle is broken. It does not last for too long as the 5-cycle is strengthened by another cycle at $n = 6212$ (Figure 5.6v) and the 36-74 cycle again becomes extinct. This time it does not revive, as the dominant ACS builds around the strengthened 5-cycle. About two thousand time steps later, at $n = 8232$ (Figure 5.6w), the graph is again fully autocatalytic but is on the verge of a major collapse. The core is just a 3-cycle and node 54 gets removed, thus destroying the only cycle in the graph. The graph at $n = 8233$ (Figure 5.6x) is left without an ACS; the system is now once again in the random phase. Within a few hundred time steps all of the structure is destroyed and the graph at $n = 8500$ (Figure 5.6z) and $n = 10000$ (Figure 5.6z) are similar to the initial graph at $n = 1$ (Figure 5.6a). At this point, I will stop following the run but eventually a new ACS arises, grows and spans the entire graph, then gets destroyed and another round starts (see Figure 5.5).

Chapter 6

Formation and Growth of Autocatalytic Sets

6.1 The random phase

For the run with $s = 100, p = 0.0025$ displayed in Figure 5.3b, the initial random graph at $n = 1$ contains no cycles, and hence no ACSs, and its Perron-Frobenius eigenvalue is $\lambda_1 = 0$. Figure 6.1 shows this initial graph.

For such a graph $X_i > 0$ for all nodes that are at the ends of the longest paths of nodes, and $X_i = 0$ for every other node (see section 4.4). In Figure 6.1, there are two paths of length 4, which are the longest paths in the graph. Both end at node 13, which is therefore the only non-zero node in the attractor for this graph. This node, then, is the only node protected from removal during the graph update. Node 13 has a high relative population but its supporting nodes do not have high relative populations. Inevitably within a few graph updates a supporting node will be removed from the graph. When that happens node 13 which presently has non-zero X_i will no longer be at the end of the longest path and hence will get $X_i = 0$. In the run node 34 is replaced at the 8th time step. After that node 13 joins the set \mathcal{L} of nodes with least X_i . Thus no structure is stable when there is no ACS. Eventually, all nodes are removed and replaced.

Figures 6.2 and 6.3 compare properties of the graphs from the first random phase of the run (from $n = 1$ to $n = 2853$, inclusive), with properties of the random graph ensemble, G_s^p , described in section 2.9. The average number of links for the 2853 graphs in the random phase is 25.2, with standard deviation 5.3. For the ensemble G_s^p , with $s = 100, p = 0.0025$, the average number of links is $ps(s-1) = 24.75$. Figure 6.2 shows that the in and out degree distributions of graphs taken from the random phase are close to the binomial distribution expected for G_s^p for smaller values of degree but depart from the binomial for larger degrees. Figure 6.3 compares the dependency distribution of the random phase with that of 10^7 graphs taken from the ensemble G_s^p . Again, the distributions are similar for smaller dependency values, and differ for higher values.

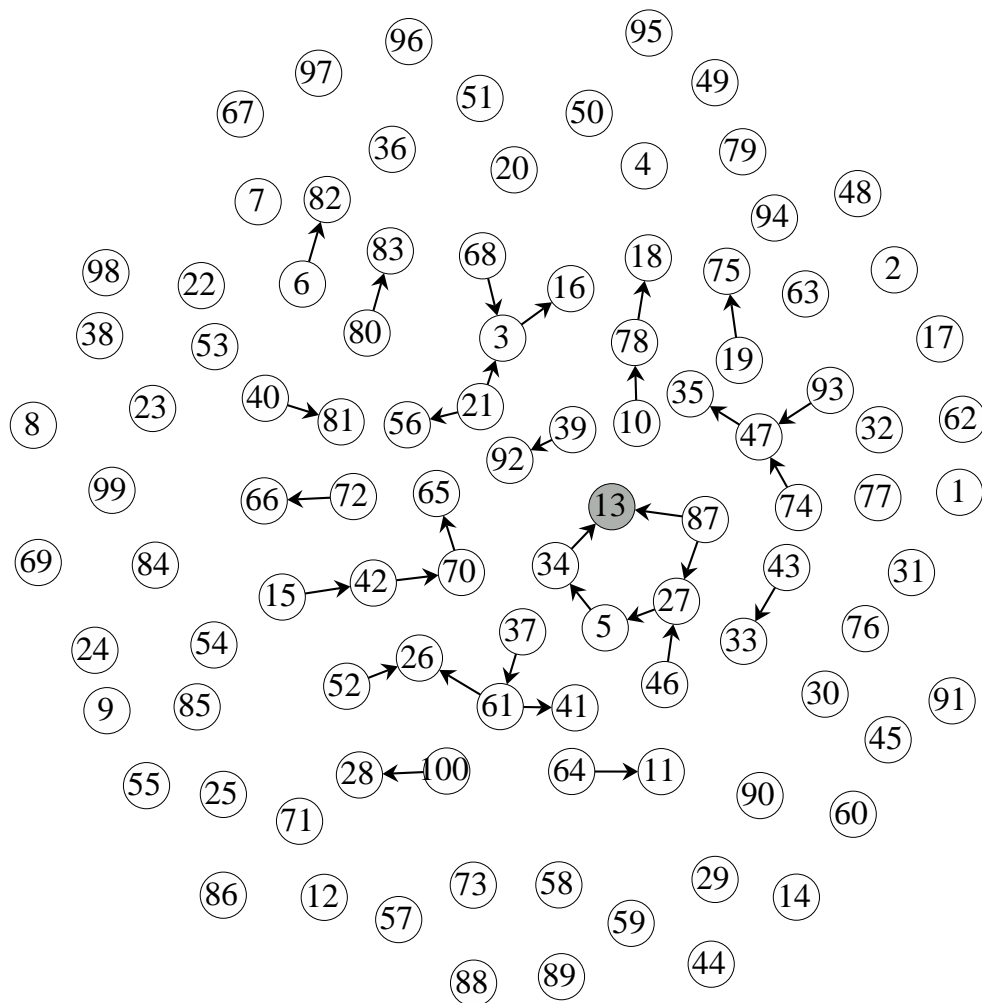


Figure 6.1: The initial random graph, at $n = 1$, for the run shown Figure 5.3b. Node 13 is the only node with non-zero X_i because it is at the end of the longest path.

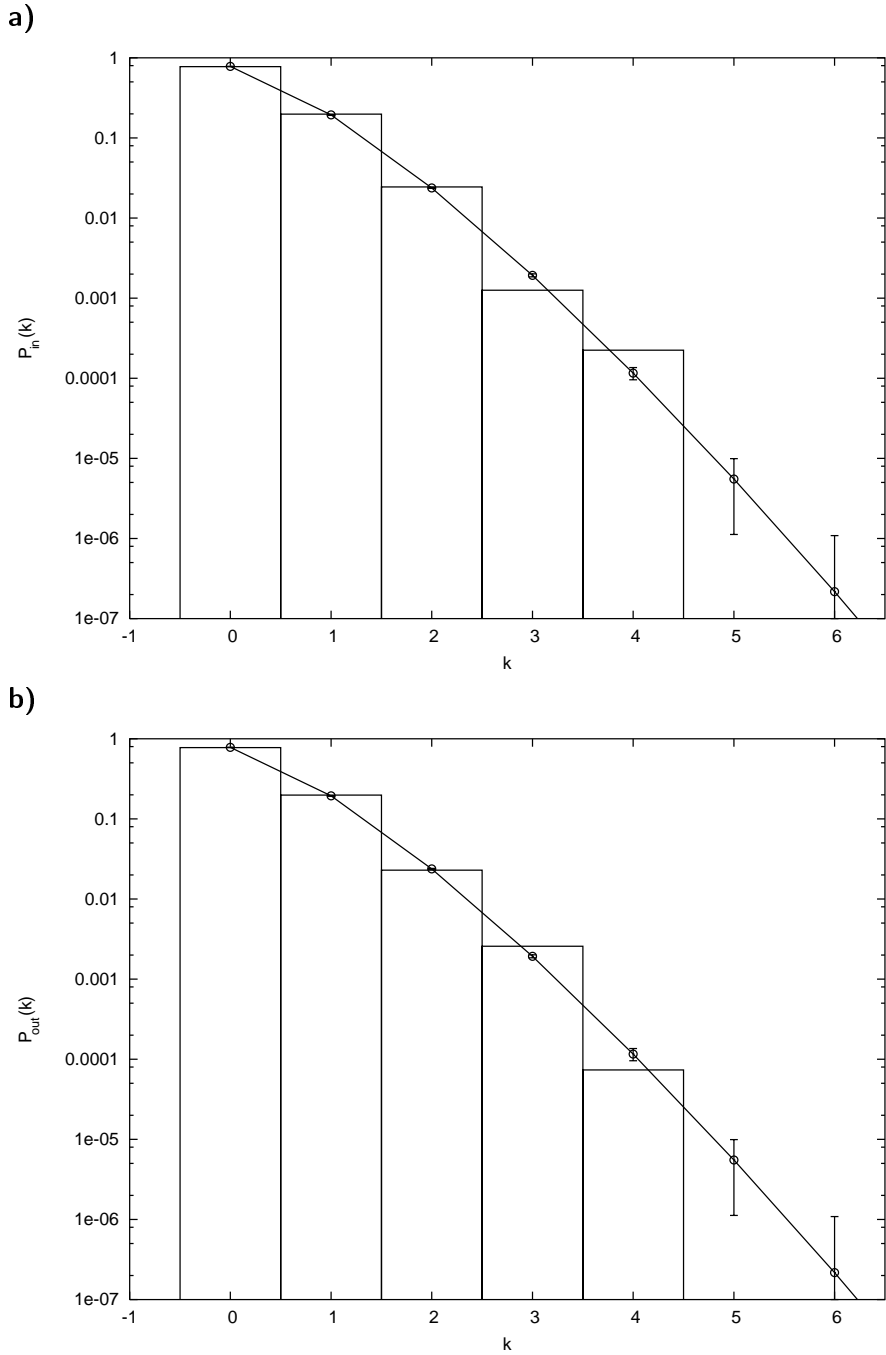


Figure 6.2: Comparison of the **a.** in-, and **b.** out-degree distributions (bars) of 2853 graphs from the random phase ($n = 1$ to $n = 2853$ of the run in Figure 5.3b) with the binomial degree distribution $B_p^{s-1}(k) \equiv {}^{s-1}C_k p^k (1-p)^{s-1-k}$ (lines with circles) expected for a random graph with $s = 100, p = 0.0025$. The error bars show the expected standard deviation, $\sqrt{\frac{B_p^{s-1}(k)[1-B_p^{s-1}(k)]}{285300}}$, of the distribution from the binomial for a finite sample of 2853 random graphs each with 100 nodes.

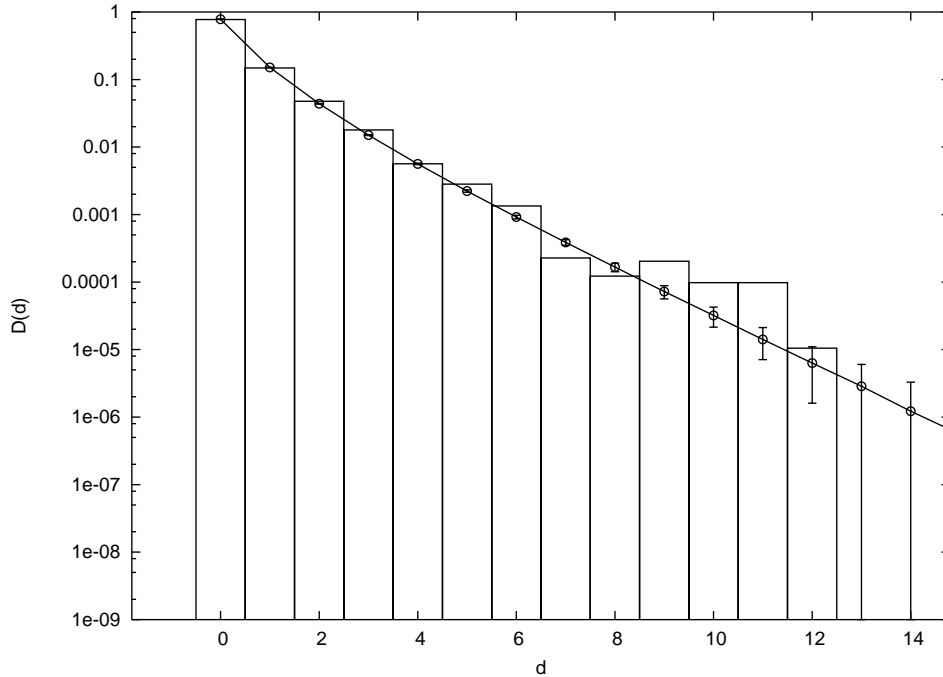


Figure 6.3: Comparison of the dependency distribution of 2853 graphs (bars) from the random phase ($n = 1$ to $n = 2853$ of the run in Figure 5.3b) with the dependency distribution (shown in figure 2.2) of 10^7 random graphs with $s = 100, p = 0.0025$ (line with circles). The error bars show the expected standard deviation, $\sqrt{\frac{D(d)[1-D(d)]}{285300}}$, of the distribution for a finite sample of 2853 random graphs each with 100 nodes (this estimate of the error assumes that the dependencies of each node is independently picked from the distribution $D(d)$ and does not take into account any correlations that would exist, even for random graphs, between dependencies of nodes of the same graph).

Although the properties of the random phase graphs do not exactly match the properties of graphs from the ensemble $G_{s,p}^p$, the main point about the graph dynamics holds nevertheless: In the random phase no graph structure is stable for very long and eventually all nodes are removed and replaced.

Note that the initial random graph is likely to contain no cycles when p is small ($ps \ll 1$). If larger values of p are chosen, it becomes more likely that the initial graph will contain a cycle. If it does, there is no random phase; the system is then in the growth phase, discussed below, right from the initial time step.

6.2 The growth phase

At some graph update an ACS is formed by pure chance. The probability of this happening can be closely approximated by the probability of a 2-cycle (the simplest ACS with 1-cycles being

disallowed) forming by chance, which is p^2s (= the probability that in the row and column corresponding to the replaced node in C , any matrix element and its transpose are both assigned unity). Thus, the ‘average time of appearance’ of an ACS is $\tau_a = 1/p^2s$, and the distribution of times of appearance is $P(n_a) = p^2s(1 - p^2s)^{n_a-1}$. This approximation is better for small p . In the run displayed in Figure 5.3b, a 2-cycle between nodes 26 and 90 formed at $n = 2854$. This is a graph that consists of a 2-cycle and several other chains and trees. For such a graph, I have shown in Example 3 in section 4.6 that the attractor has non-zero X_i for nodes 26 and 90 and zero for all other nodes. The dominant ACS consists of nodes 26 and 90. Therefore these nodes cannot be picked for removal at the graph update and, hence, a graph update cannot destroy the nodes and links of the dominant ACS. *The autocatalytic property is guaranteed to be preserved until the dominant ACS spans the whole graph.* In fact, an even stronger statement can be made (Jain and Krishna, 1998, 1999):

Proposition 6.1: λ_1 is a non-decreasing function of n as long as $s_1 < s$.

When a new node is added to the graph at a graph update, one of three things will happen:

1. The new node will not have any links from the dominant ACS and will not form a new ACS. In this case the dominant ACS will remain unchanged, the new node will have zero relative population and will be part of \mathcal{L} . For small p this is the most likely possibility.
2. The new node gets an incoming link from the dominant ACS and hence becomes a part of it. In this case the dominant ACS grows to include the new node. For small p , this is less likely than the first possibility, but such events do happen and in fact are the ones responsible for the growth of the dominant ACS.
3. The new node forms another ACS. This new ACS competes with the existing dominant ACS. Whether it now becomes dominant, overshadowing the previous dominant ACS or it gets overshadowed, or both ACSs coexist depends on the Perron-Frobenius eigenvalues of their respective subgraphs and how they are connected. Again, for small p , this is a rare event compared with possibilities 1 and 2.

Typically the dominant ACS keeps growing by accreting new nodes, usually one at a time, until the entire graph is an ACS. At this point the growth phase stops and the organized phase begins.

6.2.1 Timescale for growth of the dominant ACS

Assuming that possibility 3 above is rare enough to neglect, and that the dominant ACS grows by adding a single node at a time, one can estimate the time required for it to span the entire graph. Let the dominant ACS consist of $s_1(n)$ nodes at time n . The probability that the new node gets an incoming link from the dominant ACS and hence joins it is ps_1 . Thus in Δn

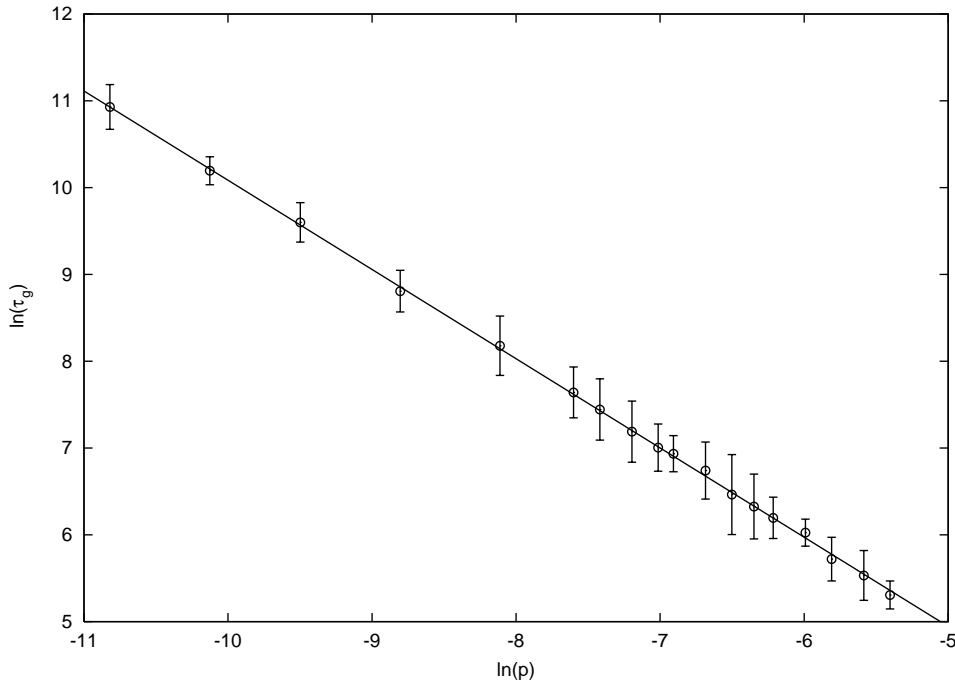


Figure 6.4: Dependence of τ_g (the growth timescale of the dominant ACS) on p . Each data point shows the average of $\ln \tau_g$ over 5 different runs with $s = 100$ and the given p value. The error bars correspond to one standard deviation of the $\ln \tau_g$ values for each p . The straight line is the best linear fit to the data points on a log-log plot. It has slope -1.03 ± 0.03 and intercept -0.20 ± 0.25 which is consistent with the expected slope -1 and intercept 0 .

graph updates, the dominant ACS will grow, on average, by $\Delta s_1 = p s_1 \Delta n$ nodes. Therefore $s_1(n) = s_1(n_a) \exp((n - n_a)/\tau_g)$, where $\tau_g = 1/p$, n_a is the time of appearance of the first ACS and $s_1(n_a)$ is the size of the first ACS ($=2$ for the run shown in Figure 5.3b). Thus s_1 is expected to grow exponentially with a characteristic timescale $\tau_g = 1/p$. The time taken from the appearance of the ACS to its spanning is $\tau_g \ln(s/s_1(n_a))$. This analytical result is confirmed by simulations (see Figure 6.4). In the displayed run, after the first ACS (a 2-cycle) is formed at $n = 2854$, it takes 1026 time steps, until $n = 3880$ for the dominant ACS to span the entire graph. This explains how an autocatalytic network structure and the positive feedback processes inherent in it can bootstrap themselves into existence from a small seed. The small seed, in turn, is guaranteed to appear on a certain timescale ($1/p^2 s$ in the present model) just by random processes.

6.3 Fully autocatalytic graphs

The growth phase continues until the dominant ACS spans the entire graph. In the displayed run this happened at $n = 3880$. Figure 6.5 shows the graph at this time – it is a fully autocatalytic graph, all nodes are part of the dominant ACS.

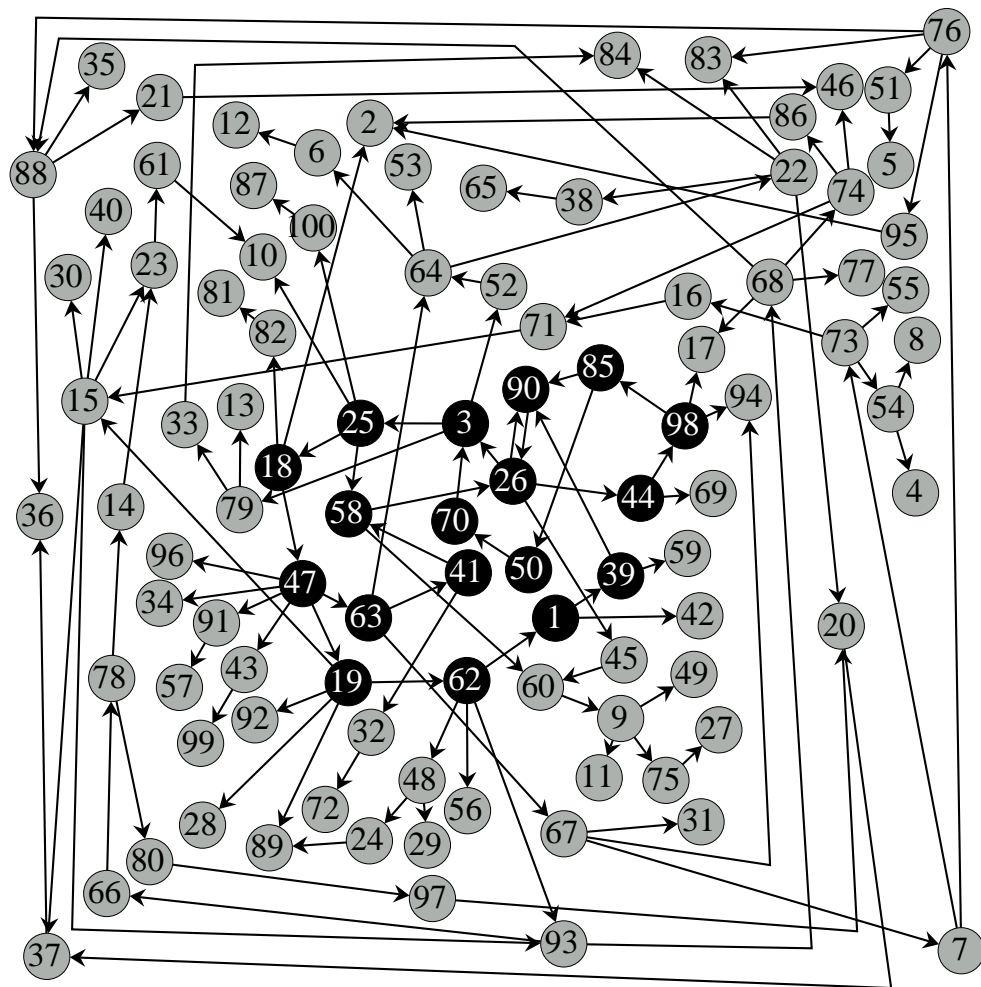


Figure 6.5: The graph, at $n = 3880$, for the run shown Figure 5.3b. For the first time in this run the graph is fully autocatalytic. All nodes are part of the dominant ACS and are non-zero in the attractor.

6.3.1 Probability of a random graph being fully autocatalytic

A fully autocatalytic graph such as this is a highly improbable structure for a random graph. Consider a graph of s nodes and let the probability of a positive link existing between any pair of nodes (except self-links) be p^* . Such a graph has on average $m^* = p^*(s - 1)$ incoming or outgoing positive links per node. For the entire graph to be an ACS, each node must have at least one incoming link, i.e. each row of the matrix C must contain at least one positive element. Hence the probability, P , for the entire graph to be an ACS is

$$\begin{aligned}
 P &= \text{probability that every row has at least one positive entry} \\
 &= [\text{probability that a row has at least one positive entry}]^s \\
 &= [1 - (\text{probability that every entry of a row is zero})]^s \\
 &= [1 - (1 - p^*)^{s-1}]^s \\
 &= [1 - (1 - m^*/(s - 1))^{s-1}]^s.
 \end{aligned}$$

Note from Figure 5.2 that at spanning the number of links is 124, i.e., $O(s)$. Thus the average degree m^* at spanning is $O(1)$. I have found this to be true in all the runs I have done where ps was $O(1)$ or less.

For large s and $m^* \sim O(1)$, $P \approx (1 - e^{-m^*})^s \sim e^{-\alpha s}$, where α is positive, and $O(1)$. Thus, a fully autocatalytic graph is exponentially unlikely to form if it were being assembled randomly (or picked at random from the random graph ensemble $G_s^{p^*}$). In the present model nodes are being added completely randomly but the underlying population dynamics and the selection imposed at each graph update result in the inevitable arrival of an ACS (in, on average, $\tau_a = 1/p^2 s$ time steps) and its inevitable growth into a fully autocatalytic graph in (on average) an additional $\sim \tau_g \ln s$ time steps.

For the displayed run if we take $m^* = ps \approx 0.25$ we get $P \approx 3 \times 10^{-66}$. Even if we take m^* to be the average degree of the graph at $n = 3880$, i.e., $m^* = 1.24$, we get $P \approx 3 \times 10^{-15}$; one would expect such a fully autocatalytic graph to take $\sim 10^{15}$ time steps to form if it were being assembled randomly, in contrast to the 3880 time steps it actually took in this run.

As mentioned in section 1.9, one of the puzzles of the origin of life is: how could a highly structured chemical network form in such a short time after the oceans condensed on the Earth? In this model, a highly non-random structure, a fully autocatalytic set, inevitably forms. Further, the time taken for it to form is extremely short, growing only as a logarithm of the size of the network. This model, therefore, suggests a mechanism – the growth of ACSs by the accretion of nodes around a small initial ACS – by which highly structured chemical networks (that are exponentially unlikely to form by chance) can form in a very short time. This mechanism, or its analogue in a more realistic chemical model, might explain the emergence of a structured chemical organization on the prebiotic Earth. This is discussed further in section 9.2.

6.3.2 Clustering coefficient

In several runs with $s = 100, p = 0.0025$ (totaling 1.55 million iterations) 160659 graphs were fully autocatalytic. The mean clustering coefficient of these 160659 graphs was 0.025, with standard deviation 0.016, which is comparable to the clustering coefficient for random graphs with the same connectivity ($p^* = 1.27/(s - 1)$, see below). The graph in Figure 6.5, in fact, has a clustering coefficient of zero: none of the neighbours of any node are connected to each other, as can be verified from the figure. Thus, the fully autocatalytic graphs produced in these runs do not have a small-world structure.

6.3.3 Degree and dependency distributions

The in-degree and out-degree distributions of the nodes of all the 160659 fully autocatalytic graphs produced in these runs are shown in Figure 6.6. The mean in-degree for nodes of these graphs was 1.27, and the standard deviation was 0.50. The mean out-degree was 1.27, with standard deviation 1.75. The distributions are compared with the binomial distribution $B_{p^*}^{s-1}(k)$ (as expected for random graphs from the ensemble $G_s^{p^*}$; $p^* = 1.27/(s - 1)$) and the shifted binomial $B_p^{s-1}(k - 1)$ (as would be expected for a *random* autocatalytic graph). The in-distribution is quite similar in functional form to the shifted binomial for small in-degrees but departs from it for higher values. In contrast, the out-distribution falls off much more slowly, though it is not scale-free either because it is not a straight line in a log-log plot (Figure 6.7). However, as $s = 100$, the allowed values for the degree of a node cover a range of only two decades. If a portion of the out-degree distribution is a power-law then it is more likely to show up for graphs with higher s , where the degree distributions would span more decades. For such networks, with larger s , whether the fully autocatalytic graphs produced are scale-free or not is an open question.

The dependency distribution of the fully autocatalytic graphs produced in the runs (Figure 6.8) has a substantially larger mean than the distribution for graphs of the random phase (compare with Figure 6.3). This is consistent with the growth of interdependency observed in Figure 5.4. Further, as evident from Figure 6.8, the dependency distribution is also clearly different from, and much narrower than, the distribution for random graphs with a comparable connectivity $p^* = 1.27/(s - 1)$. The mean dependency of nodes of the fully autocatalytic graphs (30.93, with standard deviation 14.71) is slightly larger than the mean dependency for 1.5×10^6 random graphs, $G_s^{p^*}$, with $p^* = 1.27/(s - 1), s = 100$ (23.70, with standard deviation 30.82), but the maximum dependency observed for the fully autocatalytic graphs (100) is smaller than the maximum for the random graphs (163). In all the fully autocatalytic graphs, the minimum dependency was two, and the dependency distribution is small for small values of dependency. In contrast, the dependency distribution for the random graphs is maximum at zero dependency.

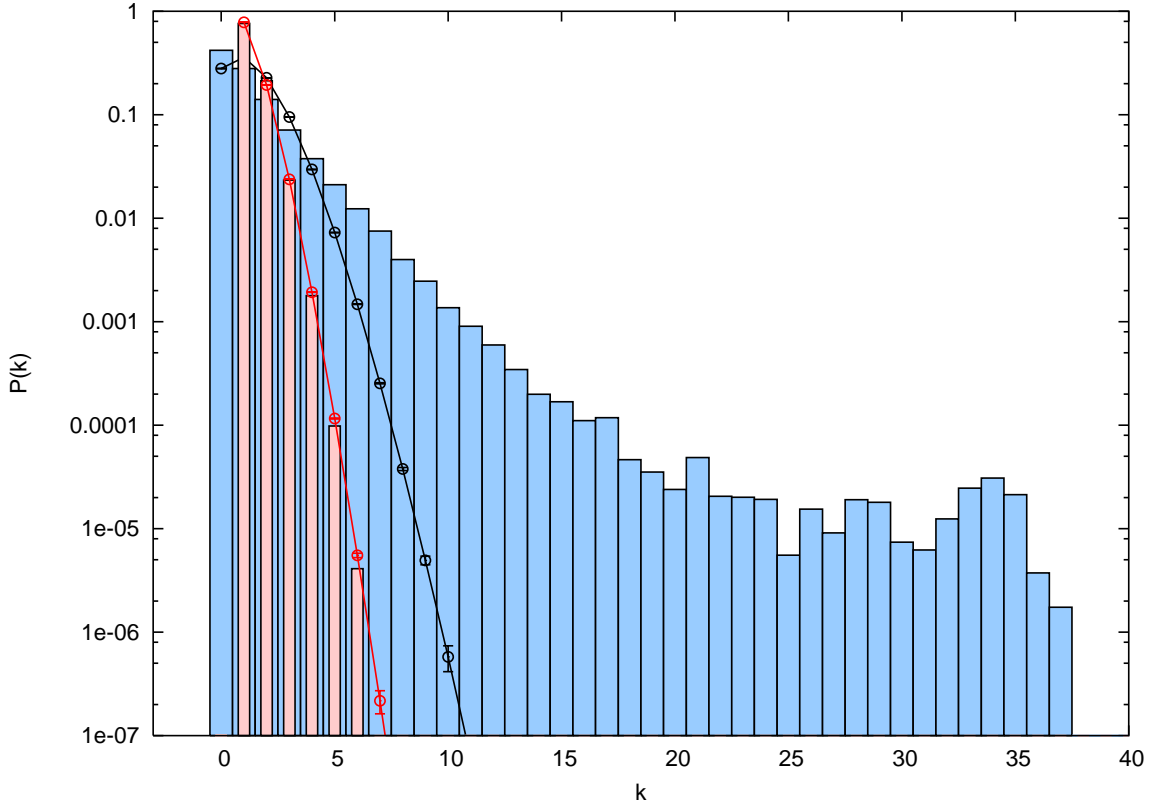


Figure 6.6: Light red bars: in-degree distribution of nodes of 160659 fully autocatalytic graphs from several runs with $s = 100, p = 0.0025$ (totaling 1.55 million iterations). Mean in-degree is 1.27. Light blue bars: out-degree distribution for the same graphs. Mean out-degree is 1.27. Black curve: the binomial distribution $B_p^{s-1}(k)$ expected for a random graph $G_s^{p^*}, p^* = 1.27/(s-1)$;

error bars are the expected standard deviation, $\sqrt{\frac{B_p^{s-1}(k)[1-B_p^{s-1}(k)]}{16065900}}$, for a finite sample of 160659 graphs. Red curve: the shifted binomial distribution $B_p^{s-1}(k-1)$ expected for a random fully autocatalytic set; error bars are the expected standard deviation, $\sqrt{\frac{B_p^{s-1}(k-1)[1-B_p^{s-1}(k-1)]}{16065900}}$.

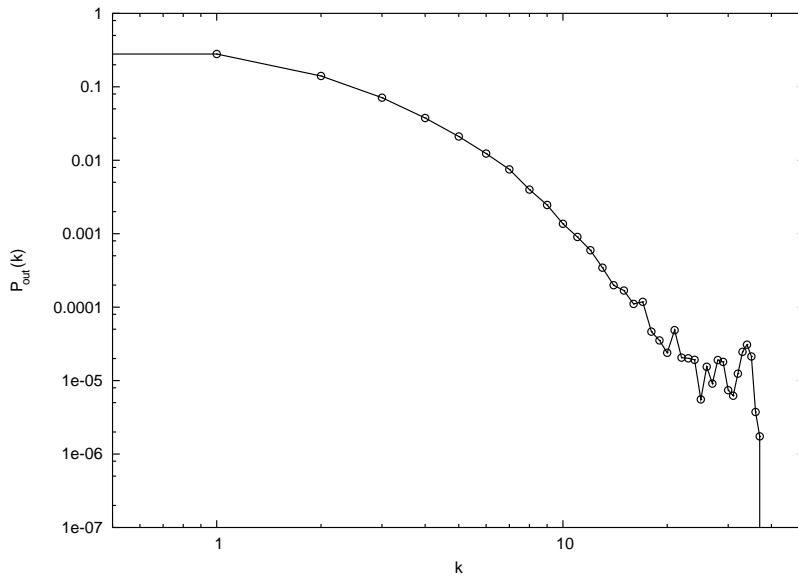


Figure 6.7: The out-degree distribution of fully autocatalytic sets in several runs with $s = 100, p = 0.0025$ (light blue bars in Figure 6.6) on a log-log plot. A scale-free distribution would be a straight line.

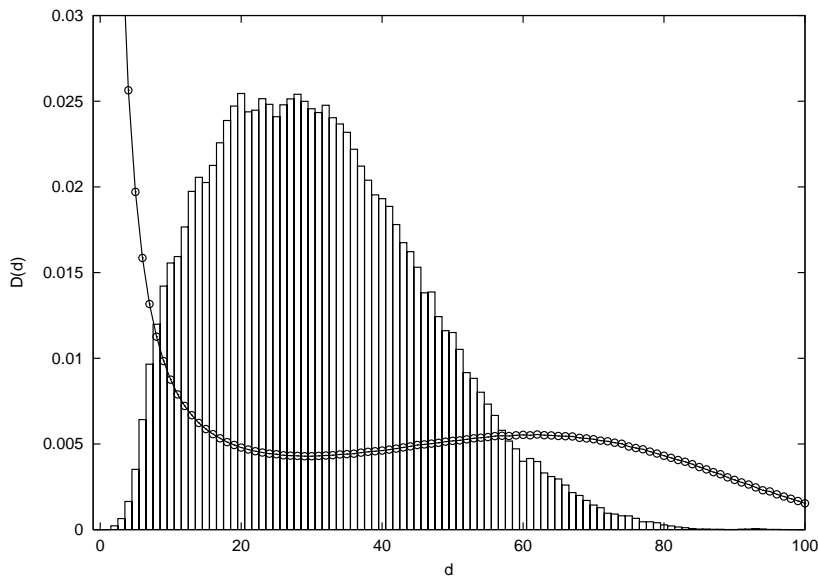


Figure 6.8: Bars: The dependency distribution of nodes of 160659 fully autocatalytic graphs from several runs with $s = 100, p = 0.0025$ (totaling 1.55 million iterations). Mean dependency is 30.93 with standard deviation 14.71. Circles: The dependency distribution of 1.5×10^6 graphs from the ensemble $G_s^{p^*}$, with $s = 100, p^* = 1.27/(s - 1)$. The mean dependency is 23.70, with standard deviation 30.82.

Chapter 7

Destruction of Autocatalytic Sets

7.1 Catastrophes and recoveries in the organized and growth phases

Once an ACS spans the entire graph the effective dynamics again changes although the microscopic dynamical rules are unchanged. At spanning, for the first time since the formation of the initial ACS, a node of the dominant ACS will be picked for removal. This is because at spanning all nodes belong to the dominant ACS and have non-zero relative populations; one node nevertheless has to be picked for removal. Most of the time the removal of the node with the least X_i will result in minimal damage to the ACS. The rest of the ACS will remain with non-zero relative populations, and the new node will repeatedly be removed and replaced until it once again joins the ACS. Thus s_1 will fluctuate between s and $s - 1$ most of the time. However, once in a while, the node that is removed happens to be playing a crucial role in the graph structure despite its low relative population. Then its removal can trigger large changes in the structure and catastrophic drops in s_1 and l . Alternatively, it can sometimes happen that the new node added can trigger a catastrophe because of the new graph structure it creates.

In Figure 5.5, which shows s_1 for the same run as that in Figure 5.3b but for a much longer time, one can observe several of the large and sudden drops in s_1 that will be discussed in this chapter. These ‘catastrophes’ in the organized and growth phases are followed by ‘recoveries’, in which s_1 rises on a certain timescale. Figure 7.1 shows the probability distribution $P(\Delta s_1)$ of changes in the number of nodes with $X_i > 0$; $\Delta s_1(n) \equiv s_1(n) - s_1(n - 1)$. The asymmetry between rises and drops as well as fat tails in the distribution are evident. For low p the probability of large drops is an order of magnitude greater than intermediate size drops (also see Figure 5.3).

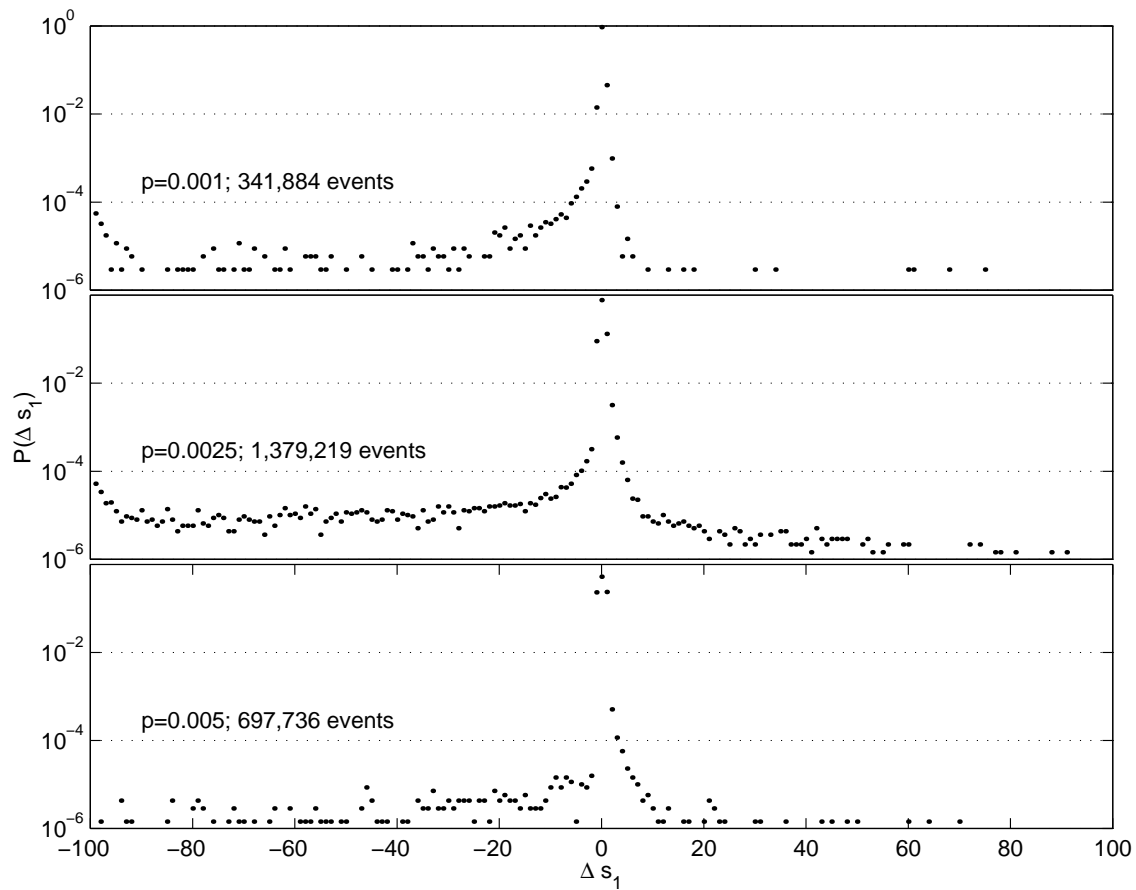


Figure 7.1: Probability distribution of changes in s_1 , the number of nodes with $X_i > 0$. $P(\Delta s_1)$ is the fraction of time steps in which s_1 changes by an amount Δs_1 in one time step in an ensemble of runs with $s = 100$ and $p = 0.001, 0.0025, 0.005$. Only time steps where an ACS initially exists are counted.

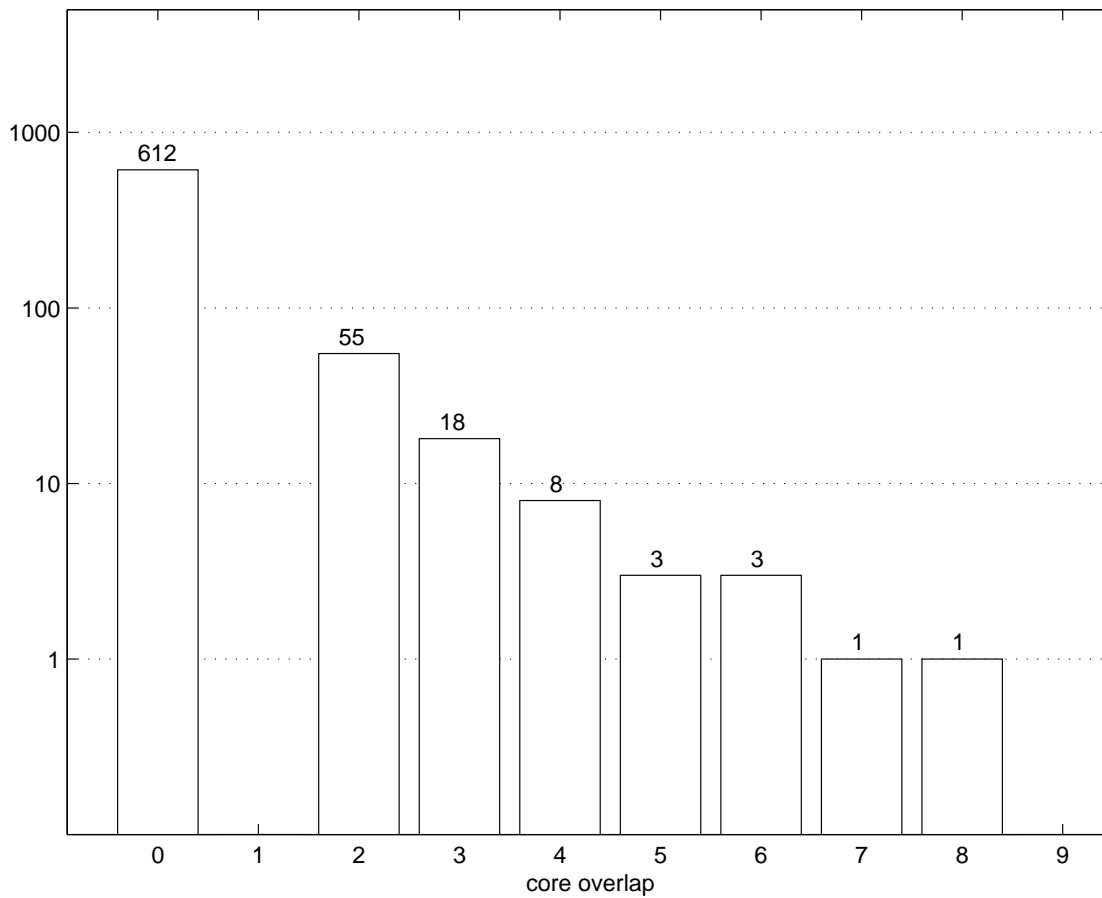


Figure 7.2: Crashes are predominantly core-shifts. A histogram of core overlaps for the 701 crashes, in which s_1 dropped by more than $s/2$, observed in several runs with $s = 100$ and $p = 0.0025$, totaling 1.55 million iterations. The attached CD contains data files for all these runs, as well as information about the 701 crashes (see appendix C).

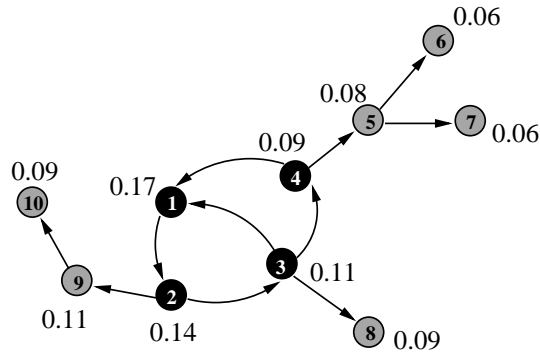


Figure 7.3: A graph with $\lambda_1 = 1.22$. The X_i values (rounded off to two decimal places) are shown adjacent to each node. Notice that if a node has only one incoming link then its X_i value is $1/\lambda_1$ times the X_i value of the node it is getting the link from. E.g. $X_6 = X_5/\lambda_1$. Thus, nodes further down a chain of single links have lower X_i . Nodes 6 and 7 have the lowest X_i .

7.2 Crashes and core-shifts

Definition 7.1: Crash.

A *crash* is a graph update event n for which $\Delta s_1(n) < -s/2$
(Jain and Krishna, 2002a,b).

A crash is an event in which a significant fraction (arbitrarily chosen as 50%) of the nodes become extinct. In several runs with $s = 100, p = 0.0025$ totaling 1.55 million iterations there were 701 crashes. The first task is to see if these large drops in s_1 are correlated to specific changes in the structure of the graph.

Definition 7.2: Core-shift.

A *core-shift* is a graph update event n for which $Ov(C_{n-1}, C_n) = 0$
(Jain and Krishna, 2002a,b).

Figure 7.2 shows a histogram of core overlaps $Ov(C_{n-1}, C_n)$ for these 701 crashes. 612 of these have zero core overlap, i.e., they are core-shifts. (If one looks at only those events in which more than 90% of the nodes went extinct, i.e., $\Delta s_1(n) < -0.9s$, then one finds 235 such events in the same runs, out of which 226 are core-shifts.) Of the remaining 89 crashes 10 were events in which the core remained unchanged and 79 were events in which the core was affected but some overlap remained between the new and old cores. Most of the crashes happen when there is a core-shift – a drastic change in the structure of the dominant ACS.

In the 612 core-shifts, the average number of incoming plus outgoing links is 2.27 for all nodes in the graph, 2.25 for the node that is removed and 1.25 for the new node. Thus the nodes whose removal or addition causes the crash are not excessively rich in links. ‘Nondescript’ nodes such as these cause system wide crashes because of their critical location in a small core (the

average core size at the 612 core-shifts is 6.3 nodes). Core-shifts in which the ACS is completely destroyed typically cause the largest damage (of 612 core-shifts these are 136 in number, with $|\Delta s_1| = 98.2 \pm 1.2$). The remaining 476 core-shifts in which an ACS exists after the core-shift have $|\Delta s_1| = 75.0 \pm 14.2$. The former constitute an increasing fraction of the crashes at smaller p values, causing the upturn in $P(\Delta s_1)$ at large negative Δs_1 for small p (Figure 7.1).

7.3 Addition and deletion of nodes from a graph

In order to understand what is happening during the crashes and subsequent recoveries I begin by examining the possible changes that an addition or a deletion of a node can make to the core of the dominant ACS.

7.3.1 Deletion of a node: keystone nodes

We have already seen how the deletion of a node can change the core – recall the discussion of keystone nodes in section 4.9: the removal of a keystone node results in a core-shift, i.e., a zero overlap between the cores of the dominant ACS before and after the removal. In an actual run a keystone node can only be removed if it happens to be one of the nodes with the least X_i . However, the core nodes are often ‘protected’ by having higher X_i . The reason for this is:

\mathbf{X} is an eigenvector of C with eigenvalue λ_1 . Therefore, when $\lambda_1 \neq 0$ it follows that for nodes of the dominant ACS, $X_i = (1/\lambda_1) \sum_j c_{ij} X_j$. If node i of the dominant ACS has only one incoming link (from the node j , say) then $X_i = X_j/\lambda_1$; X_i is ‘attenuated’ with respect to X_j by a factor λ_1 . The periphery of an ACS is a tree-like structure emanating from the core, and for small p most periphery nodes have a single incoming link. For instance, the graph in Figure 7.3, whose $\lambda_1 = 1.22$, has a chain of nodes $4 \rightarrow 5 \rightarrow 6$. The farther down such a chain a periphery node is, the lower is its X_i because of the cumulative attenuation. For such an ACS the ‘leaves’ of the periphery tree (such as node 6) will have the least X_i while core nodes will have larger X_i .

However, when $\lambda_1 = 1$ there is no attenuation. At $\lambda_1 = 1$ the core must be a cycle or a set of disjoint cycles (proposition 2.2), hence each core node has only one incoming link within the dominant ACS. All core nodes have the same value of X_i . As one moves out toward the periphery, $\lambda_1 = 1$ implies there is no attenuation, hence each node in the periphery that receives a single link from one of the core nodes will also have the same X_i . Some periphery nodes may have higher X_i if they have more than one incoming link from the core. Iterating this argument as one moves further outward from the core, it is clear that at $\lambda_1 = 1$ the core is not protected and in fact will always belong to \mathcal{L} (the set of nodes with the least X_i) if the dominant ACS spans the graph. We have already seen in section 4.9 that when $\lambda_1 = 1$ and the core is a single cycle every core node is a keystone node. Thus, when $\lambda_1 = 1$ the organization is fragile and susceptible to core-shifts caused by the removal of a keystone node.

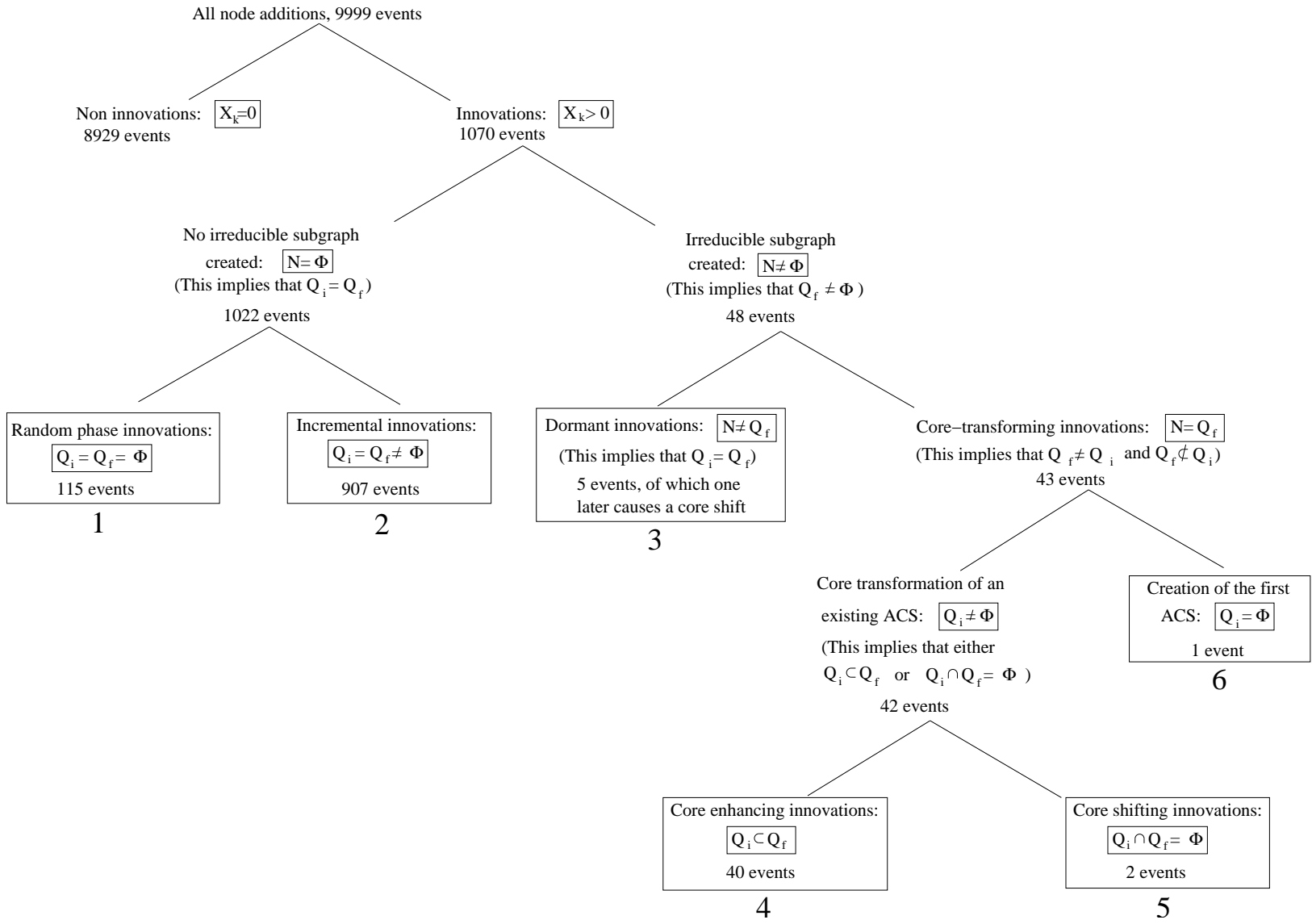


Figure 7.4: (opposite page) A hierarchy of innovations. Each node in this binary tree represents a class of node addition events. Each class has a name; the small box contains the mathematical definition of the class. All classes of events except the leaves of the tree are subdivided into two exhaustive and mutually exclusive subclasses (represented by the two branches emanating downward from the class). The number of events in each class pertain to the run of Figure 5.3b with a total of 9999 graph updates, between $n = 1$ (the initial graph) and $n = 10000$. In that run, out of 9999 node addition events, most (8929 events) are not innovations. The rest (1070 events), which are innovations, are classified according to their graph structure. X_k is the relative population of the new node in the attractor of equation (4.1) that is reached in step 1 of the graph dynamics immediately following the addition of that node. If the new node causes a new irreducible subgraph to be created, N is the *maximal* irreducible subgraph that includes the new node. If not, $N = \Phi$ (the empty set). Q_i is the core of the graph just before the addition of the node (just before step 3 of the graph dynamics) and Q_f the core just after the addition of the node. The six leaves of the innovation subtree are numbered from 1 to 6 and correspond to the classes discussed in the text. Some classes of events happen rarely (e.g., classes numbered 5 and 6) but have a major impact on the dynamics of the system. The precise impact of all these classes of innovations on the system over a short timescale (before the next graph update) as well as their probable impact over the medium term (upto a few thousand graph updates) can be predicted from the structure of N and the rest of the graph at the moment these innovations appear in a run.

7.3.2 Addition of a node: innovations

I now turn to the effects of the addition of a node. The removal and subsequent addition of a new node in a graph update creates a new graph that is likely to have a different attractor from the previous graph. In the new attractor the new node, denoted k , may become extinct, i.e., X_k may be zero, or it may survive, i.e., X_k is non-zero. If the new node becomes extinct then it remains in the set \mathcal{L} and there is no change to the dominant ACS. So I will focus on events in which the new node survives in the new attractor.

Definition 7.3: Innovation.

An *innovation* is a graph update event in which the relative population of the new node in the new attractor is non-zero, i.e. an event in which the new node survives till the next graph update (Jain and Krishna, 2002b, 2003b).

I will also use the term ‘innovation’ to refer to the new structures created – the new node and the new links brought in by the graph update event. Figure 7.4 shows a graph-theoretic classification of innovations in terms of a hierarchy. The innovations that have the least impact on the relative populations of the nodes and the evolution of the graph on a short timescale (of a few graph updates) are ones that do not affect the core of the dominant ACS, if it exists. Such innovations are of three types (see boxes 1–3 in Figure 7.4):

1. Random phase innovations. These are innovations that occur in the random phase when no ACS exists in the graph, and they do not create any new ACSs. These innovations are typically short lived and have little short or long term impact on the structure of the graph. In the displayed run the first random phase innovation appeared at $n = 79$ (node 25 in Figure 5.6c).

2. Incremental innovations. These are innovations that occur in the growth and organized phases, which add new nodes to the periphery of the dominant ACS without creating any new irreducible subgraph. See Figure 5.6f, $n = 3022$, for the first incremental innovation of the displayed run. In the short term these innovations only affect the periphery and are responsible for the growth of the dominant ACS. In a longer term they can also affect the core as chains of nodes from the periphery join the core of the dominant ACS.

3. Dormant innovations. These are innovations that occur in the growth and organized phases, which create new irreducible subgraphs in the periphery of the dominant ACS (e.g. the innovation at $n = 4696$, Figure 5.6p, that created the 2-cycle 36-74 in the periphery). These innovations too affect only the periphery in the short term. But they have the potential to cause core-shifts later if the right conditions occur (see section 7.4.3).

Innovations that do immediately affect the core of the existing dominant ACS are always ones which create a new irreducible subgraph. They are also of three types (boxes 4–6 in Figure 7.4):

4. Core enhancing innovations. These innovations result in the expansion of the existing core by the addition of new links and nodes from the periphery or outside the dominant ACS. They result in an increase of λ_1 of the graph. The innovation at $n = 3489$ (Figure 5.6l) is an example.

5. Core-shifting innovations. These are innovations that cause an immediate core-shift often accompanied by the extinction of a large number of nodes. The innovation at $n = 6062$ (Figure 5.6t) is an example (also see section 7.4.2).

6. Creation of the first ACS. This is an innovation that creates the first ACS in a graph which till then had none. In the displayed run, the first ACS was created at $n = 2853$ (Figure 5.6d,e). The innovation moves the system from the random phase to the growth phase.

Definition 7.4: Core transforming innovation.

An innovations of type 4, 5 or 6 which immediately affects the core of the dominant ACS will be called a *core transforming innovation* (Jain and Krishna, 2003a).

The following proposition makes precise the conditions under which a core transforming innovation can occur (Jain and Krishna, 2003a). Let $C'_n \equiv C_{n-1} - k$ denote the graph of $s - 1$ nodes just after the node k is removed from C_{n-1} . Q'_n will stand for the core of C'_n .

Proposition 7.1: Let N_n denote the maximal new irreducible subgraph that includes the new node at time step n . N_n will become the new core of the graph, replacing the old core Q_{n-1} , whenever either of the following conditions are true:

- (a) $\lambda_1(N_n) > \lambda_1(Q'_n)$ or,
- (b) $\lambda_1(N_n) = \lambda_1(Q'_n)$ and N_n is downstream of Q'_n .

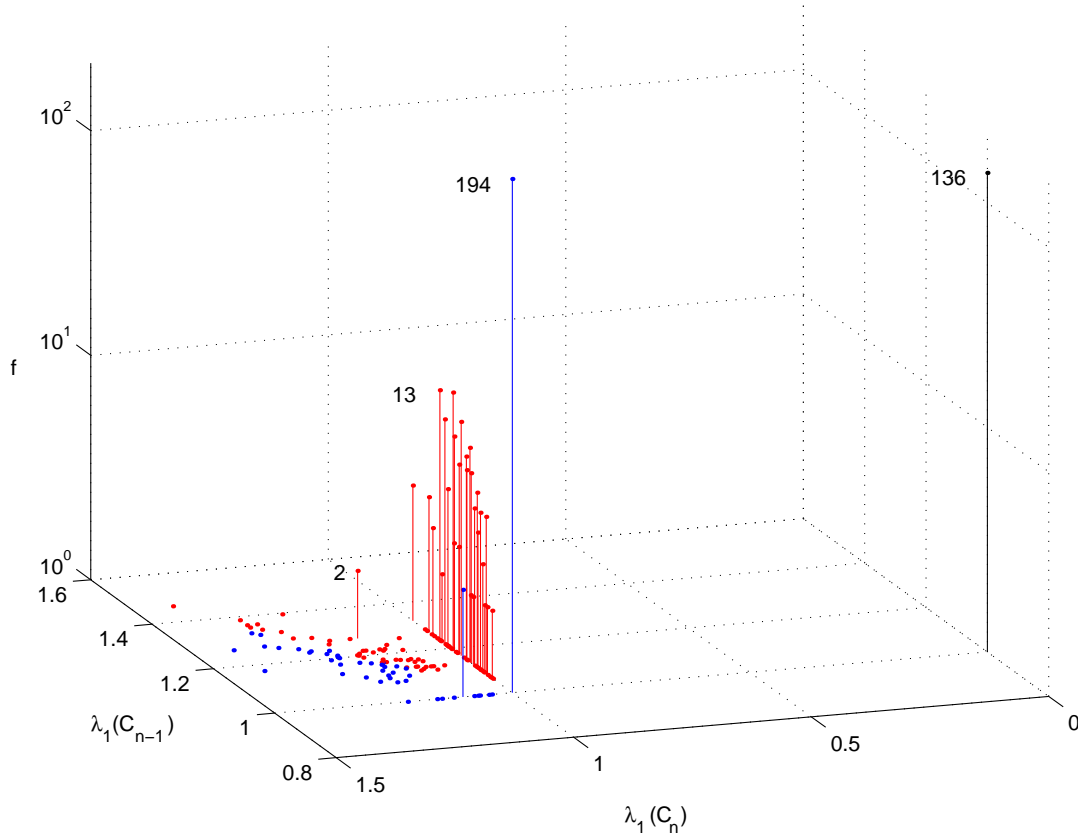


Figure 7.5: Classification of core-shifts into three categories. The graph shows the frequency, f , of the 612 core-shifts observed (see Figure 7.2) in a set of runs with $s = 100$ and $p = 0.0025$ vs. the λ_1 values before, $\lambda_1(C_{n-1})$, and after, $\lambda_1(C_n)$, the core-shift. Complete crashes (black: $\lambda_1(C_{n-1}) = 1$, $\lambda_1(C_n) = 0$), takeovers by core-transforming innovations (blue: $\lambda_1(C_n) \geq \lambda_1(C_{n-1}) \geq 1$) and takeovers by dormant innovations (red: $\lambda_1(C_{n-1}) > \lambda_1(C_n) \geq 1$) are distinguished. Numbers alongside vertical lines represent the corresponding f value.

Such a core transforming innovation will fall into category 4 above if $Q_{n-1} \subset N_n$. However, if Q_{n-1} and N_n are disjoint, we get a core-shift and the innovation is of type 5 if Q_{n-1} is non-empty or type 6 otherwise.

7.4 Classification of core-shifts

Using the insights from the above discussion of the effects of deletion or addition of a node, one can classify the different mechanisms that cause core-shifts. Figure 7.5 differentiates the 612 core-shifts observed among the 701 crashes. They fall into three categories: (i) complete crashes (136 events), (ii) takeovers by core-transforming innovations (241 events), and (iii) takeovers by dormant innovations (235 events).

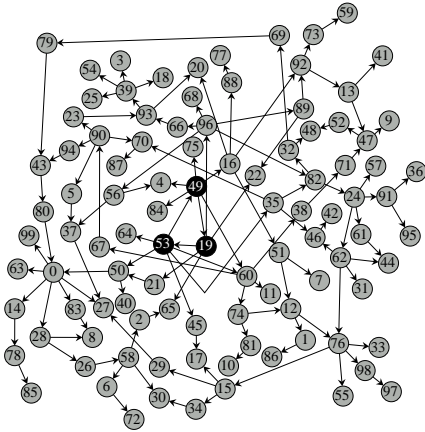
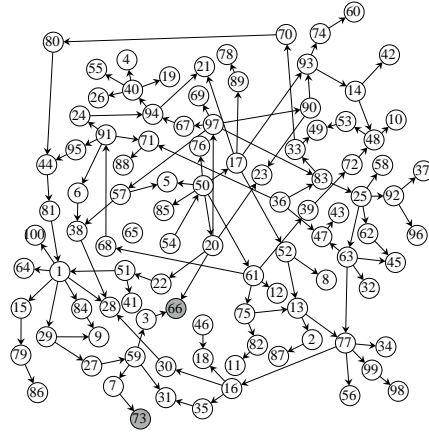
$n=8232$  $n=8233$ 

Figure 7.6: A complete crash. In the run displayed in Figure 5.3b at $n = 8232$ the core is a 3-cycle comprising nodes 20, 50 and 54. Node 54 is the node with the least X_i that is removed from the graph. This breaks the only cycle in the graph resulting in a graph, at $n = 8233$, that has no ACS. The system goes from the organized phase to the random phase, λ_1 drops from 1 to 0, and s_1 drops from 100 to 2.

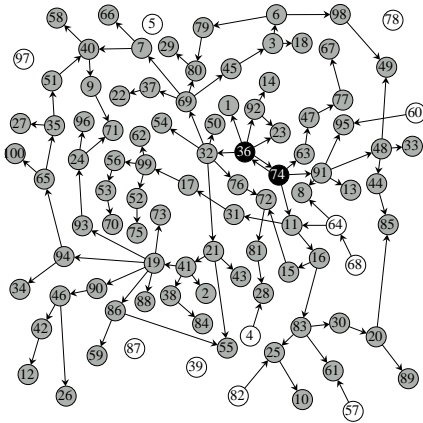
7.4.1 Complete crashes

A complete crash is an event in which an ACS exists before but not after the graph update. Such an event takes the system into the random phase. A complete crash can occur when a keystone node is removed from the graph. For example, in the run displayed in Figure 5.3b and 5.6, at $n = 8232$ (see Figure 7.6), the graph had $\lambda_1 = 1$ and its core was the simple 3-cycle of nodes 20, 50 and 54. As we have seen above, when the core is a single cycle every core node is a keystone node and is also in the set \mathcal{L} of nodes with the least X_i . Node 54 was removed, thus disrupting the 3-cycle. The resulting graph, at $n = 8233$, had no ACS and λ_1 dropped to zero. As discussed earlier, graphs with $\lambda_1 = 1$ are the ones that are most susceptible to complete crashes. This can be seen in Figure 7.5: every complete crash occurred from a graph with $\lambda_1(C_{n-1}) = 1$.

7.4.2 Takeovers by core transforming innovations

An example of a takeover by a core-transforming innovation is given in Figure 7.7, taken from the example run of Figure 5.3b. At $n = 6061$ the core was a single cycle comprising nodes 36 and 74. Node 60 was replaced at $n = 6062$ creating a 5-cycle comprising nodes 60, 21, 41, 19 and 73, downstream from the old core. The graph at $n = 6062$ has one cycle feeding into a second cycle that is downstream from it. We have already seen in section 4.6 (see the discussion of Example 4) that for such a graph only the downstream cycle is non-zero and the upstream cycle and all nodes dependent on it become extinct. Thus, the new cycle becomes the new core and the old core

n=6061



n=6062

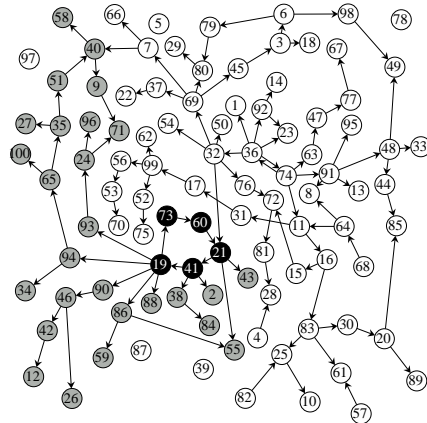
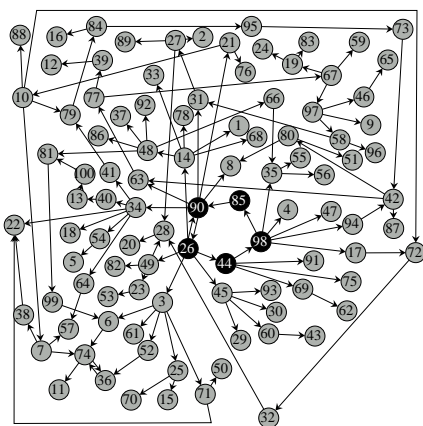


Figure 7.7: Takeover by a core-transforming innovation. In the run displayed in Figure 5.3b at $n = 6061$ the core is a 2-cycle comprising nodes 36 and 74. The graph update creates a core-transforming innovation – a new 5-cycle downstream from the 2-cycle 36-74. As a result the 2-cycle and all nodes dependent on it become extinct at $n = 6062$ and s_1 drops from 100 to 32. Because an ACS survives this event, the system is in the growth phase at $n = 6062$.

n=5041



n=5042

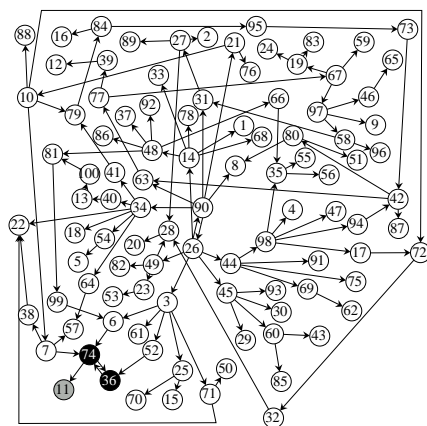


Figure 7.8: Takeover by a dormant innovation. In the run displayed in Figure 5.3b at $n = 5041$ the core has two overlapping cycles. Downstream from the core is a 2-cycle comprising nodes 36 and 74 which formed earlier at $n = 4696$. Node 85 happens to be one of the nodes with the least X_i and is removed from the graph. Thus, at $n = 5042$, the graph consists of one 2-cycle, 36-74, downstream from another 2-cycle, 26-90. As a result, the upstream cycle, 26-90, and all nodes dependent on it become extinct and s_1 drops from 100 to 3. Because an ACS survives this event, the system is in the growth phase at $n = 5042$.

becomes extinct resulting in a core-shift. This is an example of condition (b) for a core-transforming innovation. For all such events in Figure 7.5, $\lambda_1(Q'_n) = \lambda_1(C_{n-1})$ because k happened not to be a core node of C_{n-1} . Thus, these core-shifts satisfy $\lambda_1(C_n) = \lambda_1(N_n) \geq \lambda_1(Q'_n) = \lambda_1(C_{n-1}) \geq 1$ in Figure 7.5.

7.4.3 Takeovers by dormant innovations

Dormant innovations, which create an irreducible structure in the periphery of the dominant ACS that does not affect its core at that time, were discussed in section 7.3.2. An example is the 2-cycle comprising nodes 36 and 74 formed at $n = 4696$. At a later time such a dormant innovation can result in a core-shift if the old core gets sufficiently weakened.

In this case the core has become weakened by $n = 5041$, when it has $\lambda_1 = 1.24$ (Figure 7.8). The structure of the graph at this time is very similar to the graph in Figure 4.5a. Just as node 3 in Figure 4.5a was a keystone node, here nodes 44, 85, and 98 are keystone nodes because removing any of them results in a graph like Figure 4.5b, consisting of two 2-cycles, one downstream from the other.

Indeed, at $n = 5041$, node 85 is replaced and the resulting graph at $n = 5042$ has a 2-cycle (36 and 74) downstream from another cycle (26 and 90). Thus, at $n = 5042$, nodes 36 and 74 form the new core with only one other downstream node, 11, being non-zero. All other nodes become extinct resulting in a drop in s_1 by 97. A dormant innovation can takeover as the new core only following the removal of a keystone node that weakens the old core. In such an event the new core necessarily has a lower (but non-zero) λ_1 than the old core, i.e., $\lambda_1(C_{n-1}) > \lambda_1(C_n) \geq 1$ (see Figure 7.5).

Note that 85 is a keystone node and the graph is susceptible to a core-shift *because* of the innovation that created the cycle 36-74 earlier. If the cycle between 36 and 74 were absent 85 would not be a keystone node because its removal would still leave part of the core intact (nodes 26 and 90).

7.5 Timescale of crashes

I will denote by n_s the time elapsed between successive crashes, not counting the time spent in the recovery from the previous crash (i.e., the time from the previous crash to the first subsequent spanning of the graph by the dominant ACS). Figure 7.9a shows the distribution of n_s values for the 701 crashes, discussed above, observed in runs with $s = 100, p = 0.0025$. The average $\tau_s \equiv \overline{n_s} \approx 1088.3$ and the standard deviation of n_s values is ≈ 1581.0 for these 701 crashes. Figure 7.9b shows the distribution of $\log_{10} n_s$ values. The distribution and the τ_s value must be taken with caution because the distribution appears to be a very broad one (the standard deviation of n_s values is larger than τ_s) and 701 instances may not be enough to specify it accurately.

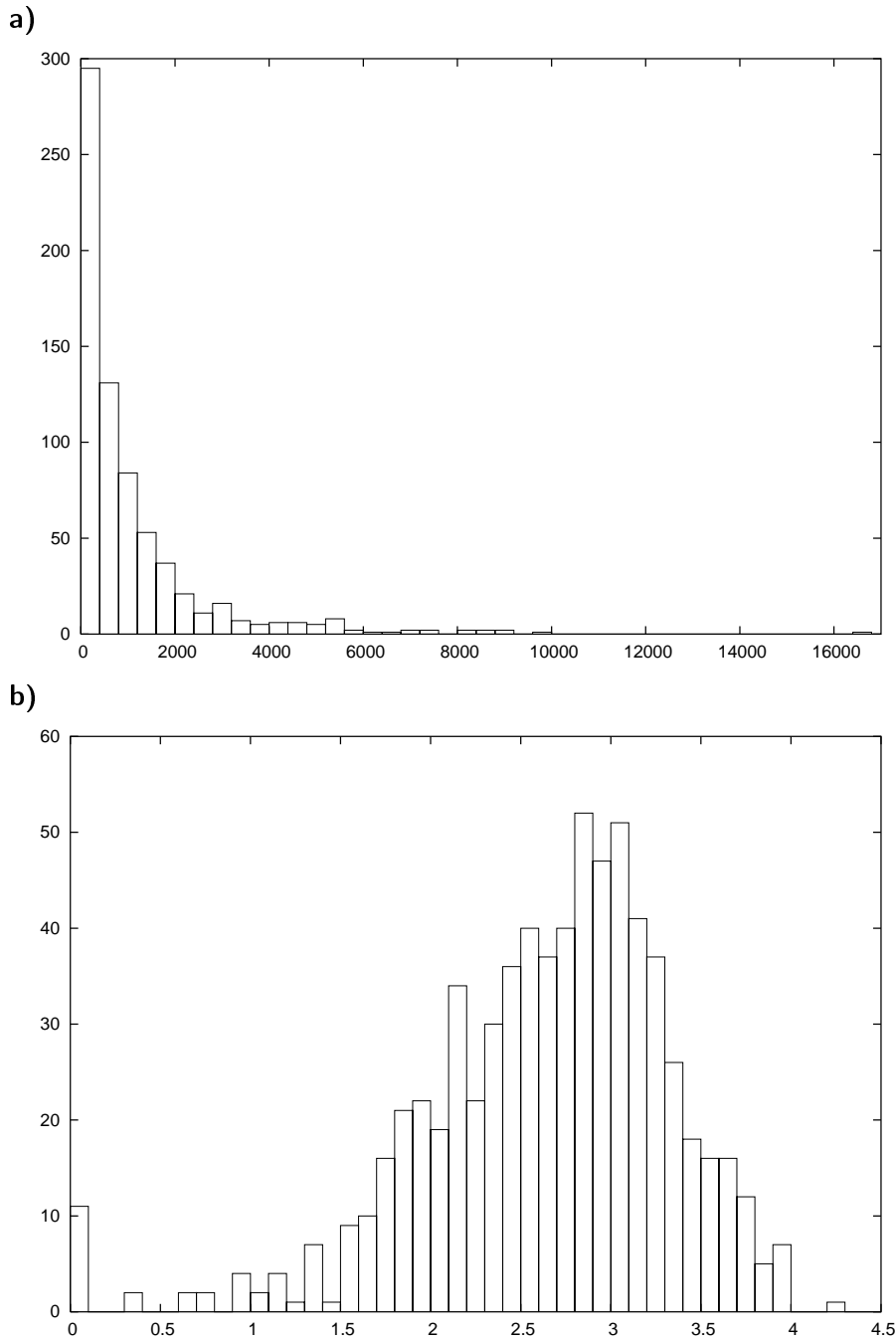
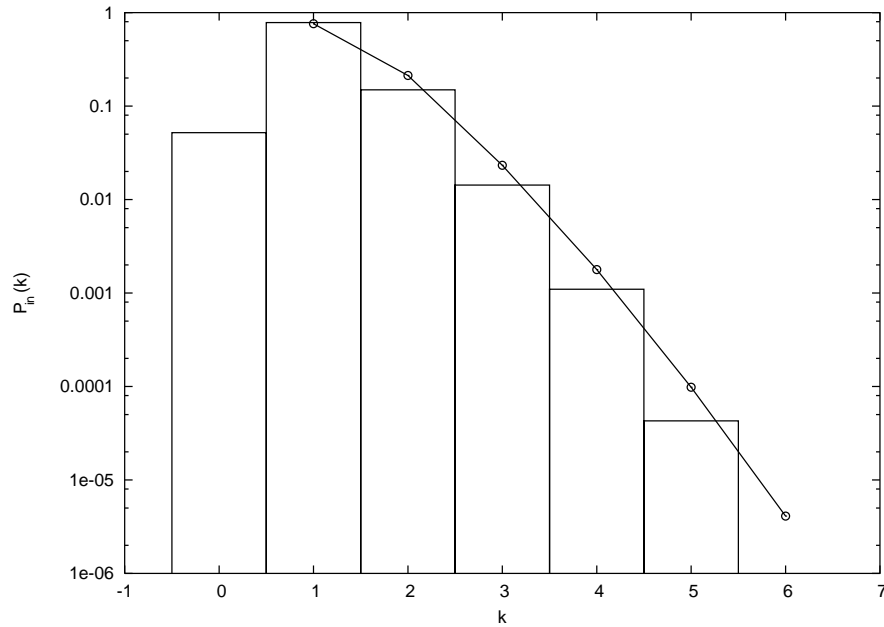


Figure 7.9: **a.** Distribution of times elapsed between crashes (not counting the recovery time from the previous crash or beginning of the run), n_s , for the 701 crashes observed in runs with $s = 100, p = 0.0025$. $\min\{n_s\} = 1, \max\{n_s\} = 16625, \tau_s \equiv \overline{n_s} \approx 1088.3$, and the standard deviation of the 701 n_s values is ≈ 1581.0 . The bin size is 400. **b.** Distribution of $\log_{10}n_s$ values for the same 701 crashes. The bin size is 0.1.

a)



b)

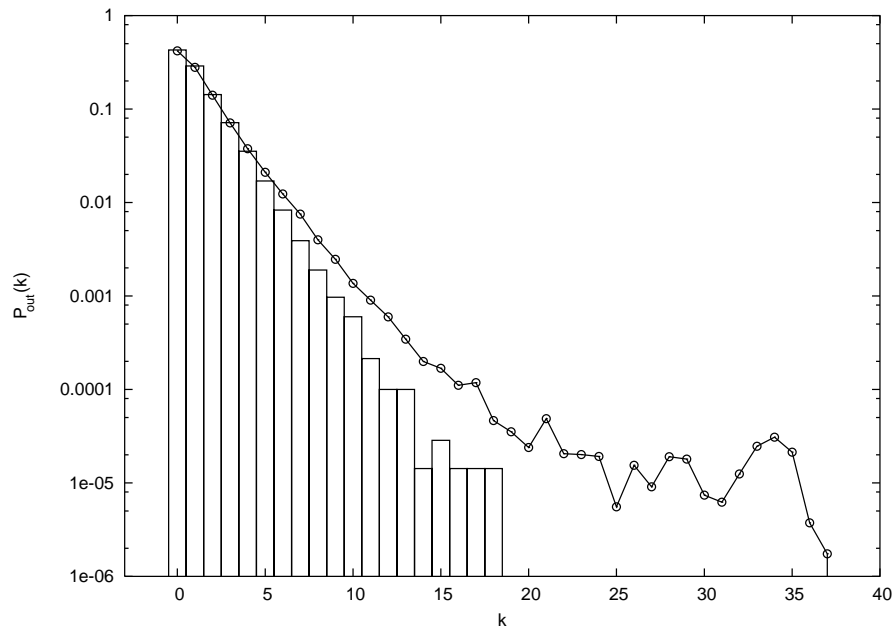


Figure 7.10: **a.** Comparison of the in-degree distribution of nodes of the 701 graphs just before each crash (bars) with the in-degree distribution of all fully autocatalytic graphs in the same runs (line with circles). **b.** Comparison of the out-degree distributions for the same graphs as in (a).

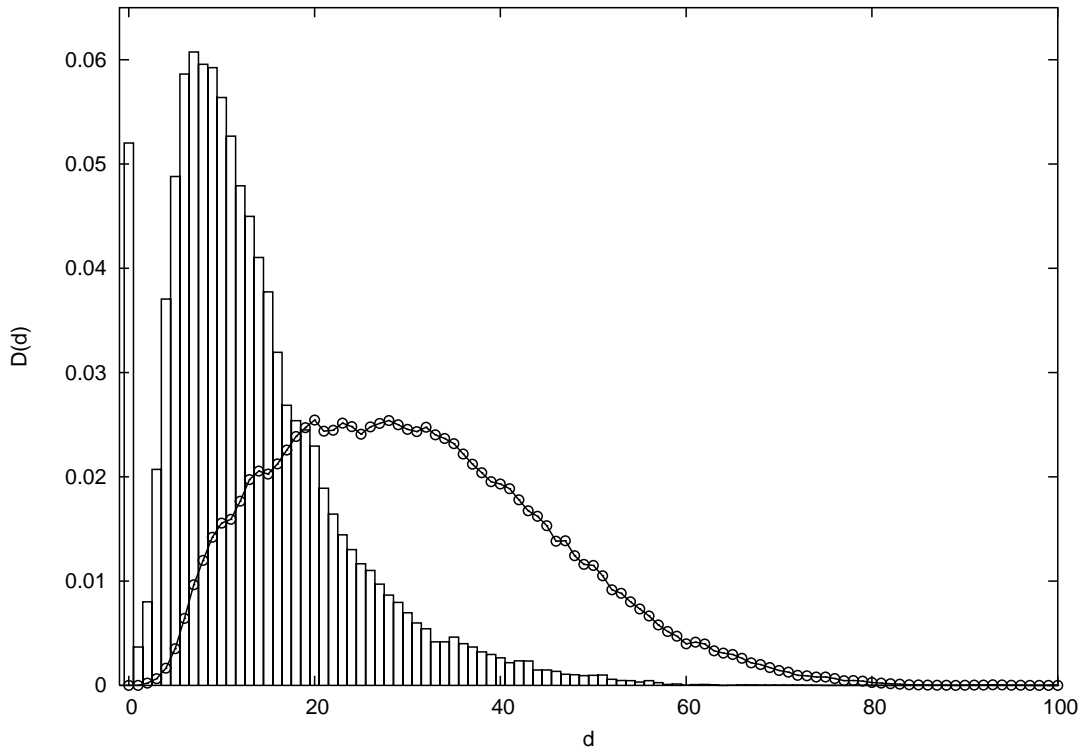


Figure 7.11: Comparison of the dependency distribution of nodes of the 701 graphs just before each crash (bars) with the distribution for all fully autocatalytic graphs in the same runs (circles).

7.6 Recoveries

After a complete crash the system is back in the random phase. In $O(s)$ graph updates each node is removed and replaced by a randomly connected node, resulting in a graph as random as the initial graph. Then the process starts again, with a new ACS being formed after an average of $1/p^2s$ time steps and then growing to span the entire graph after, on average, $(1/p) \ln(s/s_0)$ time steps, where s_0 is the size of the initial ACS that forms in this round (typically $s_0 = 2$ for small p).

After other catastrophes, an ACS always survives. In that case the system is in the growth phase and immediately begins to recover, with s_1 growing exponentially on a timescale $1/p$. Note that these recoveries happen because of innovations (mainly of type 2 and 4, and some of type 3).

7.7 Structure of the graph just before a crash

The in-degree and out-degree distributions of the nodes of the 701 graphs just before each crash are shown in Figure 7.10. The distributions are compared with the distributions for all fully autocatalytic graphs produced in the same runs. Both the distributions fall off faster than the distributions for all fully autocatalytic graphs.

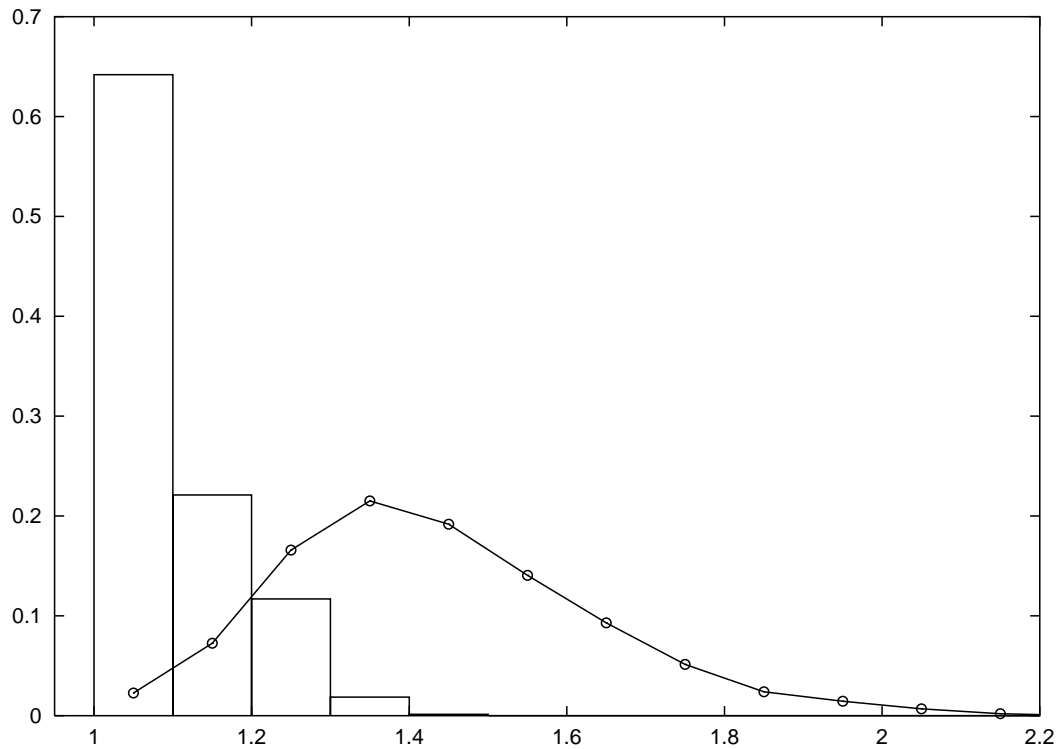


Figure 7.12: Comparison of the distribution of Perron-Frobenius eigenvalues of the 701 graphs just before each crash (bars) with the distribution for all fully autocatalytic graphs in the same runs (circles).

Another interesting difference between the graphs just before a crash and all fully autocatalytic graphs lies in their dependency distributions: The dependency distribution of the graphs before crashes (Figure 7.11) is bimodal, in contrast to the distribution for all fully autocatalytic graphs which is unimodal and has a larger mean.

Figure 7.12 compares the distribution of Perron-Frobenius eigenvalues for the 701 graphs with the distribution for all the fully autocatalytic graphs. For the graphs just before each of the 701 crashes the mean Perron-Frobenius eigenvalue is 1.07, with standard deviation 0.10 – clearly lower than the mean for the fully autocatalytic graphs, which is 1.43, with standard deviation 0.20. The three mechanisms that cause core-shifts, discussed previously, are all more likely to happen with graphs whose cores are cycles. Therefore, it is not surprising that the graph just before a crash tends to have a Perron-Frobenius value close to unity.

Chapter 8

Robustness of the ACS Growth Mechanism

8.1 Variants of the model

In this chapter, I examine the effect of various modifications to the model rules on the formation and growth of ACSs. These modifications relax several of the simplifications that have been made, which depart from realism but make the model simpler to analyze:

1. c_{ij} take values 0 and 1 only; all catalysts have the same catalytic efficiency.
2. c_{ij} take positive values only; negative links – inhibitors – are not present in the model.
3. Diagonal elements c_{ii} are zero; no self-replicators are allowed.
4. The node with the *least* X_i is removed at each graph update; extremal selection.
5. If several nodes have the same least X_i only one is removed.
6. The total number of nodes is fixed; the rate of node removals and node additions is exactly the same.
7. The population dynamics is linear in the y_i variables.

I consider the following variants of the model, that relax these simplifications:

1. **Variable link strengths.** c_{ij} , when non-zero, are allowed to take any value in the interval $[0, 1]$. This relaxes simplification (1).
2. **Negative links.** c_{ij} , when non-zero, are allowed to take negative values also. This relaxes simplifications (1) and (2).

3. **Self-replicators.** The diagonal elements, c_{ii} , are allowed to take non-zero values. This relaxes simplification (3).
4. **Non-extremal selection.** Simplification (4) is relaxed in three variants, in which the dynamics is made non-extremal in different ways:
 - (a) A fixed fraction f of the nodes with the least X_i are replaced at each graph update.
 - (b) A single node is picked for removal, with a probability proportional to $1/X_i$, at each graph update. When some nodes have $X_i = 0$ then one of them is picked randomly.
 - (c) The selection depends on a parameter, denoted q . At each graph update, the node to be removed is selected from the set of nodes with least X_i with a probability q , or randomly from all nodes with a probability $1 - q$.
5. **Variable number of nodes.** A fixed threshold x_t is chosen and at each graph update all nodes with $X_i < x_t$ are removed and one new node is brought in. This relaxes simplifications (5) and (6).
6. **Different population dynamics.** An equation for \dot{x}_i in which the first term is quadratic in the relative population variables is used instead of equation (4.1). This relaxes simplification (7).

8.2 Variable link strengths

The first modification I examine is allowing c_{ij} to take values in the interval $[0, 1]$, instead of just the values 0 or 1. The initial graph is constructed as follows: for each ordered pair (i, j) with $i \neq j$, c_{ij} is non-zero with probability p and $c_{ij} = 0$ with probability $1 - p$. If non-zero, the value of c_{ij} is randomly picked from the interval $[0, 1]$ with uniform probability. As before c_{ii} is set to zero for all i to disallow self-replicators. Step 3 of the graph dynamics – addition of a new node – is similarly modified. Apart from these alterations the model remains unchanged.

Figure 8.1 shows a run with these modifications in the rules. The same behaviour is seen. There is a ‘random phase’ where there is no ACS and the graph remains random. The chance formation of an ACS on an average timescale $\tau_a = 1/p^2s$ triggers the ‘growth phase’ in which the number of non-zero nodes grows exponentially with a characteristic timescale $\tau_g = 1/p$, until the ACS spans the entire graph.

This is expected because most of the analytical results hold, with minor modifications, for this variant too. The Perron-Frobenius theorem holds for the adjacency matrices of the graphs produced because they are still non-negative. The only significant modification in the analytical results is that now λ_1 can take values between 0 and 1 also. For example, consider the 2-cycle shown in Figure 8.2. The strengths of the two links are a and b , any real numbers in the interval $[0, 1]$. For such a graph $\lambda_1 = \sqrt{ab}$.

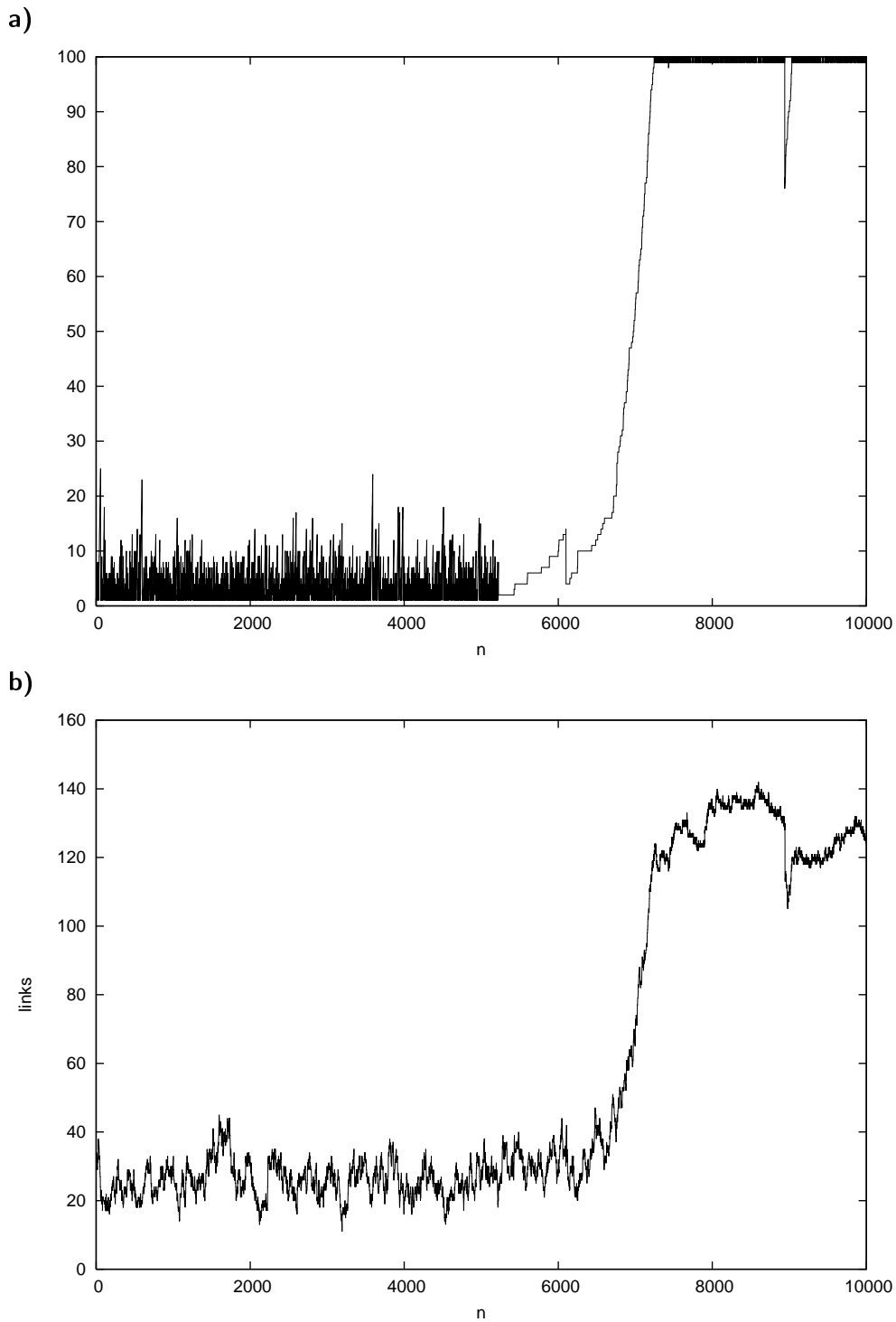


Figure 8.1: A run with $s = 100, p = 0.0025$ with variable strength links: c_{ij} when non-zero can take any value in the interval $[0, 1]$. **a.** number of nodes with $X_i > 0, s_1$, versus time, n . **b.** number of links versus n .

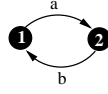


Figure 8.2: A two cycle with link strengths $a, b \in [0, 1]$. The Perron-Frobenius eigenvalue of this graph is \sqrt{ab} .

Thus, the condition $\lambda_1 \geq 1$ is changed to $\lambda_1 > 0$ in all propositions that contain it. Proposition 2.1(ii) is modified to read: If a graph C has a closed walk then $\lambda_1 > 0$. Proposition 3.2(iii) is similarly modified: If a graph C has an ACS then $\lambda_1 > 0$.

The only difference this makes to the dynamics of the system is that in this variant it is much less likely for two disjoint ACSs with the same λ_1 value to exist in some graph. In the original model two or more ACSs, typically cycles, often coexisted in runs with small p (see Figures 5.6j,u). With variable link strengths even if two disjoint cycles form the chance of their having exactly the same λ_1 value is negligible.

8.3 Negative links: emergence of cooperation

Now I generalize the model to include inhibitory reactions (where a species can decrease the rate of production of another species) along with variable link strengths. I implement this by modifying the way links are assigned in the initial random graph and to the new node at each graph update: if c_{ij} is chosen to be non-zero then it is assigned randomly a value in the interval $[-1, 1]$ if $i \neq j$ or $[-1, 0]$ if $i = j$ (self-replicators continue to be disallowed but self-inhibitors are possible). With negative links the populations can become negative. To prevent this a cutoff must be put on \dot{y}_i when y_i becomes zero:

$$\dot{y}_i = \begin{cases} r_i & \text{if } y_i > 0 \text{ or } r_i \geq 0 \\ 0 & \text{if } y_i = 0 \text{ and } r_i < 0 \end{cases} \quad (8.1)$$

$$\text{where } r_i = \sum_{j=1}^s c_{ij} y_j - \phi y_i.$$

For simplicity I retain the form of (4.2) although a more realistic chemical interpretation would require \dot{y}_i to be proportional to y_i for inhibitory reactions.

The relative population dynamics that follows from (8.1) using $x_i = y_i / \sum_{j=1}^s y_j$ is:

$$\dot{x}_i = \begin{cases} f_i & \text{if } x_i > 0 \text{ or } f_i \geq 0 \\ 0 & \text{if } x_i = 0 \text{ and } f_i < 0 \end{cases} \quad (8.2)$$

$$\text{where } f_i = \sum_{j=1}^s c_{ij} x_j - x_i \sum_{k,j=1}^s c_{kj} x_j.$$

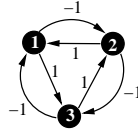


Figure 8.3: A graph that has a limit cycle attractor. The negative links, each of strength -1 , form a cycle. The positive links, each of strength 1 , form another cycle running in the opposite direction. In the attractor each x_i oscillates around a mean value $1/3$ with a frequency $2\pi\sqrt{3}$. The amplitude of oscillation depends on the initial condition but is the same for each x_i .

The cutoff in the population dynamics makes it a nonlinear equation. As a result now the attractor need not be only a fixed point. For most graphs I have encountered in simulations the attractor of (8.2) has been a fixed point. In less than 0.2% cases the attractor has been a limit cycle where the relative populations of the nodes oscillate. I have not observed any other types of attractors. The simplest type of graph having a limit cycle attractor consists of 3 nodes and is displayed in Figure 8.3. For this graph each x_i oscillates around a mean value of $1/3$ with a frequency $2\pi\sqrt{3}$. The amplitude of oscillation depends on the initial condition but is always equal for the 3 nodes. If the amplitudes are smaller than $1/3$ then none of the x_i hit zero and the cutoff in (8.2) plays no role in the oscillations. However if arbitrarily random small changes are made to the interaction strengths of the graph the oscillations of the x_i start hitting zero and the cutoff comes into play. In general the cutoff seems to play an important role in limit cycle attractors. It is only in some special cases and for particular initial conditions that the relative populations of nodes oscillate without hitting zero. Numerical observations indicate that the property of having a limit cycle attractor is structurally stable, i.e., a limit cycle attractor remains if sufficiently small changes are made to the interaction strengths of a given graph having a limit cycle attractor.

The theorems used to analyze the attractors of the original model depended on the matrix C being non-negative and hence no longer hold for the system with negative links. However numerical simulations of the system show behaviour very similar to the original system (Jain and Krishna, 2001) despite the slight bias toward negative links (because self-inhibitors are allowed but not self-replicators). Figure 8.4 shows the results of a run with $s = 100$ and $p = 0.005$. The number of nodes with $X_i \neq 0$, s_1 , after the n^{th} addition of a new node, the number of positive ($c_{ij} > 0$), l_+ , and negative links ($c_{ij} < 0$), l_- , are displayed. Similar to the original model, the curves have three distinct regions. Initially s_1 is small; most of the nodes have zero X_i . l_+ and l_- also do not vary much from their initial value ($\approx ps^2/2 = 25$) and remain approximately equal. In the second region s_1 and l_+ show a sharp increase while l_- decreases. In the third region the growth of s_1 and l_+ stops and almost all nodes have non-zero X_i in contrast to the initial period. The number of positive links have increased to several times their initial value while the number of negative links has declined to about 10. I have observed the same qualitative behaviour in several runs with p values ranging from 0.00002 to 0.01 and $s = 100, 150, 200$.

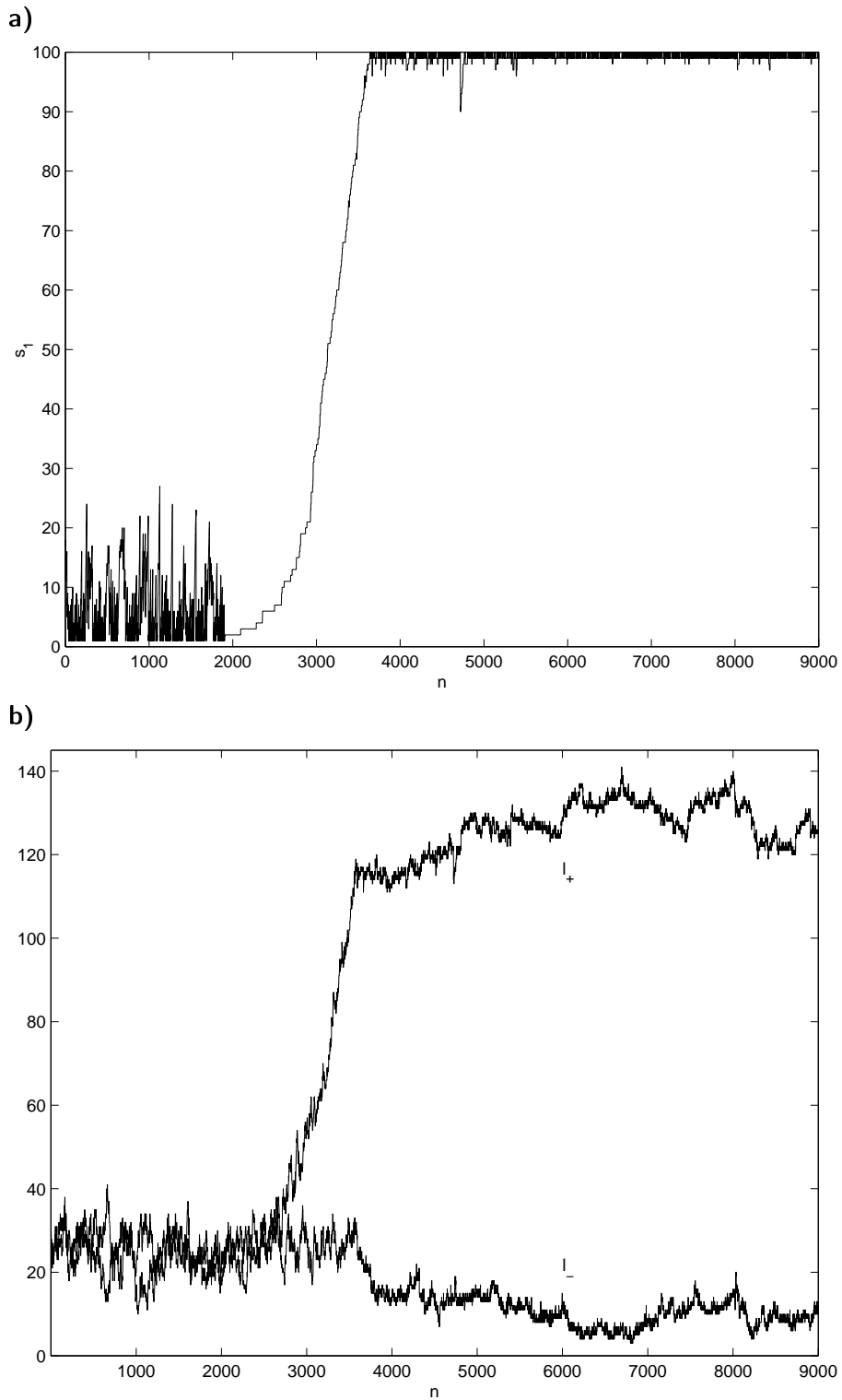


Figure 8.4: A run with $s = 100, p = 0.005$ where negative links are allowed. **a.** the number of nodes with $X_i > 0$, s_1 , versus time, n . **b.** the number of positive, l_+ , and negative links, l_- , versus n .

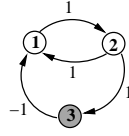


Figure 8.5: Example of a destructive parasite. A new node, 3, added to an existing 2-cycle, destroys the 2-cycle because of the negative link to node 1. The attractor is $\mathbf{X} = (0, 0, 1)^T$.

Again the explanation for the above behaviour lies in the formation and growth of autocatalytic sets. The definition of an ACS has to be slightly modified: an ACS is a subgraph, each of whose nodes has at least one incoming *positive* link from a node belonging to the same subgraph. Proposition 3(i) also has to be similarly modified: An ACS must contain a cycle of *positive* links.

Upto $n = n_a = 1904$, there is no ACS; the graph has no cycles of positive links. For such graphs, I find that $X_i = 0$ for most nodes except a few at which the longest paths of positive links terminate, with intermediate nodes not having incoming negative links. This is a numerical observation that is similar to proposition 4.2. Thus most nodes have $X_i = 0$. Nodes with $X_i \neq 0$ will also join the set \mathcal{L} of nodes with least X_i if one of their supporting nodes is picked for removal from the system. Hence, all nodes are susceptible to be removed sooner or later; the graph remains as random as the initial graph and so s_1 , l_+ and l_- hover around their initial values. The dramatic increases in s_1 and l_+ are triggered by the chance formation of an ACS at $n = n_a$. In this system too an ACS will inevitably form by pure chance sooner or later. The ‘time of appearance’ of an ACS can again be approximated by the time of formation of a 2-cycle of positive links. As one wants the 2-cycle to contain positive links only, p in the previous formula for τ_a has to be replaced by $p/2$. Thus $\tau_a \approx 4/p^2s (= 1600$ for $p = 0.005$ and $s = 100)$ and $P(n_a) = \frac{p^2s}{4}(1 - \frac{p^2s}{4})^{n_a-1}$.

From $n = 1904$ to $n = 3643$ (when s_1 first reaches s), I again find that the set of nodes with $X_i \neq 0$ is an ACS; the ‘dominant ACS’. This is also a numerical observation. The proof of proposition 4.3 no longer holds but the system nevertheless shows identical behaviour in this respect to the system with only positive links. Hence, as long as the dominant ACS does not span the entire graph, i.e. $s_1 < s$, there are nodes outside it with $X_i = 0$ which form the set \mathcal{L} . Therefore, none of the nodes in the dominant ACS can be removed in the next graph update.

All the processes that can happen in the original model when a new node is brought in (numbered 1, 2 and 3 in section 6.2) happen in this system with the same effects. The only new possibility to which the presence of negative links leads is when the new node joins the dominant ACS and some of the other nodes in the dominant ACS receive negative links from it. Then those nodes may become extinct causing s_1 to decrease. An example of this is shown in Figure 8.5. A new node, 3, is added to a previously existing 2-cycle. It gets a positive incoming link from node 2 and a negative outgoing link to node 1. This negative link destroys the ACS. In the attractor only node 3 is non-zero while node 1 and 2 have $X_i = 0$. Node 3 is like a destructive parasite that feeds on the the host ACS (nodes 1 and 2) to increase its own relative population, in the process

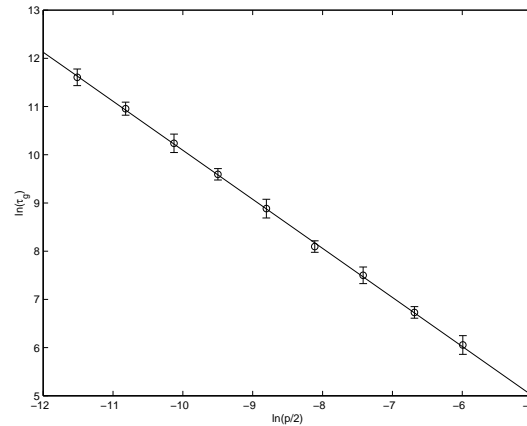


Figure 8.6: Dependence of τ_g on p for the model with negative links. Each data point shows the average of $\ln \tau_g$ over 10 different runs with $s = 100$, $x_0 = 10^{-4}$ and the given p value. The error bars correspond to one standard deviation of $\ln \tau_g$ values for each p . The best fit line has slope -1.02 ± 0.03 and intercept -0.08 ± 0.27 , consistent with the expected slope -1 and intercept 0 .

destroying the host. The negative link is essential for the destructive property of such parasites; in the system with only positive links only benign parasites are possible that do not harm the ACS upon which they are feeding. This example also shows that propositions 4.3 and 6.1 are no longer true; the set of nodes with $X_i > 0$ need not be an ACS even if an ACS exists in the graph and λ_1 can decrease while $s_1 < s$. However, destructive parasites occur rarely and do not reverse the trend of increasing s_1 – in the displayed run they formed 6 times at $n = 3388, 3478, 3576, 3579, 3592$ and 3613 , and in each case only resulted in s_1 decreasing by 1. Because the dominant ACS grows by adding positive links to the existing dominant ACS, the number of positive links increases as the ACS grows. On the other hand nodes receiving negative links often have $X_i = 0$, hence negative links get eliminated when these nodes are removed.

One can calculate the growth rate of the dominant ACS in exactly the same way as for the system with positive links because destructive parasites appear rarely. The only difference is that p must be replaced by $p/2$ because that is the probability for the added node to get a *positive* link to/from any other node. Thus once an ACS forms, s_1 locally averaged in time grows exponentially with a characteristic timescale $\tau_g = 2/p$. This is confirmed by numerical simulations (Figure 8.6).

This variant of the model, apart from being an important test of the robustness of the ACS mechanism, also allows one to address questions concerning the emergence of ‘cooperation’ because negative links can arise in the network. The negative links in the network can be considered ‘destructive’ links as they cause one species to decrease the population growth rate of another. In contrast, the positive links in the network can be considered ‘cooperative’ links. The increase of the ratio of positive to negative links, from its initial value of unity to value more than an order of magnitude larger in Figure 8.4, is evidence of the emergence of cooperation during the run.

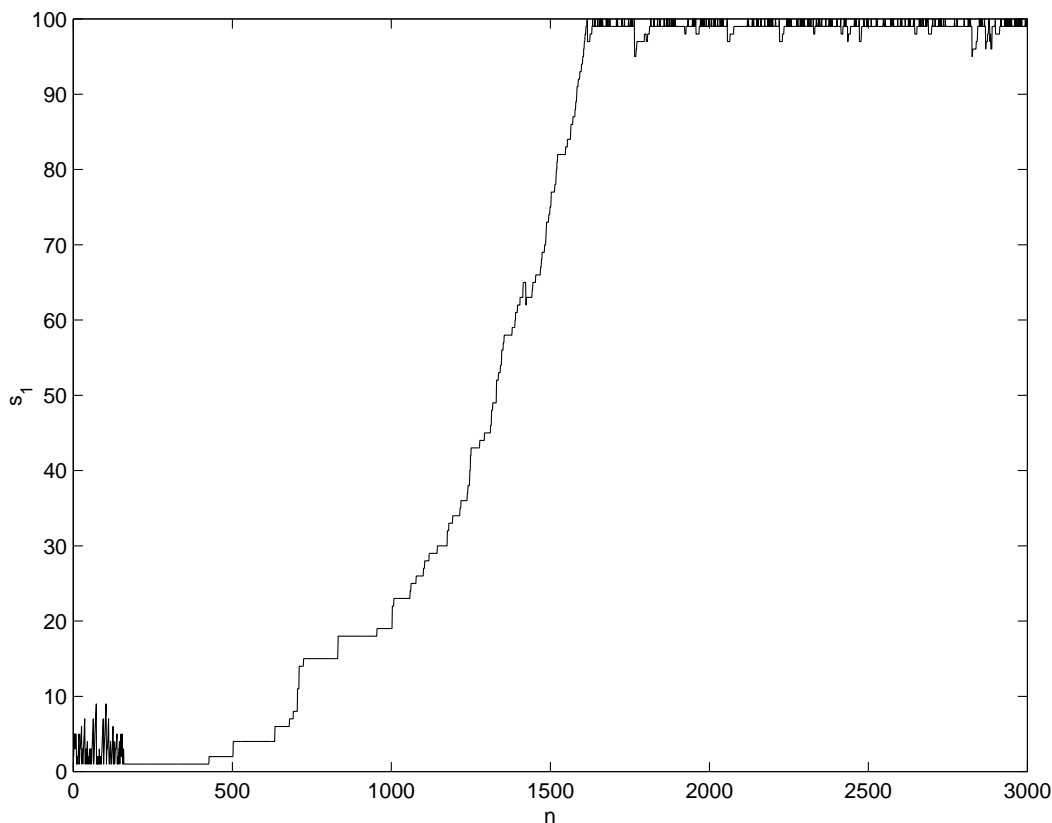


Figure 8.7: A run where self-replicators are allowed. Diagonal elements c_{ii} , when non-zero, are chosen randomly from the interval $[-1, 1]$. The run has $s = 100, p = 0.005$.

8.4 Self-replicators

In the original model, and all the variants discussed so far, self-replicators, i.e., self-links from a node to itself, are disallowed. As discussed in section 5.2.3, this was done to see whether structured chemical networks can arise even in the (forced) absence of individual self-replicators. As shown in chapter 6, structured networks do indeed form. The question that now arises is: Will allowing self-links interfere with the formation and growth of other ACSs? In fact, it does not, as evidenced by Figure 8.7, which shows a run with negative links in which self-replicators were allowed, i.e., for the initial graph and for the new node c_{ii} (when non-zero) was chosen randomly from the interval $[-1, 1]$. The probability for a self-replicator to form in a graph update event is $p/2$. The probability for a 2-cycle to form is $p^2s/4$. These are comparable when $p \approx 2/s$. Thus for small enough p , self-replicators do form, and often trigger the growth phase, but their role in the network dynamics is similar to that of any other ACS. Self-replicators have a Perron-Frobenius eigenvalue $\lambda_1 = 1$ and are, therefore, no more robust than cycles. ACSs with larger Perron-Frobenius eigenvalues out-compete self-replicators.

8.5 Non-extremal selection

The rule for removing a node can be made non-extremal in various ways. Instead of removing a single node with the least X_i one can remove more than one node or remove nodes with higher X_i also. However, even when removing nodes which do not have the least X_i it is reasonable to allow some bias in favour of nodes with a higher X_i . I consider the following possibilities:

1. A fixed fraction f of the nodes with the least X_i are replaced at each graph update.
2. A single node is picked for removal, with a probability proportional to $1/X_i$, at each graph update. When some nodes have $X_i = 0$ then one of them is picked randomly.
3. The selection depends on a parameter, denoted q . At each graph update, the node to be removed is selected from the set of nodes with least X_i with a probability q , or randomly from all nodes with a probability $1 - q$.

Figure 8.8a shows a run with $s = 100, p = 0.005$ with 2 nodes removed at each graph update; case 1 with $f = 0.02$. Figure 8.8b shows a similar run with 10 nodes removed at each graph update. Figure 8.9 shows a run with $s = 100, p = 0.005$ for case 2. In these three runs the behaviour is similar to the earlier models. An ACS forms by chance and grows until most of the graph is autocatalytic. In these cases the nodes comprising the dominant ACS are protected from removal until the size of the ACS becomes close to s . Only after the ACS has become more than $s - 2$ for Figure 8.8a, more than $s - 10$ for Figure 8.8b, or has reached s for Figure 8.9 do nodes of the dominant ACS start getting removed in the graph updates.

Case 3 is designed to interpolate between the extremal selection of the original model ($q = 1$) and the completely random run where there is no selection ($q = 0$, see black curve in Figure 5.2). Figure 8.10 displays what happens for different values of q . The basic mechanism of an ACS forming and growing remains but as q is decreased the ACS becomes increasingly short lived and susceptible to destruction. Suppose the ACS has z indispensable nodes, any of whose removal would destroy the ACS. Then the probability that an indispensable node will be removed is $(1 - q)z/s$. Hence, there exists a timescale $\tau_{ne} = s/\{z(1 - q)\}$ over which an ACS will get destroyed due to non-extremality. On the other hand for small p ACSs get destroyed even with extremal dynamics over a timescale τ_s . z does change with time but by choosing q sufficiently close to 1, one can make $\tau_{ne} \gg \tau_s$. In that case the behaviour would be the same as in the case of extremal dynamics. This is confirmed by the run in Figure 8.10c, where an ACS forms and grows until it spans the entire graph. After spanning it does not get destroyed for a substantial period of time.

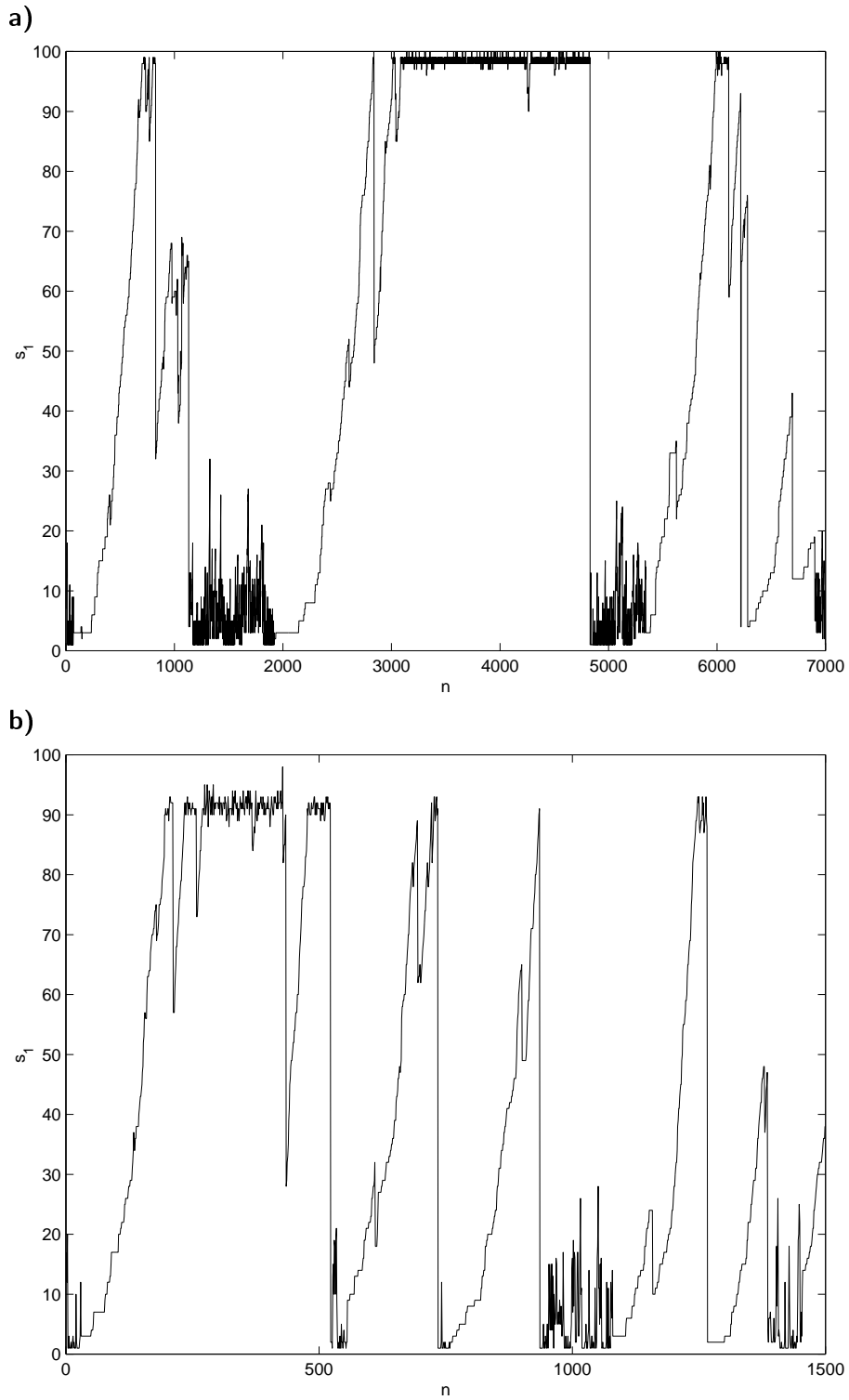


Figure 8.8: Non-extremal runs of type 1 with $s = 100, p = 0.005$. **a.** at each time step 2 nodes are replaced. **b.** at each time step 10 nodes are replaced.

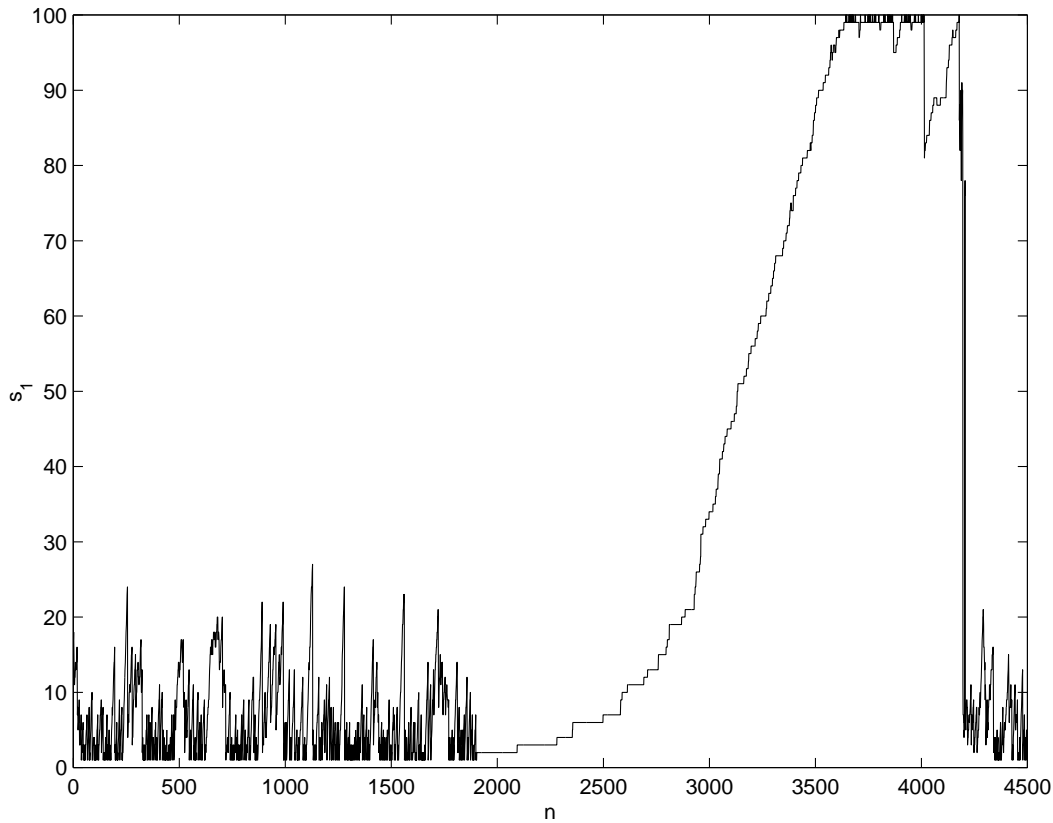


Figure 8.9: Non-extremal run of type 2 with $s = 100$, $p = 0.005$. At each time step a single node is replaced. The node is chosen with a probability proportional to $1/X_i$. If some nodes have $X_i = 0$ then one of them is randomly chosen.

These non-extremal runs seem to indicate that the ACS mechanism is stable to the introduction of non-extremality. In an ACS, organizationally important nodes, such as the core nodes, tend to have high relative populations and, therefore, these nodes are protected if there is a selective bias that favours removing nodes with less relative population. When the mechanism for choosing a node for removal is not based on the relative population of nodes, as (partially) in case 3, this protection is lost and the ACS is not as robust a structure.

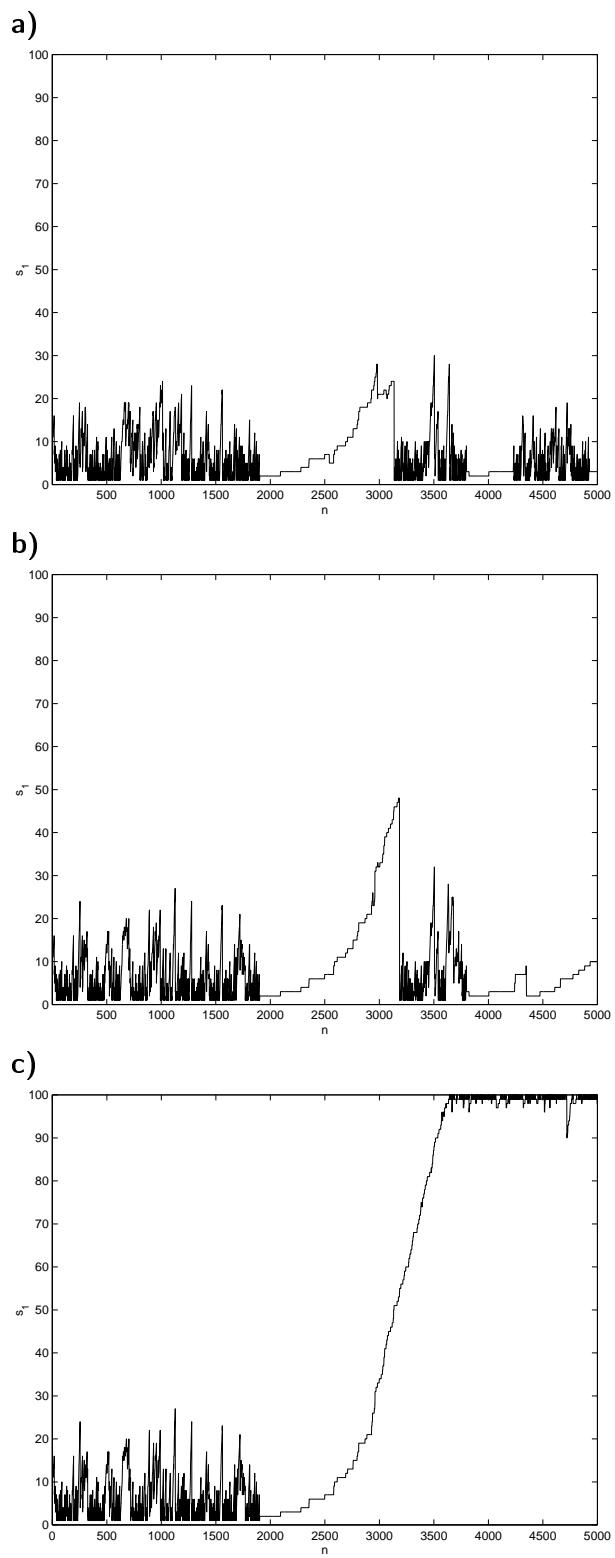


Figure 8.10: Non-extremal run of type 3 with $s = 100, p = 0.0025$. **a.** $q = 0.95$, **b.** $q = 0.99$, **c.** $q = 0.99999$.

8.6 Variable number of nodes

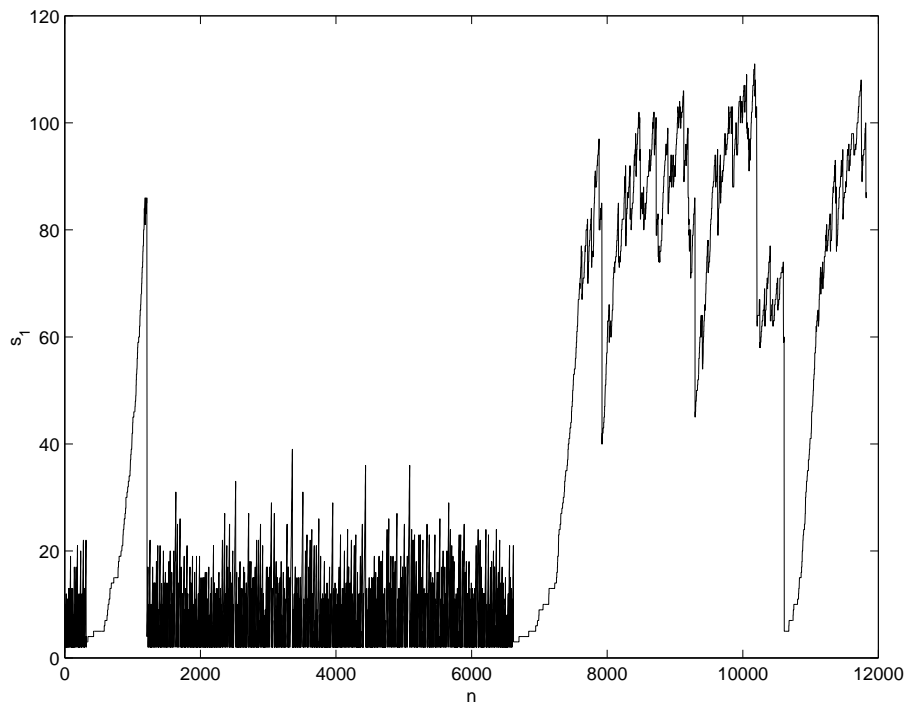
Another idealization in the original model is that at each time step exactly one node is removed and one node is introduced leaving the total number of nodes constant. A variant in which the number of nodes is not constant is the following: at each time step, all nodes with X_i below a fixed threshold, x_t , are removed (more than one node can get deleted and the number of nodes is not constant). The rest of the procedure remains the same; one new node is added, the population dynamics is allowed to run its course with the new graph, and this is iterated many times. Notice that it is also possible for none of the nodes to be removed in a particular time step if they all have relative populations above x_t . This is not possible in the original model.

This variant too shows the same qualitative behaviour (see Figure 8.11). When there is no ACS in the graph, none of the nodes remain above the threshold for long. The graph remains small, with few nodes and links. The chance formation of an ACS changes things. Again the number of links and the number of nodes are seen to rise sharply as more and more nodes get attached to the dominant ACS. A third region analogous to the organized phase can also be seen, once the ACS grows large enough for some of its nodes to have X_i values below the threshold, but the transition is not so clear because there is no upper cutoff for the number of nodes in the graph.

Because only positive links are allowed all the analytical results, including theorems 3.1 and 4.1, hold for this variant too. In the initial graph, if there is no ACS, most of the nodes will have $X_i = 0$. All of these nodes will be removed from the graph leaving a graph with very few nodes and only those links assigned to the new node. Throughout the random phase the graph will consist of only very few nodes. As soon as the first ACS forms the graph will consist only of that ACS and the added node. The ACS grows whenever the new node joins it. Here there is a slight difference from the original model. The rare events where several nodes, including the new node, simultaneously join the dominant ACS are not possible in this variant. It is also not possible for an ACS that went extinct for some reason to be resurrected (as happened in Figures 5.6j,u) – in this variant the extinct nodes would all be removed from the graph immediately.

Despite the absence of an explicit upper cutoff, the number of nodes cannot grow indefinitely. Because $\sum_{i=1}^s x_i = 1$ always, the number of nodes cannot grow much larger than $1/x_t$. In the run shown above the threshold is $x_t = 0.005$ and the number of nodes remains well below $200 = 1/0.005$.

a)



b)

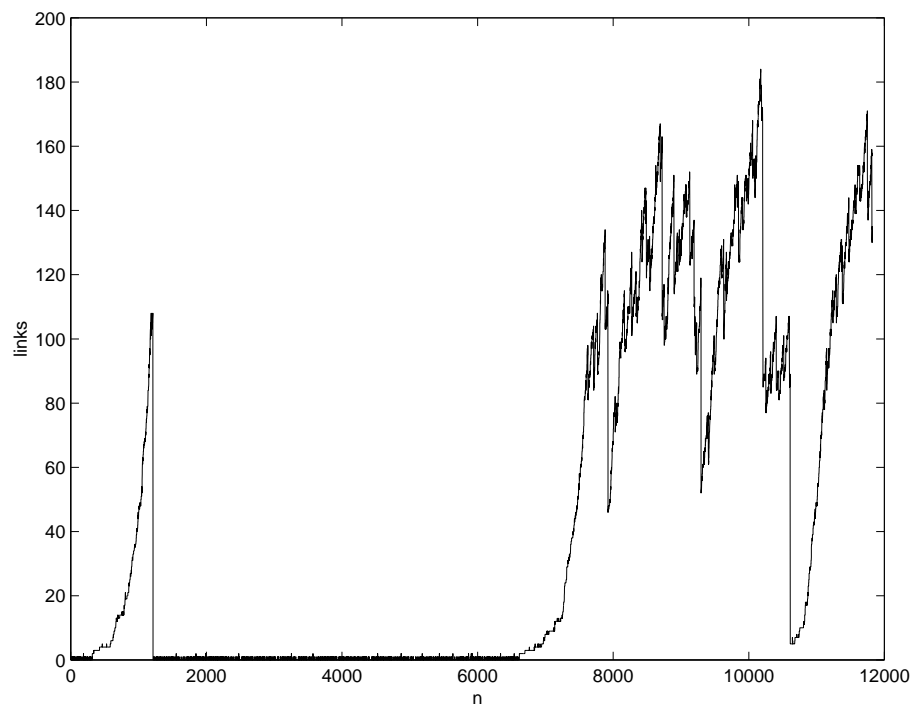


Figure 8.11: A run with variable number of nodes. At each time step all nodes with $X_i < 0.005$ are removed. A single new node is added and assigned links with existing nodes with a probability $p = 0.005$. **a.** the number of nodes in the graph, s_1 , as a function of time, n . **b.** the total number of links in the graph as a function of n .

8.7 Different population dynamics

Replicator equation.

A variant where the qualitative behaviour does change drastically is one where equation (4.1) is replaced by the replicator equation (Hofbauer and Sigmund, 1988):

$$\dot{x}_i = x_i \left[\sum_{j=1}^s c_{ij} x_j - \sum_{k,j=1}^s x_k c_{kj} x_j \right]. \quad (8.3)$$

The name ‘replicator’ comes from the fact that the equation models self-replicating species, for example in model ecosystems (Hofbauer and Sigmund, 1988; Drossel and McKane, 2003). Because \dot{x}_i is proportional to x_i , the relative population of species i can only grow if it is non-zero in the first place; once $x_i = 0$ it will always stay zero, as expected for self-replicators. The replicator equation can have a variety of attractors depending on the coupling constants c_{ij} and the initial conditions – fixed points, limit cycles, heteroclinic cycles and chaotic attractors have been observed (Hofbauer and Sigmund, 1988). The replicator equation has also been used in the hypercycle model of the origin of life (Eigen and Schuster, 1979).

The other rules of the model are unchanged, making it an evolving version of the hypercycle model. Figure 8.12 shows a typical run. When there is no ACS the number of nodes with non-zero X_i fluctuates wildly, even reaching as high as 40 or more for short periods of time. However, no graph structure is stable for very long and the graph remains random. The times when there is an ACS are the periods in Figure 8.12 when s_1 remains at some small constant value for a large number of graph updates. Yet, nothing resembling a growth phase is seen and the system eventually relapses into the random phase. What is happening is that small (hyper)cycles do form but quickly get destroyed when a graph update creates a parasite. This observed behaviour is consistent with existing work on well-stirred hypercycles and replicator networks (Niesert et al., 1981; Happel and Stadler, 1998; Tokita and Yasutomi, 2003).

Niesert et al. (1981) have identified three instabilities to which hypercycles are susceptible. Two are of relevance here: Figure 8.13a illustrates the parasite instability mentioned above. For the graph shown here, if $a > 1$, the attractor of equation (8.3) is $\mathbf{X} = (0, 0, 1)^T$ for generic initial conditions. Thus, the nodes of the core cycle have the least X_i . Figure 8.13b illustrates the short-circuit instability. For generic initial conditions the system always reaches an attractor where node 4, part of the longer cycle, is zero – in general, when long hypercycles are short-circuited by a new link, only the smaller hypercycle survives. These two instabilities are responsible for preventing a large, structured network from forming when the replicator equation (8.3) is used in place of equation (4.1) for the population dynamics.

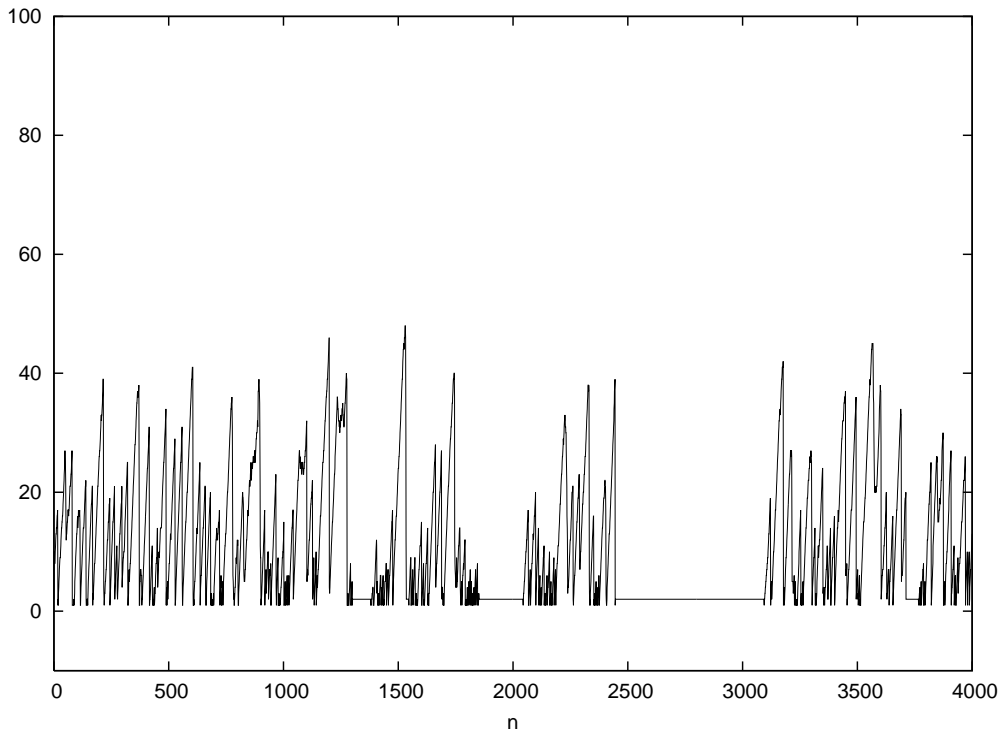


Figure 8.12: Number of nodes with $X_i > 0$, s_1 , versus time, n , for a run with the replicator equation used for the population dynamics. For this run, $s = 100$, $p = 0.0025$.

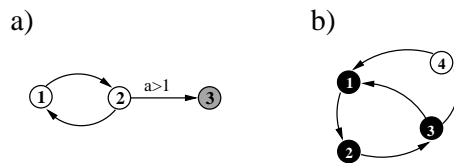


Figure 8.13: **a.** Example of the parasite instability of hypercycles. The links between nodes 1 and 2 are of strength unity. When $a > 1$ the attractor of the replicator equation for this graph is $\mathbf{X} = (0, 0, 1)^T$ for generic initial conditions. **b.** Example of the short-circuit instability of hypercycles. All link strengths are unity. The attractor of the replicator equation for this graph is $\mathbf{X} = (1, 1, 1, 0)^T / 3$ for generic initial conditions.

A generalization of the replicator equation.

The replicator equation is a special case of a more general equation in which the first term is quadratic in the relative population variables:

$$\dot{x}_i = \sum_{j,k=1}^s A_{ijk} x_j x_k - x_i \sum_{l,j,k=1}^s A_{ljk} x_j x_k. \quad (8.4)$$

This equation preserves the normalization of x_i because $\sum_{i=1}^s \dot{x}_i = 0$. The equation models a chemistry where two catalysts are (simultaneously) required for the production of each molecular species. It reduces to equation (8.3) in the special case where one of the catalysts is the product itself: $A_{ijk} = \delta_{ij} c_{jk}$, where $\delta_{ij} = 1$ if $i = j$ and zero if $i \neq j$.

In this case, the simplest ACS would consist of three species: species 1 and 2 catalyze species 3, species 2 and 3 catalyze species 1, and species 3 and 1 catalyze species 2. Consider the case where one periphery node is added to this ACS – let species 1 and 2 also catalyze the production of species 4, and let species 4 not be a catalyst for any of the other species. Numerical simulations show that, unlike the replicator case, here both the core and the periphery nodes have non-zero relative populations in the attractor for generic initial conditions. The ratio of the relative populations of the periphery to the core nodes depends on the link strengths but the core nodes 1, 2 and 3 remain with non-zero relative populations even if the link to the periphery node is stronger than the links between core nodes. Therefore, unlike the special case of the replicator equation, when equation (8.4) is used for the population dynamics it is possible for small ACSs to grow by adding periphery nodes.

Chapter 9

Concluding Remarks

In this thesis I have studied a model of an evolving catalytic network. I have discussed some of the issues and questions of interest related to the evolution of networks in section 1.6. Here, I summarize the interesting phenomena observed in the model, their implications for some of those questions, as well as the limitations and possible extensions of the model.

9.1 Interesting features of the model

1. **Rich dynamical behaviour: three phases and multiple timescales.** For small p the system always appears to be moving from one unstable, or quasi-stable, state to another. It never appears to reach a stable state. Three 'phases' of behaviour are observed (see section 5.4). A 'random phase' in which the graph remains sparse and consists only of trees, chains and isolated nodes. The 'growth phase' is triggered by the chance formation of a small ACS which then grows by accreting nodes to itself. Finally, the 'organized phase' begins when the ACS spans the entire graph. There are transitions from each phase to other phases (except that there is never a transition from the growth phase to the random phase). The appearance of different structures dynamically generates multiple timescales: τ_a in the random phase, τ_g in the growth phase and τ_s in the organized phase (see sections 6.2 and 7.5).
2. **Growth of structure, interdependence and cooperation.** Starting from an initial random graph, the system spontaneously self-organizes into a highly structured graph. This process is triggered by the chance, but inevitable, formation of an ACS, which then grows by accreting other nodes to it, until eventually the entire graph becomes an ACS (section 6.2). The resultant fully autocatalytic graph is highly non-random, occupying an exponentially small (as a function of s) volume of graph space (section 6.3.1). Nevertheless starting from a sparse graph the dynamics inevitably leads the system into this exponentially small volume in a time that grows only as $\ln s$. The growth of exponentially unlikely chemical organizations on the prebiotic Earth in a short time is a puzzle that has been discussed in section 1.9.

The growth of autocatalytic sets in this model might shed some light on this puzzle – the implications for the origin of life are discussed further in section 9.2. Along with the growth of non-random structure, the interdependence of the species also grows with the ACS. The fully autocatalytic sets that form have an interdependency almost two orders of magnitude larger than that of random phase graphs (sections 5.4 and 6.3.3). A variant of the model, where negative links are also allowed, exhibits the emergence of cooperation. The formation and growth of ACSs in this variant is accompanied by an increase in the number of cooperative, positive links between species and a decrease in the number of destructive, negative links. The ratio of cooperative to destructive links rises from unity, in the random phase, to an order of magnitude larger in the organized phase (section 8.3). The formation and growth of ACS might be one of the mechanisms responsible for the spontaneous emergence of cooperation in a variety of contexts.

3. **Structure of fully autocatalytic graphs.** The graphs produced at the end of the growth phase have several interesting structural features. Firstly, they are fully autocatalytic. However, they are not random fully autocatalytic graphs, as evidenced by their broad, though not scale-free, out-degree distribution which is displayed in Figures 6.6 and 6.7 (however, whether runs from other parameter ranges produce scale-free graphs or not remains an open question). An interesting feature is that the in-degree distribution spans a much smaller range than the out-degree distribution. While the fully autocatalytic graphs have a small clustering coefficient (section 6.3.2), they do consist of an irreducible core that is more clustered, from which grow the chains and trees that form the periphery. These observations suggest that, in addition to the commonly studied properties of small-worldness and scale-freeness, it might be interesting to examine real networks for properties such as autocatalysis, a core-and-periphery structure, a difference between the in- and out-degree distributions, etc.
4. **Large extinctions: destruction of ACSs.** ACSs not only form and grow, but over long times also get destroyed. The destruction of an ACS is usually sudden and accompanied by the extinction of a large number of species, a ‘crash’. The asymmetry between rises and drops of s_1 as well as fat tails in the distribution of crash sizes (Figure 7.1) are seen in the fossil record (Newman and Palmer, 1999) and in financial markets (Bouchaud, 2001; Johansen and Sornette, 2001). An interesting feature of the distribution of drops in s_1 is its bimodal structure for low p – the probability of large drops in s_1 is an order of magnitude greater than intermediate size drops. A similar bimodality is observed in distribution of earthquake sizes in an earthquake model described by Carlson and Langer (1989), but the mechanism causing it is different.
5. **Causes of large extinctions: core-shifts, innovations and keystone species.** A variety of mechanisms have been suggested as causes of large extinction events in macroevolution (Maynard-Smith, 1989; Glen, 1994) and finance (Bouchaud, 2001; Johansen and Sornette,

2001). The largest of the extinction events in this model are usually core-shifts – a discontinuous change of the core of the dominant ACS in a single graph update. It is interesting that such core-shifts can be caused both by the removal of an important ‘keystone’ species as well as by graph structures created by the new species, ‘innovations’ (section 7.4). One can distinguish two processes involving innovations, both having analogues in the real world. One is exemplified by the appearance of the automobile that made the horse drawn carriage and its ancillary industries obsolete. This is like the example of the core-transforming innovation shown in Figure 7.7 where the graph update produced an irreducible structure that was ‘stronger’ than the existing core. This structure became the new core, driving the old core and nodes dependent on it to extinction. The subsequent development of other industries dependent on the automobile mirrors the growth of the ACS around the new core. The second process is exemplified by the emergence of the body plans of several phyla that are dominant today. It is believed that while these body plans originated in the Cambrian era more than 520 million years ago (Valentine et al., 1999), the organisms with these body plans played no major role till about 250 million years ago. They started flourishing only when the Permian extinction depleted the other species that were dominant till that time (Erwin, 1996). This is similar to the events shown in Figure 7.8 where an earlier innovation had lain dormant for a while without disturbing the existing core, but when the latter became sufficiently weak, took over as the new core.

6. **Predicting crashes.** Certain graph theoretic markers could possibly be used to predict whether a crash is imminent (section 7.7). The Perron-Frobenius eigenvalue, λ_1 , is one such marker. Most of the large extinctions are core-shifts, caused by the removal of keystone species, takeover by core-transforming innovations, or takeover by dormant innovations. The graph is most susceptible to these core-shifts when its $\lambda_1 = 1$ or close to it. The dependency distribution is another marker: it is bimodal for graphs preceding a crash. The in and out-degree distributions also appear to fall off faster, as a function of degree, for graphs just before a crash, than for the fully autocatalytic graphs produced in the same runs. In combination, these different markers might indicate whether a given graph has an enhanced probability of suffering a crash.
7. **Analytical tractability of the model.** The analytical tractability of the model is a result of the linearity of the y_i dynamics. Equation (4.1) is nonlinear but, as it originates via a nonlinear change of variables from a linear equation, equation (4.2), its attractors can be easily analyzed in terms of the underlying linear system. The attractors are always fixed points and are just the Perron-Frobenius eigenvectors of the adjacency matrix of the graph. Theorems 3.1 (the eigenvector profile theorem) and 4.1 (the attractor profile theorem) form the backbone of the analytic results about the population dynamics. Note that while the y_i dynamics in the present model is essentially linear as long as the graph is fixed, it is highly nonlinear over long timescales. Because of the coupling of the population and graph dynamics, over long

timescales the 'coupling constants' c_{ij} in equation (4.2) are not constant but implicitly depend upon the y_i , thus making the evolution highly nonlinear. The simplifying device of widely separated timescales for the graph dynamics and the population dynamics (the population variables reach their attractor before the graph is modified) results in a piecewise linear y_i dynamics that is easier to analyze. The analytic results about the population dynamics have been used in the analysis of the graph dynamics: results such as proposition 6.1, as well as average timescales of appearance and growth of an ACS use insight about the attractors of the population dynamics to predict aspects of the graph dynamics.

8. **Predictability and historicity in the network evolution.** There is an interesting mixture of predictability and historicity in the model dynamics. The detailed structure of the dominant ACS is dependent on the chance events that happen throughout the run. Many complicated processes are possible, such as formation of new disconnected ACSs or the reinforcement of an old overshadowed ACS before it was completely broken up (Figures 5.6j,u). Thus, the actual growth of the ACS is usually very complicated with the dominant ACS often undergoing drastic changes in structure caused purely by chance events. However, despite the historical particularities of a given run several aspects are predictable. The non-decreasing nature of λ_1 in the growth phase is a rule that holds for every run with any values of the parameters s and p (see proposition 6.1, section 6.2). Other results, such as the timescales of appearance and growth of the ACS, are predictable for ensembles of runs with the same value of s and p (section 6.2). Also, as discussed above, the transitions from the organized to the growth or random phases that involve the sudden extinction of a large number of species, might be predictable.
9. **Correlation between graph structure of perturbations and their impact on the evolution of the network.** The network evolves by periodic perturbations, that involve the removal and addition of nodes, and there is a correlation between the graph theoretic nature of the perturbation and its short and long term impact. The perturbations can be broadly placed in two classes based on their effect on s_1 :
 - (i) 'Constructive perturbations': these include the birth of a new organization (an innovation of type 6), the attachment of a new node to the core (an innovation of type 4) and an attachment of a new node to the periphery of the dominant ACS (an innovation of type 2).
 - (ii) 'Destructive perturbations': these include complete crashes and takeovers by dormant innovations (both caused by the loss of a keystone node), and takeovers by core-transforming innovations (innovations of type 5). The word 'destructive' is used only in the sense that several species become extinct on a short timescale (a single graph update) after such a perturbation. In fact, over a longer timescale (ranging from a few to several hundred graph updates), the 'destructive' takeovers by innovations usually trigger a new round of 'constructive' events like incremental innovations (type 2) and core enhancing innovations (type 4).

The maximum upheaval is caused by those perturbations that introduce new irreducible structures in the graph (innovations of type 4, 5 and 6) or those that destroy the existing irreducible structure. For example, the creation of the first ACS at $n = 2854$ triggered the growth phase in the run of Figure 5.3b. Other examples of large upheavals are core-shifts due to takeover by a core-transforming innovation at $n = 6061$, takeover by a dormant innovation at $n = 5041$, and a complete crash at $n = 8233$.

10. **Context dependence of the effective dynamics of the network evolution.** It is characteristic of evolutionary systems, such as this model, that as different (graph) structures spontaneously appear, the nature of selective pressure on existing structures and hence the effective dynamics changes. In the present model the effective dynamics appears to be different in each of the phases even though the microscopic rules remain the same. Thus, in the random phase, because there is no ACS, the graph updates are almost random. In the growth phase there is competition between ACS and non-ACS structures. The dynamics essentially involves the growth of the dominant ACS by the accretion of nodes outside it. Once the entire graph becomes an ACS and the organized phase begins, the effective dynamics once again changes. Now there are no nodes outside the dominant ACS, yet some node has to be removed at each graph update. The competition now shifts to within the ACS – between core and periphery nodes. Typically the core nodes are protected by a higher relative population, therefore most of the graph updates involve periphery nodes. As the periphery realigns itself around stronger core nodes it can happen that a weak core node may be removed at some graph update. Over a long period of time such events may cause the core to become fragile and susceptible to core-shifts. Thus ACSs, which were robust in one phase, become fragile in another. Robust and fragile structures are also found in highly designed systems (Carlson and Doyle, 1999). A different system, in which the selective pressures and effective dynamics change as different structures arise, is discussed by Cohen, M., et al. (2001).
11. **Robustness of the ACS growth mechanism to changes in model rules.** The basic model has a number of simplifying features that depart from realism but enhance analytical tractability. These are listed in chapter 8 along with variants of the model that relax those simplifications. As shown in that chapter, in most cases relaxing the various idealizations does not change the qualitative behaviour. A variant where the qualitative behaviour does change drastically is one where equation (4.1) is replaced by the replicator equation, making it an evolving version of the hypercycle model (Eigen and Schuster, 1979). In this case small (hyper)cycles do form but quickly get destroyed when a graph update creates a parasite. Consequently, large complex networks cannot form. However, the replicator equation is a special case of a more general equation. In the more general case, unlike the hypercycle model, the ACSs that arise do not get destroyed by parasites (nodes belonging to the periphery). This robustness, one expects, would allow them to evolve into complex networks, as in the original model.

9.2 Implications for the origin of life

As discussed in chapter 1, one of the possible scenarios for which the model might be relevant is for the evolution of a chemical network in a pool on the prebiotic Earth. From the point of view of the origin of life problem the main conclusions are:

1. The model shows the emergence of a chemical organization where none exists. A small ACS emerges spontaneously by random processes and then grows until the entire system is autocatalytic.
2. The graph structures that emerge (ACSs) are collective self-replicators even though none of their components (individual nodes) are self-replicators.

As mentioned in section 1.9, one of the puzzles of the origin of life is the emergence of structured non-random chemical organizations in a relatively short time. A highly structured organization, whose timescale of forming by pure chance is exponentially large (as a function of the size of the system), forms in this model on a very short timescale that grows only logarithmically with the size of the system. Under the assumption that the present model captures what happens in a prebiotic pool, the timescale for a fully autocatalytic chemical organization to grow in the pool is $\tau_g = 1/p$, in units of the graph update time step. This time unit corresponds to the periodicity of the influx of new molecular species, hence it ranges from a day (for tides) to a year (for floods). Further, in the present model the 'catalytic probability' p is the probability that a random small peptide or RNA molecule will catalyze the production of another, and this has been estimated by Kauffman (1993) as being in the range 10^{-5} to 10^{-10} . With this range of values for p , the timescale, τ_g , for a fully autocatalytic chemical organization to grow in the pool lies in the range 10^3 to 10^{10} years. The time taken for the first cells to arise on Earth, a few hundred million years after the oceans condensed (Joyce, 1989; Schopf, 1993), lies within this range. However, 10^3 to 10^{10} years is a very wide interval. A tighter prediction, and therefore a better test of the model, would require a more accurate value for the catalytic probability p for peptides and catalytic RNA, and a chemically more realistic model.

These speculations might be complementary to some other approaches to the origin of life. Autocatalytic organizations of polypeptides could enter into symbiosis with the autocatalytic citric acid cycle proposed by Wächterhäuser (1990) and Morowitz et al. (2000). The latter would help produce, among other things, amino acid monomers needed by the former; the former would provide catalysts for the latter. It is conceivable that lipid membranes (that have been argued by Segré et al., 2000, 2001, to have their own catalytic dynamics) could form and surround autocatalytic sets, of the kind discussed here, in an enclosure. These 'cells' may contain different ACSs, or different parts of the same ACS, thereby endowing them with different fitness levels; such a population could evolve by natural selection. It is also conceivable that such autocatalytic sets of polypeptides formed an enabling environment for the formation and maintenance of self-replicating molecules such as those needed for an RNA world.

9.3 Limitations of the model as a description of a chemical network

I have interpreted the model as a chemical system, with nodes representing molecular species and the links representing catalytic interactions. This interpretation raises some questions. For example, what does it mean to remove a node from the graph? This effectively means that that molecular species cannot be produced again for a finite time until, at some later graph update, a new node comes in with exactly the same links as the one removed. If the species to be removed has a catalyst, then this is inconsistent with the assumption that there is a constant supply of all required reactants. In the random and growth phases this does not happen – in all cases the removed node either has no incoming links, or the X_i values of all its catalysts are zero. In the organized phase too, for runs with small p ($ps < 1$), a large fraction of graphs have $s_1 < s$ in which case the node that is removed (one of the nodes outside the dominant ACS) either has no incoming links or, if it does, all its catalysts have $X_i = 0$ (otherwise the node would be part of the dominant ACS). However, when $s_1 = s$, i.e., all nodes have non-zero X_i values, then the removed node always has a catalyst with a non-zero X_i value. Most of the time such removals do not significantly disturb the graph structure. However, in some cases they have drastic effects – for instance, complete crashes (section 7.4.1).

Another question concerns the structure of the molecules in the system. In this model, the identity of the molecular species is defined solely by their interactions and their structure is not specified at all. In reality, it is the structure of molecules that determines their chemical properties. The absence of structure in the model precludes its use in addressing a different problem of the origin of life: How did long proteins with strong and highly specific catalytic properties form from the short, weakly catalytic polypeptides existing initially?

Other weaknesses of the interpretation of the model as a chemical system lie in the assumptions behind the functional form of f_i , in particular, the dependence of \dot{x}_i only on the relative populations of catalysts of i and not on the reactants. Such an assumption implies that the reactants are all present and have unchanging concentrations, i.e., they are buffered and there is effectively a constant supply of reactants. This can lead to the uncontrolled growth in the population of some, or all, molecular species. In reality, the reactants will eventually get consumed thereby truncating the growth of population. Further, the dependence of the growth rate on reactants would make the dynamics nonlinear and hence oscillations and chaotic dynamics might occur. The form of f_i precludes the possibility of this kind of dynamics. The choice of f_i also does not allow for the possibility of other types of chemical reactions, such as conversion of one substrate to another, or cleavage and ligation of molecules, which might be important for the prebiotic pool scenario.

Another limitation is the absence of spatial degrees of freedom. Thus, the model applies only to a well-stirred chemical reactor and cannot address the emergence of spatial structure and its effect on the dynamics of the system. As prebiotic pools need not be well-stirred it would be more appropriate to use reaction-diffusion equations to model the x_i dynamics (Bhalla, 2003).

These are the most serious limitations. Apart from them, the model has several simplifications that aid in the analysis of its dynamical behaviour. These are listed below:

1. All catalysts have the same catalytic efficiency.
2. Inhibitors – negative links – are not present in the model.
3. Self-replicators are not allowed.
4. The selection is extremal; the node with the *least* X_i is removed at each graph update.
5. The total number of nodes is fixed; the rate of node removals and node additions is exactly the same.

Variants of the model, in which the rules are modified to relax these simplifications, were described in chapter 8 and show the same qualitative behaviour as the original model. Therefore, these are not serious limitations.

9.4 Possible extensions of the model

The above limitations of the model suggest possible directions in which it would be worthwhile to extend the model. Firstly, the structure of the molecular species could be explicitly introduced into the model. This would require specifying some rules to determine the catalytic properties of a molecule from its structure. The structure of the molecular species should determine the reactions in which the molecule will participate. Then there would be no need to remove a node from the graph. In such a model one could explicitly study the evolution of certain structural features of molecules in the system – for instance their length.

Another direction in which to extend the model as a description of a chemical system would be to introduce the reactants explicitly, and also include other kinds of reactions, e.g., reactions in which one molecular species is converted to another type of molecular species. In the reductive citric acid cycle discussed above, a crucial reaction involves the splitting of citrate into two smaller molecules, which then undergo various reactions until each is re-converted into citrate. Therefore, including these kind of reactions is necessary to study the emergence of this kind of autocatalytic set in a chemical network. These changes fit within the general framework described in section 1.7.

Going beyond that framework, spatial degrees of freedom could be added to the model by using reaction-diffusion equations for the x_i dynamics. However, it is computationally difficult to solve such equations for complicated geometries (Press et al., 1992). A compromise might be achieved by simulating a finite number of compartments, within each of which the system is well mixed, and allowing some exchange or diffusion across compartment boundaries (Bhalla, 2003). Then different ACSs could exist in different compartments and interact with each other. This is likely to be computationally easier to simulate and at the same time allows some spatial differentiation.

9.5 Modeling other systems within the same framework

The general framework described in section 1.7 can be used to model systems other than chemical networks. For example, an ecosystem could be modeled. In that case the nodes would represent biological species while the links would represent interactions such as prey-predator, competitive or symbiotic interactions between species. Here removing a node that has become extinct is not a problem because the species are self-replicators (once a species becomes extinct its chance of being recreated can be neglected). However, the self-replicating character of the species in this interpretation must also be reflected in the population dynamics. The Lotka-Volterra equation, replicator equation or other more complicated dynamical equations may be tried (Drossel and McKane, 2003). In modeling an ecosystem one might also wish to modify the way the new node is assigned links. While a random assignment might be interpreted as the invasion of the ecosystem by an entirely alien species, one might also want to include the possibility of an existing species mutating.

Another system that might be modeled in this manner is a genetic regulatory network. The nodes would represent the genes. The x_i would represent the level of expression of a gene, and the links would represent regulatory interactions between the protein product of one gene and another gene. Here again one might wish to allow a new node (a new gene) to be a mutated copy of an existing gene. One might also wish to include other processes that change the graph such as gene duplications.

A third way to modify the graph dynamics would be to allow the rewiring of existing links. This might be most relevant when using the model to describe an economic system, with the nodes representing economic 'agents' such as buyers and sellers, or companies, or nations.

Appendix A

Proofs of Propositions

Proposition 2.1: If a graph, C ,

- (i) has no closed walk then $\lambda_1(C) = 0$,
- (ii) has a closed walk then $\lambda_1(C) \geq 1$.

(i) If a graph has no closed walk then all walks are of finite length. Let the length of the longest walk of the graph be denoted r . If C is the adjacency matrix of a graph then $(C^k)_{ij}$ equals the number of distinct walks of length k from node j to node i . Clearly $C^m = 0$ for $m > r$. Therefore all eigenvalues of C^m are zero. If λ_i are the eigenvalues of C then λ_i^k are the eigenvalues of C^k . Hence, all eigenvalues of C are zero, which implies $\lambda_1 = 0$. This proof was supplied by V. S. Borkar.

(ii) If a graph has a closed walk then there is some node i that has at least one closed walk to itself, i.e. $(C^k)_{ii} \geq 1$, for infinitely many values of k . Because the trace of a matrix equals the sum of the eigenvalues of the matrix, $\sum_{i=1}^s (C^k)_{ii} = \sum_{i=1}^s \lambda_i^k$, where λ_i are the eigenvalues of C . Thus, $\sum_{i=1}^s \lambda_i^k \geq 1$, for infinitely many values of k . This is only possible if one of the eigenvalues λ_i has a modulus ≥ 1 . By the Perron-Frobenius theorem, λ_1 is the eigenvalue with the largest modulus, hence $\lambda_1 \geq 1$. This proof was supplied by R. Hariharan. \square

Proposition 2.2: If all the basic subgraphs of a graph C are cycles then $\lambda_1(C) = 1$, and vice versa.

For any cycle of k nodes whose adjacency matrix is A , it follows that A^k is the identity matrix $(A^k)_{ij} = \delta_{ij}$ (for each i there is a closed walk of length k from node i to itself, and there are no other walks of length k). Therefore, each eigenvalue, λ , of A satisfies $\lambda^k = 1$, i.e., $|\lambda| = 1$. The Perron-Frobenius eigenvalue of A must be real, therefore, $\lambda_1(A) = 1$. Thus, if all basic subgraphs of a graph C are cycles then $\lambda_1(C) = 1$.

If $\lambda_1(C) = 1$ then the basic subgraphs must be irreducible, they cannot be single nodes. Assume that one of the basic subgraphs is not a cycle. Let its adjacency matrix be A . Because A is

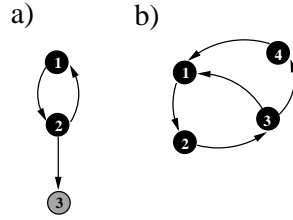


Figure A.1: **a.** A graph that is an ACS, but not irreducible (e.g. there is no path from node 3 to node 1). **b.** A graph that is irreducible but is not a cycle. Removing the link from node 3 to node 1 would convert it into a cycle.

irreducible, every row has at least one non-zero entry. Construct A' by removing, from each row of A , all non-zero entries except one that can be chosen arbitrarily. Thus A' has exactly one non-zero entry in each row. Clearly the column vector $\mathbf{x} = (1, 1, \dots, 1)^T$ is a right eigenvector of A' with eigenvalue 1 and hence $\lambda_1(A') \geq 1$. Also $A > A'$, therefore, by the Perron-Frobenius theorem for irreducible matrices, $\lambda_1(A) > \lambda_1(A') \Rightarrow \lambda_1(A) > 1$. But this contradicts the earlier assumption that $\lambda_1(A) = 1$. Hence, if $\lambda_1(C) = 1$, all the basic subgraphs must be cycles. \square

Proposition 3.1: (i) All cycles are irreducible graphs and all irreducible graphs are ACSs.

(ii) Not all ACSs are irreducible graphs and not all irreducible graphs are cycles.

(i) Clearly in a cycle, there is a path from every node i to any other node j hence all cycles are irreducible. In every irreducible graph each node must have an incoming link from one of the other nodes. Hence all irreducible graphs are ACSs.

(ii) This is proved by providing two counterexamples. Figure A.1a shows an ACS that is not an irreducible graph, and Figure A.1b shows an irreducible graph that is not a cycle. \square

Proposition 3.2: (i) An ACS must contain a closed walk. Consequently,

(ii) If a graph C has no ACS then $\lambda_1(C) = 0$.

(iii) If a graph C has an ACS then $\lambda_1(C) \geq 1$.

(i) Let A be the adjacency matrix of a graph that is an ACS. Then by definition, every row of A has at least one non-zero entry. Construct A' by removing, from each row of A , all non-zero entries except one that can be chosen arbitrarily. Thus A' has exactly one non-zero entry in each row. Clearly the column vector $\mathbf{x} = (1, 1, \dots, 1)^T$ is an eigenvector of A' with eigenvalue 1 and hence $\lambda_1(A') \geq 1$. Proposition 2.1 therefore implies that A' contains a closed walk. Because the construction of A' from A involved only removal of some links, it follows that A must also contain a closed walk. (ii) and (iii) follow from part (i) and propositions 2.1(i) and (ii), respectively. \square

Proposition 3.3: If $\lambda_1(C) \geq 1$, then the subgraph of any PFE of C is an ACS.

Let \mathbf{x} be a PFE of a graph. Renumber the nodes of the graph so that $x_i > 0$ only for $i = 1, \dots, k$. Let C be the adjacency matrix of this graph. As \mathbf{x} is an eigenvector of the matrix C

$$\sum_{j=1}^s c_{ij}x_j = \lambda_1 x_i,$$

$$\Rightarrow \sum_{j=1}^k c_{ij}x_j = \lambda_1 x_i.$$

Because $x_i > 0$ for $i = 1, \dots, k$ and $\lambda_1 \neq 0$, it follows that $\sum_{j=1}^k c_{ij}x_j > 0$ for each $i \in \{1, \dots, k\}$. Therefore, for each $i \in \{1, \dots, k\}$ there exists a j such that $c_{ij} > 0$. Hence the $k \times k$ submatrix $C' \equiv (c_{ij})$, $i, j = 1, \dots, k$, has at least one non-zero entry in each row. Thus each node of the subgraph corresponding to this submatrix has an incoming link from one of the other nodes in the subgraph. Hence the subgraph is an ACS. \square

Lemma A: Let A be a submatrix of a non-negative matrix B . Denote the Perron-Frobenius eigenvalue of A by $\lambda_1(A)$ and that of B by $\lambda_1(B)$. Then $\lambda_1(A) \leq \lambda_1(B)$.

Renumber the nodes so that B can be written as:

$$B = \left(\begin{array}{c|c} A & C_1 \\ \hline C_2 & C_3 \end{array} \right).$$

Consider the matrix

$$B' = \left(\begin{array}{c|c} A & 0 \\ \hline 0 & 0 \end{array} \right),$$

and denote its Perron-Frobenius eigenvalue by $\lambda_1(B')$.

Because $B' \leq B$ we have $\lambda_1(B') \leq \lambda_1(B)$ from the Perron-Frobenius theorem.

Also $\lambda_1(B') = \max\{0, \lambda_1(A)\}$.

Hence, $\lambda_1(B') = \lambda_1(A)$.

Therefore $\lambda_1(A) \leq \lambda_1(B)$. \square

Proposition 3.4: Let \mathbf{x} be a PFE of a graph C , and let C' denote the adjacency matrix of the subgraph of \mathbf{x} . Let $\lambda_1(C')$ denote the Perron-Frobenius eigenvalue of C' . Then $\lambda_1(C') = \lambda_1(C)$ and C' must contain at least one of the basic subgraphs of C .

Let the nodes be numbered such that $x_i > 0$ only for $i = 1, \dots, k$. Because \mathbf{x} is an eigenvector of the matrix C we have $\sum_{j=1}^s c_{ij}x_j = \lambda_1 x_i$; $i = 1, \dots, s$ ($\lambda_1(C)$ has been abbreviated to λ_1).

$$\Rightarrow \sum_{j=1}^k c_{ij}x_j = \lambda_1 x_i; \quad i = 1, \dots, k.$$

Therefore $(x_1, x_2, \dots, x_k)^T$ is an eigenvector of the submatrix $C' = (c_{ij})$, $i, j = 1, \dots, k$, with eigenvalue λ_1 . Also by lemma A, $\lambda_1(C') \leq \lambda_1$. Therefore $\lambda_1(C') = \lambda_1$. It follows that the subgraph C' must contain a strong component with Perron-Frobenius eigenvalue λ_1 . That strong component would be present in C also and would be one of its basic subgraphs. Hence there exists at least one basic subgraph of C that is non-zero in any PFE of C . \square

Lemma B: Let C be an $s \times s$ non-negative irreducible matrix with Perron-Frobenius eigenvalue λ_1 and let $E = \text{Adj}(C - \lambda_1 I)$. Then either $E > 0$ or $E < 0$.

As E is the adjoint of $C - \lambda_1 I$ and $|C - \lambda_1 I| = 0$, it follows that $E(C - \lambda_1 I) = 0$ and $(C - \lambda_1 I)E = 0$. Hence any column of E is either a PFE of C or is a column of zeroes. If it is a PFE then by the Perron-Frobenius theorem it is either strictly positive or strictly negative. A similar result holds for the rows of E . Hence either $E = 0$ or E has all elements non-zero. If E has all elements non-zero then it follows that either $E > 0$ or $E < 0$.

I now show that one element of E is non-zero. The (s, s) element of E is $|D - \lambda_1 I|$ where D is the matrix C with the last row and column deleted. Consider the matrix

$$C' = \left(\begin{array}{c|c} D & 0 \\ \hline 0 & 0 \end{array} \right).$$

Clearly $C' \leq C$. Because C is irreducible it cannot have a zero column or row; if it did there would be no path to or from that node to other nodes. Hence $C' \neq C$, which implies, as a consequence of the Perron-Frobenius theorem for irreducible matrices, that λ_1 is not an eigenvalue of C' and, therefore, is not an eigenvalue of D either. Hence $E_{ss} = |D - \lambda_1 I| \neq 0$.

Therefore, either $E > 0$ or $E < 0$. \square

Proposition 3.5: If a node is non-zero in a PFE then all nodes it has access to are non-zero in that PFE.

Let i be a node that is non-zero in the PFE \mathbf{x} . Let j be any node downstream from it. Therefore there exists a positive integer k such that $(C^k)_{ji} > 0$.

Assume that $x_j = 0$. As $\sum_{l=1}^s (C^k)_{jl} x_l = \lambda_1^k x_j$,

$$\Rightarrow \sum_{l=1}^s (C^k)_{jl} x_l = 0,$$

$\Rightarrow (C^k)_{jl} x_l = 0$, for each $l = 1, \dots, s$. This is a contradiction because $x_i > 0$ and $(C^k)_{ji} > 0$.

Hence $x_j > 0$. \square

Proposition 3.6: If a node is upstream from a basic subgraph then that node is zero in any PFE.

Let the nodes be renumbered so that the last few – nodes $r, r+1, \dots, s$ – form a basic subgraph of the graph C . Let node p be some other node that is upstream from this basic subgraph, i.e., there exists a positive integer k such that $(C^k)_{rp} > 0$. Let \mathbf{x} be a PFE of C . Then:

$$\sum_{j=1}^s (C^k)_{ij} x_j = \lambda_1^k x_i; \quad i = 1, \dots, s.$$

The equations for $i = r, r+1, \dots, s$ can be written in matrix form as follows:

$$A \begin{pmatrix} x_1 \\ \vdots \\ x_{r-1} \end{pmatrix} + (D^k - \lambda_1^k I) \begin{pmatrix} x_r \\ \vdots \\ x_s \end{pmatrix} = 0,$$

where $A_{ij} = (C^k)_{i+r-1, j}$ ($i = 1, \dots, m; j = 1, \dots, r-1; m \equiv s - r + 1$),

and $D_{ij} = C_{i+r-1, j+r-1}$ ($i, j = 1, \dots, m$) is the adjacency matrix of the basic subgraph.

$$\Rightarrow (D^k - \lambda_1^k I) \begin{pmatrix} x_r \\ \vdots \\ x_s \end{pmatrix} = \begin{pmatrix} b_1 \\ \vdots \\ b_m \end{pmatrix}, \quad (\text{A.1})$$

with $\mathbf{b} \equiv (b_1, b_2, \dots, b_m)^T \leq 0, \neq 0$.

Let us assume that node p is non-zero in the PFE, i.e. $x_p > 0$. Also $(A)_{1p} \equiv (C^k)_{rp} > 0$, therefore $b_1 < 0$.

Let R_i denote the i^{th} row of $D^k - \lambda_1^k I$.

Because $|D^k - \lambda_1^k I| = 0$,

$$\Rightarrow R_1 = \sum_{j=2}^m \alpha_j R_j, \quad (\text{A.2})$$

with at least one α_j being non-zero.

(A.1) gives

$$\sum_{i=1}^m (R_j)_i x_{i+r-1} = b_j; \quad j = 1, \dots, m.$$

Multiply the above equation by α_j and sum from $j = 2$ to $j = m$.

$$\begin{aligned} \Rightarrow \sum_{i=1}^m \sum_{j=2}^m \alpha_j (R_j)_i x_{i+r-1} &= \sum_{j=2}^m \alpha_j b_j, \\ \Rightarrow \sum_{i=1}^m (R_1)_i x_{i+r-1} &= \sum_{j=2}^m \alpha_j b_j, \\ \Rightarrow b_1 &= \sum_{j=2}^m \alpha_j b_j. \end{aligned} \tag{A.3}$$

From (A.2) we have

$$\begin{aligned} (R_1)_i &= \sum_{j=2}^m \alpha_j (R_j)_i, \\ \Rightarrow (D^k - \lambda_1^k I)_{1i} &= \sum_{j=2}^m \alpha_j (D^k - \lambda_1^k I)_{ji}. \end{aligned} \tag{A.4}$$

Let $E = \text{Adj}(D^k - \lambda_1^k I)$. By definition

$$\begin{aligned} \sum_{j=1}^m E_{ij} (D^k - \lambda_1^k I)_{ji} &= |D^k - \lambda_1^k I| = 0; \quad i = 1, \dots, m, \\ \Rightarrow (D^k - \lambda_1^k I)_{1i} &= - \sum_{j=2}^m \frac{E_{ij}}{E_{i1}} (D^k - \lambda_1^k I)_{ji}; \quad i = 1, \dots, m. \end{aligned}$$

Comparing with (A.4) we have

$$\alpha_j = - \frac{E_{ij}}{E_{i1}} < 0,$$

because from lemma B either $E > 0$ or $E < 0$ (as D is irreducible it follows that D^k is irreducible hence lemma B is applicable).

$$\Rightarrow \sum_{j=2}^m \alpha_j b_j \geq 0.$$

Therefore from (A.3)

$$\Rightarrow b_1 \geq 0.$$

However, we are given that $b_1 < 0$. Hence the assumption that $x_p > 0$ has led to a contradiction. The only other possibility is that $x_p = 0$ in the PFE. \square

Proposition 3.7: If a node does not have access from a basic subgraph then it is zero in any PFE.

Let the $k \times k$ submatrix A consist of all the strong components that do not have access from any basic subgraph of C . The matrix C can be written as:

$$C = \left(\begin{array}{c|c} A & 0 \\ \hline R & B \end{array} \right),$$

where B consists of all the basic subgraphs of C and all the nodes having access from them. Let \mathbf{x} be a PFE of C . The eigenvector equations give:

$$(A - \lambda_1 I) \begin{pmatrix} x_1 \\ \vdots \\ x_k \end{pmatrix} = 0. \quad (\text{A.5})$$

A has no basic subgraphs of C , hence λ_1 is not an eigenvalue of A . Therefore (A.5) has only the trivial solution $x_i = 0$; $i = 1, \dots, k$. \square

Theorem 3.1: Eigenvector profile theorem

For any graph C , determine all the basic subgraphs of C . Denote them by D_1, \dots, D_K . Determine which of these does not have any other D_i downstream from it. Denote these by E_1, \dots, E_N . Then:

- (i) For each $i = 1, \dots, N$ there exists a unique (upto constant multiples) PFE in which the nodes of E_i and all nodes having access from them are non-zero and all other nodes are zero. It is evident that these PFEs are simple. Moreover these are the only simple PFEs of the graph C .
- (ii) Any PFE is a linear combination of these N simple PFEs.

The first statement follows from propositions 3.4–3.7. To prove the second statement, I first write

the matrix as follows:

$$C = \left(\begin{array}{c|cc} A & 0 & 0 \\ \hline & E_1 & \\ P & \cdot & 0 \\ & \cdot & \\ & E_N & \\ \hline Q & R & D \end{array} \right).$$

A contains all the nodes $i = 1, \dots, p-1$ that don't have access from any E_i . Thus all nodes in A will be zero in any PFE \mathbf{x} . D contains all nodes $i = p+m+1, \dots, s$ having access from some E_i , i.e. $R \neq 0$. As $x_1, \dots, x_{p-1} = 0$ the eigenvector equations for each E_i are:

$$(E_i - \lambda_1 I) \begin{pmatrix} x_{l_i} \\ \vdots \\ x_{l_i+m_i} \end{pmatrix} = 0.$$

Because each E_i is irreducible the above equations have solutions that are unique upto constant multiples. Denote these solutions by $x_j^{(i)}$; $j = l_i, \dots, l_i + m_i$. The equations for D are:

$$\begin{aligned} R \begin{pmatrix} x_p \\ \vdots \\ x_{p+m} \end{pmatrix} + (D - \lambda_1 I) \begin{pmatrix} x_{p+m+1} \\ \vdots \\ x_s \end{pmatrix} &= 0, \\ \Rightarrow (D - \lambda_1 I) \begin{pmatrix} x_{p+m+1} \\ \vdots \\ x_s \end{pmatrix} &= \mathbf{b}, \end{aligned}$$

where $\mathbf{b} \leq 0, \neq 0$.

Consider the case where only one of the E_i is non-zero. Denote the \mathbf{b} for that case by $\mathbf{b}^{(i)}$ and the corresponding (unique) solution of the above equations by $x_j^{(i)}$; $j = p+m+1, \dots, s$. For the general case where more than one E_i is non-zero, \mathbf{b} will be a linear combination of the $\mathbf{b}^{(i)}$ because x_k , for each node k in each E_i , is unique upto constant multiples. Hence the general solution for x_{p+m+1}, \dots, x_s will also be a linear combination of $x_{p+m+1}^{(i)}, \dots, x_s^{(i)}$. Rothblum (1975) provides a different proof that uses the principle of mathematical induction. \square

Proposition 3.8: Every node in the core of a simple PFE has access to every other node of the PFE subgraph. No periphery node has access to any core node.

From theorem 3.1 it follows that the subgraph of any simple PFE is the subgraph induced by the nodes of one of the basic subgraphs E_i (defined in the statement of theorem 3.1) and all nodes having access from E_i . The core nodes are the nodes of E_i . Because E_i is irreducible, it is evident that every core node has access to every other core node. Further, every periphery node has access from some, and therefore all, nodes of E_i . Thus, each core node has access to every other node of the PFE subgraph.

Now assume there is some periphery node p that has access to some core node r . Also r has access to p , therefore p is strongly connected to r . In that case p would also be part of the basic subgraph E_i , i.e., p would be a core node, not a periphery node. Thus, no periphery node can have access to any core node. \square

Proposition 4.1: For any graph C ,

- (i) Every eigenvector of C that belongs to the simplex J is a fixed point of equation (4.1), and vice versa.
- (ii) Starting from any initial condition in the simplex J , the trajectory converges to some fixed point (generically denoted \mathbf{X}) in J .
- (iii) For generic initial conditions in J , \mathbf{X} is a Perron-Frobenius eigenvector (PFE) of C .
- (iv) If C has a unique (upto constant multiples) PFE, it is the unique stable attractor of equation (4.1).
- (v) If C has more than one linearly independent PFE, then \mathbf{X} can depend upon the initial conditions. The set of allowed \mathbf{X} is a linear combination of a subset of the PFEs. The interior of this set in J may then be said to be the 'attractor' of (4.1), in the sense that for generic initial conditions all trajectories converge to a point in this set.

The proof uses the Jordan canonical form of the matrix C (Horn and Johnson, 1985):

$$J = \begin{pmatrix} J_{s_1}(\lambda_1) & & & 0 \\ & J_{s_2}(\lambda_2) & & \\ & & \ddots & \\ & & & J_{s_k}(\lambda_k) \\ 0 & & & & \end{pmatrix},$$

with $s_1 + s_2 + \dots + s_k = s$.

Each $J_{s_i}(\lambda_i)$ is called a Jordan block and is an $s_i \times s_i$ matrix of the form:

$$J_{s_i}(\lambda_i) = \begin{pmatrix} \lambda_i & 1 & & & 0 \\ & \lambda_i & 1 & & \\ & & \lambda_i & \cdot & \\ & & & \cdot & \cdot \\ & & & & \cdot & \cdot \\ & & & & & 1 \\ 0 & & & & & \lambda_i \end{pmatrix}.$$

The λ_i are the eigenvalues of C . The λ_i need not be distinct; there may be more than one Jordan block with the same diagonal. It is known that any complex matrix can be put in the above form by a similarity transformation, i.e. there exists a non-singular matrix P such that $C = PJP^{-1}$, and moreover, the form of J is unique barring rearrangements of the Jordan blocks (Horn and Johnson, 1985). The columns \mathbf{p}_i of P form k 'Jordan chains' $\{\mathbf{p}_1, \dots, \mathbf{p}_{s_1}\}, \{\mathbf{p}_{s_1+1}, \dots, \mathbf{p}_{s_1+s_2}\}, \dots, \{\mathbf{p}_{s-s_k+1}, \dots, \mathbf{p}_s\}$ that satisfy the following equations:

$$\begin{aligned} C\mathbf{p}_1 &= \lambda_1\mathbf{p}_1, \\ C\mathbf{p}_i &= \lambda_1\mathbf{p}_i + \mathbf{p}_{i-1}; \quad i = 2, \dots, s_1, \\ C\mathbf{p}_{s_1+1} &= \lambda_2\mathbf{p}_{s_1+1}, \\ C\mathbf{p}_{s_1+i} &= \lambda_2\mathbf{p}_{s_1+i} + \mathbf{p}_{s_1+i-1}; \quad i = 2, \dots, s_2, \\ &\vdots \\ C\mathbf{p}_{s-s_k+1} &= \lambda_k\mathbf{p}_{s-s_k+1}, \\ C\mathbf{p}_{s-s_k+i} &= \lambda_k\mathbf{p}_{s-s_k+i} + \mathbf{p}_{s-s_k+i-1}; \quad i = 2, \dots, s_k. \end{aligned}$$

Thus $\mathbf{p}_1, \mathbf{p}_{s_1+1}, \dots, \mathbf{p}_{s_k-1+1}$ are eigenvectors of C with eigenvalues $\lambda_1, \lambda_2, \dots, \lambda_k$ respectively. It can be shown that there is one and only one linearly independent eigenvector of C associated with each Jordan block and vice versa (Horn and Johnson, 1985). The other columns of P are called 'generalized eigenvectors' of C .

Now consider the underlying dynamics (4.2) from which (4.1) is derived: Because (4.1) is independent of ϕ , we can set $\phi = 0$ in (4.2) without any loss of generality. With $\phi = 0$ the general solution of (4.2), which is a linear system, can be schematically written as:

$$\mathbf{y}(t) = e^{Ct}\mathbf{y}(0),$$

where $\mathbf{y}(0)$ and $\mathbf{y}(t)$ are column vectors.

Using the Jordan canonical form of C in the general solution of (4.2) we find:

$$\mathbf{y}(t) = P e^{Jt} P^{-1} \mathbf{y}(0).$$

Now

$$e^{Jt} = \begin{pmatrix} e^{J_{s_1}(\lambda_1)t} & & & & 0 \\ & e^{J_{s_2}(\lambda_2)t} & & & \\ & & \cdot & & \\ & & & \cdot & \\ & 0 & & & e^{J_{s_k}(\lambda_k)t} \end{pmatrix},$$

where

$$e^{J_{s_i}(\lambda_i)t} = e^{\lambda_i t} \begin{pmatrix} 1 & t & \frac{t^2}{2} & \cdot & \cdot & \frac{t^{s_i-1}}{(s_i-1)!} \\ & 1 & t & \cdot & \cdot & \frac{t^{s_i-2}}{(s_i-2)!} \\ & & \cdot & & \cdot & \\ & & & \cdot & \cdot & \\ & & & & \cdot & t \\ 0 & & & & & 1 \end{pmatrix}.$$

Let

$$\mathbf{Y} = P \lim_{t \rightarrow \infty} e^{Jt} P^{-1} \mathbf{y}(0).$$

Then the attractor of (4.1) will be $\mathbf{X} = \mathbf{Y} / \sum_{i=1}^s Y_i$ and only the fastest growing components in \mathbf{Y} will contribute to \mathbf{X} . Therefore, in calculating \mathbf{Y} , I will keep only the fastest growing terms and set all others to zero for convenience.

First consider the case where $\mathbf{y}(0)$ is unrestricted – any initial condition is allowed. Then some components of $P^{-1} \mathbf{y}(0)$ could be zero. If all the components corresponding to a particular Jordan block are zero in $P^{-1} \mathbf{y}(0)$ then that Jordan block will not contribute to $e^{Jt} P^{-1} \mathbf{y}(0)$. Further, among the Jordan blocks that do have some non-zero components in $P^{-1} \mathbf{y}(0)$, only the ones with the largest λ_i will survive in the $t \rightarrow \infty$ limit because of the $e^{\lambda_i t}$ term. Let the Jordan blocks that survive be the first K ones (the nodes can always be renumbered to achieve this). From the structure of $e^{J_{s_i}(\lambda_i)t}$ it then follows that the only non-zero components of $e^{Jt} P^{-1} \mathbf{y}(0)$ will be the components $1, 1 + s_1, 1 + s_1 + s_2, \dots, 1 + \sum_{j=1}^{K-1} s_j$. Therefore $\mathbf{Y} = t^r e^{\lambda t} \sum_i' c_i \mathbf{p}_i$, with i being summed over the set $\{1, 1 + s_1, 1 + s_1 + s_2, \dots, 1 + \sum_{j=1}^{K-1} s_j\}$. c_i, r, λ are constants and \mathbf{p}_i is the i th column of P . Then, the attractor is $\mathbf{X} = c_0 (c_1 \mathbf{p}_1 + c_{1+s_1} \mathbf{p}_{1+s_1} + \dots + c_k \mathbf{p}_k)$, where c_0 is a constant chosen to make $\sum_{i=1}^s X_i = 1$, and $k = 1 + \sum_{j=1}^{K-1} s_j$. Notice that $\mathbf{p}_1, \mathbf{p}_{1+s_1}, \dots, \mathbf{p}_k$ are all eigenvectors of C with eigenvalue λ . Therefore \mathbf{X} is a fixed point, and is an eigenvector of C . This proves (i) and (ii).

Theorem 4.1: Attractor profile theorem

- 1) Determine all the strong components of the given graph C . Denote these by C_1, \dots, C_M .
- 2) Determine which of these are basic subgraphs. Denote them by D_1, \dots, D_K .
- 3) Construct a graph, denoted D^* , with K nodes, representing the D_i , and a link from node j to node i if there is a path from any node of D_j to any node of D_i that does not contain a node of any other basic subgraph.
- 4) Determine which of the D_i are at the ends of the longest paths in the above graph D^* . Denote these by $F_i, i = 1, \dots, N$.

For each $i = 1, \dots, N$ there exists a unique (upto constant multiples) PFE that has only nodes of F_i and all nodes having access from them non-zero, and all other nodes zero. The attractor set consists of all linear combinations of these PFEs that lie on the simplex J .

It has already been shown (proposition 4.1) that the attractor \mathbf{X} is a linear combination of those PFEs of C that correspond to the largest Jordan blocks with eigenvalue λ_1 . Therefore to prove this theorem it suffices to show that the PFEs corresponding to the largest Jordan blocks with eigenvalue λ_1 are precisely those PFEs corresponding to the subgraphs F_i that are at the ends of the longest paths in D^* .

It can be shown that the size of the largest Jordan block with eigenvalue λ_1 is equal to the length of the longest path in the graph D^* (see Rothblum, 1975, where it is called the index of C). It is also shown by Rothblum that for each basic subgraph D_i there is a sequence of generalized eigenvectors $\mathbf{y}^1, \dots, \mathbf{y}^h$, where h is the length of the longest path in D^* starting at D_i , such that $(C - \lambda_1 I)\mathbf{y}^1 = 0$, $(C - \lambda_1 I)\mathbf{y}^k = \mathbf{y}^{k-1}$ (where $k = 2, \dots, h$) and $y_j^k > 0$ if and only if the longest path from a node of D_i to node j when projected onto the graph D^* has a length k .

Let the length of the longest path in D^* be r and consider one such path starting at, say, D_j and ending at some F_i . Then, corresponding to this path, there is a sequence of r generalized eigenvectors that includes the PFE in which only F_i and nodes having access from it are non-zero. Thus there is a Jordan block of size r corresponding to the PFE in which only F_i and all nodes having access from it are non-zero. This is also the largest Jordan block. Therefore the PFEs corresponding to the largest Jordan blocks with eigenvalue λ_1 are precisely those PFEs corresponding to the subgraphs F_i that are at the ends of the longest paths in D^* . The attractor set will consist of linear combinations of these PFEs. \square

Proposition 4.2: For any graph with $\lambda_1(C) = 0$, in the attractor only the nodes at the ends of the longest paths are non-zero. All other nodes are zero.

Consider a graph consisting only of a linear chain of $r + 1$ nodes, with r links, pointing from node 1 to node 2, node 2 to 3, etc. The node 1 (to which there is no incoming link) has a constant population y_1 because the r.h.s of (4.2) vanishes for $i = 1$ (taking $\phi = 0$). For node 2, we get $y_2 = y_1$, hence $y_2(t) = y_2(0) + y_1 t \sim t$ for large t . Similarly, it can be seen that y_k grows as t^{k-1} . In general, it is clear that for a graph with no cycles, $y_i \sim t^r$ for large t (when $\phi = 0$), where r is the length of the longest path terminating at node i . Thus, nodes with the largest r dominate for sufficiently large t . Because the dynamics (4.1) does not depend upon the choice of ϕ , $X_i = 0$ for all i except the nodes at which the longest paths in the graph terminate. \square

Proposition 4.3: For any graph C ,

- (i) For every \mathbf{X} belonging to the attractor set, the set of nodes i for which $X_i > 0$ is the same and is uniquely determined by C . The subgraph formed by this set of nodes will be called the 'subgraph of the attractor' of (4.1) for the graph C .
- (ii) If $\lambda_1(C) \geq 1$, the subgraph of the attractor is an ACS.

This is a corollary to theorem 4.1. The set of nodes j for which $X_j > 0$ consists of nodes in all the subgraphs F_i described in the statement of theorem 4.1, and all nodes having access from them. This set evidently depends only on C . Further \mathbf{X} is a PFE of C . Therefore, from proposition 3.3 the subgraph of the attractor \mathbf{X} is an ACS if $\lambda_1(C) \geq 1$. \square

Proposition 6.1: λ_1 is a non-decreasing function of n as long as $s_1 < s$.

Let the adjacency matrix of the graph at time step n be denoted C_n and its Perron-Frobenius eigenvalue be denoted $\lambda_1(C_n)$. Removing a node with the least X_i from this matrix gives an $(s - 1) \times (s - 1)$ matrix that I denote T .

From lemma B, $\lambda_1(T) \leq \lambda_1(C_n)$.

Because $s_1 < s$ the removal of the node with the least X_i leaves the dominant ACS (denoted D_n) unaffected, i.e., D_n is a subgraph of T .

$\Rightarrow \lambda_1(D_n) \leq \lambda_1(T) \leq \lambda_1(C_n)$.

However $\lambda_1(C_n)$ is an eigenvalue of D_n . Hence, $\lambda_1(D_n) = \lambda_1(C_n)$,

$\Rightarrow \lambda_1(T) = \lambda_1(C_n)$.

Now a new node is added to T to get C_{n+1} . Because T is a subgraph of C_{n+1} , it follows that $\lambda_1(C_{n+1}) \geq \lambda_1(T)$,

$\Rightarrow \lambda_1(C_{n+1}) \geq \lambda_1(C_n)$. \square

Proposition 7.1: Let N_n denote the maximal new irreducible subgraph that includes the new node at time step n . N_n will become the new core of the graph, replacing the old core Q_{n-1} , whenever either of the following conditions are true:

- (a) $\lambda_1(N_n) > \lambda_1(Q'_n)$ or,
- (b) $\lambda_1(N_n) = \lambda_1(Q'_n)$ and N_n is downstream of Q'_n .

After a node is removed from the graph C_{n-1} , the resultant graph is C'_n which has the core Q'_n . Now a new node is added to this graph to get C_n . This graph contains the irreducible subgraph N_n . Clearly if $\lambda_1(N_n) > \lambda_1(Q'_n)$ then N_n is the only basic subgraph of C_n and will therefore be its core. But if $\lambda_1(N_n) = \lambda_1(Q'_n)$ then it is only one of the basic subgraphs of C_n . By definition Q'_n , because it is the core of C'_{n-1} , contains those basic subgraphs that are at the ends of the longest chains of basic subgraphs in C'_{n-1} . Therefore, N_n will be a basic subgraph at the end of the longest chain of basic subgraphs in C_n only if it is downstream from some node of Q'_n . If this is so, then it will be the single basic subgraph at the end of the longest chain, and therefore will be the core of C_n . \square

Appendix B

Programs to simulate the model

This appendix describes two programs, included in the attached CD, that can be used to simulate the model and its variants. The programs differ in the way the attractor is found at each time step. The first program uses theorem 4.1. The second numerically integrates equation (4.1) to find the attractor. These different methods will be described below, in sections B.4 and B.5, but first I will describe what is common to the two programs. Both programs are written in C++, however they can be easily translated to C because I have used only certain small convenient features of C++ and no object oriented code.

B.1 Variables and data types

The two parameters of the model are s , the total number of nodes of the graph, which is specified by the variable named `n` of type `int` (integer), and p , the catalytic probability, which is specified by the variable named `lprob` of type `double` (double precision real number).

The dynamical variables are the graph C , whose adjacency matrix is stored as a two dimensional $s \times s$ array of type `double`, and the relative populations x_i which are stored as a one dimensional array of type `double`.

B.2 Creating the initial random graph

The initial random graph is created in the function `makec4`. For each $i, j \in \{1, \dots, s\}$, I generate a (pseudo)random number of type `double` uniformly distributed in the interval $[0, 1]$. If the random number is less than p then c_{ij} is assigned unity, otherwise it is assigned zero. For generating (pseudo)random numbers uniformly distributed in the interval $[0, 1]$ I have used the routine `ran1` from Numerical Recipes (Press et al., 1992). However, as Press et al. do not allow Numerical Recipes routines to be distributed publicly, I have replaced calls to `ran1` in the programs included in the attached CD by calls to the internal random number generator `drand48`. The function call is `drand48()` and returns a number of type `double` uniformly distributed in the interval $[0, 1]$.

The variable `idum` of type `long` (long integer) is used to set the initial seed of the random number generator using the function `srand48`.

B.3 The graph update

Once the attractor is known, the set \mathcal{L} of nodes with the least X_i has to be determined. Because the X_i are stored as data type `double` it makes sense to choose a threshold such that two numbers differing by less than the threshold will be considered equal. In the programs, the threshold has been chosen to be 10^{-5} . Note that in the case where theorem 4.1 is used to determine the attractor, the set \mathcal{L} is known exactly in most cases; there are few situations where the threshold is actually required.

After the set \mathcal{L} is determined, one picks an arbitrary node out of this set for removing from the graph. This node is picked by choosing a random number from the set $\{0, 1, \dots, l-1\}$, where l is the size of the set \mathcal{L} (if r is a random number in the interval $[0, 1]$ generated using `ran1` or `drand48`, then `int(1*r)` is a random integer between 0 and l , inclusive).

Once the node to be removed is decided, say node k , the graph update is done by the function call `update4(k)`. All the elements of the matrix in that row and column are reassigned to 0 or 1 by the same procedure used to create the initial matrix, i.e., a random number is generated and for each $i \neq k$, c_{ik} is assigned unity if the random number is less than p , and is assigned zero otherwise, and similarly for c_{ki} . The function `update4` also sets x_k to x_0 (the variable `xin` of type `double`) and rescales all other x_i so that $\sum_{i=1}^s x_i = 1$.

B.4 Program that uses the attractor profile theorem

B.4.1 Determining which node to remove

The crucial step involves the determination of the set, \mathcal{L} , of nodes with the least X_i at each time step. The results from chapter 4, in particular theorem 4.1, are used to do this.

1. Determine all the strong components of the given graph. Denote these by C_1, C_2, \dots, C_M .
2. Determine which of these are basic subgraphs. Denote them by D_1, \dots, D_K .
3. Construct a graph, D^* , of K nodes representing the D_i with a link from node j to node i if there is a path from any node of D_j to any node of D_i that does not contain a node of any other basic subgraph.
4. Determine which of the D_i are at the ends of the longest paths in the above graph D^* . Denote these by F_i .

5. For each F_i construct a vector with (arbitrary) non-zero values assigned to those components corresponding to nodes in F_i and all nodes having access from them. Set all other components to zero.
6. (a) If there are any nodes that are zero in all these vectors then they form the unique set \mathcal{L} for generic initial conditions.
 (b) If no nodes are zero, then first the PFE corresponding to each F_i is determined using Matlab. This is done by constructing the adjacency matrix of the subgraph induced by all nodes in F_i and all nodes having access from them and using Matlab's eig function to determine the (unique) PFE of this matrix. Then,
 If there is only one F_i , its PFE is used to determine \mathcal{L} . Because its PFE is unique upto constant multiples, the set \mathcal{L} is also unique and independent of the (generic) initial conditions. If there is more than one F_i , then \mathcal{L} depends on the initial conditions. In this case X_i is taken to be a linear combination of the PFEs corresponding to each F_i , with the coefficients of the linear combination being random numbers generated by ran1 or drand48. The set \mathcal{L} is then determined from these values of X_i .

This last case only occurs for graphs in which several ACSs coexist and the whole graph is spanned by these ACSs. Such a situation occurs very rarely. Thus when $s_1 < s$ the set \mathcal{L} is unique and independent of initial conditions. When $s_1 = s$ most of the time there is only one F_i in which case again \mathcal{L} is unique and independent of initial conditions but has to be determined numerically (using Matlab). Finally, very rarely, when $s_1 = s$ and there is more than one F_i in the graph then the set \mathcal{L} depends on the initial conditions and an arbitrary linear combination of PFEs is taken as the attractor. The function that implements this algorithm in the program is called thmeig.

Note that the code was written to work with Matlab 5.2 and therefore may require some modifications to work with other versions of Matlab.

B.4.2 Output files

Having specified the values of the variables n (the size of the graph), lprob (the catalytic probability), xin (the relative population assigned to each new node) and idum (the initial random seed), the program produces a run with the specified number of graph updates. Several output files are created, which consist of one or more columns of data. Each row corresponds to an iteration of the graph dynamics and different filenames are used for storing different quantities. The list below shows the naming scheme I have used for the output files:

1. *.1 : the total number of links.
2. *.px : column 1 has the number of nodes with $X_i > 10^{-5}$, column 2 has the number of nodes with $X_i > 0$ calculated (using theorem 4.1) in thmeig if there is an ACS, or -1 if there is no ACS in the graph.

3. `*.lm` : the Perron-Frobenius eigenvalue of the graph.
4. `*.min` : information about each graph update, which node was replaced, which new links were assigned. This can be used to reconstruct all the graphs later using the program `mtx.cpp` included in the attached CD (see appendix C).
5. `*.c1no` : the number of irreducible subgraphs of the graph.
6. `*.c1ev` : the Perron-Frobenius eigenvalue of each irreducible subgraph.
7. `*.cn` : number of core nodes.
8. `*.cs` : list of core nodes.
9. `*.0num` : number of nodes with $X_i = 0$.
10. `*.0nodes` : list of nodes with $X_i = 0$.

Any filename can be substituted for `*`. I typically use a name that contains information about the values given to `n`, `lprob` and `idum`, thereby allowing me to distinguish one type of run from another.

B.5 Program that finds the attractor numerically

B.5.1 Numerical method for determining the attractor

As an alternative to the above program that uses theorem 4.1, I have included, in the attached CD, a program that numerically integrates equation (4.1) to find its attractor. The program uses a 5th order adaptive Runge-Kutta scheme based on the algorithm given in Numerical Recipes (Press et al., 1992). The function that implements this in the program is called `dyneig`. A call to `dyneig` replaces the call to `thmeig` in the previous program.

I have included this alternate program for two reasons. One, for several variants of the model, such as the variant with negative links (section 8.3), theorems 3.1 and 4.1 do not hold. Then the only option is to use a numerical method to find the attractor – many of the variants discussed in chapter 8 have been simulated using this method.

The second reason is historical. When I initially began working on this model, theorems 3.1 and 4.1 did not exist (in my mind). All the initial runs were done using the numerical method. Some patterns were consistently observed in these runs. For example, whenever there was a 2-cycle downstream from another, and these were the only basic subgraphs, then the upstream 2-cycle was always zero. These observations were the stepping stones that led to the theorems.

B.5.2 Output files

As in the previous program, the following variables must be set before running the program: `n` (the size of the graph), `lprob` (the catalytic probability), `xin` (the relative population assigned to each new node) and `idum` (the initial random seed). For a given run, the program produces four output files, each of which consist of one or more columns of data, and are named as follows:

1. `*.l` : the total number of links.
2. `*.px` : column 1 has the number of nodes with $X_i > 10^{-5}$, column 2 has a flag that is 1 if the set of nodes with $X_i > 10^{-5}$ is an ACS and 0 otherwise.
3. `*.S1` : list of nodes having $X_i > 10^{-5}$.
4. `*.min` : information about each graph update, which node was replaced, which new links were assigned. This can be used to reconstruct all the graphs later using the program `mtx.cpp` included in the attached CD (see appendix C).

Appendix C

Contents of the attached CD

The attached CD contains the following files:

- `contents`: The contents of the CD; this list.
- `thesis.pdf`: This thesis in PDF format.
- `thesis.ps`: This thesis in Postscript format.
- `Programs/thmrns.cpp`: A program to simulate the model, that uses theorem 4.1 (see section B.4).
- `Programs/rk5runs.cpp`: A program to simulate the model, that uses a 5th order Runge-Kutta method to integrate equation (4.1) (see section B.5).
- `Programs/mtx.cpp`: A program to extract the adjacency matrix of the graph at any given iteration, from the `*.min` file produced by `thmrns.cpp` or `rk5runs.cpp`. The program requires the seed used to initialize the random number generator for that run.
- `Programs/mtx2gw.cpp`: A program to convert the adjacency matrix files produced by `mtx.cpp` to the LEDA format.
- `Programs/calcddeg.cpp`: A program to calculate the in, out and total degree distributions for some or all graphs of a run from the `*.min` file produced by `thmrns.cpp` or `rk5runs.cpp`. The program requires the seed used to initialize the random number generator for that run.
- `Programs/calcddep.cpp`: A program to calculate the interdependency and dependency distribution for some or all graphs of a run from the `*.min` file produced by `thmrns.cpp` or `rk5runs.cpp`. The program requires the seed used to initialize the random number generator for that run.

- `Programs/rndgraph.cpp`: A program to produce a set of graphs drawn from the ensemble G_s^p , and to calculate the degree and dependency distribution.
- `Data/t01s1n100.*`: The data files produced by `thmrns.cpp` for a run with $s = 100, p = 0.001$. This is the run displayed in chapter 5 (see Figures 5.2 and 5.3a).
- `Data/t025s*n100.*`: The data files produced by `thmrns.cpp` for runs with $s = 100, p = 0.0025$ and different seeds. These are the set of runs, totaling 1.55 million iterations, mentioned in sections 6.3.2, 6.3.3 and 7.2. `t025s1n100.*` is the run displayed in chapter 5 (see Figures 5.2 and 5.3b).
- `Data/t05s3n100.*`: The data files produced by `thmrns.cpp` for a run with $s = 100, p = 0.005$. This is the run displayed in chapter 5 (see Figures 5.2 and 5.3c). Note that these data files, and the ones above, were produced by a version of `thmrns.cpp` that uses `ran1` as the random number generator and, therefore, are likely to differ from runs with the same random seed that are produced by the program provided in the CD, which uses `drand48`.
- `Data/crashes.txt`: A list of iterations, for each of the runs `t025s*n100.*` with $s = 100, p = 0.0025$, at which the graph update resulted in a crash. The core overlap for each crash is also given.
- `Graphs/n*.gw`: The graphs of Figure 5.6 in LEDA format.
- `Graphs/n*.mtx`: The adjacency matrices of the graphs shown in Figure 5.6.

Bibliography

- Adamic, L. A., Lukose, R. M. and Huberman, B. A. (2003) Local search in unstructured networks, in *Handbook of Graphs and Networks*, eds. Bornholdt, S. and Schuster, H. G. (Wiley-VCH, Berlin) pp. 295–317.
- Albert, R. and Barabási, A.-L. (2002) Statistical mechanics of complex networks, *Rev. Mod. Phys.* **74**, 47–97.
- Albert, R., Jeong, H. and Barabási, A.-L. (1999) Diameter of the world wide web, *Nature* **400**, 130–131.
- Albert, R. Jeong, H. and Barabási, A.-L. (2000) Error and attack tolerance of complex networks, *Nature* **406**, 378–382.
- Amaral, L. A. N., Scala, A., Barthélémy, M. and Stanley, H. E. (2000) Classes of small-world networks, *Proc. Natl. Acad. Sci. (USA)* **97**, 11149–11152.
- Arbib, M. A., ed. (1995) *Handbook of Brain Theory and Neural Networks* (MIT Press, Cambridge).
- Bagley, R. J. and Farmer, J. D. (1991) Spontaneous emergence of a metabolism, in *Artificial Life II*, eds. Langton, C. G., Taylor, C., Farmer, J. D. and Rasmussen, S. (Addison Wesley, Redwood City) pp. 93–140.
- Bagley, R. J., Farmer, J. D. and Fontana, W. (1991) Evolution of a metabolism, in *Artificial Life II*, eds. Langton, C. G., Taylor, C., Farmer, J. D. and Rasmussen, S. (Addison Wesley, Redwood City) pp. 141–158.
- Bak, P. and Sneppen, K. (1993) Punctuated equilibrium and criticality in a simple model of evolution, *Phys. Rev. Lett.* **71**, 4083–4086.
- Barabási, A.-L. and Albert, A. (1999) Emergence of scaling in random networks, *Science* **286**, 509–512.

- Bhalla, U. S. (2002) Mechanisms for temporal tuning and filtering by postsynaptic signaling pathways, *Biophys. J.* **83**, 740–752.
- Bhalla, U. S. (2003) Understanding complex signaling networks through models and metaphors, *Prog. Biophys. Mol. Biol.* **81**, 45–65.
- Bhalla, U. S. and Iyengar, R. (1999) Emergent properties of biological signaling pathways, *Science* **283**, 381–387.
- Bhalla, U. S., Ram, P. T. and Iyengar, R. (2002) MAP kinase phosphatase as a locus of flexibility in a mitogen-activated protein kinase signaling network, *Science* **297**, 1018–1023.
- Biswal, B. and Dasgupta, C. (2002a) Neural network model for apparent deterministic chaos in spontaneously bursting hippocampal slices, *Phys. Rev. Lett.* **88**, 088102/1–4.
- Biswal, B. and Dasgupta, C. (2002b) Stochastic neural network model for spontaneous bursting in hippocampal slices, *Phys. Rev. E* **66**, 051908/1–18.
- Bollobás, B. (1998) *Modern Graph Theory* (Springer, New York).
- Bollobás, B. (2001) *Random Graphs, Second Edition* (Cambridge Univ. Press, Cambridge).
- Bollobás, B. and Riordan, O. M. (2003) Mathematical results on scale-free random graphs, in *Handbook of Graphs and Networks*, eds. Bornholdt, S. and Schuster, H. G. (Wiley-VCH, Berlin) pp. 1–34.
- Bornholdt, S. and Schuster, H. G. (2003) *Handbook of Graphs and Networks* (Wiley-VCH, Berlin).
- Bose, I. (2002) Biological networks, Preprint: <http://www.arxiv.org/abs/cond-mat/0202192>.
- Bouchaud, J.-P. (2001) Power laws in economics and finance: Some ideas from physics, *Quant. Finance* **1**, 105–112.
- Broder, A., Kumar, R., Maghoul, F., Raghavan, P., Rajagopalan, S., Stata, R., Tomkins, A. and Wiener, J. (2000) Graph structure in the web, *Comput. Netw.* **33**, 309–320.
- Callaway, D. S., Newman, M. E. J., Strogatz, S. H. and Watts, D. J. (2000) Network robustness and fragility: Percolation on random graphs, *Phys. Rev. Lett.* **85**, 5468–5471.
- Camacho, J., Guimerà, R. and Amaral, L. A. N. (2002) Robust patterns in food web structure, *Phys. Rev. Lett.* **88**, 228102/1–4.
- i Cancho, R. F. and Solé, R. V. (2001) The small-world of human language, *Proc. R. Soc. London B* **268**, 2261–2265.

- Carlson, J. M. and Doyle, J. (1999) Highly optimized tolerance: A mechanism for power laws in designed systems, *Phys. Rev. E* **60**, 1412–1427.
- Carlson, J. M. and Langer, J. S. (1989) Mechanical model of an earthquake fault, *Phys. Rev. A* **40**, 6470–6484.
- Chen, Y., Rangarajan, G. and Ding, M. (2003) General stability analysis of synchronized dynamics in coupled systems, *Phys. Rev. E* **67**, 026209–026213.
- Chowdhury, D., Stauffer, D. and Kunwar, A. (2003) Unification of small and large timescales for biological evolution: Deviations from power law, *Phys. Rev. Lett.* **90**, 068101/1–4.
- Cohen, R., Erez, K., ben-Avraham, D. and Havlin, S. (2000) Resilience of the Internet to random breakdowns, *Phys. Rev. Lett.* **85**, 4626–4628.
- Cohen, R., Erez, K., ben-Avraham, D. and Havlin, S. (2001) Breakdown of the Internet under directed attack, *Phys. Rev. Lett.* **86**, 3682–3685.
- Cohen, M. D., Riolo, R. L. and Axelrod, R. (2001) The role of social structure in the maintenance of cooperative regimes, *Rationality and Society* **13**, 5–32.
- Dhar, D., Barma, M., Chakrabarti, B. K. and Taraphder, A. (1987) The travelling salesman problem on a randomly diluted lattice, *J. Phys. A* **20**, 5289–5298.
- Dorogovtsev, S. N. and Mendes, J. F. F. (2001) Language as an evolving word web, *Proc. R. Soc. London B* **268**, 2603–2606.
- Dorogovtsev, S. N. and Mendes, J. F. F. (2002) Evolution of networks, *Adv. Phys.* **51**, 1079–1187.
- Dorogovtsev, S. N. and Mendes, J. F. F. (2003a) *Evolution of Networks: From Biological Nets to the Internet and WWW* (Oxford Univ. Press, Oxford).
- Dorogovtsev, S. N. and Mendes, J. F. F. (2003b) Accelerated growth of networks, in *Handbook of Graphs and Networks*, eds. Bornholdt, S. and Schuster, H. G. (Wiley-VCH, Berlin) pp. 318–341.
- Drossel, B. and McKane, A. J. (2003) Modeling food webs, in *Handbook of Graphs and Networks*, eds. Bornholdt, S. and Schuster, H. G. (Wiley-VCH, Berlin) pp. 218–247.
- Dube, P., Borkar, V. and Manjunath, D. (2002) Differential join prices for parallel queues: Social optimality, dynamic pricing algorithm and applications to Internet pricing, in *Proceedings of the IEEE INFOCOM 2002 Conference*, pp. 276–283.
- Dyson, F. (1985) *Origins of Life* (Cambridge Univ. Press, Cambridge).

- Edwards, J. S., Ibarra, R. U. and Palsson, B. O. (2001) In silico predictions of Escherichia coli metabolic capabilities are consistent with experimental data, *Nature Biotechnology* **19**, 125–130.
- Eigen, M. (1971) Self-organization of matter and the evolution of biological macromolecules, *Naturwissenschaften* **58**, 465–523.
- Eigen, M., McCaskill, J. and Schuster, P. (1989) The molecular quasi-species, *Adv. Chem. Phys.* **75**, 149–263.
- Eigen, M. and Schuster, P. (1979) *The Hypercycle: A Principle of Natural Self-Organization* (Springer, Berlin).
- Erdős, P. and Rényi, A. (1959) On random graphs, *Publicationes Mathematicae* **6**, 290–297.
- Erwin, D. H. (1996) The mother of mass extinctions, *Sci. Am.* **275**, 56–62.
- Faloutsos, M., Faloutsos, P. and Faloutsos, C. (1999) On power-law relationships of the Internet topology, *ACM SIGCOMM Comp. Commun. Rev.* **29**, 251–262.
- Farkas, I. J., Derényi, I., Barabási, A.-L. and Vicsek, T. (2001) Spectra of “real-world” graphs: Beyond the semicircle law, *Phys. Rev. E* **64**, 026704/1–12.
- Farkas, I. J., Jeong, H., Vicsek, T., Barabási, A.-L. and Oltvai, Z. N. (2003) The topology of the transcription regulatory network in the yeast, *Saccharomyces cerevisiae*, *Physica A* **318**, 601–612.
- Farmer, J. D., Kauffman, S. and Packard, N. H. (1986) Autocatalytic replication of polymers, *Physica D* **22** 50–67.
- Fell, D. A. and Wagner, A. (2000) The small-world of metabolism. *Nature Biotechnology* **18**, 1121–1122.
- Fontana, W. (1991) Algorithmic chemistry, in *Artificial Life II*, eds. Langton, C. G., Taylor, C., Farmer, J. D. and Rasmussen, S. (Addison Wesley, Redwood City) pp. 159–209.
- Fontana, W. and Buss, L. (1994) The arrival of the fittest: Toward a theory of biological organization, *Bull. Math. Biol.* **56**, 1–64.
- Gade, P. M., Cerdeira, H. A. and Ramaswamy, R. (1995) Coupled maps on trees, *Phys. Rev. E* **52**, 2478–2485.
- Goh, K.-I., Kahng, B. and Kim, D. (2001) Spectra and eigenvectors of scale-free networks, *Phys. Rev. E* **64**, 051903/1–5.

- Govindan, R. and Tangmunarunkit, H. (2000) Heuristics for Internet map discovery, *Proc. 2000 IEEE INFOCOM Conference*, pp. 1371–1380.
- Glen, W., ed. (1994) *The Mass Extinction Debates* (Stanford Univ. Press, Stanford).
- Gutfreund, H. (1995) *Kinetics for the Life Sciences* (Cambridge Univ. Press, Cambridge).
- Happel, R. and Stadler, P. F. (1998) The evolution of diversity in replicator networks, *J. Theor. Biol.* **195**, 329–338.
- Harary, F. (1969) *Graph Theory* (Addison Wesley, Reading).
- Hartwell, L. H., Hopfield, J. J., Leibler, S. and Murray, A. W. (1999) From molecular to modular cell biology, *Nature* **402**, C47–C52.
- Hofbauer, J. and Sigmund, K. (1988) *The Theory of Evolution and Dynamical systems* (Cambridge Univ. Press, Cambridge).
- Hong, J.-I., Feng, Q., Rotello, V. and Rebek Jr., J. (1992) Competition, cooperation and mutation: Improving a synthetic replicator by light irradiation, *Science* **255**, 848–850.
- Horn, R. and Johnson, H. (1985) *Matrix Analysis* (Cambridge Univ. Press, New York).
- Huberman, B. A. and Adamic, L. A. (1999) Growth dynamics of the world wide web, *Nature* **401**, 131.
- Ito, T., Chiba, T., Ozawa, R., Yoshida, M., Hattori, M. and Sakaki, Y. (2001) A comprehensive two-hybrid analysis to explore the yeast protein interactome, *Proc. Natl. Acad. Sci. (USA)* **98**, 4569–4574.
- Jain, S. and Krishna, S. (1998) Autocatalytic sets and the growth of complexity in an evolutionary model, *Phys. Rev. Lett.* **81**, 5684–5687. Preprint: <http://www.arxiv.org/abs/adap-org/9809003>.
- Jain, S. and Krishna, S. (1999) Emergence and growth of complex networks in adaptive systems, *Computer Physics Comm.* **121-122**, 116–121. Preprint: <http://www.arxiv.org/abs/adap-org/9810005>.
- Jain, S. and Krishna, S. (2001) A model for the emergence of cooperation, interdependence and structure in evolving networks, *Proc. Natl. Acad. Sci. (USA)* **98**, 543–547. Preprint: <http://www.arxiv.org/abs/nlin.AO/0005039>.
- Jain, S. and Krishna, S. (2002a) Crashes, recoveries and 'core-shifts' in a model of evolving networks, *Phys. Rev. E* **65**, 026103/1–4. Preprint: <http://www.arxiv.org/abs/nlin.AO/0107037>.

- Jain, S. and Krishna, S. (2002b) Large extinctions in an evolutionary model: the role of innovation and keystone species, *Proc. Natl. Acad. Sci. (USA)* **99**, 2055–2060. Preprint: <http://www.arxiv.org/abs/nlin.AO/0107038>.
- Jain, S. and Krishna, S. (2003a) Graph theory and the evolution of autocatalytic networks, in *Handbook of Graphs and Networks*, eds. Bornholdt, S. and Schuster, H. G. (Wiley-VCH, Berlin) pp. 355–395. Preprint: <http://www.arxiv.org/abs/nlin.AO/0210070>.
- Jain, S. and Krishna, S. (2003b) Innovation in evolution: Insights from a network perspective, Preprint.
- Jalan, S. and Amritkar, R. E. (2003) Self-organized and driven phase synchronization in coupled maps, *Phys. Rev. Lett.* **90**, 014101/1–4.
- Janaki, T. M. and Gupte, N. (2003) Connectivity strategies to enhance the capacity of weight-bearing networks, *Phys. Rev. E* **67**, 021503/1–6.
- Jeong, H., Mason, S., Barabási, A.-L. and Oltvai, Z. N. (2001) Lethality and centrality in protein networks, *Nature* **411**, 41–42.
- Jeong, H., Tombor, B., Albert, A., Oltvai, Z. N. and Barabási, A.-L. (2000) The large-scale organization of metabolic networks, *Nature* **407**, 651–654.
- Johansen, A. and Sornette, D. (2001) Large stock market price drawdowns are outliers, *J. Risk* **4(2)**, 69–110.
- Jordán, F., Takács-Sánta, A. and Molnár, I. (1999) A reliability theoretical quest for keystones, *OIKOS* **86**, 453–462.
- Joyce, G. F. (1989) RNA evolution and the origins of life, *Nature* **338**, 217–223.
- Joyce, G. F., Schwartz, A. W., Miller, S. L. and Orgel, L. E. (1987) The case for an ancestral genetic system involving simple analogues of the nucleotides, *Proc. Natl. Acad. Sci. (USA)* **84**, 4398–4402.
- Kaneko, K. (1989) Pattern dynamics in spatio-temporal chaos, *Physica D* **34**, 1–41.
- Kauffman, S.A. (1971) Cellular homeostasis, epigenesis and replication in randomly aggregated macromolecular systems, *J. Cybernetics* **1**, 71–96.
- Kauffman, S. A. (1983) Autocatalytic sets of proteins, *J. Theor. Biol.* **119**, 1–24.
- Kauffman, S. A. (1993) *The Origins of Order* (Oxford Univ. Press, New York).
- Kinzel, W. (2003) Theory of interacting neural networks, in *Handbook of Graphs and Networks*, eds. Bornholdt, S. and Schuster, H. G. (Wiley-VCH, Berlin) pp. 199–217.

- Kirman, A. (2003) Economic networks, in *Handbook of Graphs and Networks*, eds. Bornholdt, S. and Schuster, H. G. (Wiley-VCH, Berlin) pp. 273–294.
- Koch, C. and Laurent, G. (1999) Complexity and the nervous system, *Science* **284**, 96–98.
- Kohn, K. W. (1999) Molecular interaction map of the mammalian cell cycle control and DNA repair systems, *Mol. Biol. Cell* **10**, 2703–2734.
- Kirschner, M. and Gerhart, J. (1998) Evolvability, *Proc. Natl. Acad. Sci. (USA)* **95**, 8420–8427.
- Kumar, R., Raghavan, P., Rajagopalan, S., Sivakumar, D., Tomkins, A. S. and Upfal, E. (2000) The web as a graph, *Proc. 19th ACM SIGACT-SIGMOD-AIGART Symp. Principles of Database Systems*, pp. 1–10.
- Lauffenburger, D. A. (2000) Cell signaling pathways as control modules: Complexity for simplicity? *Proc. Natl. Acad. Sci. (USA)* **97**, 5031–5033.
- Lee, D. H., Severin, K., Yokobayashi, Y. and Ghadiri, R. M. (1997) Emergence of symbiosis in peptide self-replication through a hypercyclic network, *Nature* **390**, 591–594.
- Liljeros, F., Edling, C. R., Amaral, L. A. N., Stanley, H. E. and Åberg, Y. (2001) The web of human sexual contacts, *Nature* **411**, 907–908.
- Lindgren, K. and Nordahl, M. G. (1994) Artificial food webs, in *Artificial Life III*, ed. Langton, C. G. (Addison Wesley, Redwood City) pp. 73–103.
- Manna, S. S. (2003) Diffusion limited friendship network: A model for six degrees of separation, Preprint: <http://www.arxiv.org/abs/cond-mat/0304047>.
- Maslov, S. and Sneppen, K. (2002) Specificity and stability in topology of protein networks, *Science* **296**, 910–913.
- Maslov, S., Sneppen, K. and Alon, U. (2003) Correlation profiles and motifs in complex networks, in *Handbook of Graphs and Networks*, eds. Bornholdt, S. and Schuster, H. G. (Wiley-VCH, Berlin) pp. 168–198.
- Maynard-Smith, J. (1989) The causes of extinction, *Phil. Trans. R. Soc. B* **325**, 241–252.
- Milo, R., Shen-Orr, S., Itzkovitz, S., Kashtan, N., Chklovskii, D. and Alon, U. (2002) Network motifs: Simple building blocks of complex networks, *Science* **298**, 824–827.
- Montoya, J. M. and Solé, R. V. (2002) Small-world patterns in food webs, *J. Theor. Biol.* **214**, 405–412.
- Morowitz, H. J., Kostelnik, J. D., Yang, J. and Cody, G. D. (2000) The origin of intermediary metabolism, *Proc. Natl. Acad. Sci. (USA)* **97**, 7704–7708.

- Mukherjee, G. and Manna, S. S. (2003) Quasistatic scale-free networks, *Phys. Rev. E* **67**, 012101/1–4.
- Nagel, K. (2003) Traffic networks, in *Handbook of Graphs and Networks*, eds. Bornholdt, S. and Schuster, H. G. (Wiley-VCH, Berlin) pp. 248–272.
- Newman, M. E. J. (2000a) Scientific collaboration networks I: Network construction and fundamental results, *Phys. Rev. E* **64**, 016131/1–8.
- Newman, M. E. J. (2000b) Scientific collaboration networks II: Shortest paths, weighted networks and centrality, *Phys. Rev. E* **64**, 016132/1–7.
- Newman, M. and Palmer, R. G. (1999) Models of extinction: A review, Preprint: <http://www.arxiv.org/abs/adap-org/9908002>.
- Newman, M. E. J., Strogatz, S. H. and Watts, D. J. (2001) Random graphs with arbitrary degree distributions and their applications, *Phys. Rev. E* **64**, 026118/1–17.
- Niesert, U., Harnasch, D. and Bresch, C. (1981) Origin of life: between Scylla and Charybdis, *J. Mol. Evol.* **17**, 348–353.
- Paine, R. T. (1969) A note on trophic complexity and community stability, *Am. Nat.* **103**, 91–93.
- Pandit, S. A. and Amritkar, R. E. (1999) Characterization and control of small-world networks, *Phys. Rev. E* **60**, R1119–R1122.
- Pandit, S. A. and Amritkar, R. E. (2001) Random spread on the family of small-world networks, *Phys. Rev. E* **63**, 041104/1–7.
- Pastor-Satorras, R., Vázquez, A. and Vespignani, A. (2001) Dynamical and correlation properties of the Internet, *Phys. Rev. Lett.* **87**, 258701/1–4.
- Pastor-Satorras, R. and Vespignani, A. (2003) Epidemics and immunization in scale-free networks, in *Handbook of Graphs and Networks*, eds. Bornholdt, S. and Schuster, H. G. (Wiley-VCH, Berlin) pp. 111–130.
- Pérez, C. J., Corral, A., Díaz-Guilera, A., Christensen, K. and Arenas, A. (1996) On self-organized criticality and synchronization in lattice models of coupled dynamical systems, *Int. J. Mod. Phys. B* **10**, 1111–1151.
- Press, W. H., Teukolsky, S. A., Vetterling, W. T. and Flannery, B. P. (1992) *Numerical Recipes in C, Second Edition* (Cambridge Univ. Press, Cambridge).
- Ramaswamy, R. (1997) Synchronization of strange nonchaotic attractors, *Phys. Rev. E* **56**, 7294–7296.

- Ravasz, E., Somera, A. L., Mongru, D. A., Oltvai, Z. N. and Barabási, A.-L. (2002) Hierarchical organization of modularity in metabolic networks, *Science* **297**, 1551–1555.
- Redner, S. (1998) How popular is your paper? An empirical study of the citation distribution, *Eur. Phys. J. B* **4**, 131–134.
- Robinson, D. F. and Foulds, L. R. (1980) *Digraphs: Theory and Techniques* (Gordon and Breach, New York).
- Rossler, O. E. (1971) A system theoretic model of biogenesis, *Z. Naturforschung* **26b**, 741–746.
- Rothblum, U. G. (1975) Algebraic eigenspaces of non-negative matrices, *Linear Algebra and Appl.* **12**, 281–292.
- Scala, A., Amaral, L. A. N. and Barthélémy, M. (2001) Small-world networks and the conformation space of a short lattice polymer chain, *Europhys. Lett.* **55**, 594–600.
- Schopf, J. W. (1993) Microfossils of the early archean apex chert: New evidence of the antiquity of life, *Science* **260**, 640–646.
- Seglen, P. O. (1992) The skewness of science, *J. Am. Soc. Inf. Sci.* **43**, 628–638.
- Segré, D., Ben-Eli, D. and Lancet, D. (2000) Compositional genomes: Prebiotic information transfer in mutually catalytic noncovalent assemblies, *Proc. Natl. Acad. Sci. (USA)* **97**, 4112–4117.
- Segré, D., Ben-Eli, D., Deamer, D. W. and Lancet, D. (2001) The lipid world, *Origins of Life and Evol. of the Biosphere* **31**, 119–145.
- Sen, P. and Chakrabarti, B. K. (2001) Small-world phenomena and the statistics of linear polymers, *J. Phys. A* **34**, 7749–7755.
- Sen, P., Dasgupta, S., Chatterjee, A., Sreeram, P. A., Mukherjee, G. and Manna, S. S. (2003) Small-world properties of the Indian railway network, *Phys. Rev. E* **67**, 036106/1–5.
- Seneta, E. (1973) *Non-Negative Matrices* (George Allen and Unwin, London).
- Sengupta, A. M., Djordjevic, M. and Shraiman, B. I. (2002) Specificity and robustness in transcription control networks, *Proc. Natl. Acad. Sci. (USA)* **99**, 2072–2077.
- Shen-Orr, S. S., Milo, R., Mangan, S. and Alon, U. (2002) Network motifs in the transcriptional regulation network of *Escherichia coli*, *Nature Genet.* **31**, 64–68.
- Sinha, S. (2002) Random coupling of chaotic maps leads to spatiotemporal synchronization, *Phys. Rev. E* **66**, 016209–016215.
- Sinha, S. and Chakrabarti, B. K. (1999) Dynamical transitions in network models of collective computation, *Current Science* **77(3)**, 420–428.

- Solé, R. V. and Manrubia, S. C. (1996) Extinction and self-organized criticality in a model of large-scale evolution, *Phys. Rev. E* **54**, R42–R45.
- Solé, R. V. and Montoya, J. M. (2001) Complexity and fragility in ecological networks, *Proc. R. Soc. London B* **268**, 2039–2045.
- Solé, R. V., Pastor-Satorras, R., Smith, E. and Kepler, T. (2002) A model of large-scale proteome evolution, *Adv. Complex Syst.* **5**, 43–54.
- Stadler, P. F., Fontana, W. and Miller, J. H. (1993) Random catalytic networks, *Physica D* **63**, 378–392.
- Strogatz, S. H. (2000) From Kuramoto to Crawford: Exploring the onset of synchronization in populations of coupled oscillators, *Physica D* **143**, 1–20.
- Strogatz, S. H. (2001) Exploring complex networks, *Nature* **410**, 268–276.
- Suguna, C., Chowdhury, K. K. and Sinha, S. (1999) Minimal model for complex dynamics in cellular processes, *Phys. Rev. E* **60**, 5943–5949.
- Tokita, K. and Yasutomi, A. (1999) Mass extinction in a dynamical system of evolution with variable dimension, *Phys. Rev. E* **60**, 842–847.
- Tokita, K. and Yasutomi, A. (2003) Emergence of a complex and stable network in a model ecosystem with extinction and mutation, *Theor. Popul. Biol.* **63**, 131–146.
- Uetz, P., Giot, L., Cagney, G., Mansfield, T. A., Judson, R. S., Knight, J. R., Lockshon, D., Narayan, V., Srinivasan, M., Pochart, P., Qureshi-Emili, A., Li, Y., Godwin, B., Conover, D., Kalbfleisch, T., Vijayadamar, G., Yang, M., Johnston, M., Fields, S. and Rothberg, J. M. (2000) A comprehensive analysis of protein-protein interactions in *Saccharomyces cerevisiae*, *Nature* **403**, 623–627.
- Valentine, J. W., Jablonski, D. and Erwin, D. H. (1999) Fossils, molecules and embryos: New perspectives on the Cambrian explosion, *Development* **126**, 851–859.
- Vázquez, A., Flammini, A., Maritan, A. and Vespignani, A. (2003) Modeling of protein interaction networks, *ComplexUs* **1**, 38–44.
- Wächterhäuser, G. (1990) Evolution of the first metabolic cycles, *Proc. Natl. Acad. Sci. (USA)* **87**, 200–204.
- Wagner, A. (2001) The yeast protein interaction network evolves rapidly and contains few redundant duplicate genes, *Mol. Biol. Evol.* **18**, 1283–1292.

- Watts, D. J. (1999) *Small Worlds: The Dynamics of Networks between Order and Randomness* (Princeton Univ. Press, Princeton).
- Watts, D.J. and Strogatz, S. H. (1998) Collective dynamics of 'small-world' networks, *Nature* **393**, 440–442.
- White, J. G., Southgate, E., Thomson, J. N. and Brenner, S. (1986) The structure of the nervous system of the nematode *Caenorhabditis elegans*, *Philos. Trans. R. Soc. London B* **314**, 1–340.
- Williams, R. J. and Martinez, N. D. (2000) Simple rules yield complex food webs, *Nature* **404**, 180–183.

Acknowledgments

I would like to thank Sanjay Jain and Chandan Dasgupta for being my PhD advisors, and Diptiman Sen for being my acting advisor for a year. I thank Sanjay Jain, in collaboration with whom this work was done, for suggesting the models discussed in this thesis. Chandan Dasgupta has always been ready to provide advice when I wanted it and has not seemed to mind if I didn't follow the advice. Sriram Shastry's constant interest in the details of my work and the opportunities he has provided me outweigh a rather heavy suitcase. I thank V. Vinay, V. Nanjundiah and H. R. Krishnamurthy for serving on my comprehensive examination committee.

Ramesh Hariharan and Vivek Borkar provided proofs for two propositions used in the analysis of the model. Thanks are due to William Cheswick, Dennis Bray and Hawoong Jeong who kindly gave me permission to use their images in this thesis, and to the COSIN project that has made data about a number of real networks publicly available. Many thanks to the Lyx team for an excellent free software that made the process of writing this thesis easier and faster.

I thank the Harishchandra Research Institute, NBI/NORDITA, Santa Fe Institute, Bell Laboratories, Rutgers Univ., Rockefeller Univ. and Princeton Univ. for their hospitality.

G. Rangarajan, Kim Sneppen, Maya Paczuski, Andrei Ruckenstein, Boris Shraiman, Anirvan Sengupta, members of the Bell Labs Biology Bandwagon, Vikram Soni, Ravi Mehrotra, Eric Siggia and William Bialek provided invaluable comments and complaints about this work, that have helped shape my understanding of it.

I am obliged to the Council of Scientific and Industrial Research, Govt. of India, for a research fellowship. Fortunately, circumstances never resulted in my testing their condition that, being unmarried, I would never marry again while my first wife was still alive – the bizarreness of which condition is only exceeded by their classification of fellows into the three categories: unmarried, married and female.

Thanks to the students, staff and faculty (in particular Raghu, Ritesh, Poulouse and Aavishkar the blue-nosed porcupine) for maintaining a breathable atmosphere at CTS. Special thanks are due to Janardhana who made life in CTS vastly easier by efficiently and invisibly taking care of numerous small tasks.

Working with Dhruba, Randhir, Joby, Pinaki and others in the SCouncil has been very interesting — not least in illuminating the essentially feudal structure of IISc, designed to maintain, as the bottom rung, an inexpensive and *grateful* labour force. In addition, during my stint in the SCouncil, I benefited from four crash courses: Beautifying IISc in 30 Days, Eradicating Child Labour from IISc in Six Easy Steps, Practical Lessons for the Modern Witch-hunter, and How to Talk at Important Meetings for Dummies.

If I survived coursework, it is both because of and despite my Integrated PhD classmates. Their names, in descending order of weirdness:

Shubra > Prabudhha > Ayash > Dhruba > Pinaki > Nandan > Rangeet.

This list misses out Sundar, who is no less weird, but his weirdness is orthogonal to the others. Thanks for (among many many other things that I can't remember right now) teaching me how to cycle.

In these six years many friends have left for other places. I remember them with fondness and miss their company: Aditi, Niruj, Arti, Rjoy, Dandy, Sumana, Devyani, Sundar, Raju, Baliga, Poulouse, Prithu, Raghavan, Subroto and Rsidd. Fortunately, new friendships have also formed: Osho, Ayesha, Moushumi and Natasha will be remembered for helping me and others during CTS parties, impromptu chocolate pastries, agreeing to be a murder victim and dropping a snake onto (well, close to) my foot, respectively.

My memories of IISc will also include: heavy metal education at Styx, courtesy Niruj; Dandy taking us to the edge of urbanity; Vatsa's views on mixing quantum field theory with alcohol; Raju and Negi frightening me out of my wits by mistaking a cow for an elephant; and the pool incident, which deserved a quieter night.

Much of my time recently has been spent in the welcome company of Bhavtosh, Moyna, Raghu, Joby, Toby and Vivek. Thanks to Vivek for catalyzing puns and other wordsmithings. Perhaps one day we'll finish the movie, the play and some junk we started. Toby and I share a common love for Calvin and Hobbes. From Chembra to World Cups to Rallyk and 'Walk in the Woods', he's always been great company and great competition. Joby has made a positive difference to the lives of many people and he can count me among them. The small amount of time I have spent at the tmsc classes and the construction colony with him have been more educative than all the coursework I did in IISc. I will miss Joby every time I see a bird that I can't identify, or hear a bird that I can't see.

It's difficult to adequately describe the kind of crucial life support those closest to me have provided. I hope they will extrapolate from the few words I have managed to put down. My parents have, successfully, tread the narrow path between pressurizing me with their opinions and abandoning me to my own decisions. Bhavtosh, Moyna and Raghu: If at all we drift apart, I hope it will only be geographically.